Analyses of melittin-induced ADAM10 and -17-activation and of phosphatidylserine exposure for ADAM17-mediated substrate processing

Dissertation

zur Erlangung des Doktorgrades

der Mathematisch-Naturwissenschaftlichen Fakultät

der Christian-Albrechts-Universität zu Kiel

vorgelegt von

Anselm Sommer

Kiel, 2014

Erster Gutachter: Prof. Dr. Thomas Roeder
Zweiter Gutachter: Prof. Dr. Karina Reiss

Tag der mündlichen Prüfung: 30.01.2015

Zum Druck genehmigt: 30.01.2015

Gez. Prof. Dr. Wolfgang J. Duschl, Dekan

TABLE OF CONTENT

1. Introduction

1.1. The family of "A Disintegrin And Metalloproteases"

Proteolysis represents a crucial regulatory mechanism for cells. It plays a role in irreversible modifications of proteins and controls protein function. This includes post-translational modifications, such as removal of signal sequences and maturation of precursor proteins, activation and deactivation of enzymes and receptors and processing of cytokines and growth factors. The latter are often mediated by family members of "A Disintegrin And Metalloproteases" (ADAMs). ADAMs are typical type-I transmembrane glycoproteins which cleave the ectodomains of type-I and type-II transmembrane or glycosylphosphatidylinositol- (GPI-) anchored proteins (Reiss and Saftig, 2009). This process is referred to as "shedding" (Figure 3). Shedding takes place in every cell type. The substrates are cleaved in close proximity to the transmembrane domain. The resulting ectodomains as well as the membrane bound stubs exhibit diverse and crucial effects of ADAM-functions. For instance, shed growth factors like TGF-α induce proliferation in a paracrine and autocrine manner by activating the epidermal growth factor receptor (EGFR). The most important sheddases belong to the ADAM family and will be introduced in this chapter.

1.1.1. Classification & Members

ADAMs are zinc-dependent-metalloproteinases and belong to the group of metzincins (Wolfsberg et al., 1995). This protease family shares a highly conserved zinc-binding amino acid sequence (HExxHxxGxxH) with three histidines in their catalytically active center. C-terminal, this motif is followed by a methionine turn (Bode et al., 1993). Metzincins are divided in four groups: matrix-metalloproteases (MMPs), astacines, serralysines and adamalysines (Figure 1). ADAMs are assigned to the adamalysines in the MEROPS classification (Rawlings et al., 2008). Adamalysines include also the protease families "a disintegrin and metalloproteinase with thrombospondin motifs" (ADAMTSs) and snake venom metalloproteases (SVMPs).

ADAM proteases have been identified in many species, inter alia in the nematode *Caenorhabditis elegans*, the fruit fly *Drosophila melanogaster*, the fission yeast *Schizosaccharomyces pombe* and in all investigated vertebrates (Blobel, 1997; Edwards et al., 2008; Wolfsberg and White, 1996). Thirteen family members of the so far identified 21 human members are proteolytically active (ADAMDEC-1, ADAM-8, -9, -10, -12, -15, -17, -19, -20, -21, -28, -30 and 33). The others lack one or more features in the active Zn^{2+}-binding site and may rather play a role in protein-protein interaction than proteolysis. Within the group of the proteolytic active members

ADAM10 and -17 are most extensively studied due to their crucial physiological importance (Reiss and Saftig, 2009). In this thesis, the main focus will be on ADAM17.

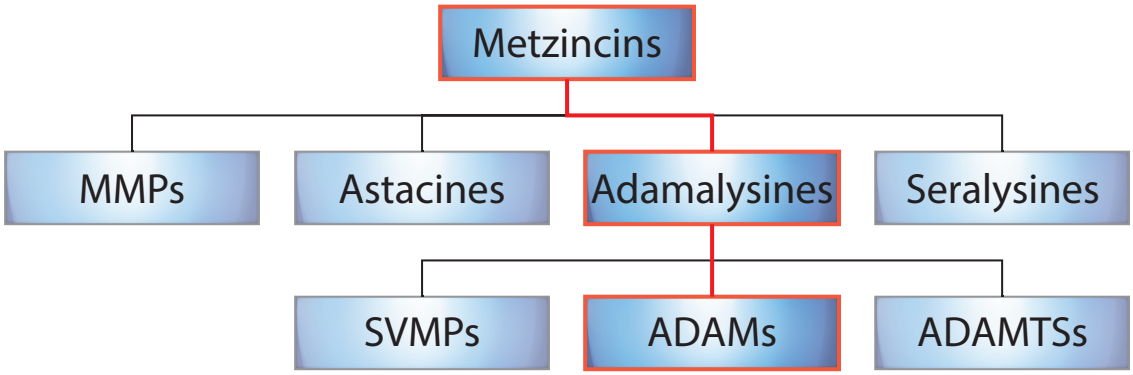

Figure 1: Metzincin family of Zn^{2+}-dependent metalloproteases. The superfamily of metzincins consist of matrix metalloproteases (MMPs), astacines, serralysines and adamalysines. The "a disintegrin and metalloproteases" (ADAMs) are assigned to the group of adamalysines together with snake venom metalloproteases (SVMPs) and " a disintegrin and metalloprotease with thrombospondin motifs" (ADAMTSs)(Rawlings et al. 2008).

1.1.2. Structure of ADAM17 and ADAM10

ADAMs consists of a typical sequence of protein domains. Most ADAMs possess a signal sequence at their N-terminus, followed by a pro-domain, a metalloprotease domain, a disintegrin domain, a cysteine-rich region, a EGF-like domain, a transmembrane domain and a cytoplasmic tail (Figure 2)(Stone et al., 1999). ADAM10 and -17 are atypical members of this family; they contain a pro-, catalytic- disintegrin- and a membrane proximal domain with a α/β fold and a stalk region followed by a transmembrane domain and a cytoplasmic tail (Figure 2) (Düsterhöft et al., 2014; Lorenzen et al., 2012; S. Takeda, 2009).

The signal sequence directs the ADAM to the secretory pathway and is cleaved off afterwards. The pro-domain acts as an intramolecular chaperone and keeps the enzyme inactive until it is removed by a furin type pro-protein convertase (Lum et al., 1998; Roghani et al., 1999; Schlöndorff et al., 2000). Recent studies suggest that ADAM17 is still able to cleave its substrate at the cell surface with an intact pro-domain (Lum et al., 1998; Roghani et al., 1999; Schwarz et al., 2013a). However removal of the pro-domain generally occurs during the transit through the Golgi system as maturation step before ADAMs get in contact with their substrates.

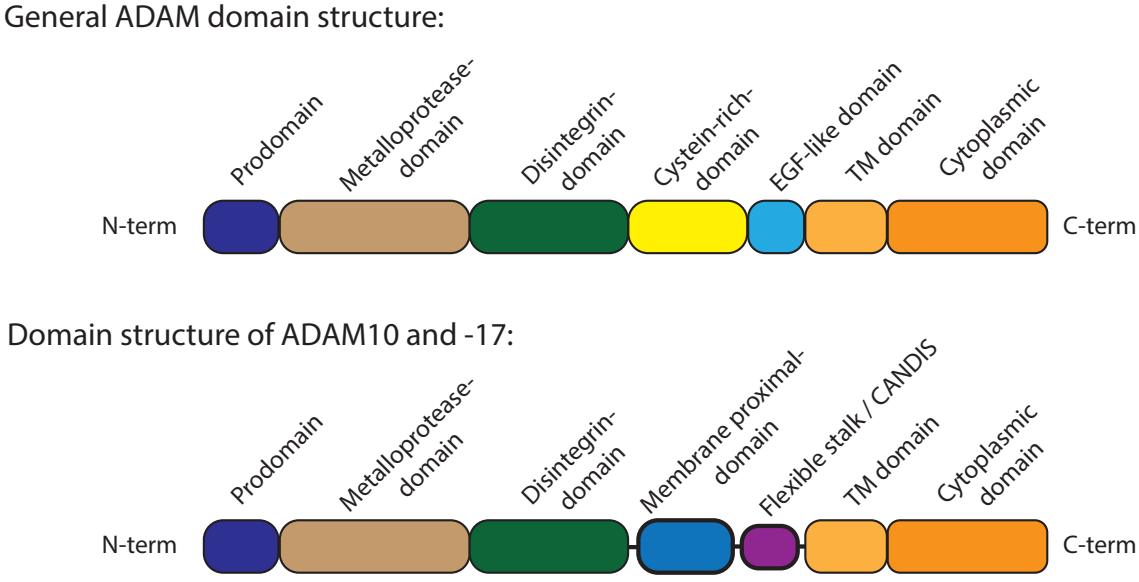

Figure 2: Schematic view of the domain structure of ADAMs in general and ADAM10 and -17. The catalytic active members of the ADAM family consist of a signal sequence (not shown), a prodomain, a metalloprotease-, a disintegrin-, a cysteine-rich-, a transmembrane- and a cytoplasmic domain. ADAM10 and -17 have instead of the cysteine-rich and EGF-like domain, a membrane proximal domain and a flexible stalk. The flexible stalk of ADAM17 have been named "conserved ADAM seventeen dynamic interaction sequence" (CANDIS) (Düsterhöft et al., 2014).

A disintegrin domain follows the metalloprotease domain. The disintegrin domain of ADAM17 promotes cell-cell contacts and adhesion through binding to $\alpha_5\beta_1$-integrins (White, 2003). Integrins are transmembrane receptors linking the cytoskeleton to the extracellular matrix (ECM), thus providing cell adhesiveness. Several members of the ADAM family bind to integrins (Arribas et al., 2006). The binding of ADAM17 to integrins results in a steric inhibition (Trad et al., 2013). Although ADAM10 contains a disintegrin domain, it is unclear if ADAM10 binds to integrins.

The membrane proximal domain (MPD) and the stalk region of ADAM17 play important roles in multimerisation, substrate recognition and activity regulation (Lorenzen et al., 2012; 2011). Interestingly, the MPD and the stalk region bind only to the type I transmembrane proteins IL1RII and IL6R and not to the type II transmembrane proteins pro-TNF-α and TNFRII (Düsterhöft et al., 2013; Lorenzen et al., 2012). These first studies on the role of the MPD did not distinguish between the stalk region and the MPD. The recently defined MPD (amino acids 581-642) contains 10 cysteines with one thioredoxin motif ($C_{600}XXC_{603}$), which are targets for protein-disulfide isomerases (PDIs) (Düsterhöft et al., 2013). PDIs catalyze breaking and formation of disulfide-bonds between cysteines. Within the MPD, three cysteine-bridges can be reshuffled. This restructuring leads to a conformational change of the MPD from a flexible (active/open) form to an inflexible (inactive/closed) form (Düsterhöft et al., 2013). It was shown that extracellular PDIs have the potential to negatively regulate ADAM17 activity (Bennett et

al., 2000; Willems et al., 2010). The small stalk region of ADAM17 is named “conserved ADAM seventeen dynamic interaction sequence” (CANDIS, amino acids 643-671) and consists of highly conserved amino acids, which form a α-helical structure. This domain contributes to IL6R-, but not to TNF-α interaction (Düsterhöft et al., 2014).

The transmembrane region of ADAM17 is an α-helical structure and is also involved in the function. A GPI-anchored ADAM17 construct lacking the transmembrane domain (TMD) loses its ability to shed TGF-α, TNF-α and L-selectin (X. Li et al., 2007). In addition, replacement of the TM domain of ADAM17 with the transmembrane region of PDGFR (Platelet derived growth factor receptor), restored the ability to shed TNF-α and L-selectin but not TGF-α (X. Li et al., 2007). These findings indicate that the TM domain is involved in substrate recognition but the mechanism is still unclear.

The intracellular part of ADAM17, the cytotail, contains phosphorylation- and a SH3-binding sites, which might play a role in activity regulation, transport and localization (Schwarz et al., 2013b; P. Xu and Derynck, 2010). Interestingly, deletion mutants of the ADAM17 cytotail are still fully functional (Le Gall et al., 2010).

Less is known about the structure-function relationship of ADAM10. The structural organization is comparable to its close relative ADAM17. The cytoplasmic tail of ADAM10 is dispensable for stimulated shedding, but exhibits an inhibitory effect on constitutive shedding (Maretzky and Evers et al. manuscript in preparation). Furthermore, the cytoplasmic tail of ADAM10 may play a role in transport and localization, as it contains sorting signals and binding sites for interaction partners (Marcello et al., 2013; Wild-Bode et al., 2006).

Taken together, still many questions regarding to the structure-function relationship of ADAM10 and -17 remain unanswered. Nevertheless each domain of ADAM10 and -17 contributes to the protease function by either regulating the proteolytic activity directly, or by binding to substrates or integrins and probably also by regulating the proteases localization.

1.2. Physiological roles of ADAM10 and ADAM17

ADAM10 and -17 exert different physiological roles in health and disease and in embryonic development. They are expressed in all organs and cell types in different quantities and so are their substrates. The importance of ADAM10 and -17 in cell function and pathophysiology will be outlined in this chapter.

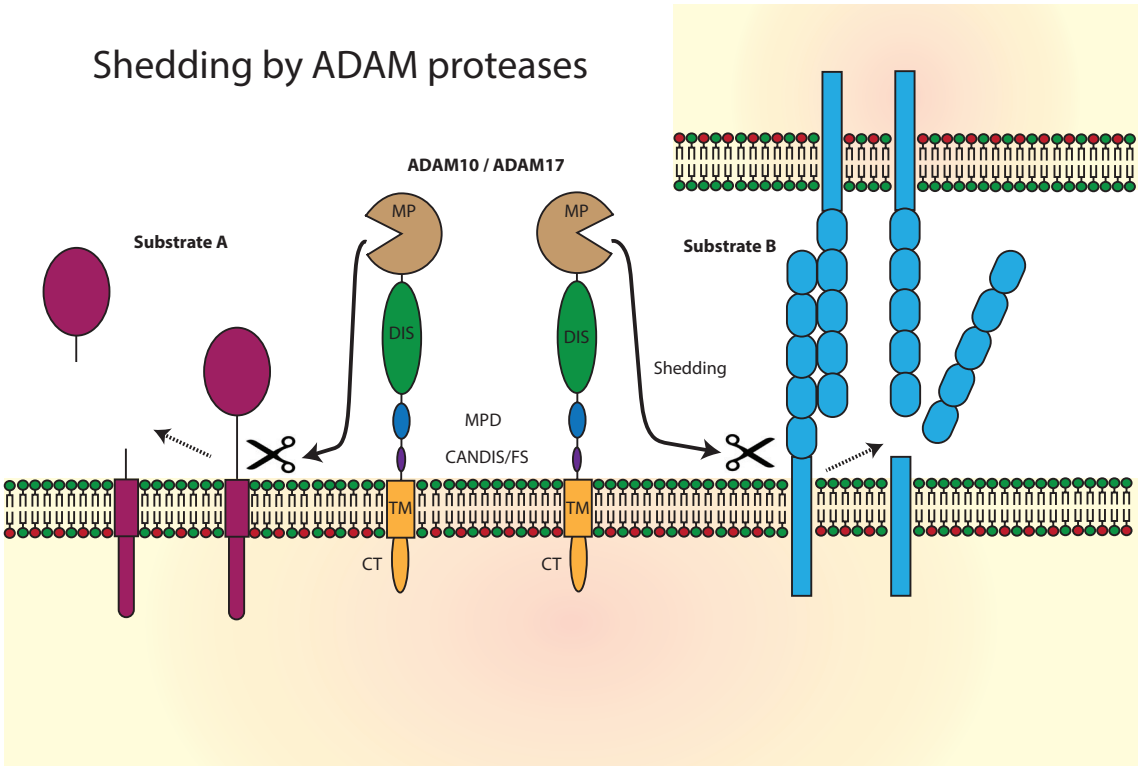

Figure 3: Schematic view of ADAM10 and ADAM17-mediated substrate shedding: Depicted are the generalized shedding events of substrate A (such as an EGFR-ligand) and substrate B (such as a cell-adhesion molecule) by ADAM10 or -17. Both proteases cleave their substrate in close proximity to the cell surface (MP: metalloprotease domain; Dis: disintegrin domain; MPD: membrane proximal domain; CANDIS: conserved ADAM17 dynamic interaction sequence; FS: flexible stalk; TM: transmembrane domain; CT: cytotail).

1.2.1. Substrate diversity

Several dozen substrates are identified for ADAM10 and -17 (Scheller et al., 2011). These substrates include e.g. cytokines, growth factors, receptors and cell adhesion molecules. ADAM17 was first described as "TNF-α converting enzyme" (TACE) due to its ability to shed pro-TNF-α and release this pro-inflammatory cytokine (Black et al., 1997; Moss et al., 1997). Some ADAM10 and -17 substrates, which are of special interest for this thesis, are listed in Table 1 and Table 2. Several substrates are exclusively cleaved by one of the two proteases, like TNF-α by ADAM17 and E-cadherin by ADAM10, others can be cleaved by both proteases, such as APP and CX3CL1 (fractalkine) (Buxbaum et al., 1998; Christian, 2012; Hundhausen et al., 2003; Lammich et al., 1999). ADAM10 or -17 substrates do not contain a specific consensus sequences in their cleavage site, but all substrates are shed close to the membrane. Nevertheless ADAM10 and -17 have preferences in their cleavage site specifity for some amino acids. While both cleave N-terminal of leucine, ADAM10 shows additional preferences towards aromatic amino acid, whereas ADAM17 prefers valine at the P1´ site (Tucher et al., 2014).

Table 1: Important ADAM10 substrates.

Substrate	Function	Reference
Notch	Development; tissue repair	(Pan and Rubin, 1997)
VE-cadherin	Cell-cell adhesion	(Schulz et al., 2008)
N-cadherin	Cell-cell adhesion	(Reiss et al., 2005)
CX3CL1	Immunity	(Hundhausen et al., 2003)
E-cadherin	Cell-cell adhesion	(Maretzky et al., 2005)
Betacellulin	EGFR-ligand, proliferation	(Sahin et al., 2004)
APP	Non amyloidogenic pathway	(Lammich et al., 1999)

Table 2: Important ADAM17 substrates.

Substrate	Function	Reference
TGF-α	EGFR-ligand, proliferation	(Sahin et al., 2004)
HB-EGF	EGFR-ligand, proliferation	(Sahin et al., 2004)
TNF-α	Pro-inflammatory cytokine	(Black et al., 1997), (Moss et al., 1997)
IL6-R	Immunity	(Garbers et al., 2011)
JAM-A	Cell-cell adhesion	(Koenen et al., 2009)
L-selectin	Cell-cell adhesion, immunity	(Hafezi-Moghadam et al., 2001)
TNFR1	Immunity	(D Alessio et al., 2012)
VEGFR	Vasculogenesis, angiogenesis	(Swendeman et al., 2008)

1.2.2. Cell adhesion and leukocyte transmigration

One important feature of ADAM10 and -17 function is the ability to shed cell adhesion molecules. Cell adhesion molecules (CAMs) are proteins connecting cells with the ECM and to other cells, maintaining organized structures of cells and tissues. CAMs include members of the Ig superfamily, cadherins, integrins and selectins. Several substrates of ADAM10 and -17 are classified to these groups, such as neuronal-, epithelial and vascular endothelial cadherins (N-, E-, and VE-cadherin), junctional adhesion molecule A (JAM-A) or leukocyte selectin (L-selectin). ADAM10-induced N- and E-cadherin cleavage results not only in dramatic changes in the adhesiveness of cells; it results also in a redistribution of β-catenin. This in turn results in β-catenin-induced gene expression (Maretzky et al., 2005; Reiss et al., 2005). Furthermore, VE-cadherin shedding increases the permeability of endothelial cell monolayers and T-cell transmigration (Schulz et al., 2008).

ADAM17 sheds the endothelial tight junction protein JAM-A after treatment with inflammatory cytokines (Koenen et al., 2009). The soluble JAM-A fragment blocks endothelial migration and transendothelial migration of neutrophils *in vitro* and decreases neutrophil infiltration in a murine air pouch model (Koenen et al., 2009). In this context of leukocyte transmigration, L-selectin is involved in the binding and rolling of leukocytes to the endothelial wall. This pro-

motes transendothelial migration of leukocytes to the site of inflammation. ADAM17-mediated shedding of L-selectin weakens the binding to endothelial cells and increases the velocity of rolling (Hafezi-Moghadam et al., 2001; Tang et al., 2011). In general, the shedding of adhesion molecules weakens not only cell adhesion and promotes leukocyte transmigrations, it also paves the way for cell migration and proliferation in development and tissue repair.

1.2.3. EGFR signaling in proliferation and migration

The tyrosine kinase epithelial growth factor receptor EGFR, also known as ERBB1, is one of the most versatile receptors. Several ligands for the EGFR are known (Table 3). All of them are expressed as membrane spanning proforms and are proteolytically released by ADAM10 or -17. This leads to autocrine and paracrine signaling (Blobel, 2005). EGFR signaling regulates many key processes in cell biology, such as proliferation, migration, survival and differentiation during development, tissue homeostasis, repair and tumorigenesis (Yarden and Sliwkowski, 2001). An overview about ADAM-mediated transactivation of the EGFR is depicted in Figure 4.

Table 3 EGFR Ligands: All EGFR-ligands are proteolytically released by either ADAM10 or ADAM17. These ligands activate then EGFR-dependent signaling cascades.

Substrate	Protease	Reference
Pro-EGF	ADAM10	(Cohen, 1965; Sahin et al., 2004)
Pro-TGF-α	ADAM17	(Derynck et al., 1984; Sahin et al., 2004)
Pro-AREG	ADAM17	(Sahin et al., 2004; Shoyab et al., 1989)
Pro-HB-EGF	ADAM17	(Higashiyama et al., 1991; Sahin et al., 2004)
Pro-BTC	ADAM10	(Sahin et al., 2004; Shing et al., 1993)
Pro-Epigen	ADAM17	(Sahin and Blobel, 2007; Strachan et al., 2001)
Pro-Epiregulin	ADAM17	(Sahin et al., 2004; Toyoda et al., 1995)

Upon binding of a ligand, two receptor molecules dimerize (Ferguson et al., 2003; Ogiso et al., 2002). Consequently, the cytoplasmic kinase domains are drawn near each other. As a result the cytoplasmic domains of each molecule are reciprocally phosphorylated (Xue and Lucocq, 1998). This enables binding of the adaptor protein Grb-2 via SH2-domains. Grb-2 recruits SOS (son of sevenless), which binds to Grb2 (growth factor receptor-bound protein 2) via two domains and activates Ras. Ras is a monomeric GTPase. The activated Ras induces a kinase cascade, which amplifies and spreads the signal. This signaling cascade induces the activation of ERK1/2 (extracellular-signal regulated kinase). ERK is a “mitogen activated protein” (MAP) kinase which phosphorylates several transcription factors and other effector proteins leading to proliferation, migration, survival and differentiation of the cell (Yarden and Sliwkowski, 2001).

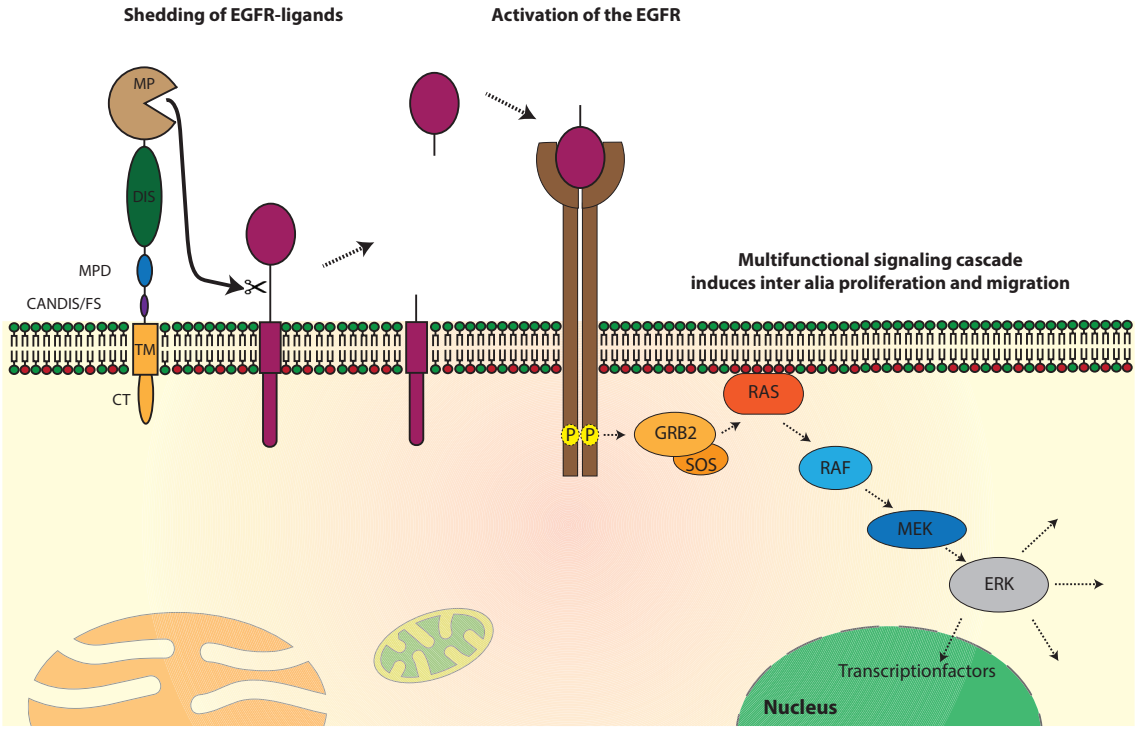

Figure 4: Transactivation of EGFR-signaling by ADAM-mediated growth factor shedding. Proteolytic release of EGFR-ligands by ADAM10 or -17 activates EGFR-signalling. A process referred to as transactivation. Upon binding of the ligand, the intracellular kinase domains of the homodimer phosphorylate each other and initiate a signaling cascade via GRB2, SOS, RAS, RAF, MEK and ERK1/2. Activated ERK1/2 phosphorylates several effector molecules including transcription factors. This induces for example proliferation and migration of the cells.

1.2.4. Pathophysiology & disease models

The importance of ADAM10 and -17 for (patho-) physiology and embryonic development becomes especially apparent with regard to mice models. Genetically modified mice and disease models provide a more holistic view in the function of these proteases. Mice which express an inactive variant of ADAM17 (*tace*$^{\Delta Zn/\Delta Zn}$) die between embryonic day 17.5 and birth (Peschon et al., 1998). T-cells derived from these mice fail to release TNF-α. Additionally, these mice phenotypically resemble TGF-α knockout mice, suggesting a crucial role of ADAM17 in EGFR signaling (Luetteke et al., 1993; Mann et al., 1993).

The functions of ADAM17 in adult mice were investigated by using conditional knockouts. Mice lacking active ADAM17 in myeloid cells are protected from LPS-induced endotoxin shock. This is due to lower TNF-α serum levels compared to wildtype mice (Horiuchi et al., 2007a). High serum levels of TNF-α are associated with rheumatoid arthritis, sepsis and other inflammatory pathologies (Zelová and Hošek, 2013). Mice expressing only ~5 % ADAM17 compared to wildtype, are viable but show a decreased fertility. These mice are more prone to

severe inflammation in a dextran sulfate sodium-induced colitis model. In that case the phenotype is caused by defective tissue repair as a consequence of impaired EGFR signaling (Chalaris et al., 2010).

Mice lacking ADAM10 die at embryonal day 9.5 and show severe malformations in the nervous and cardiovascular system (Hartmann et al., 2002). The phenotypes of these mice have striking similarities with those that carry a Notch receptor deletion (Krebs et al., 2000). Conditional ADAM10 knockout mice lacking ADAM10 in neural precursor cells die prenatally. They have disrupted cortex and a reduced ganglionic eminence, caused by defective neuronal differentiation (Jorissen et al., 2010). In vasculature, endothelial specific knockout of ADAM10 leads to increased branching and density of retinal vasculature which also recapitulates the phenotype observed in notch knockouts (Glomski et al., 2011).

Taken together, the dominant effects of ADAM10 or -17 knockouts *in vivo* are mostly due to defective TNF-α and EGFR signaling for ADAM17 and Notch signaling for ADAM10.

1.3. Regulation of ADAM10 and ADAM17 activity

Several different mechanisms regulate the activity of ADAM10 and -17. This includes the expression, maturation and transport and the rapid activation of the shedding events. These mechanisms are an important subject of research. The principles of ADAM10 and -17 activity regulations will be summarized in this chapter.

1.3.1. Regulation of ADAM10 and ADAM17 protein expression, maturation and transport

The regulation of transcriptional expression is poorly characterized despite the fact that ADAM10 and -17 expression is increased in several cancer types and associated with malignant cancer progression (Arribas et al., 2006; Borrell-Pagès et al., 2003; Ding et al., 2004; Gavert et al., 2005; Yoshimura et al., 2002). The expression of ADAM17 in endothelial cells can be upregulated by certain cytokines and growth factors (Bzowska et al., 2004). However, the mechanisms remain poorly understood. In contrast to the transcriptional control, post-translational regulation is described for most ADAMs. The first step is the removal of the inhibitory prodomain by furin convertases, which occurs during the transit through the Golgi (Lum et al., 1998; Roghani et al., 1999). Inhibition of furin results in less ADAM17 substrate shedding and consequently, overexpression of furin increases ADAM17 substrate shedding (Peiretti et al., 2003). Interestingly, Peiretti et al. also showed that pro-domain processing by furin is not a prerequisite

for ADAM17 surface expression. Nevertheless, prodomain processing is not a endogenously regulated step that controls the activity of ADAM17. More important than prodomain processing is the transport and localization of ADAM17. Recent findings revealed that iRhom1 and -2, inactive members of the rhomboid protease family are required for ADAM17 maturation. In mice, iRhom2 is necessary to promote trafficking of ADAM17 in immune cells (Adrain et al., 2012; Issuree et al., 2013; McIlwain et al., 2012). The other member of the murine iRhoms is iRhom1. It contributes to the maturation of ADAM17 in non-immune cells. A loss of either iRhom has a partially inhibitory effect, whereas double deficient cells have no ADAM17 activity (Christova et al., 2013). In iRhom2-deficient mouse embryonic fibroblast, stimulated shedding of some substrates, such as HB-EGF and Kit-Ligand-2 is impaired, but shedding of other substrates seems to be normal (Maretzky et al., 2013).

Protein binding partners are also known for ADAM10. Tetraspanins, a highly conserved transmembrane protein family, contribute to the maturation of ADAM10. It was shown that tetraspanin12 is able to regulate ADAM10-dependent amyloid precursor protein (APP) processing through enhanced maturation of ADAM10 (D. Xu et al., 2009). Additionally, tetraspanin15 regulates trafficking and activity of ADAM10 by promoting the endoplasmic reticulum (ER) exit and stabilizing mature ADAM10 at the cell surface in mammalian cell lines (Prox et al., 2012).

Immunofluorescence studies suggest that the majority of ADAM17 is localized in perinuclear compartments and mature ADAM17 was found at the cell surface (Schlöndorff et al., 2000). Additionally, ADAM17 is packaged into lipid rafts during the transport through the Golgi and this spatial distribution contributes to the proteolytic function (Tellier et al., 2006).

Taken together, protein-binding partners and lipid environments of ADAM10 and -17 are important for the maturation, transport and localization. Furthermore, these proteins and lipids may control the substrate selectivity and the proteolytic function of these proteases.

1.3.2. The rapid activation of ADAM10- and -17-dependent shedding

ADAM10 and -17 are constitutively active, but the shedding can rapidly be enhanced by several stimuli. These stimuli include some cytokines, G-protein coupled receptors (GPCR) -ligands, growth factors and unphysiological stimuli like phorbol esters, such as Phorbol-12-Myristat-13-Acetat (PMA) and ionophores like ionomycin. These multifaceted activators of ADAM-mediated shedding imply different signaling cascades, all leading to the rapid activation of ADAM17 and/or ADAM10 shedding, but the general underlying mechanism remains poorly characterized. Some important principles of these activating mechanisms will be outlined in this chapter. In general, three receptor classes transmit signals from the outside that can induce rapid

activation of ADAM10 and/or -17. These receptor classes are ligand-gated ion channels, g-protein coupled receptors (GPCRs) and receptors with own or associated kinase activity.

1.3.2.1 Ligand-gated ion channels

Ligand-gated ion channels are membrane-spanning channels allowing ions like Na^+, K^+, Cl^-, or Ca^{2+} to pass the membrane upon binding of a ligand. This receptor class consists of three superfamilies, the cys-loop superfamily (nicotinic receptors, $GABA_A$ and $GABA_C$ receptors, glycine receptors, and some glutamate, histamine and serotonin activated anionic channels), the ATP-gated ion channels (P2X1-P2X7) and the glutamate activated cationic ion channels (NMDA receptors, AMPA receptors, kainate receptors etc.).

One example for ADAM activation through ligand-gated ion channels is the NMDA receptor. The N-methyl-D-aspartate (NMDA) receptor is a non-selective cation channel involved in synaptic plasticity (Traynelis et al., 2010). Stimulation of this receptor, for example with glutamate, leads to an influx of Na^+ and Ca^{2+} and an efflux of K^+ and results in increased ADAM10-dependent N-cadherin cleavage in neuronal cells (Reiss et al., 2005; Uemura et al., 2006). ADAM-mediated shedding can also be induced by another cation channel, the P2X7. The P2X7 is a trimeric ATP-gated cation channel, which plays important roles in health and disease (Bartlett et al., 2014). Activation of this channel allows Na^+, Ca^{2+} and K^+ to pass the plasma membrane leading to an increase in cytosolic calcium levels. This is followed by enhanced ADAM-mediated shedding of CD23 and L-selectin in B- cells (Gu et al., 1998), of IL6-receptor in T-cells (Garbers et al., 2011) and CXCL16 in peripheral B-lymphocytes (Pupovac et al., 2013) .

1.3.2.2 G-protein coupled receptors

G-protein coupled receptors are a large group of seven-transmembrane domain receptors with nearly 800 predicted human genes. They are involved in many physiological and pathophysiological processes, such as homeostasis, inflammation, sensory perception and neuronal signal transmission and many more (Heng et al., 2013). GPCRs transduce extracellular signals to coupled intracellular heterotrimeric G-proteins. Upon binding of the ligand and activation of the G-protein the α-subunit dissociates from the β/γ subunits and each amplifies a second messenger response by activating or inhibiting various effector molecules. Four main classes of α-subunits are described ($G\alpha_s$, $G\alpha_{i/0}$, $G\alpha_{q/11}$ and $G\alpha_{12/13}$ (Gilman, 1987)), which activate distinct signaling events (reviewed in (Marinissen and Gutkind, 2001; Neves et al., 2002; Perez and Karnik, 2005). ADAM-mediated shedding can be activated by several GPCR ligands. These ligands include *inter alia* lysophosphatidic acid (LPA), angiotensin II, thrombin, bradykinin, carbachol and acetylcholine. Stimulation of epithelial cells with these agents leads to a rapid activation of

ADAM-mediated shedding and transactivation of EGFR signaling by releasing EGFR ligands like HB-EGF and TGF-α (Prenzel et al., 1999; Schäfer et al., 2004).

1.3.2.3 Receptors with own or associated kinase activity

Receptors with their own kinase activity include the receptor tyrosine kinases (RTKs) like the EGFR, the vascular endothelial growth factor receptor 2 (VEGFR2) and the fibroblast growth factor receptor 2b (FGFR2b). RTKs promote migration and proliferation of cells (Iwashita and Kobayashi, 1992). The EGFR signaling and their consequences are depicted in chapter 1.2.3.

One example for RTK-induced ADAM-mediated shedding is the VEGFR2. The VEGFR2 promotes proliferation of endothelial cells by transactivating EGFR and ERK1/2 signaling via ADAM17-dependent release of EGFR-ligands (Maretzky et al., 2011a). Another example is the keratinocyte specific FGFR2b, which promotes ADAM17-dependent EGFR activation in epithelial cells (Maretzky et al., 2011a).

Furthermore, Toll-like receptors (TLRs) are also involved in ADAM activation. They belong to the pattern recognition receptors, responsible for recognizing pathogenic molecules like lipopolysaccharides (LPS). Stimulation of TLRs triggers the innate immunity by activating NFκB and other effector molecules (reviewed in (Akira and K. Takeda, 2004)). Additionally, activation of TLRs through LPS increases ADAM10 and -17-mediated "T cell immunoglobulin and mucin domain 3" (TIM-3) shedding in monocytes (Möller-Hackbarth et al., 2013). In LPS-induced acute pulmonary inflammation alveolar recruitment of neutrophil and monocyte is reduced in mice lacking ADAM10 in hematopoietic cells (Pruessmeyer et al., 2014). These findings indicate important roles for ADAM10 and -17 in TLR-induced innate immunity response, but the mechanisms involved remain unexplored.

1.3.2.4 Intracellular signaling involved in ADAM regulation

Various receptor ligands induce rapid activation of ADAM10 and -17 shedding by multifaceted intracellular signaling. No distinct signaling pathway is known that is responsible for the activation of ADAM10 or -17. Nevertheless, some general mechanisms are often associated with increased ADAM10 and -17 proteolytic activity. This includes kinase activation and elevation of intracellular Ca^{2+} levels.

Several kinases take part in the regulation of ADAM17 activity. Most of them are able to phosphorylate ADAM17 at threonine 735 (T735). These kinases are protein kinase C (PKC) (Killock and Ivetić, 2010), protein kinase G (Chanthaphavong et al., 2012), src kinase (Maretzky et al., 2011b), phosphoinositide-dependent kinase 1 (PDK1) (Zhang et al., 2006), p38-mitogen-activated protein kinase (p38-MAPK) (P. Xu and Derynck, 2010) and ERK (Rousseau et al.,

2008). The phosphorylation of T735 increases the transport of ADAM17 to the surface (Soond et al., 2005) and prevents dimerization of ADAM17, which is a prerequisite for TIMP3 binding (P. Xu et al., 2012). TIMP3 is a physiological inhibitor of several metalloproteases including ADAM17 (Amour et al., 1998). Nevertheless, ADAM17 phosphorylation seems not to be the final activation step because rapid activation does not depend on TIMP3 removal and ADAM17 lacking the cytotail can still be activated (Le Gall et al., 2010; Reddy et al., 2000).

Another mechanism often associated with the rapid activation of ADAM-mediated shedding is elevation of intracellular Ca^{2+} (Horiuchi et al., 2007b; Le Gall et al., 2009). Cytosolic calcium increase can occur either by extracellular Ca^{2+} influx, or by depletion of intracellular stores. The first is mediated by ion channels, like the ATP-gated channel P2X7 (Bartlett et al., 2014; Pupovac et al., 2013). The latter is often caused by $G_{q/11}$-coupled GPCR signaling, such as through thrombin activated PAR-1 (Hirano and Kanaide, 2003; Schulz et al., 2008).

Phorbol esters and ionophores are the most used unphysiological stimuli of ADAM-mediated shedding. Whereas phorbol esters like PMA induce ADAM17 substrate shedding through PKC activation, ionophores like ionomycin activate ADAM10 and -17 substrates shedding via Ca^{2+} influx (Horiuchi et al., 2007b; Le Gall et al., 2009; Sahin et al., 2004).

Taken together, the underlying mechanisms how kinases and/or Ca^{2+}-levels contribute to the final activation of ADAM-mediated shedding remain unclear.

1.3.3. Membrane dynamics as a regulatory mechanism for ADAM10 and -17 function

All cells are surrounded by membranes, which define the border between intracellular and extracellular space. These membranes are composed of a lipid bilayer containing proteins that span the bilayer and/or interact with the lipids (Meer et al., 2008). Since ADAMs and their substrates are transmembrane proteins embedded in this bilayer, it can be speculated that the lipid environment plays a role in the regulation of the shedding events. 5% of the eukaryotic genes encode for lipid synthases or lipid modifying proteins making up more than thousand different lipids (Sud et al., 2007). These vast numbers of lipids do not only contribute to barrier properties of membranes, they are also involved in energy storage, signaling events and interaction with proteins (Capelluto, 2013; Meer et al., 2008). The potential role of cell membranes, their lipid composition and their biophysical properties on ADAM-mediated shedding will be summarized in this chapter.

1.3.3.1 Membrane lipids: distribution and biophysical properties

The major structural lipids in eukaryotic membranes are the amphiphilic glycerophospholipids phosphatidylcholine (PtdCho), phosphatidylethanolamine (PtdEtn), phosphatidylserine (PtdSer), phosphatidylinositol (PtdIns) and phosphatidic acid (PA) (Figure 5).

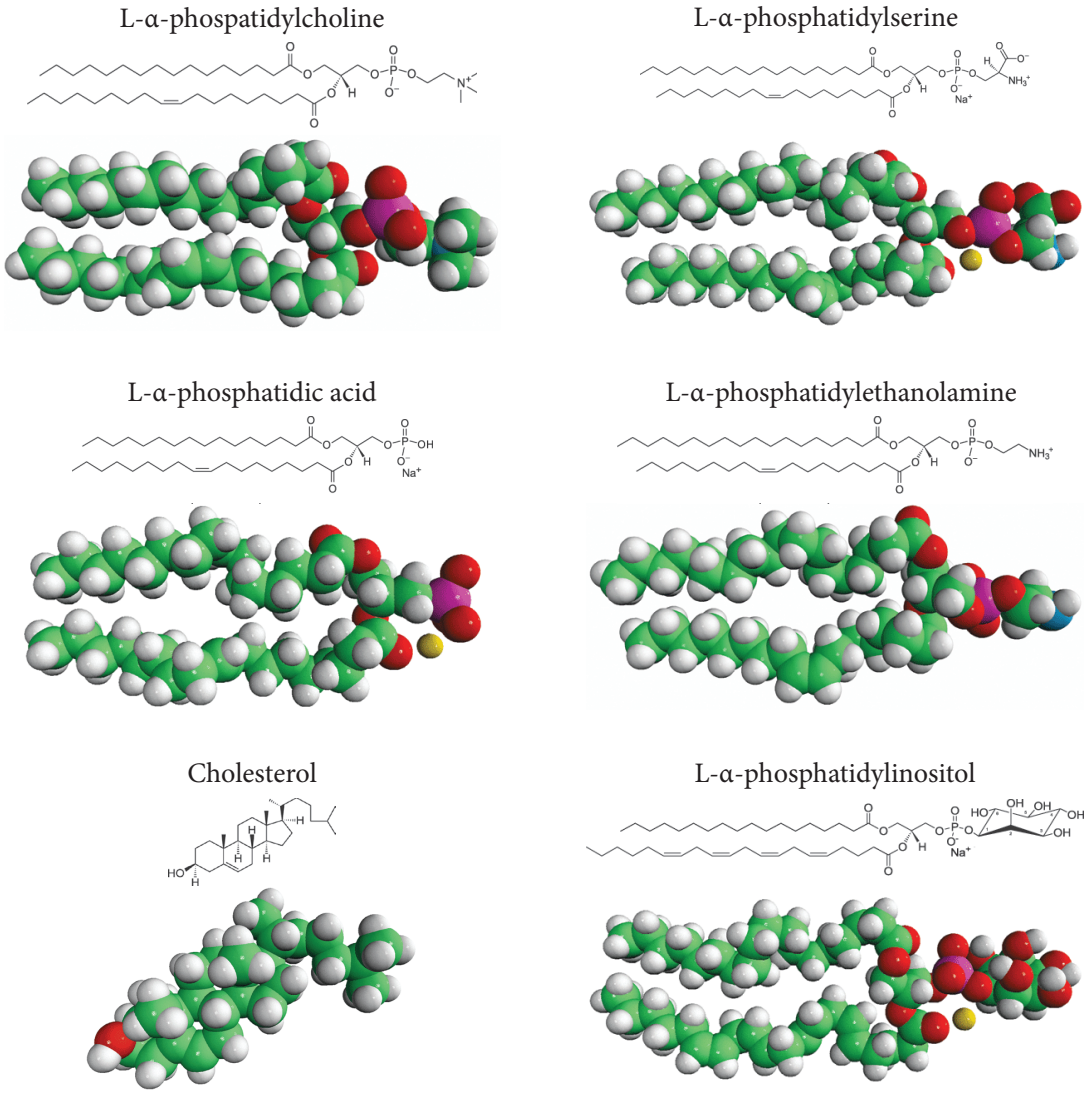

Figure 5: Structures of the major lipids in eukaryotic membranes. Depicted are the structural formulas and the 3-D structures of the most abundant naturally occurring lipids L-α-phosphatidylcholine, L-α-phosphatidylserine, L-α-phosphatidic acid, L-α-phosphatidylethanolamine, cholesterol and L-α-phosphatidylinositol. (Pictures are taken from Avanti® Polar Lipids, Inc.).

Their hydrophobic part consists of a diacylglycerol (DAG) and saturated or cis-unsaturated fatty acid chains of variable length. The hydrophilic part bears the characteristic head group. Together, these parts of the lipid determine the molecular shape and the biophysical properties. The most abundant lipid is PtdCho (J. E. Vance and D. E. Vance, 2008). Most of them have one cis-unsaturated fatty acyl chain and a nearly cylindrical structure. These properties makes PtdCho

spontaneously build planar bilayers (J. E. Vance and D. E. Vance, 2008). Among the phospholipids, several carry a negatively charged head group. These include the monoacidic phospholipids like PtdSer and phosphadidylglycerol (PG) and the diacidic PA. Another, the PtdIns contains one negative charge, but can be conjugated with additional phosphate groups. These acidic phospholipids are often involved in ionic binding of proteins and will be discussed in more detail in 1.3.3.3.

Another class of structural lipids are sphingolipids. Their hydrophobic backbone consists of ceramide. The most abundant sphingolipids are sphingomyelin (SM) and glycosphingolipids (GSL). Most sphingolipids have saturated or trans-unsaturated fatty acyl chains, which provides them with the ability to aggregate more closely to each other in the membrane than phospholipids. Another class of important structural lipids are sterols. In mammalian cells cholesterol is the predominant form. It contributes to the rigidity of membranes by modulating membrane fluidity.

The different lipids and membrane proteins are not evenly distributed in a leaflet of the bilayer. Several findings suggest the participation of membrane proteins in organizing large functional complexes (Simons and Ikonen, 1997). Similar to proteins, lipids also tend to group together mediating lipid-lipid and lipid-protein interactions (J. E. Vance and D. E. Vance, 2008). Together, this leads to a 2-dimensional patchiness of the cell membrane. Additionally, lipids of the plasma membrane display an asymmetric distribution between the two leaflets, with PtdSer and PtdEtn enriched in the cytosolic leaflet and SM and GSL in the non-cytosolic leaflet (Meer et al., 2008). This asymmetric distribution is accomplished either by insertion of the lipid in one leaflet and continual retention of the lipid in the leaflet, or by ATP-dependent flippases (P-type ATPases and ABC transporters) (Pomorski and Menon, 2006). The asymmetric distribution of lipids has important functional consequences. On the one hand, it allows proteins to interact with a lipid specifically at one site, on the other hand, the imbalance can contribute to membrane bending, allowing vesicle budding (Pomorski and Menon, 2006). The distribution of lipids is highly regulated and changes can cause multiple effects. In apoptosis PtdSer translocates to the outer leaflet and serves as a signal for phagocytosis and propagates the blood coagulation (Devitt and Marshall, 2011; Lentz, 2003). The loss of lipid asymmetry could be caused by the action of lipid scramblases, which function in an ATP-independent manner to randomize lipids between the leaflets (Pomorski and Menon, 2006). Lipid scramblases are typically activated by intracellular Ca^{2+} elevation (Bucki et al., 2001).

1.3.3.2 The role of lipid rafts and membrane fluidity in ADAM regulation

Certain lipids and proteins have the tendency to build lipid-lipid, lipid-protein and/or protein-protein interactions in the membrane. This leads to compartmentalization and specialized membrane areas which are involved in endocytosis, signaling and many other functions (Simons and Ikonen, 1997). These membrane areas have distinct lipid and protein composition due to phase separation of different lipids. One kind of specialized membrane areas are lipid rafts. Lipid rafts are defined as sphingolipid- and cholesterol-enriched ordered patches of specific proteins. Most of the lipids in rafts are thought to be enriched in saturated and longer fatty acids, what makes the rafts high ordered and less fluid (Simons and Sampaio, 2011).

ADAM17 is incorporated in lipid rafts during the transport through the Golgi (Moreno-Càceres et al., 2014; Tellier et al., 2006). Consequently it was shown that disruption of lipid rafts through cholesterol depletion increases the ADAM-mediated shedding of several substrates. These substrates include among others CD30 (Tresckow et al., 2004), IL6R (Matthews et al., 2003), TNF-α, TNFR1 and TNFR2 (Tellier et al., 2006). Although ADAM10 is not sequestered in lipid rafts, ADAM10-mediated substrate processing can also be rapidly activated by cholesterol depletion (Kojro et al., 2001). That is shown *inter alia* for the ADAM10 substrates CD44 (Murai et al., 2011), N-cadherin (Reiss et al., 2005), L1-CAM (Mechtersheimer et al., 2001) and APP (Kojro et al., 2001). ADAM-mediated shedding is also driven by membrane fluidity. Unsaturated free fatty acids increase shedding of VE-cadherin and L-selectin of endothelial cells and leukocytes. This effect could be ascribed to increased fluidity of the plasma membrane and not to changes in ADAM enzymatic activity (Reiss et al., 2011).

Taken together, the membrane environment and its biophysical properties play an important role in regulating ADAM function by localizing the proteases and their substrates in specific regions and by mobilizing or immobilizing ADAM10 and -17 in the membrane.

1.3.3.3 Protein-Lipid Interactions

The most apparent protein-lipid interaction is that of transmembrane proteins, which span the lipid bilayer (Contreras et al., 2011) The kind of interaction of a lipid with a transmembrane protein is defined by the relative residence time of a particular lipid at the protein-lipid interface (A. G. Lee, 2003). When a lipid shows a low affinity to a transmembrane domain (TMD), it is considered as a bulk lipid and shows a fast exchange rate with other lipids. Lipids that show a specific interaction with the transmembrane domain due to hydrophobic matching to the protein or by specific interactions with the polar head group are appointed as annular lipids. These annular lipids surround the protein and build a shell (annulus) (Anderson and K. Jacobson, 2002). Lipids that are highly specific bound or integrated in transmembrane protein complexes are

considered as non-annular lipids. Although the TMD and the lipid environment seems to play a role for ADAM17-mediated shedding, no specific interactions with lipids are proven up to now (Le Gall et al., 2010; X. Li et al., 2007; Tellier et al., 2006).

Another type of protein-lipid interactions are ionic interactions at the inner and outer layer of the membrane. Certain phospholipids are negatively charged (see 1.3.3.1) and can interact with proteins via polybasic residues (L. Li et al., 2014). These proteins include membrane proteins, soluble proteins and viral proteins. Some of these proteins have specific binding pockets like the pleckstrin homology (PH) domain from phospholipase C β1, which binds PtdIns(4,5)P2 (Razzini et al., 2000) or the C2 domain from Synaptotagmin-1, which binds PtdSer (Honigmann et al., 2013). Synaptotagmin-1 is the main calcium sensor for neuronal exocytosis. It contains two Ca^{2+}-binding domains (C2A and C2B). In that case Ca^{2+} acts as bridge for the binding of the negatively charged PtdSer to the binding pocket of synaptotagmin-1 and enables exocytosis (Honigmann et al., 2013). Proteins without specific binding pocket can ionically bind to phospholipids through less structured polybasic sequences. Examples for these ionic protein-lipid binding are the src kinase (Buser et al., 1994; Sigal et al., 1994) and HIV-1 Nef (Gerlach et al., 2009). The NH2-terminus of the src kinase contains a myristoylated glycin that can integrate into the plasma membrane and a polybasic motif in close proximity that binds to PtdSer (Buser et al., 1994; Murray et al., 1997; Sigal et al., 1994). The HIV-1 Nef has three membrane binding moieties which enable Nef to bind to the plasma membrane. Nef contains an N-terminal myroistoyl-modification, followed by a polybasic amino acid cluster and some aromatic residues. The membrane binding of Nef occurs in two steps: first by fast ionic protein-lipid interaction and insertion of the myroistoyl group, followed by slow insertion of the aromatic residues in the membrane (Gerlach et al., 2009). These protein-lipid interactions are often crucial for the proper functions of the proteins and determine the activity state of these proteins. One example is the T-cell receptor: binding of the ITAM region to the membrane and insertion of tyrosine side chains into the membrane prevents the spontaneous phosphorylation of the tyrosines. Upon activation an increase in local Ca^{2+} concentration and a decrease in local PtdSer disrupts this binding allowing tyrosine phosphorylation (Gagnon et al., 2012; Shi et al., 2013).

1.3.3.4 Membrane disturbing peptides

Bacterial pore forming toxins (PFTs) and antimicrobial peptides (AMPs) have the ability to perturb the plasma membrane by insertion. Whereas PFTs are secreted by bacteria and serve as virulence factors, antimicrobial peptides are part of the innate immune system and are released after TLRs and NLRs (Nod like receptors) activation.

The first hint that membrane-disturbing peptides can modulate ADAM function was published in 1996. Cells exposed to *streptococcus pyogenes* streptolysin-O (SLO) or to *E. coli* HlyA showed increased shedding of the ADAM substrates CD14 and IL-6R (Walev et al., 1996). This response is probably linked to P2X receptor activation because Skals et al. could show that the hemolysis properties of HlyA are accelerated by P2X channel opening in response to initial ATP release through the HlyA pore (Skals et al., 2009).

Another example is the human antimicrobial peptide LL-37. It is stored in specific granula in immune and epithelial cells and is released in pathogenic infections. It permeates microbial membranes by building transmembrane pores (C.-C. Lee et al., 2011). Beside this primary target, LL-37 can act on eukaryotic cells. It induces fibroblast growth in a P2X7 dependent manner and activates the innate immune response at the airway epithelial surface by transactivating the EGFR (Tjabringa et al., 2003; Tomasinsig et al., 2008). In keratinocytes LL-37 contributes to wound healing by provoking migration of the cells via transactivation of the EGFR receptor (Tokumaru et al., 2005). These findings indicate the involvement of ADAM-mediated shedding in the LL-37 provoked physiological effects. Although not proven, a possible mechanism is that LL-37 activates P2X receptors direct or indirect, which in turn activates ADAM-mediated shedding and transactivation of the EGFR.

The serine protease inhibitor kazal type 9 (SPINK9) has structural similarities to AMPs. Recently Sperrhacke et al. could show that SPINK9 operates in a comparable way as LL-37. In keratinocytes it promotes wound healing by transactivation of the EGFR in a P2-receptor- and ADAM-dependent manner (Sperrhacke et al., 2014).

Another AMP-related peptide is the bee venom component melittin (Lavialle et al., 1980). Bee venom consists of several bioactive peptides including apamin, adolapin, mast cell-degranulating peptide and melittin. In this complex venom, melittin is the greates part, constituting 50% of the whole venom (Raghuraman and Chattopadhyay, 2007). Melittin is a amphipathic peptide of 26 residues and contains a hydrophobic stretch of 19 amino acids followed by a cluster of four positively charged residues at the C-terminus (RSCB protein databank number 2MLT). Melittin has several bioactive functions. For example, it is able to integrate into cell membranes causing membrane perturbations (Dawson et al., 1978; Lavialle et al., 1980; Schoch and Sargent, 1980; Sessa et al., 1969). Melittin is also been discussed as anti-cancer drug and substitute for conventional antibiotics (Duclohier, 2010; Oršolić, 2012). Several cancer cells can be selectively destroyed by melittin *in vitro* (Son et al., 2007). Additionally, its potential as an anti-cancer drug has been tested in animal models for hepatocellular carcinoma, breast cancer and prostate cancer, with positive outcome (Liu et al., 2008; Russell et al., 2004; Soman et al., 2009). Furthermore melittin is ascribed as anti-inflammatory, anti-arthritic and pain-killing substance (Son et al., 2007). The underlying mode of action of melittin remains largely unknown.

Beside the membrane interaction melittin is able to activate phospholipase A2 (PLA_2) and it promotes arachidonic acid synthesis (Vernon and Bell, 1992). The activation of PLA_2 and activation of caspase-3 are reported to contribute to the anti-cancer effects of melittin (D.-O. Moon et al., 2006). If melittin influences ADAM-mediated shedding is unknown. One part of this thesis deals with investigations if and when how melittin affects ADAM-mediated functions.

2. Aim of this thesis

The diverse and crucial effects of ADAM-mediated shedding in many physiological and pathophysiological situations are subjects of intense research. ADAM proteases participate e.g. in cancer progression, inflammation and tissue homeostasis. A better understanding of the regulating mechanisms, which control ADAM functions would expand the knowledge about pathophysiological conditions and may lead to new pharmacological targets. Many signaling events can drive ADAM activation. These include kinase activation and calcium elevation. The resulting cleavage of the ADAM substrates occurs outside of the cells in short proximity to the cell membrane. ADAM10 and ADAM17 lacking their cytotail can still be activated. This leads to the conclusion that the final signaling step, which transforms the signal from the inside to the outside, is independent of the intracellular part of the ADAMs. Since membrane composition and membrane dynamics affect ADAM activity and function, the hypothesis arises that the membrane plays a role as ultimate trigger for shedding and may also be involved in the transformation of the activation signal from the inside to the outside of the cells. The aim of this thesis consists of two parts. The first part deals with the effect of the bee venom component melittin on ADAM function. Melittin is a membrane disturbing peptide with anti-microbial, anti-inflammatory and anti-cancer properties. In this context ADAMs release pro-inflammatory cytokines as well as EGFR ligands and may promote inflammation and cancer progression. How melittin affects ADAM-mediated shedding is unknown and this question is investigated in the first section of this thesis.

In the second part, the role and function of membrane lipids, in particular phosphatidylserine, in determining ADAM activity is analyzed. The dynamic distribution of membrane lipids, as well as their properties to interact with and regulate proteins became more and more apparent in recent years. A prime candidate for inside-out signaling is PtdSer. PtdSer, normally localized in the inner leaflet of the cell membrane, can rapidly be exposed to the outside. A process originally described for apoptosis, in which the permanent exposition affects the whole membrane. Recent reports link the PtdSer exposure also to other cell functions and highlight that this exposure can be transient. The potential role of the membrane dynamic and PtdSer exposure on ADAM activity is investigated in the second section of this thesis.

3. Material and Methods

3.1. Equipment and consumables

Table 4: Consumables

Consumable	Provider
96-well plates, flat bottom	Sarstedt AG & Co, GER
Cell culture dishes, 10 cm	Sarstedt AG & Co., GER
Cell culture flask, 75 cm^2	Sarstedt AG & Co., GER
Cell culture plates, 12-, 24-, 96-well	Sarstedt AG & Co., GER
Cell scraper, 16 cm, 25 cm	Sarstedt AG & Co., GER
Cover slips	Menzel-Gläser GmbH, GER
Falcon centrifuge tubes	Sarstedt AG & Co., GER
Glass flasks, 1000 ml, 300 ml	Schott AG, GER
Imaging Dishes with glass bottom CG (175 µm), surface treated	PAA (GE Healthcare), USA
Microscope slides	Menzel-Gläser GmbH, GER
Microtubes with thread	Sarstedt AG & Co., GER
Neubauer chamber	Brand GmbH & Co. KG, GER
Nitrogen tank	AIR LIQUIDE Deutschland GmbH, GER
Parafilm	American National Can Company, USA
Pasteur pipettes	Carl Roth GmbH & Co. KG
Petri dishes	Sarstedt AG & Co., GER
Plastic box, airtight	EMSA GmbH, GER
PVDF membrane, 0.45 µm	Carl Roth GmbH & Co. KG
Serological pipettes, 5 ml, 10 ml, 25 ml	Sarstedt AG & Co., GER
Syringe filter, 0.45 µm pore size	Sarstedt AG & Co., GER
Whatman paper, 1.5 mm	Carl Roth GmbH & Co. KG

Table 5: Standard equipment

Equipment	Manufacturer
-80°C Freezer Forma 900 Series	Thermo Scientific, USA
Analytical balance	Kern & Sohn GmbH, GER
Analytical balance	Denver Instruments, USA
Biophotometer	Eppendorf, GER
Centrifuge 5417R, fixed angle rotor F45-30-11	Eppendorf, GER
Centrifuge 5424, fixed angle rotor FA45-24-11	Eppendorf, GER
Centrifuge 5804R fixed angle rotor F34-6-38	Eppendorf, GER
Centrifuge 5810R, swing-out rotor A-4-62	Eppendorf, GER
Centrifuge Heraeus Multifuge X3R, fixed angle rotor F14-6x250LE	Thermo Scientific, USA
Chemiluminescence detector Fusion FX7	Peqlab, GER
Digital camera EOS 1100D with microscope	Canon, JPN

adapter	
Exhaust pump, BVC professional	Vacuubrand, GER
Freezing container, Nalgene Mr. Frosty	Thermo Fisher Scientific Inc., USA
Heating block	Eppendorf, GER
Heating cabinet	Memmert, GER
Incubator Hera cell 150	Thermo Scientific, USA
Light microscope, invers	Hund, GER
Magnetic stirrer CB162	Stuart, USA
Microwve oven	Samsung, GER
NanoDrop 1000 spectrophotometer	Peqlab, GER
PH-meter pH211	HANNA Instruments GmbH, GER
Plate Reader EL800	Biotek Instruments GmbH, GER
Plate reader FLx800	Biotek Instruments GmbH, GER
Power Supply EV231	Peqlab, GER
Power Supply PAC300	Bio-Rad Laboratories, Inc., GER
Roller mixer, Stuart SRT6	Bibby Scientific Ltd., UK
Semi dry electroblotter, PerfectBlue	Peqlab, GER
Shaking incubator Minitron	Infors HT, GER
Single channel pipettes	Abimed GmbH, GER
Sonificator	Bandelin electronic GmbH, GER
Sterile work bench	Köttermann GmbH & Co. KG, GER
Tank electroblotter Web S	Peqlab, GER
Thermocycler peqSTAR 96 universal	Peqlab, GER
Tilting shaker Unitwist-RT	Uniequip, GER
Tube rotator MACSmix™	Miltenyi Biotech, GER
Vortexer Vortex Genie	IKA, GER
Water bath GFL1004	GFL, GER
Water purification system, TKA GenPure	TKA, GER

3.2. Chemicals

Table 6: Chemicals and provider

Chemical	**Provider**
1,10-Phenantrolin	Roth, GER
1,2-dioleoyl-*sn*-glycero-3-phospho-L-serine (PtdSer)	Avanti Polar Lipids, USA
1,2-dioleoyl-*sn*-glycero-3-phosphocholine (PtdCho)	Avanti Polar Lipids, USA
ADAM peptide substrate (soluble)	Enzo Life Sciences, USA
Adenosinetriphosphate (ATP)	Sigma, GER
Agar Agar	Roth, GER
Ammoniumperoxidisulfate (APS)	Roth, GER
Ampicillin	Roth, GER

AnnexinV-FITC	Sigma, GER
Apyrase from potato	Sigma, GER
Bapta-AM	Tocris Bioscience, UK
BCIP® /NBT, Sigma Fast™	Sigma, GER
Benzoylbenzoyl-ATP (bz-ATP)	Sigma, GER
Bovine serum albumin (BSA)	Sigma, GER
Bradford *Coomassie Plus*	Fermentas, USA
Calciumchloride ($CaCl_2$)	Roth, GER
Cetuximab C225	Merck, GER
Collagen from rat tail	Roche, GER
Di-sodiumphosphate (NH_2POH_4)	Roth, GER
DIDS (4,4'-Diisothiocyanatostilbene-2,2'-disulfonic acid disodium salt)	Invitrogen, USA
Dimethylsulfoxid (DMSO)	Roth, GER
Dulbecco´s Modified Eagle Medium (DMEM), High Glucose (4.5 g/l)	GE Healthcare, USA
ECL Advanced	GE Healthcare, USA
Epithelial growth factor (EGF), recombinant human	Immunotools, GER
Ethanol 96 % (EtOH)	Roth, GER
Ethanolamine	Sigma, GER
Ethylene glycol tetraacetic acid (EGTA)	Roth, GER
Ethylenediaminetetraacetic acid (EDTA)	Roth, GER
Evans blue	Tocris Bioscience, UK
Fetal calf serum (FCS)	GE Healthcare
Fibroblast growth factor 7 (FGF7), recombinant human	Immunotools, GER
GI254023X (GI)	GlaxoSmithKline, UK
Glucose	Roth, GER
Glycerin	Roth, GER
Glycine	Roth, GER
Gö6976	Sigma, GER
GW280264X (GW)	GlaxoSmithKline, UK
Hexokinase from *saccharomyces cerevisiae*	Sigma, GER
Hydrochloric acid (HCl)	Roth, GER
Hydroxyurea	Sigma, GER
Ionomycin (IO)	Calbiochem, GER
Isopropanol	Roth, GER
L-α-phosphatidylcholine (PtdCho, Egg, Chicken)	Avanti Polar Lipids, USA
L-α-phosphatidylserine (PtdSer, Brain, Porcine)	Avanti Polar Lipids, USA
LSM 1077	
Magnesiumchloride ($MgCl_2$)	Merck, GER

Magnesiumsulfate ($MgSO_4$)	Merck, GER
Marimastat (MM)	Tocris Bioscience, UK
Melittin	Produced by J. Andrä (FZ Borstel)
Mercaptoethanol	Roth, GER
Methanol (MeOH)	Roth, GER
Milk powder	Roth, GER
MTT (3-(4,5-Dimethylthiazol-2-yl)-2,5-diphenyltetrazoliumbromide	Sigma, GER
O-phospho-l-serine (OPLS)	Sigma, GER
p-Nitrophenyl phosphate (pNPP) tablets	Sigma, GER
Penicillin/Streptomycin (100x)	GE Healthcare
Phorbol-12-myristat-13-acetat (PMA)	Sigma, GER
Phosphatase-inhibitor mix (PhosStop)	Roche, GER
Phosphocholin (PC)	Sigma, GER
Potassiumchloride (KCl)	Merck, GER
Potassiumdihydrogenphosphate (KH_2PO_4)	Roth, GER
PP2	Calbiochem GER
PP2	Calbiochem, GER
PPADS	Sigma, GER
Propidium iodide	Sigma, GER
Protease-inhibitor mix *Complete*	Roche, GER
Proteinmarker PageRuler™	Thermo Scientific, USA
pSIVA™-IANBD	Imgenex Corp., USA
Saccharose	Roth, GER
SITS (4-Acetamido-4'-isothiocyanato-2,2'-stilbenedisulfonic acid disodium salt hydrate)	Sigma, GER
Sodiumchloride (NaCl)	Roth, GER
Sodiumdodecylsulfate (SDS)	Roth, GER
Staurosporine from *streptomyces sp.*	Sigma, GER
Suramin	Sigma, GER
TAPI-0	Sigma, GER
Tetramethylethylendiamin (TEMED)	Roth, GER
Transfectionreagent *Turbofect*	Thermo Scientific, USA
Tris	Roth, GER
Triton X-100	Roth, GER
Trypsin-EDTA	GE Healthcare
Trypton/Pepton from casein	Roth, GER
Tween®20	Roth, GER
Yeast extract	Roth, GER

3.3. Kits & ELISAs

All Kits and enzyme linked immunosorbent assays (ELISAs) were performed according to manufacturer´s instructions.

Table 7: Commercial kits and enzyme linked immunosorbent assays.

Kit	Provider
CellTiter Glo© Luminescence Cell Viabilty Assay	Promega, USA
PureYield™ MidiPrep Kit	Promega, USA
PureYield™ Midiprep-Kit	Promega, USA
QuickChange® II Site-directed Mutagenesis	Stratagene, USA
sTNFR1/TNFRSF1A ELISA DuoSet (human)	R&D Systems, USA
TGF-α ELISA DuoSet (human)	R&D Systems, USA

3.4. Software

Table 8: Software used for this thesis

Software	Developer
Adobe CC 2014 (Photoshop, Illustrator, InDesign, AcrobatPro, Media Encoder)	Adobe Systems, USA
AxioVision	Zeiss, GER
Bio 1D	Vilber Lourmat, GER
Clone Manager 9	Scientific & Educational Software, USA
FluoView FV10-ASW 4	Olympus corporation, JPN
Fusion 15.17	Vilber Lourmat, GER
GraphPad Prism 5	GraphPad Software Inc., USA
ImageJ 1.47m	NIH, USA
Microsoft Office 2011	Microsoft Corp., USA
Papers 3	Mekentosj B.V., Netherlands
QuickChange® Primer Design (http://stratagene.com/qcprimerdesign)	Stratagene, USA
UCSF Chimera 1.1	University of California, USA

3.5. Stimulants and inhibitors

Table 9: Stimulants and inhibitors used for this thesis

Name	Utilization	Concentration*
Apyrase	ATPase	2 U/ml
Bapta-AM	Ca^{2+}-chelator (membrane permeable)	50 µM
bz-ATP	P2X7 agonist	300 µM
Cetuximab	EGFR-blocking antibody	10 µg/ml
DIDS	Inhibition of PtdSer exposure	100 µM

EGF	EGFR-ligand	4 nM
EGTA	Ca^{2+}-chelator (membrane impermeable)	3 mM
Evans blue	P2-receptor inhibitor	1 µM
FGF7 (fibroblast growth factor 7)	FGFR2b-ligand	20 ng/ml
GI254023X (GI)	Preferential ADAM10 inhibitor	3 µM
GW280264X (GW)	Preferential ADAM10 and -17 inhibitor	3 µM
Hexokinase	ATP-Hydrolase	2 U/ml
Hydroxyurea	Inhibition of proliferation	2 mM
Ionomycin (IO)	Ca^{2+}-ionophor	1 µM
Marimastat	General metalloprotease-inhibitor	10 µM
Melittin	Bee venom component	1 µM
OPLS	Competition for PtdSer binding	10 mM
PC	Control for OPLS	10 mM
PMA	PKC-activator	200 ng/ml
PP2	Src-kinase-inhibitor	10 µM
PPADS	P2(X)-receptor inhibitor	100 µM
SITS	Inhibition of PtdSer exposure	500 µM
Staurosporine	PKC-inhibitor	1 µM
Suramin	P2-receptor inhibitor	50 µM

*Unless indicated otherwise

3.6. Antibodies

Table 10: Primary antibodies

Antigen	Reactivity*	Provider	Species	Used dilution (WB)
E-cadherin	h	BD Bioscience	Mouse	1:2500
EGFR	h	Cell signaling	Rabbit	1:3000
ERK1/2	h	Cell signaling	Mouse	1:3000
GAPDH	h, m	Santa Cruz	Rabbit	1:500
N-cadherin	h, m	BD Bioscience	Mouse	1:2500
Phospho-EGFR	h	Cell signaling	Rabbit	1:3000
Phospho-ERK1/2	h	Cell signaling	Rabbit	1:3000
VE-cadherin	h	Santa Cruz	Mouse	1:1000

*Reactivity: h: human; m: mouse

Table 11: Secondary antibodies

Name	Coupling	Provider	Used dilution (WB)
Goat-α-mouse IgG	POD	Jackson ImmunoResearch	1:10000
Goat-α-rabbit IgG	POD	Jackson ImmunoResearch	1:10000

3.7. Plasmids

Table 12: Plasmids

Name	Vector	Provider
ADAM17-3X	pcDNA3.1 (Invitrogen)	Mutated ADAM17-WT
ADAM17-E/A	pcDNA3.1 (Invitrogen)	C. Blobel (HSS, New York)
ADAM17-WT	pcDNA3.1 (Invitrogen)	C. Blobel (HSS, New York)
P2X7	pcDNA3.1 (Invitrogen)	C. Blobel (HSS, New York)
TGFα-AP	pAPtag5 (GenHunter)	C. Blobel (HSS, New York)

3.8. General buffer recipes

Table 13: General buffer recipes.

6x SDS sample buffer	0.75 M Tris 12 % SDS 6.54 M Glycerin 6 mM EDTA 120 mM DTT 0.15 % Bromphenole blue pH 6.8
Alkaline phosphatase (AP) buffer	100 mM NaCl 100 mM Tris 20 mM $MgCl_2$ pH 9.5
Annexin binding buffer	10 mM HEPES 140 mM NaCl 2.5 mM $CaCl_2$ pH 7.4
Cell lysis buffer for AP-assays	1 mM EDTA 10 mM 1,10-Phenantrolin* 2,5 % (v/v) Triton-X-100 in H_2O
Cell lysis buffer for western blotting	5 mM Tris 1 mM EGTA 250 mM Saccharose 1 % (v/v) Triton-X-100 10 mM 1,10-Phenantrolin* 1 x *Complete* protease inhibitor mix (Roche)* 1 x *PhosStop* phosphatase inhibitor mix (Roche)*
Electrophoresis buffer	25.1 mM Tris 192 mM Glycin 0.1 % SDS pH 8.8
Erythrocyte lysis buffer	M $KHCO_3$

	0.15 M NH_4Cl 0.1 mM EDTA pH 7.5
PBS	137 mM NaCl 2.7 mM KCl 1.8 mM KH_2PO_4 10.1 mM Na_2HPO_4
Resolving gel buffer	1.5 M Tris 0.4 % SDS pH 8.8
Stacking gel buffer	0.5 M Tris 0.4 % SDS pH 6.8
Stripping buffer for PVDF membranes	62.5 mM Tris 20 % (w/v) SDS 0.7 % (v/v) 2-mercaptoethanol*
TBS	20 mM Tris 1.17 M NaCl 10 mM EDTA
TBST	20 mM Tris 1.17 M NaCl 10 mM EDTA 0.1% Tween-20
Transfer buffer for western blotting	192 mM Glycin 25 mM Tris 10 % MeOH pH 8.5

*Before use freshly added

3.9. Cell culture

3.9.1. Cell lines

Table 14: Cell types used

Cell line	Type	Growth Medium
ADAM10 and/or -17-deficient MEFs	Generated from knockout mice (Biochemistry Kiel)	DMEM + 10 % FCS + Pen/Strep*
CHO-K1	Chinese hamster ovary cells, epithelial like	Hams F12 + 10 % FCS + Pen/Strep*
Cos-7	SV40 transformed cell line from kidney of *cercopithecus aethiops*, fibroblast cells	DMEM + 10 % FCS + Pen/Strep*
Granulocytes	Primary human granulocytes (freshly prepared from blood)	RPMI
HaCaT	Human keratinocytes, immortalized	DMEM + 10 % FCS + Pen/Strep*
HEK293	Human embryonic kidney cells, epithelial	DMEM + 10 % FCS + Pen/Strep*
HUVEC	Primary human umbilical vein endothelial cells	EGM + Supplements** + Pen/Strep*
Monocytes	Primary human monocytes (freshly prepared from blood)	RPMI
Murine embryonic fibroblasts (MEF)	Immortalized Fibroblasts	DMEM + 10 % FCS + Pen/Strep*
PBMC	Primery peripheral blood mononuclear cells (freshly prepared from blood)	RPMI
PSA3	CHO-K1 cell line lacking functional PSS1	Hams F12 + 10 % FCS + Pen/Strep* + 10 µM ethanolamin

* Penicillin/Streptomycin: 100 U/ml

**Endothelial supplements: 2 % FCS; Endothelial cell growth mixture 0.4 %, EGF 0.1 ng/ml, FGF 1 ng/ml, heparin 90 µg/ml, hydrocortisone 1 µg/ml (all obtained from Promocell as mixture).

3.9.2. Cultivation of eukaryotic cell lines

All cells were cultured at 37° C at 5 % CO_2 in a humidified atmosphere. All media and buffers were stored at 4° C and preheated to 37° C before use.

The adhesion cells were grown in T75 cell culture flasks until they reached a confluency of 80 - 90 %. At this stadium they were either passaged for further propagation or seeded in cell culture plates for experiments. For passaging and seeding, the cells were once washed with PBS

and afterwards for round about 5 min incubated with trypsin-EDTA until they detach. To stop the proteolytic activity of trypsin, serum-containing medium was added (5 ml). Subsequently the cells were split in a 1:3 ratio into new flasks or seeded in the appropriate density in 6-, 12-, 24-, or 96-well plates. If needed the cells were counted before seeding to adjust the appropriate density (see 3.9.6).

The used suspension cells were all primary human blood cells, which were fresh prepared for each experiment and not cultivated for longer periods.

3.9.3. Preparation of blood cells

Blood samples from healthy donors were immediately mixed with heparin to a final concentration of 1 U/ml to prevent blood clotting. To prepare granulocytes and monocytes, whole blood samples were diluted with sterile PBS in a 1:2 ratio. 25 ml of this mixture were overlaid on 12.5 ml LSM 1077 in 50 ml falcon tubes. The tubes were transferred to a centrifuge and a density gradient was established by centrifuging for 30 min at 300 xg (RT, without break). In this gradient the cells separate on the basis of their weight and size and different fractions can be seen by eye (Figure 6). The red pellet contains erythrocytes and granulocytes. Upon this, a layer with LSM and granulocytes and a small band with PBMCs follow. This PBMC layer contains monocytes and lymphocytes. On top of the tube is a layer of cell free plasma.

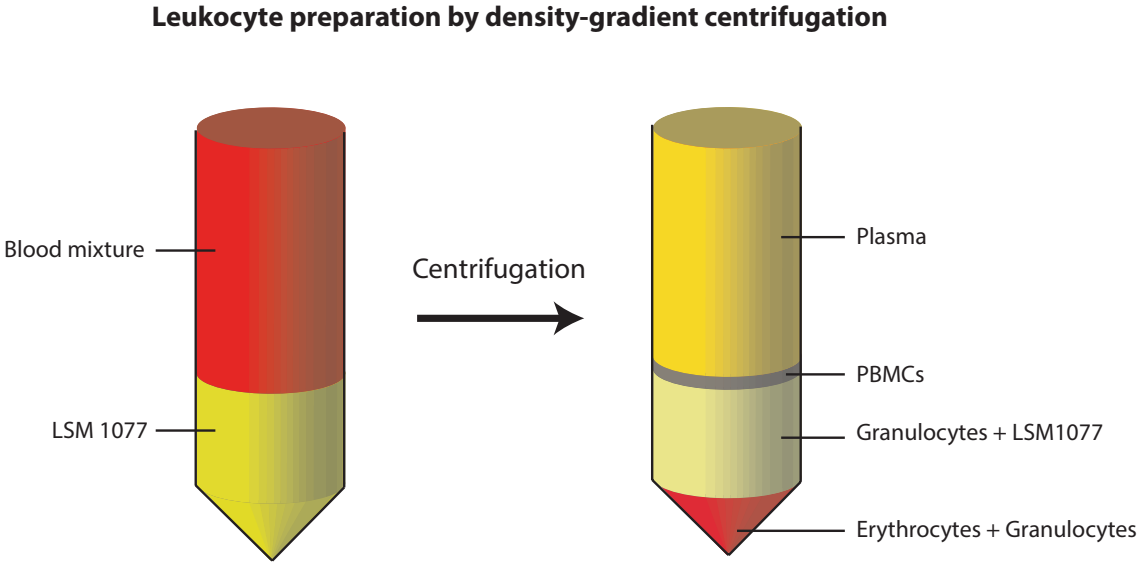

Figure 6: Scheme of the blood cell distribution before and after density gradient centrifugation. 25 ml blood mixture is layered on top of 12.5 ml LSM 1077 (left side). After centrifugation for 30 min at 300 xg the blood cells are separated on the basis of their size and weight with erythrocyte and granulocytes at the bottom, plasma on top and PBMCs and granulocytes between.

To isolate monocytes from the PBMC fraction, the fraction was removed and three times washed through centrifugation (300 xg, RT) with PBS. Than the cells were diluted in RPMI medium and plated into cell culture plates and incubated for 2-3 h at 37° C and 5 % CO_2 in a humidified atmosphere. After this timespan, monocytes were adhered to the plate bottom and the non-monocytes can be washed away. Subsequent the monocytes were used in experiments.
To isolate granulocytes, the granulocytes-containing fractions were washed three times with PBS (300 xg, RT). Subsequent, the erythrocytes were removed by re-suspending the cell pellet in ice-cold erythrocyte lysis buffer for 2 min. Then the suspension was centrifuged for 5 min and the supernatant removed. This procedure was repeated until the cell pellet was apparently free of erythrocytes. Finally, the granulocytes were washed three times with PBS, resuspended in RPMI and used for experiments.

3.9.4. Cryopreservation of eukaryotic cells

For long time storage, eukaryotic cells were stored at -196° C in liquid nitrogen. Therefor 80-90 % confluent cells are washed and trypsinised as described in 3.9.2. Then the cells were re-suspended in 1 ml of the corresponding medium containing 20 % FCS and 10 % DMSO and transferred into a freezing container. The freezing container contains MeOH, which guarantees a slow cool down of the cells. To support the slow cool down, the cells were stored for the first 24 h at -80° C before they were transferred into liquid nitrogen.

3.9.5. Collagenisation of cell culture dishes

Some cell types cannot grow on plastic surfaces. These kinds of cells need additional matrix compounds to which they can adhere. To these cells belong the primary endothelial cells HUVECs. To promote the adhesion and growth of HUVECs, cell culture flasks and plates were coated with collagen. Collagen from rat-tail was suspended in PBS containing 0.02 M HCl to a concentration of 2000 µg/ml and stored at 4° C. The flasks and plates were coated with collagen at a final concentration of 20 µg/ml in PBS for at least 30 min. Then the plates and flasks were washed three times with PBS and dried before seeding the cells.

3.9.6. Cell counting

If indicated, the cells were counted before seeding and performing the experiments. Therefore, the trypsinized cells were centrifuged for 5 min with 300 xg at room temperature. Afterwards the cell pellet was resuspended in the corresponding medium and 10 µl of the cell suspension was diluted in a 1:1 or 1:10 ration in PBS with trypan blue. The final trypan blue concentration

was 0.2 %. Trypan blue stains dead cells but is excluded from viable cells. The cell count of viable cells was determined by counting the cells in a Neubauer counting chamber. By counting the viable cells in all four squares of the chamber the cell concentration of the cell suspension was calculated as follows:

$$\frac{Cells}{ml} = \frac{cell\ count}{4} * dilution\ factor * 10^4$$

3.10. MTT-based cell viability assay

Metabolic activity was determined in 96-well plates in triplicates by quantifying the reduction of MTT ((3-(4,5-Dimethylthiazol-2-yl)-2,5-diphenyltetrazodium bromide) to formazan. Adhesion cells were grown to confluency and suspension cells were counted and 200.000 cells per well were used. The cells were incubated with the indicated amount of melittin in 100 µl serum free medium for 30 min. Untreated and 2.5 % Triton-X treated cells served as control. Afterwards medium was replaced by 100 µl of 0.5 mg/ml MTT in 10 % standard cell culture medium and 90 % PBS and incubated for 2 h at 37° C. Formed formazan crystals were dissolved by adding 100 µl of 10 % Triton-X in isopropanol. Extinction was measured at 590 nm and absorbance values were normalized to untreated and Triton-X treated controls.

3.11. Determination of ATP-release

The CellTiter-Glo® Luminescent Cell Viability Assay (Promega) was used to determine the release of soluble ATP. The assay was performed according to manufacturer´s instructions and slightly adapted to measure extracellular ATP. In brief, cells were grown to confluency and incubated in 100 µl serum free medium with the indicated amounts of melittin for 30 min. Afterwards the supernatant was removed and centrifuged to remove cell debris. 50 µl of the conditioned supernatant was mixed in a 1:1 ratio with the luminescent substrate. After 10 min at room temperature the luminescence was determined in a plate reader with an integration time of 1 s per well. The obtained luminescence values were interpolated with the values of an ATP standard curve ranging from 0 nM to 4000 nM, which were done in parallel.

3.12. Stimulation, cell lysis and collection of supernatants

For the shedding analyses by western blotting, AP-assays or ELISAs all cells were stimulated as follows. If not otherwise indicated, all cells were pre-incubated for 1 h in serum free medium before stimulation. Inhibitors were added 15 min before the stimulation started to ensure that all target molecules are blocked. For all stimulants and inhibitors the corresponding solvent controls were used to exclude unspecific side effects. After the indicated stimulation period the medium was removed and centrifuged at 13.000 rcf at 4° C for 5 min to remove cell debris. The cleared supernatants were either immediately used for ELISA- or AP-assays or stored at -20° C for later analyses. Depending on the kind of assay, different cell lysis buffer were used (Table 13). Cell lysis was always performed on ice or at 4° C in the fridge. For western blotting analyses, the cells were directly lysed through adding 100-200 µl pre-chilled lysis buffer in the wells and freezing and thawing them for three times in a row. Afterwards the lysis solution was transferred into Eppendorf tubes and incubated for 30 min on ice. The lysed cell solution was cleared by centrifugation at 13.000 rcf at 4° C for 5 min. The supernatants, containing the proteins, were either directly used or stored at -20° C for later analyses.

For AP-assays the cells were lysed by adding 200 µl lysis buffer to the wells and the plates were incubated for 30 min and slow shaking at 4° C. Afterwards the lysis solution was transferred to Eppendorf tubes and incubated for further 30 min on ice. Finally, the solution was cleared by centrifugation at 13.000 rcf at 4° C for 5 min. The cleared solution was than directly used for AP-assays.

3.13. Bradford protein concentration determination

To determine the protein concentration in lysed cell solutions the Bradford protein concentration assay was used (Bradford, 1976). Therefor 200 µl of a ready-to-use *Coomassie Plus* solution was mixed with 1 µl of the cell lysate. 1 µl pure lysisbuffer served as control. The extinction was measured at 595 nm in a plate reader. The protein concentrations were calculated by interpolation with a BSA standard curve.

3.14. SDS polyacrylamide gel electrophoresis

The SDS polyacrylamide gel electrophoresis is a standard procedure to separate proteins according to their size ranging from 5 to 2000 kDa due to the uniform pore size provided by the polyacrylamide gel. Therefor 50 µg proteins per sample were boiled up to 95° C in 1x SDS sample buffer for 5 min. The now denaturated proteins were loaded onto the gel as well as the protein size marker *PageRuler*™. The stacking gel had by default 4.5 % and the resolving gel

10 % polyacrylamide (Table 15). The electrophoresis was performed at 30 mA and a maximum of 150 V.

Table 15: Composition of the SDS polyacrylamide gels

Stacking Gel 4.5 %	2.9 ml H_2O 1.25 ml Stacking gel buffer 825 µl Acrylamide/Bisacrylamide, 30%, 37.5:1 30 µl APS 10 % (w/v) 15 µl TEMED
Resolving Gel 10 %	4.03 ml H_2O 2.5 ml Resolving gel buffer 3.33 ml Acrylamide/Bisacrylamide, 30%, 37.5:1 60 µl APS 10 % (w/v) 30 µl TEMED

3.15. Western blotting

To transfer the electrophoretically resolved proteins from the gel to a polyvenylidene fluoride (PVDF) membrane either the semid-dry or the tank blotting procedure were used. The semi-dry blotting was used for subsequent detection of cadherins and the tank blotting for subsequent detection of phosphorylated and unphosphorylated EGFR and ERK1/2. In brief, for both procedures the PVDF membrane was prepared by activating it in MeOH. The activated membrane and the gel were put between to *Whatman paper* with the membrane oriented to the anode and the gel at the side of the cathode. The transfer was performed at XX for XX for the semi-dry blotting and at 80 mA for 12 h for the tank blotting.

3.16. Immunological detection of transferred proteins

To block unspecific antibody binding the membrane was incubated for 1 h at room temperature in TBST with 5 % milk powder. Afterwards the membrane was incubated with the indicated antibody dilution (Table 10) in blocking solution for 1h at room temperature. Antibodies from *Cell signaling* were incubated overnight at 4° C. After the first antibody incubation, the membrane was washed three times for 5-15 min with TBST to remove excessive antibody binding. A second antibody with reactivity against the species of the first antibody was than incubated for 1h in TBST (Table 11). Unbound antibody was again washed away three times for 5-15 min with TBST. The antibody tagged proteins were detected with the peroxidase substrate *ECL Advanced* and the emitted chemiluminescence was recorded with a CCD camera (Fusion FX7, Peqlab).

3.17. Stripping of PVDF membranes

The removal of the first and secondary antibodies of the PVDF membrane allows detecting different targets with different antibodies by using the same membrane. This method is called "stripping". In this thesis it was for example used to subsequently stain phosphorylated and unphosphorylated ERK1/2 as well as p-EGFR and EGFR. To strip the antibodies off the membrane, the membrane was incubated for 15-45 min in stripping buffer at 65° C (Table 13). The further procedure was than analogue to chapter 3.16

3.18. Enzyme-linked immunosorbent assay

The enzyme linked immunosorbent assays used in this thesis were designed to detect soluble human TGF-α and TNFR1, respectively. Both are distributed by R&D Systems and were used according to the manufacturer´s instructions with a slight adaption. Instead of 100 µl sample and 100 µl antibody dilutions per well, 50 µl were used.

3.19. Cell cycle analysis

The cell cycle analysis was performed by Anja Fries (University Mainz). In brief, HaCaT keratinocytes were cultured overnight in medium containing FCS before starvation of 48 h. Subsequently, medium containing various agents was added and cells were incubated for 24 h. For FACS analyses, cells were trypsinized and fixed with 75% ethanol in PBS/EDTA for ≥ 12 h at 4°C. Samples were centrifuged and re-suspended in PBS with EDTA (1 mM), containing 10 µg/ml RNase. Propidium iodide staining was performed at a final concentration of 2 µg/ml.

3.20. *In vitro* wound healing assay

HaCaT keratinocytes were seeded in 12-well plates and grown until they reached confluence. A cell free area was introduced by scraping the monolayer with a pipette tip (10 µl). To avoid a proliferative effect, the cells were treated with 2 mM hydroxyurea for 24 h. For stimulation experiments, serum free medium containing metalloprotease inhibitors or DMSO as solvent control were added. After 15 min of preincubation the cells were treated with 0.5 µM melittin. The cells were photographed before and 24 h after stimulation by using an inverted phase-contrast microscope (Zeiss). The cell free area was quantified using AxioVision (Zeiss) before and after stimulation, respectively.

3.21. Transient transfection of eukaryotic cells

The insertion of expression vectors into eukaryotic cells was done by lipofection. The transfection solution was prepared as follows. For single transfection 100 µl serum free medium was supplemented with 0.5 µg plasmid and subsequently 1 µl *Turbofect* in a small tube. The tube was inverted a few times and incubated at room temperature for 20 min. For double transfection 0.5 µg of plasmid 1 and 0.5 µg plasmid 2 were added to 100 µl serum free medium and 1.5 µl *Turbofect* was added afterwards. The cells were transfected at 60-80 % confluence and the medium was changed to 500 µl serum free medium. The transfection solutions described above were then added in drops to the cells. After 6 h the medium was changed to normal growth medium including FCS. 24 h after transfection the cells were used for stimulation experiments, such as for AP-assays.

3.22. Phosphatidylserine deprivation with PSA3 cells

PSA3 cells were cultivated in Hams F12 medium supplemented with 10 % FCS, 10 µM ethanolamine and penicillin/streptomycin (Pen/Strep). For phosphatidylserine (PS) deprivation, cells were cultured in starvation medium consisting of Hams F12 with 6 % dialyzed FCS + Pen/Strep with or without 10 µM ethanolamine. For AP-assay experiments, PSA3 cells were transfected after 72 h PS deprivation for 6 h in Hams F12 only. Thereafter medium was changed again to the starvation medium. All AP-assays and imaging experiments were done after 96 h of PS deprivation as described.

3.23. Shedding experiments with alkaline phosphatase coupled substrates

The proteolytic activity of ADAM17 in its wildtype or mutated form was determined with alkaline phosphatase (AP) tagged substrates. These substrates (e.g. TGF-α-AP) carry an alkaline phosphatase at their extracellular domain, which is released in the supernatant after ADAM17-mediated cleavage. These substrates were transfected into eukaryotic cells as described in chapter 3.21. The activity of the AP can be determined by the hydrolysis of the colorless substrate p-nitrophenylphosphat (p-NPP) to the yellow p-nitrophenol (p-NP). The ratio between the AP-activity in the supernatant to the AP-activity in the cell lysates is a direct measure for the relative quantity of shed ADAM17-substrates. 24 h after transfection the cells were stimulated, lysed and the supernatant collected as described (chapter 3.12).

3.24. Fluorescence microscopy

3.24.1. Life cell imaging

Time-lapse imaging was performed with an inverted confocal microscope (Fluoview FV1000, Olympus) equipped with an environmental chamber using a UPLSAPO 60x oil immersion objective and 2x zoom. Before starting the experiments the chamber was equilibrated to 37°C in a humidified atmosphere. The cells were seeded in glass bottom imaging dishes (PAA) and grown till semi-confluency. Cells were allowed to rest for at least 1h in the microscope stage. PSIVA-IANBD (Imgenex) was added to the cells in a final concentration of 6.25 µg/ml 5 min before acquisition started. PSIVA-IANBD was excited at 488 nm and emission was recorded at 520 nm every 30 s or 60 s. Laser and detector settings were the same for each single experiment.

3.24.2. AnnexinV staining of cells

Cells were seeded on glass coverslip and grown until semi-confluence. After indicated stimulation/inhibiton periods coverslips were immediately incubated with 1:20 solution of FITC-AnnexinV (Sigma) in Annexin-Binding-Buffer (Table 13) for 5 min in the dark at room temperature, washed twice with ABB and were fixed for 15 min with 3 % PFA. After fixation coverslips were washed six times with PBS, once with *Aqua dest* and mounted in embedding medium. Image acquisition was performed with an inverted confocal microscope (Fluoview FV1000, Olympus) using a UPLSAPO 60x oil immersion objective and 2x zoom. FITC-AnnexinV was excited at 488 nm and emission was recorded at 520 nm. All images were acquired with the same laser and detection settings.

3.24.3. Fluorescence quantification

Image analysis was done with ImageJ 1.47m. Fluorescence area above background fluorescence was determined and correlated to the cell growth area. AnnexinV staining: for each group, three independent coverslips, each with 6-8 images of different areas were analyzed. The mean fluorescence area of each coverslip was taken for statistical analysis. Control and stimulated groups were compared with an unpaired, one-tailed t-test (*$p<0.05$).

3.25. Electrostatic surface modeling

Computational modeling of electrostatic protein surfaces was used to obtain an impression of the ionic charge distribution in the membrane proximal domain of ADAM17. The structures (accession number: 2M2F) were prepared with the PDB2PQR tool of the UCSF chimera software package using the CHARMM force field method and the electrostatic potential map was calculated with the Adaptive Poisson-Boltzmann Solver (APBS) (Baker et al., 2001; Dolinsky et al., 2007; 2004; MacKerell et al., 1998; Unni et al., 2011).

3.26. Preparation of lipid aggregates/liposomes

Liposomes were prepared as 1 mM aqueous dispersions of the phospholipids in buffer (5 mM Hepes, 100 mM KCl, pH 7.0) as follows. The lipids were dissolved in chloroform to a concentration of 1 mg/mL. The solvent was evaporated under a stream of nitrogen, buffer was added, and sonicated with a Branson sonicator (Branson Ultrasonics Corporation, Danbury, USA) for 1 min (1 mL solution). Subsequently, the preparation was cooled for 30 min at 4 °C and two times heated for 30 min at 60 °C and cooled to 4 °C. Preparations were stored at 4 °C overnight prior to measurements.

3.27. Isothermal titration calorimetry and surface acoustic wave biosensor measurements

The isothermal titration calorimetry (ITC) and the surface acoustic wave biosensor measurements (SAW) were performed at the Department of Biophysics, Forschungszentrum Borstel. Lena Heinböckel and Christian Nehls carried out these experiments. In brief, the binding of the MPD with PtdCho or PtdSer liposomes was analysed by microcalorimetric measurements on an ITC200 (GE Healthcare, Munich, Germany). 0.5 mM solutions of the open and closed form of MPD in 5 mM HEPES were titrated 20 times in 1.5 µL injections to 250 µL 0.1 mM PtdSer or PtdCho liposome dispersions. Final lipid:protein ratio was 5:3 [M:M]. The enthalpy changes were recorded versus time. The heats of dilution were determined in control experiments by injecting peptide solution into buffer (5 mM HEPES, pH 7.4). Measurements were performed at 37 °C.

For the SAW measurements, gold-coated chips (S-sens K5 Biosensor Quartz Chips, SAW Instruments GmbH, Bonn, Germany) were functionalized as described before (Andrä et al. 2008). A functionalized chip was incubated overnight in ethanol and placed into the reader unit of the S-sens K5 readout system (SAW Instruments GmbH, Bonn, Germany). Biomolecular interac-

tion processes on the surface of the sensor chip can result in changes of phase and amplitude of the surface acoustic wave. Changes of these parameters correlate with mass loading and viscoelastic alterations (Andrä et al. 2008). Measurements were performed at a continuous flow of measuring buffer (5 mM HEPES, pH 7.4) of 20 μL/min at 22 °C. By injection of 100 μL of poly- L-lysine (PLL, 50 μg/mL, Fluka, Basel, Switzerland) a positively charged layer was formed on top of the negatively charged CM-dextran matrix. 100 µl phospholipid liposomes (300 μg/ml) (PtdSer liposomes or PtdCho (9):PtdSer (1) liposomes) were injected and immobilized on the positively ionized surface. The liposomes were dissolved in 150 mM NaCl, 5 mM HEPES, pH 7.4 to ensure a homogenous surface coverage. Subsequently, 100 µl of 20 µg/ml solutions of the open and closed form of MPD in 5 mM HEPES were injected. Changes of phase and amplitude induced by the interaction of MPD with the lipid bilayer were recorded versus time.

3.28. Mutagenesis

For mutagenesis the QuickChange® II Site-directed Mutagenesis kit (Stratagene) was used according to the manufacturers' instructions. Felix Kordowski (Institute of Dermatology and Allergology, UKSH Kiel) carried out the mutagenesis primer design and reactions.

3.28.1. Plasmid

The pcDNA-ADAM17 plasmid that was used for the mutagenesis experiments consists of the pcDNA3.1 expression vector (Invitrogen) and a 2484 bp fragment, which encodes for the murine ADAM17. The coding sequence contains the whole length ADAM17 with the prodomain as well as a hemaglutinin (HA) tag. This HA-tag is C-terminal added to the cytoplasmic tail of ADAM17. This plasmid was kindly provided by Carl Blobel (Hospital for Special Surgery, New York).

3.28.2. Oligonukleotides

The primer oligonucleotides that were used to introduce site directed mutagenesis in the pcDNA-ADAM17 expression plasmids were designed with the online tool QuickChange® Primer Design (http://stratagene.com/qcprimerdesign). The primers were then ordered from Sigma Aldrich. The sequences of the mutagenesis primer pair are depicted in Table 16.

Table 16: Mutagenesis primer pair for the mutation of ADAM17.

A17 3x forward	5'-gcagagcaaaagaacttgtttttgggggagggggccatgtacagtagggttttgcg-3'
A17 3x reverse	5'-cgcaaaaccctactgtacatggccccctccccccaaaaacaagttcttttgctctgc-3'

3.28.3. Mutagenesis reaction

The mutagenesis reaction was carried out according to the manufacturers' instructions. In brief, a polymerase chain reaction was performed with the *PfuUltra HF* DNA-polymerase in the presence of the pcDNA-ADAM17 expression plasmid and the mutagenesis primer pair. The during the PCR synthesized new plasmids carrying the mutation do not have bacterial methylated DNA and are therefor protected against the afterwards performed digestion with *Dpn I* endonuclease. The resulting plasmids were than amplified in *E. coli XL1 blue* (3.28.5), isolated (3.28.7) and sequenced (3.28.8).

3.28.4. Preparation of chemical competent cells

Table 17: Buffer and solutions for the preparation of chemical competent cells.

LB medium	171 mM NaCl 10 % (w/v) Trypton/Pepton 5 % (w/v) Yeast extract
Tris buffer	0.1 mM NaCl 5 mM Tris 5 mM $MgCl_2$
$CaCl_2$-solution	0.1 mM $CaCl_2$ 5 mM Tris 5 mM $MgCl_2$

To obtain chemical competent *E. coli* cells, XL1 blue cells were treated with $CaCl_2$. Therefore, bacteria from an overnight culture were diluted 1:100 with LB medium and cultivated at 37° C and 200 rpm until they reached a optical density (OD_{600}) around 0.4-0.6. The cells were than cooled down for 20 min on ice and centrifuged afterwards (5 min, 5000 xg). A cell pellet of a 50 ml suspension was re-suspended in 20 ml pre-chilled Tris-buffer and centrifuged again for 10 min at 4° C for 10 min. Subsequently the cell pellet was re-suspended in 20 ml $CaCl_2$ solution and incubated for 20 min on ice. After this incubation, the cells were centrifuged (10 min, 5000 xg, 4° C) and re-suspended in 2 ml of the $CaCl_2$ solution. Once again, the cells were incubated on ice for 1 h and filled up with 500 µl glycerin. This cell suspension was immediately shock frosted in liquid N_2 and stored in aliquots of 50 µl at -80° C.

3.28.5. Transformation of chemical competent bacteria

Table 18: Medium and solutions for the transformation of bacteria

SOC medium	0.5 % (w/v) Yeast extract 2.0 % (w/v) Trypton 10 mM NaCl 2.5 mM KCl 10 mM $MgCl_2$ 10 mM $MgSO_4$ 20 mM Glucose
LB/Amp plates	171 mM NaCl 1% (w/v) Trypton/Pepton 0.5 % (w/v) Yeast extract 1.5 % (w/v) Agar Agar 0.1 mg/ml Ampicillin

For the transformation process of cells, 50 µl of the above-described chemical competent *XL1 blue* were gently thawed on ice and mixed with 1 µl plasmid. This mixture was first incubated for 45 min on ice and then warmed up for exactly 40 s to 42° C. The cells were cooled down for 5 min on ice and filled up with 300 µl SOC medium. This bacteria culture was than incubated for 1 h at 37° C at 200 rpm. Afterwards the cell suspension was plated onto LB/Amp plates and incubated overnight at 37° C. Colonies were picked with a sterile pipette tip and incubated in 5 ml LB medium containing ampicillin. This preculture was grown to an OD_{600} of 0.5 and used for the preparation of glycerol stocks.

3.28.6. Preparation of bacterial glycerol stocks

For long time storage of transformed bacteria, glycerol stocks were prepared. For this, 850 µl of a bacteria culture were mixed with 150 µl glycerol. This suspension was shock frosted in liquid nitrogen and afterwards stored at -80° C.

3.28.7. Isolation of plasmid DNA from *E.coli*

To amplify and isolate plasmids from transformed bacteria, 250 µl LB medium containing ampicillin was inoculated with bacteria from glycerol stocks. This bacteria culture was incubated overnight at 37° C and 200 rpm. The plasmids were isolated with the PureYield™ MidiPrep kit (Promega) according to the manufacturer´s instructions.

3.28.8. DNA sequencing

The sequences of the mutated plasmids were verified by commercial DNA sequencing (Seqlab). Therefor, 650 ng plasmid DNA was mixed with 20 pmol of the sequencing primer SeqpcDNA3.1BGHrev (5´-CTAGAAGGCACAGTCGAG-3´) in a volume of 7 µl and send in to Seqlab.

3.29. Cleavage experiments with a soluble fluorogenic ADAM substrate

Cos7 cells were transfected in 24 well plates with 0.5 µg of the ADAM17-plasmids (wildtype, E/A or 3x), or with the empty control plasmid (pcDNA3.1) for 6 h. 24 h after transfection medium was changed to DMEM only with 10 µM fluorogenic ADAM substrate (Enzo Life Sciences) and the cells were incubated for 6 h at 37°C and 5 % CO_2 in a humidified atmosphere. Afterwards fluorescence in the supernatant was determined at 485 nm excitation and 530 nm emission.

4. Results

4.1. Melittin modulates keratinocyte function through P2-receptor-dependent ADAM activation

The first part of the results section deals with the influence of the bee venom component melittin on ADAM-mediated shedding. These results have been published in the Journal of Biological Chemistry in 2012 (see supplements (Sommer et al., 2012)).

4.1.1. Melittin affects cellular viability

Melittin is known to induce necrosis and apoptosis in high concentrations, while low concentrations enhance cell migration (Maher and McClean, 2008). To exclude potential cytotoxic side effects and define sublethal concentrations, MTT reduction was measured and taken as parameter for cell viability. Viable and metabolically active cells reduce the yellow tetrazolium MTT to purple formazan, what can be quantified. As shown in Figure 7 (A-E) all cells tested responded to melittin treatment with a dose-dependent decrease in MTT reduction.

Human umbilical vein endothelial cells (HUVECs) and murine embryonic fibroblasts (MEFs) were least sensitive to melittin treatment (Figure 7 B-C). 4 µM and 2 µM melittin were sufficient for significant lowering of MTT reduction in HUVECs and MEFs In contrast to these cells, human monocytes were most sensitive and were not used in the following experiments (Figure 7A). Concentrations of ≥ 0.5 µM melittin lead to a significant decrease in MTT reduction in monocytes. The MTT reduction in human neutrophil granulocytes and HaCaT keratinocytes were significantly decreased at ≥ 1 µM and ≥ 2 µM melittin respectively (Figure 7 D-E). These results were in line with the previously reported tolerable threshold of 1 µM melittin for HaCaT keratinocytes (Drechsler and Andrä, 2011).

In conclusion, these results indicate that melittin concentrations between 0.5 µM and 1 µM were tolerable for most cell types. Thus, these concentrations were used for the following experiments, except for MEFs where higher concentrations were needed to stimulate significant shedding.

To test whether melittin treatment lead to ATP release, ATP concentrations in the supernatant of HaCaT keratinocytes were measured (Figure 7 F). ATP concentrations were determined by luciferase bioluminescence measurements (CellTiter-Glo Luminescent Cell Viability Assay (Promega)). Melittin treatment elicited ATP-release dose-dependently. It became detectable in nanomolar concentrations even when non-toxic melittin concentrations were used (Figure 7 F).

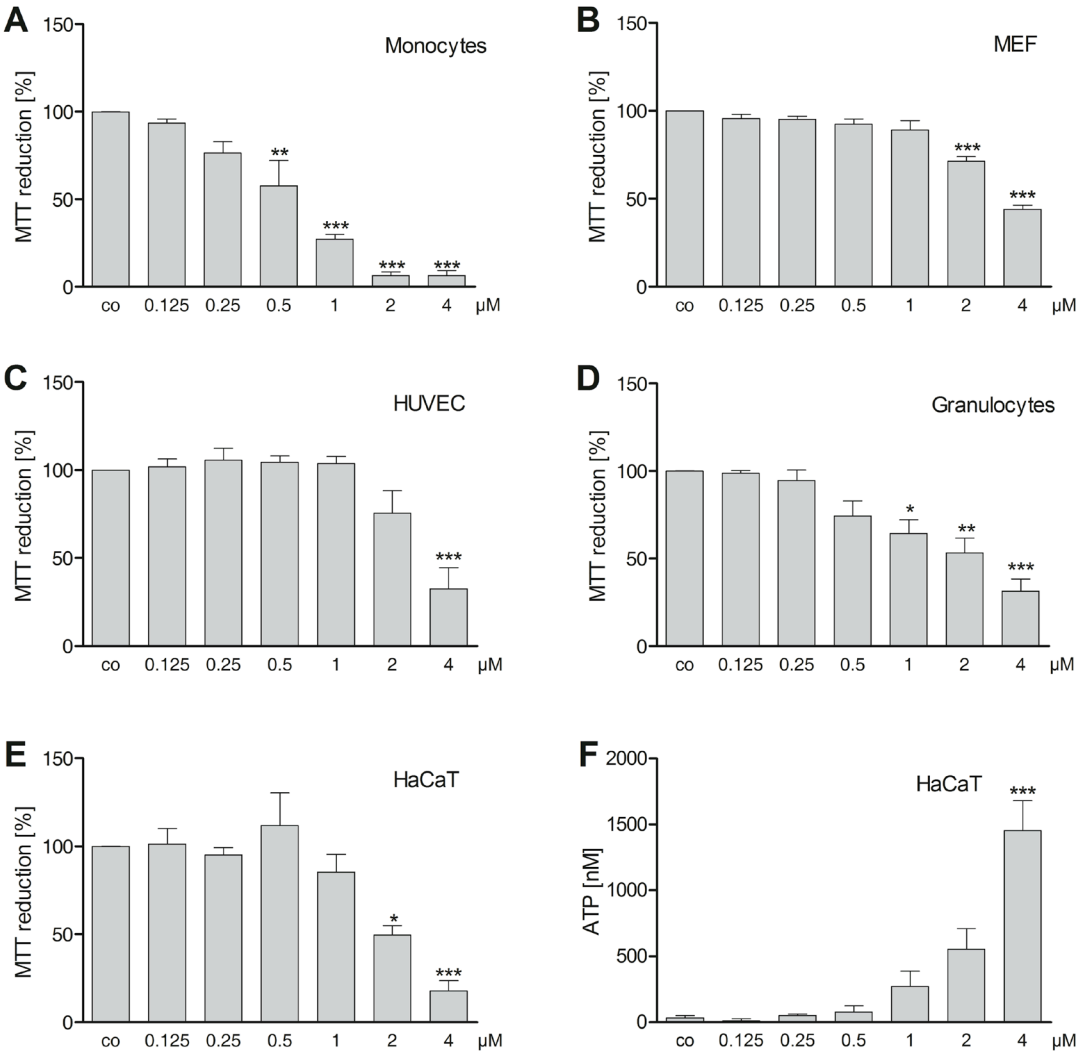

Figure 7: Low concentrations of melittin do not affect cell viability. Primary human monocytes (A), murine embryonic fibroblasts (MEFs) (B), human umbilical vein endothelial cells (HUVECs) (C), primary human granulocytes (D) and HaCaT keratinocytes (E, F) were incubated with different concentrations of melittin for 30 min. Thereafter, cells were incubated for 2 h with MTT allowing MTT reduction. MTT reduction was determined by absorbance measurements and taken as a parameter for viability. Absorbance values of melittin treated cells were normalized to untreated (100 %) and 2.5 % Triton-X treated cells (0 %) (A-E). ATP release of melittin treated HaCaT keratinocytes was determined by a luminescence ATP-dependent luciferase based Assay. Luminescence values were interpolated with a ATP standard curve (F). Data represent mean values ± S.E. of three independent experiments all measured in triplicates. * Indicates significant difference compared to control (* $p < 0.05$, ** $p < 0.01$, *** $p < 0.001$).

4.1.2. Melittin induces ADAM-dependent substrate cleavage

To elicit if melittin would stimulate ADAM10-dependent shedding, N-cadherin processing in MEFs was determined. Therefore a monoclonal antibody against the C-terminus of N-cadherin was used to visualize the C-terminal fragment (CTF) and the full length N-cadherin in immunoblots of melittin treated MEF cell lysates (Figure 8 A). The generation of N-cadherin CTF in wildtype cells was compared with ADAM10-deficient fibroblast. Melittin dose-dependently evoked shedding of N-cadherin in wildtype cells. ADAM10-deficient MEFs exhibited no N-cadherin shedding.

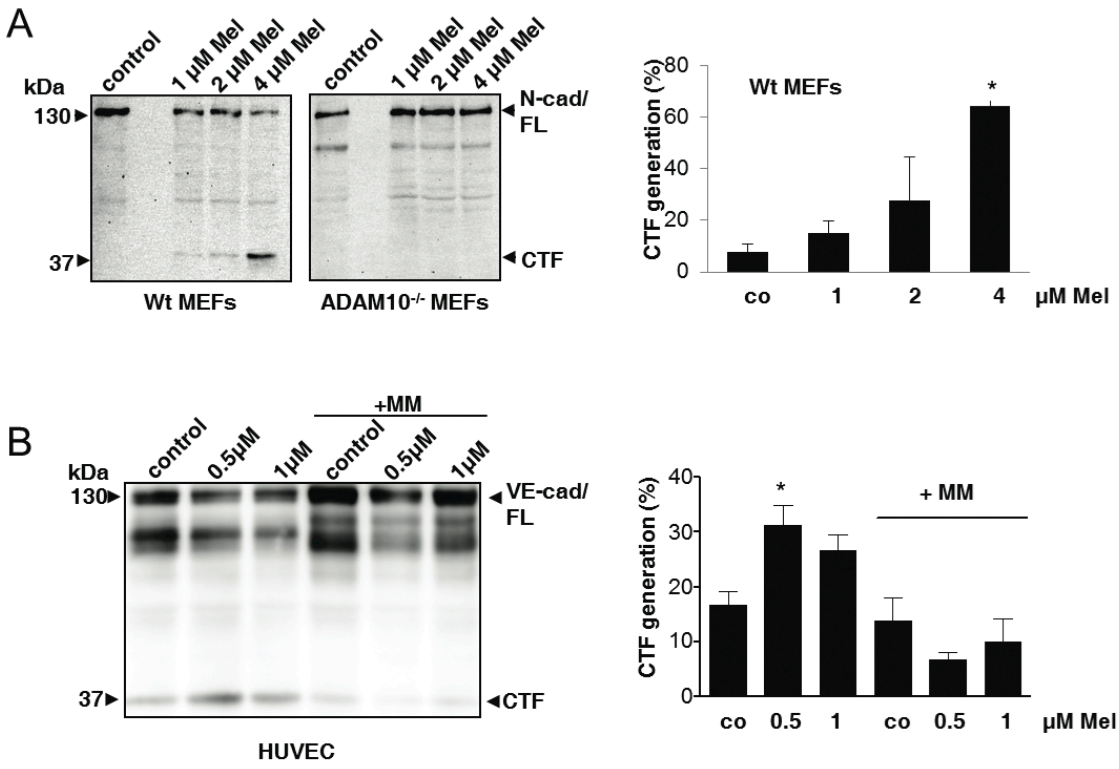

Figure 8: Melittin increases ADAM-mediated shedding in different cell types. A: MEFs were mock treated (control) or stimulated with increasing amounts of melittin for 30 min. Total cell extracts from wildtype-MEFs (Wt) and ADAM10$^{-/-}$-MEFs were subjected to immunoblot analysis and stained with a C-terminal anti-N-cadherin antibody. N-cadherin CTF generation was calculated by densitometric analysis of three independent experiments (right panel). Results are expressed as mean ± S.E. (n=3). * Indicates significant increase in CTF generation compared to control (* $p < 0.05$). **B:** HUVECs were stimulated with melittin in the presence or absence of broad-spectrum metalloprotease inhibitor marimastat (MM, 10 µM). VE-cadherin cleavage was analyzed with a C-terminal VE-cadherin antibody by immunoblot. Densitometric analysis of three independent experiments is shown in the right panel (* $p < 0.05$).

To verify these results in another cell type, melittin treated HUVECs were analyzed for VE-cadherin shedding (Figure 8 B). Melittin induced VE-cadherin shedding at concentrations of

0.5 µM and 1 µM. This shedding was inhibited by the broad-spectrum metalloprotease inhibitor marimastat (MM). In addition, ADAM17-mediated L-selectin cleavage in humane neutrophil granulocytes was analyzed by FACS analysis by our cooperation partners in Mainz (Anja Fries, Isabell Cornelsen and Sucharit Bhakdi; Institute of Medical Microbiology and Hygiene, Gutenberg University Mainz). They could show that 0.5 µM melittin induces a rapid decrease of L-selectin surface expression and that this decrease was metalloprotease-dependent (see supplements) (Sommer et al., 2012). In conclusion, melittin in sublethal dosages evokes ADAM10- and ADAM17-dependent shedding in different cell types.

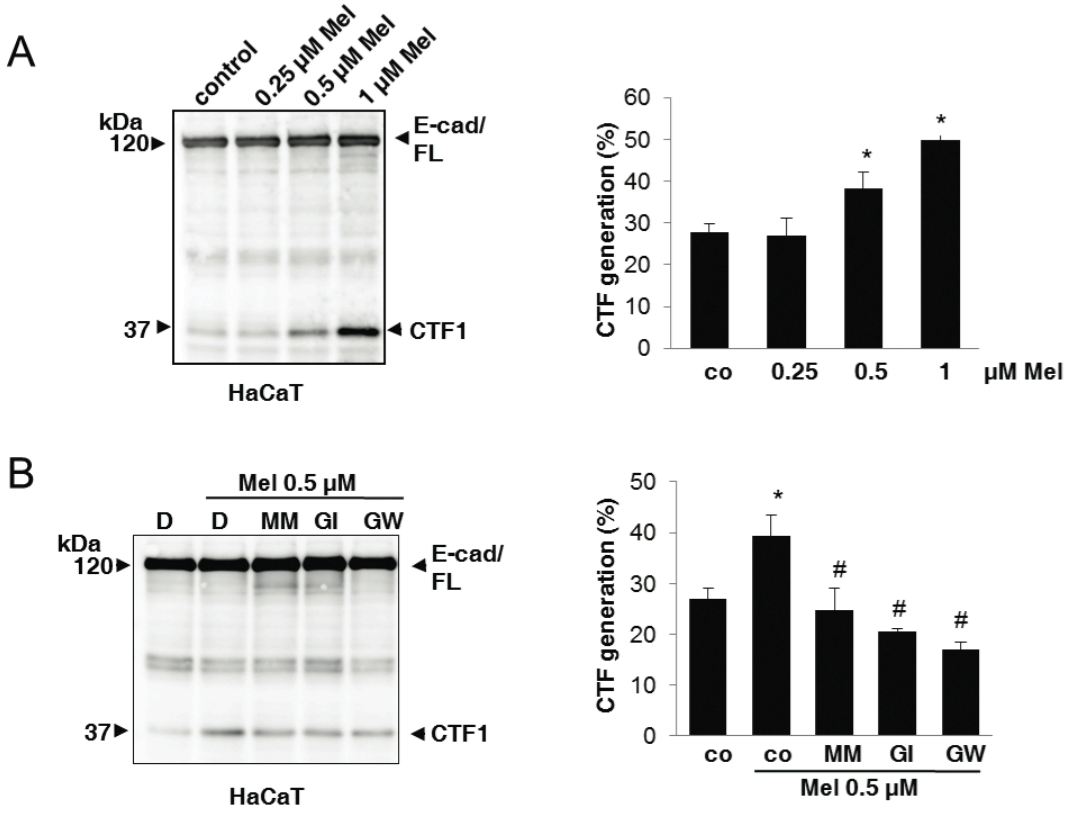

Figure 9: Melittin augments ADAM-dependent E-cadherin shedding. A: After incubation with melittin (Mel), HaCaT cell pellets were subjected to immunoblot analyses using a C-terminal E-cadherin antibody. Densitometric analysis of E-cadherin CTF generation was calculated of three independent experiments (*right panel*). Results are expressed as mean ± S.E. (n=3). **B:** Cells were pre-incubated with the ADAM10 inhibitor GI254023X (GI, 3 µM), the ADAM10/-17 inhibitor GW280264 (GW, 3 µM), the metalloprotease inhibitor marimastat (MM. 10µM), or DMSO (D) as control for 10 min before stimulation. E-cadherin CTF generation was calculated by densitometric analyses of three independent experiments (*right panel*). Melittin significantly increased E-cadherin proteolysis (*, $p < 0.05$). MM, GI and GW significantly decreased this effect (#, $p < 0.05$).

4.1.3. Melittin induces ADAM-dependent E-cadherin shedding and transactivation of the EGFR in keratinocytes

The effect of melittin on HaCaT keratinocytes was then further investigated. In these cells, E-cadherin is preferentially cleaved by ADAM10 (Maretzky et al., 2008), while shedding of TGF-α is ADAM17-dependent (Peschon et al., 1998). Melittin dose-dependently increased E-cadherin shedding (Figure 9 A). The increase was significant at concentrations of 0.5 and 1 µM. This effect could be significantly reduced by the use of broadspectrum metalloprotease inhibitor marimastat and also by the preferential ADAM10 inhibitor GI245023X (GI) and GW280264 (GW), an inhibitor for ADAM10 and -17 (Figure 9 B).

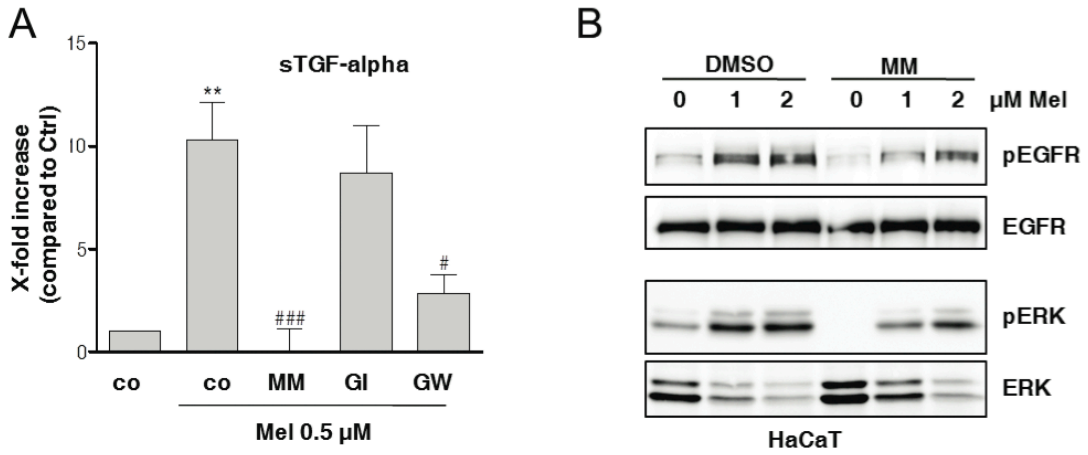

Figure 10: Melittin induces EGFR activation in HaCaT keratinocytes. A: Release of TGF-α from melittin (Mel) treated HaCaT keratinocytes were analyzed by ELISA and compared to mock treated cells. Cells were preincubated with the ADAM10 inhibitor GI254023X (GI, 3 µM), the ADAM10/-17 inhibitor GW280264 (GW, 3 µM), the metalloprotease inhibitor marimastat (MM. 10µM), or DMSO (co) as control for 10 min before stimulation with melittin (Mel, 0.5 µM, 30 min). Data represent mean values of five independent experiments with S.E. Melittin significantly increased TGF-α release (**, $p < 0.01$). This effect was significantly decreased by the use of MM and GW (#, $p < 0.05$; ###, $p < 0.001$). **B:** HaCaTs were treated with 0.5 µM melittin for 30 min in the presence or absence of marimastat (MM, 10 µM). Whole cell lysates were subjected to immunoblot analyses for pEGFR and pERK1/2 respictively. Representative westernblots are shown for EGFR phosphorylation and ERK1/2 phosphorylation with EGFR and ERK included as loading control.

Melittin simultaneously provoked release of TGF-α in the supernatant as measured by ELISA. As expected the release of TGF-α was strongly inhibited by marimastat and the ADAM10 and -17 inhibitor GW, but only weakly affected by the preferential ADAM10 inhibitor GI (Figure 10 A). TGF-α is one of seven EGFR ligands, which is critically involved in cell differentiation, migration and proliferation (chapter 1.2.3) Therefore it followed that melittin stimulation might lead to EGFR transactivation. To test this immunoblots were stained with specific antibodies against phosphorylated and unphosphorylated EGFR and ERK respectively. Indeed,

exposure of melittin induced EGFR phosphorylation with downstream activation of ERK1/2 (Figure 10 B). Again, this effect was prevented by the use of marimastat. In summary, melittin provokes ADAM-mediated E-cadherin and TGF-α cleavage. This results in EGFR transactivation and subsequent ERK1/2 phosphorylation.

4.1.4. Melittin induces keratinocyte proliferation and migration

The result that melittin induces EGFR and ERK1/2 activation in an ADAM-dependent manner, suggests that functional consequences might follow the shedding process. To test this hypothesis, proliferation and migration analyses were performed. Incubation of HaCaT keratinocytes with melittin resulted in increased proliferation, as determined by propidium iodide (PI) cell cycle analysis (Figure 11). Cell cycle analysis was performed by Isabell Cornelsen (Institute of Medical Microbiology and Hygiene, Gutenberg University Mainz). The melittin-induced proliferation was comparable to that of recombinant EGF, which was used as positive control and was abrogated by the use of TAPI-0, a broadspectrum metalloprotease inhibitor.

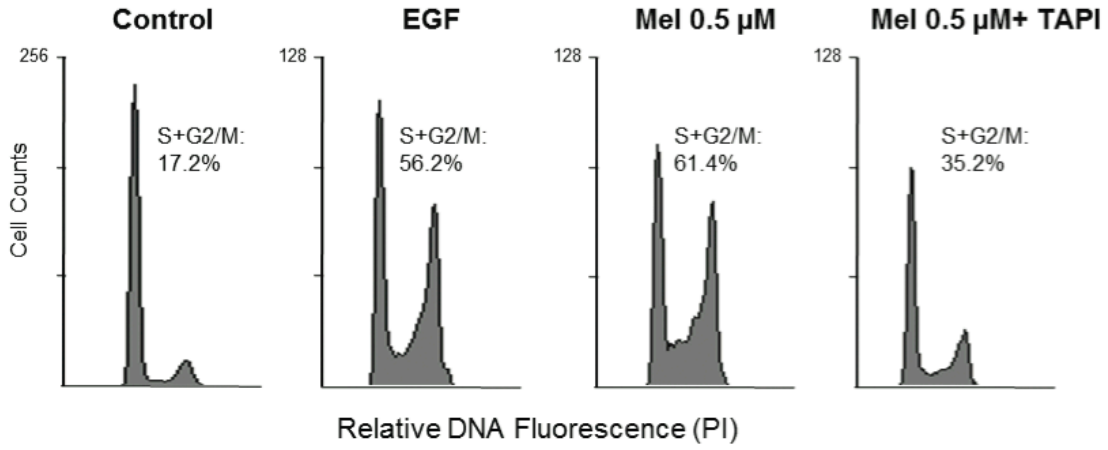

Figure 11: Melittin augments metalloprotease-dependent proliferation of HaCaT keratinocytes. Cell cycle analysis was done by propidium iodide (PI) staining and flow cytometry. Cells were seeded at 20,000 cells/well in microtiter plates and stimulated with EGF (4 nM) as positive control and with melittin (0.5 µM). After 24h increased percentages of EGF and melittin treated cells were in S+G2/M phase. TAPI-0 (10 µM) abrogated the melittin induce effect. Analyses are representatives of two independent experiments (performed by I. Cornellsen, Mainz).

To address the role of melittin in HaCaT keratinocyte migration, an *in vitro* model for wound healing was used. In confluent HaCaT cultures scrape wounds were generated with pipette tips and cells were allowed to migrate for 24 h. This assay was performed in the presence of 2 mM hydroxyurea to prevent keratinocyte proliferation (Firth and Putnins, 2004). While mock treated cells just started to cover the denuded area, melittin treatment lead to almost complete wound closure. This effect was abolished in the presence of marimastat or by the use of cetuximab

(Figure 12). Cetuximab is a monoclonal antibody, which blocks access of ligands to the EGFR preventing EGFR activation. In conclusion, application of melittin in low concentration induces proliferation and migration of keratinocytes in a metalloprotease- and EGFR-dependent manner.

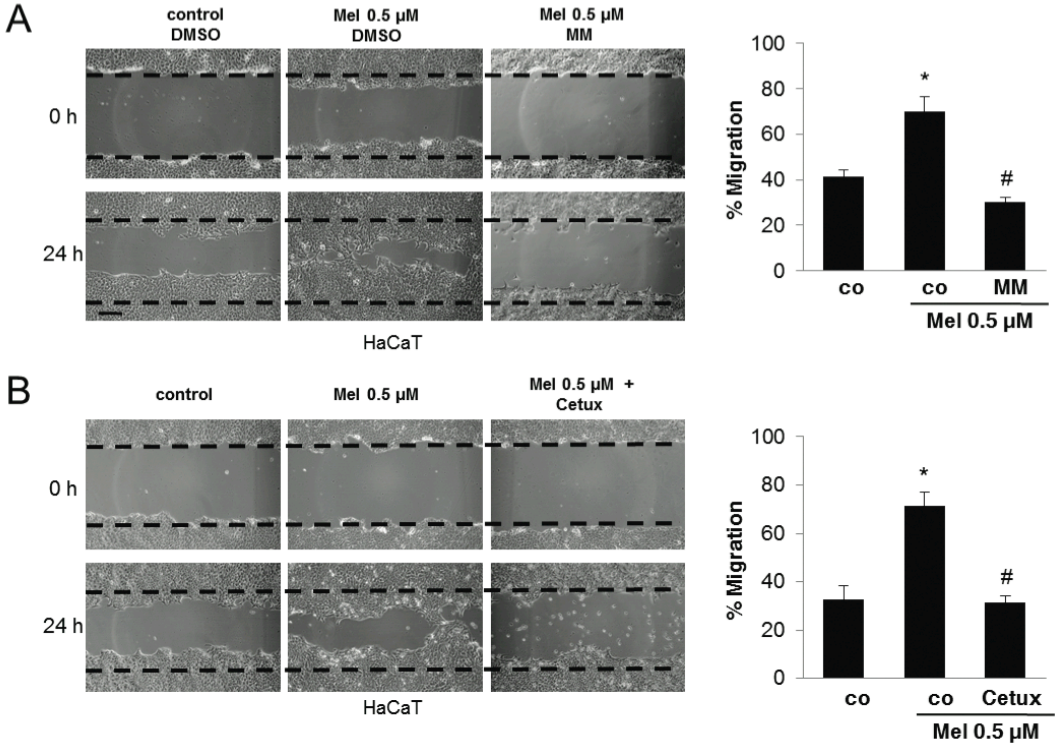

Figure 12: Melittin induces migration in HaCaT keratinocytes. Cells were grown to confluence and a cell-free area was introduced by scratching with a pipette tip. After washing, cells were mock treated or treated with melittin (0.5 µM) in the presence or absence of marimastat (MM, 10 µM) (A) or with the EGFR-blocking antibody cetuximab (Cetux, 10 µg/ml) (B). Migration was evaluated after 24 h. Micrographs of one of three independent experiments are shown. Bar: 100 µm. Migration of three independent assays are quantified (*right panel*). Asterisk (*) indicates a significant increase compared to mock treated samples (*, $p < 0.05$, $n = 3$). MM and Cetux significantly inhibited melittin-induced migration (#, $p < 0.05$, $n = 3$).

4.1.5. Melittin-induced effects are not due to altered ADAM10/-17 expression, membrane fluidity or cytosolic Ca^{2+} increase.

Reiss et al. showed that free fatty acids augmented ADAM-mediated shedding by increasing membrane fluidity (Reiss et al., 2011). To rule out that melittin, as membrane-modulating substance, affects the fluidity of membranes, steady-state fluorescence anisotropy measurements were performed. These experiments were done by Gerald Gimpl (Department of Biochemistry, Gutenberg-University Mainz). In brief, the diffusion of fatty acyl chains in HaCaT keratinocytes was determined using diphenyl hexatriene as a probe. Melittin in concentrations that induced

ADAM substrate processing exerted no effects on membrane fluidity (see supplements) (Sommer et al., 2012).

To exclude that melittin-induced effects are due to altered ADAM10 or -17 expression levels or maturation, Real-Time PCR (RT-PCR) and immunoblot analysis were performed. This was done by Nancy Speck (Institute of Dermatology and Allergology, UKSH Kiel). Melittin treatment did not significantly increase RNA expression or protein levels of ADAM10 and -17 (Sommer et al., 2012).

Another possible mechanism for ADAM activation is elevation of cytosolic Ca^{2+}. Melittin stimulation has been shown to stimulate Ca^{2+} influx in different cell types (Choi et al., 1992; Sharma, 1993). To find out whether extracellular calcium influx would contribute to ADAM activation, HaCaT keratinocytes were stimulated with increasing amounts of melittin in calcium containing and in calcium-free medium. Cytosolic calcium increase was measured by fluorescence spectroscopy (done by Gerald Gimpl, Department of Biochemistry, Gutenberg-University Mainz). Intracellular calcium increase was apparent in Ca^{+}-containing and Ca^{2+}-free medium. In Ca^{2+}-free medium the cytosolic increase was lower compared to the increase in Ca^{2+}-containing medium. This indicated that melittin induced the influx of extracellular Ca^{2+} as well as release of Ca^{2+} from intracellular stores. In immunoblot analyses for E-cadherin shedding and EGFR signaling neither chelation of intracellular nor extracellular calcium affected the cellular response (see supplements, Sommer et al., 2012).

4.1.6. Melittin effects depend on ATP-release and P2 receptor activation

Purinergic P2 receptors are involved in several physiological processes (Erb et al., 2006). They are divided in two families, the P2X receptors, which are ATP-gated ion channels and the P2Y receptors, which are G-protein-coupled receptors. Both receptor families are able to participate in the activation of ADAM-mediated shedding (chapter 1.3.2). HaCaT keratinocytes express P2X and P2Y receptors (P2R). Since melittin elicited ATP release the participation of P2 receptors in melittin evoked effects were investigated. Therefore experiments were performed using the broad-spectrum P2R inhibitor pyridoxalphosphate-6-azophenyl-2′,4′,-disulfonic acid (PPADS). As shown in Figure 13 A, PPADS abolished melittin-induced ERK1/2 phosphorylation dose-dependently (upper panel). Additionally, melittin induced E-cadherin shedding was strongly reduced by PPADS to an extent comparable with marimastat effects (lower panel). This result was confirmed by the use of the broad-spectrum P2R inhibitors suramin (Figure 13 B) and Evans blue (Figure 14A). Both compounds reduced melittin-stimulated E-cadherin shedding and ERK1/2 phosphorylation in HaCaTs.

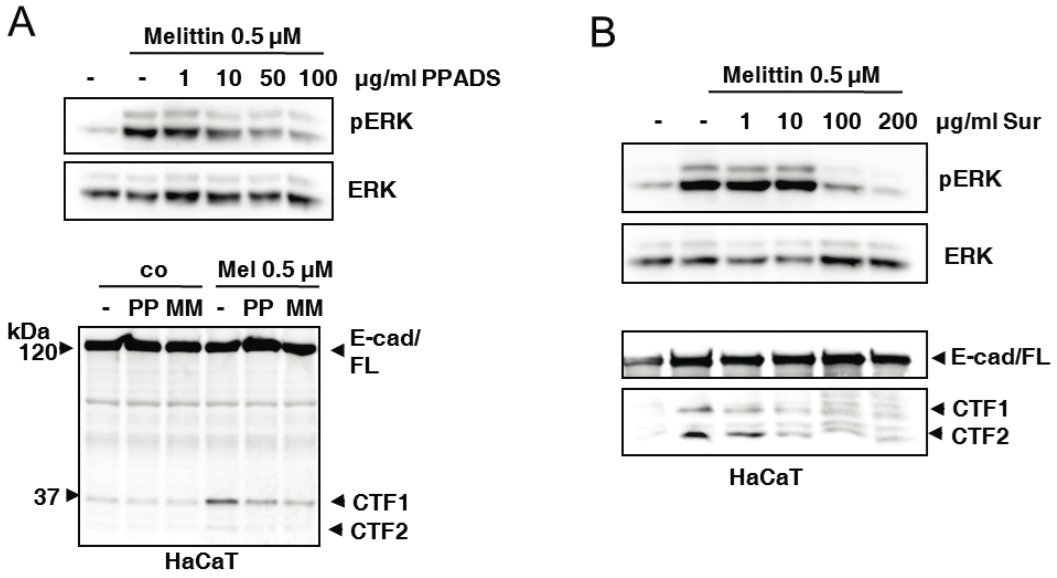

Figure 13: P2 receptor inhibitors strongly reduced melittin-stimulated shedding of E-cadherin and ERK1/2 phosphorylation HaCaT keratinocytes. A: Cells were stimulated with 0.5 µM melittin in the presence of increasing amounts of PPADS. Representative western blot analysis of ERK1/2 phosphorylation with an immunoblot of total ERK1/2 as a loading control is shown in the upper panel. PPADS (PP, 100 µM) inhibition of melittin-induced E-cadherin shedding was almost as effective as marimastat (MM, 10 µM) lower panel. **B:** The P2R antagonist suramin (Sur) decreased melittin-induced ERK1/2 phosphorylation and E-cadherin CTF generation at 100 µM and 200 µM concentrations. One representative immunoblot of three independent experiments is shown for all analyses.

To further validate the role of ATP in melittin-induced ADAM activation, HaCaTs were stimulated with melittin in the presence or absence of increasing amounts of the ATPase hexokinase. Addition of hexokinase reduced ERK1/2 phosphorylation and E-cadherin shedding dose-dependently, although the effects were not completely abrogated (Figure 14B). Human embryonic kidney 293 (HEK293) cells express only little amounts of P2Y receptors and do not express P2X receptors (Schachter et al., 1997). These cells showed a strikingly increased response to melittin stimulation when transfected with P2X7 (Figure 14 B). This response was abrogated by pretreatment with marimastat and by treatment with the ATPase apyrase. Stimulation with the P2X7 agonist benzoyl-ATP (bzATP) elicited comparable effects and was used as positive control.

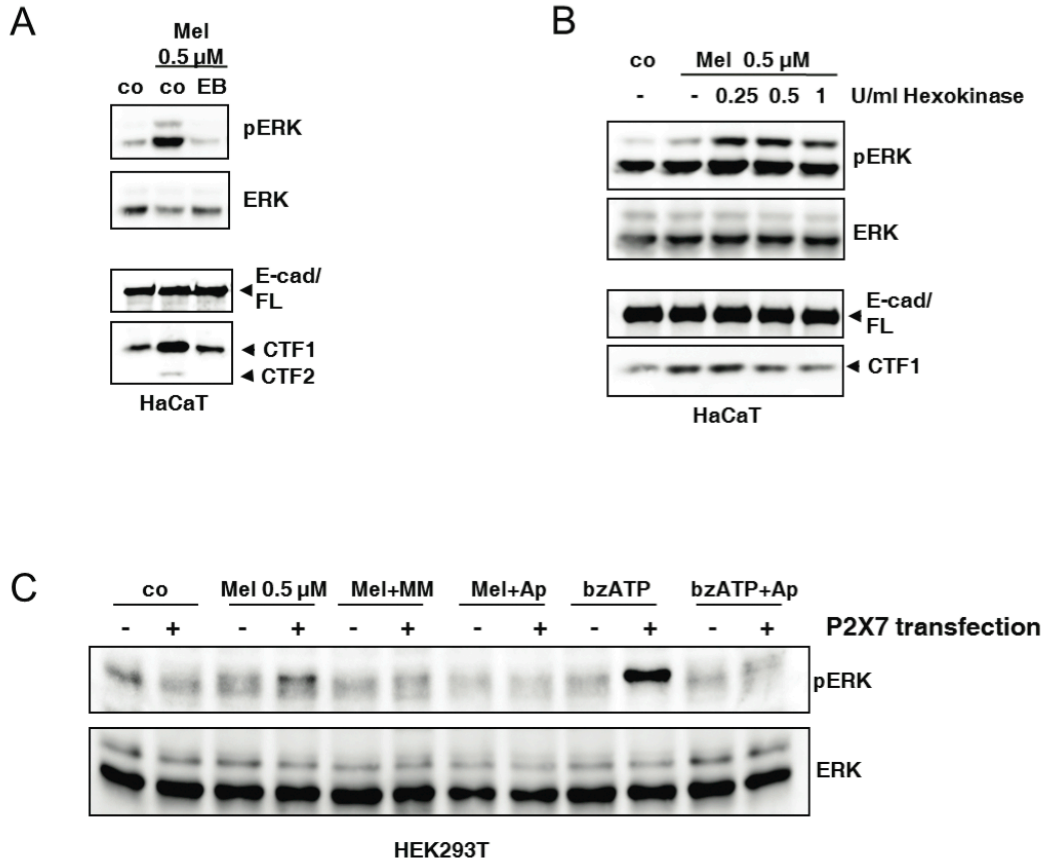

Figure 14: P2 receptor signalling is involved in activation of melittin effects in HaCaT keratinocytes. A: immunoblot analyses for ERK1/2 phosphorylation and E-cadherin C-terminal fragment (CTF) generation showed that the P2R inhibitor Evans Blue (EB, 1 µM) strongly reduced the melittin evoked effects. **B:** Cells were treated with 0.5 µM melittin for 30 min with increasing amounts of the ATPase hexokinase. Hexokinase dose-dependently reduced melittin-induced ERK1/2 phosphorylation and E-cadherin CTF generation. **C:** HEK293T cells were mock-transfected or transfected with P2X7. 48 h afterward, cells were stimulated with melittin (0.5 µM) in the presence of marimastat (MM, 10 µM) or ATPase apyrase (Ap, 2 units/ml). Stimulation with bzATP was used as positive control. Transfection with P2X7 increased melittin-stimulated ERK1/2 phosphorylation, which was abolished in the presence of Ap or MM. One representative immunoblot of three independent experiments is shown for all analyses.

4.2. The role of phosphatidylserine exposure for ADAM17-mediated proteolysis

Based on the result that melittin evokes ADAM-mediated shedding in an ATP- and P2-receptor dependent manner the hypothesis arises that PtdSer exposure could be a trigger for ADAM activation. P2 receptor activation, in particular P2X7 activation is known to induce several membrane changes including PtdSer exposure (Qu and Dubyak, 2009). The P2X7-induced PtdSer exposure can be irreversible but also transient. The transient PtdSer exposure is important for myotube formation and was additionally shown for neutrophils stimulated with chemotactic peptides (Frasch et al., 2004; van den Eijnde et al., 2001). The potential role of PdtSer exposure for ADAM activation is investigated in this second part of the thesis.

4.2.1. The ADAM10 and -17 stimulants melittin and ionomycin induce fast PtdSer exposure

To analyze if the ADAM10 and ADAM17 stimulants melittin and ionomycin promote PtdSer exposure, confocal life cell imaging experiments were performed with the PtdSer probe PSIVA-IANBD. PSIVA-IANBD is an annexin XII based polarity sensitive dye that fluoresces only when it is bound to the cell membrane. HaCaT keratinocyte were seeded in glass-bottom imaging dishes and were grown until semi-confluency. The imaging was performed with an inverted confocal microscope (Fluoview FV1000, Olympus) in a humidified atmosphere at 37° C. Cells were allowed to rest for at least one hour in the microscope stage. PSIVA-IANBD was added in a final concentration of 6.25 µg/ml 5 min before acquisition started. The dye was excited at 488 nm and emission was recorded at 520 nm every 30 s. After an initial period of 15 min melittin or ionomycin was added to a final concentration of 1 µM and the imaging was continued for further 30 min. As shown in Figure 15 A and in the supplementary movies, melittin induced a fast and transient PtdSer exposure, which spreads almost over the whole cell surface and reached a maximum between 10 and 15 min before it slowly declined. The potent ADAM activator ionomycin induced a fast PtdSer exposure in the first 5 min followed by a slight elevation of PtdSer exposure over the whole imaging period (Figure 15 B and supplementary movies). In contrast to melittin, the ionomycin-induced PtdSer exposure was permanent.

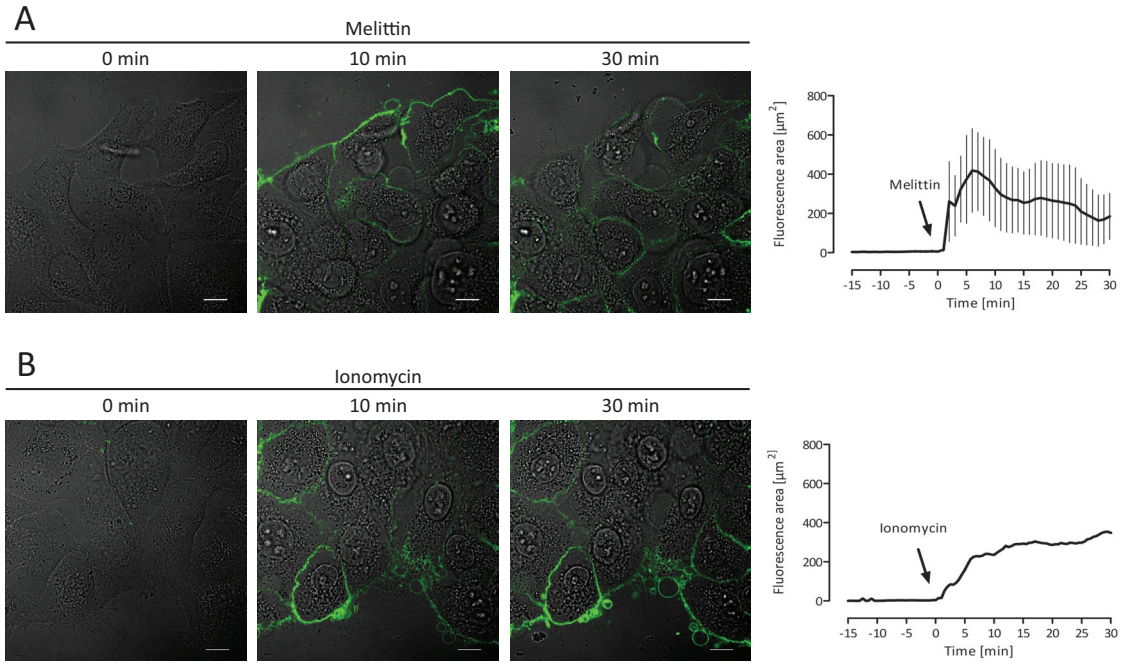

Figure 15: ADAM-activators melittin and ionomycin induce fast phosphatidylserine exposure. Confocal life cell imaging was performed with HaCaT keratinocytes in a humidified atmosphere at 37° C using the PtdSer-binding fluorescence probe pSIVA-IANBD. Melittin (1 µM, A) or ionomycin (0.5 µM, B) was added 15 min after starting the experiment. Imaging was performed for at least 30 min after addition of the stimulants. Representive images of melittin or ionomycin treated cells at different time points are shown on the left panel (bars represent 10 µm). Mean fluorescence area was calculated by using ImageJ1.47 and corrected for cell growth area (right panel, melittin n=5 ± S.E., ionomycin n=1).

4.2.2. Phosphatidylserine exposure correlates with ADAM17-mediated shedding

The strong PtdSer exposure induced by melittin or ionomycin raised the question if it correlates with ADAM-mediated shedding. Therefore, different inhibitors were used, which are known to inhibit the most important signaling pathways leading to ADAM17 activation. Cells were analyzed in parallel for PtdSer exposure and ADAM17 activity. HaCAT keratinocytes were grown on coverslips, treated with the ADAM stimulants melittin, ionomyin, PMA or FGF7 with or without the corresponding inhibitor and stained afterwards for PtdSer exposure with annexinV-FITC. In parallel, cells were treated the same way and analyzed for ERK1/2 phosphorylation as a read out for ADAM17-mediated shedding (Figure 16). As shown in Figure 16 A, melittin induced a strong PtdSer exposure in HaCaT keratinocytes. This exposure was significantly inhibited by the P2-receptor antagonist PPADS. For quantification, the mean fluorescence area was analyzed of 6-8 images of three independent coverslips for each group with ImageJ1.47 and

corrected for cell growth area. The obtained data were tested for significance with ANOVA analysis and Bonferroni multiple comparison test. In correlation to the PtdSer exposure, melittin-induced ERK1/2 phosphorylation was inhibited by the use of PPADS. Ionomycin elicited PtdSer exposure and ERK1/2 phosphorylation was inhibited with the calcium chelator EGTA (Figure 16B). The selective ADAM17 activators PMA and FGF7 induced PtdSer exposure that was punctuated in contrast to that of melittin and ionomycin (Figure 16 C and D). PMA stimulated PtdSer exposure and ERK1/2 phosphorylation was inhibited with the PKC inhibitor staurosporin. FGF7 induced PtdSer exposure and ERK1/2 phosphorylation were inhibited by the src-kinase inhibitor PP2. In summary, inhibition of ADAM17 activation correlated with inhibition of PtdSer exposure as evidenced by the analyses of ERK1/2 phosphorylation and annexin-FITC staining.

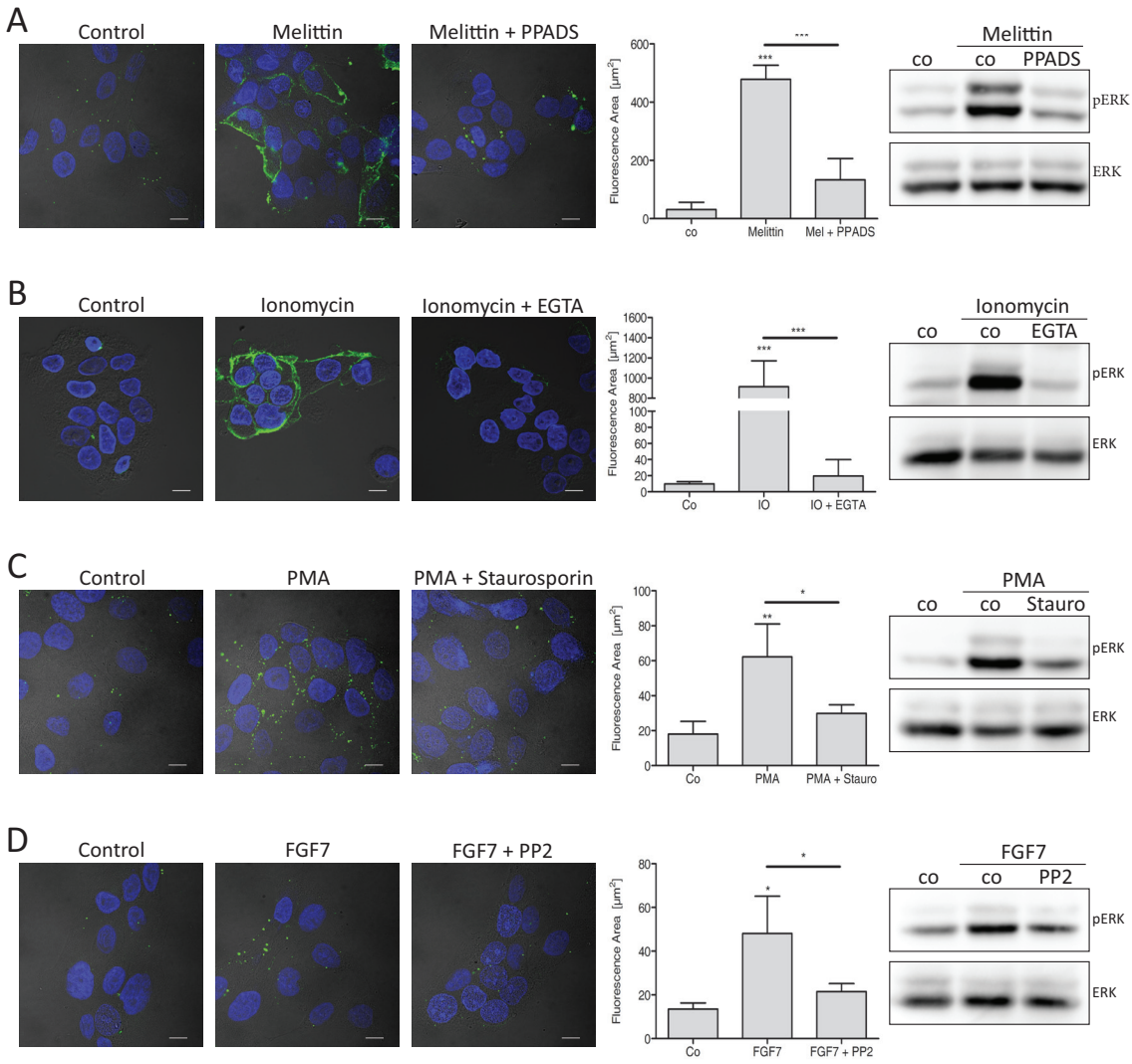

Figure 16: ADAM activators induce PtdSer exposure and correlating ERK1/2 phosphorylation. Inhibitors targeting the signaling of these stimulants decrease significantly PtdSer exposure and ERK1/2 phosphorylation. HaCaTs were grown on cover slips and mock treated (control, co), pretreated with the indicated inhibitors PPADS (100 µM), EGTA (10 mM), staurosporine (1 µM) or PP2 (10 µM) for 15 min before addition of the stimulants melittin (**A,** 1 µM), ionomycin (**B,** 1 µM), PMA (**C,** 300 ng/ml) or FGF7 (**D,** 100 ng/ml) respectively. Cells were stimulated for 15 min and immediately stained with annexinV-FITC for PtdSer exposure. Representative images of each group are shown on the left (bars represent 10 µm). Image analysis was done with ImageJ1.47m. Fluorescence area above background was determined and correlated to the cell growth area. For each group three independent coverslips, each with 6-8 images of different areas were analyzed (ANOVA, Bonferroni multiple comparison post test: *, $p<0.05$; **, $p<0.01$; ***, $p<0.001$). pERK immunoblot analysis were undertaken in parallel experiments as readout for ADAM17 sheddase function. One representative blot out of three is shown on the right side.

4.2.3. Inhibition of phosphatidylserine exposure abolish ADAM17-mediated shedding

To prevent PtdSer exposure in cells the stilbene disulfonate derivative 4,4 -diisothiocyanatostilbene-2,2-disulfonic acid (DIDS) was used. The inhibition of PtdSer translocation was verified by confocal life cell imaging with the PtdSer binding probe PSIVA-IANBD. DIDS is known as universal nonspecific Cl^--channel inhibitor that block Ca^{2+}-activated and volume-regulated Cl^- channels and anion exchangers. In cortical neurons and cardiomyocytes DIDS was shown to prevent apoptotic cell shrinkage and mildly attenuated cell death induced by various apoptotic stimuli without affecting caspase activation and DNA damage (d'Anglemont de Tassigny et al., 2008; Malekova et al., 2007; Wei et al., 2004). Beside these effects DIDS is often used as PtdSer scrambling inhibitor. It abolishes P2X7-induced PtdSer exposure and consequently CD62L shedding in lymphocytes (Elliott et al., 2005). Modulation of Ca^{2+} homeostasis may cause these effects as experiments in red blood cells (RBCs) stimulated with ionomycin indicate (Kucherenko et al., 2013). HaCaT keratinocytes stimulated with melittin (0.5 μM) and imaged with the PtdSer probe PSIVA-IANBD exhibited fast and transient PtdSer exposure (Figure 17 A). Pretreatment of HaCaT with 100 μM DIDS completely abolished melittin-induced PtdSer exposure (Figure 17 B and supplementary movies). In contrast to solely melittin treated cells, DIDS together with melittin treated cells appeared to be rounded.

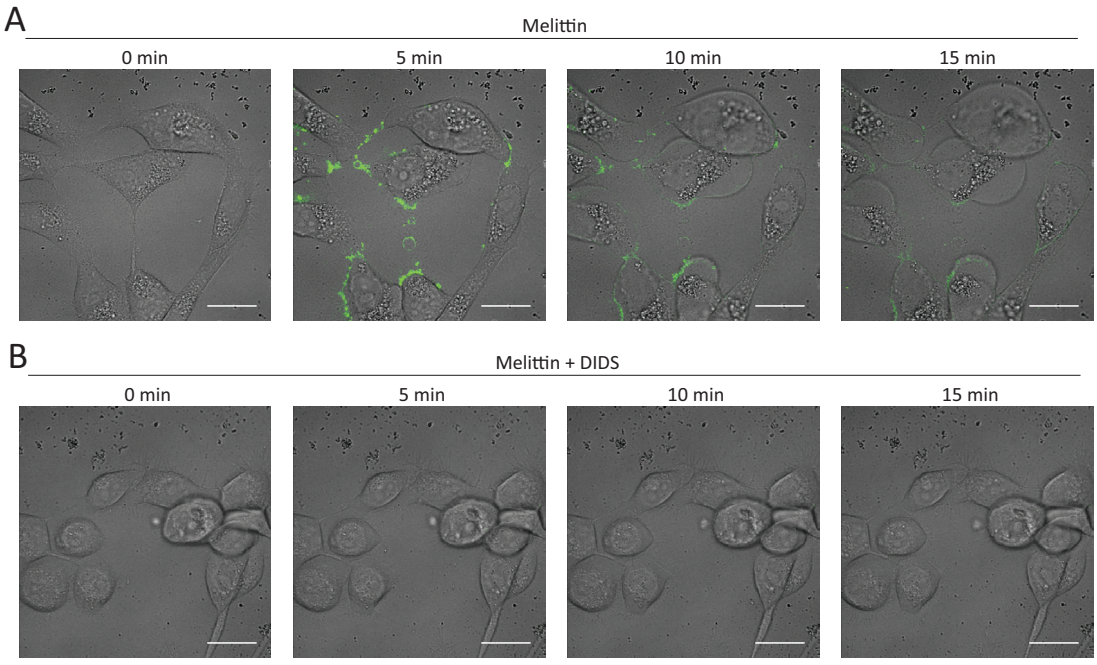

Figure 17: DIDS inhibits melittin-induced PtdSer exposure: Confocal life cell imaging was performed with HaCaT keratinocytes in a humidified atmosphere at 37° C using the PtdSer-binding fluorescence probe pSIVA-IANBD. **A**: HaCaT keratinocytes were treated with 1 µM melittin. **B:** Cells were preincubated for 10 min with DIDS (100µM) and afterwards stimulated with 1µM melittin at timepoint 0. Representive images of melittin and melittin + DIDS treated cells at different time points are shown (bars represent 10 µm).

To analyze the effect of DIDS on stimulated ADAM17-mediated shedding, HaCaT keratinocytes were stimulated in the presence and absence of DIDS and marimastat with melittin, ionomycin, PMA and FGF7 and were analysed for ERK1/2 phosphorylation. As shown in Figure 18 A, all stimuli increased ERK1/2 phosphorylation similar to what observed before. These increases in ERK1/2 phosphorylation were inhibited by preincubation with marimastat or DIDS. This indicates that DIDS may inhibit ADAM17 proteolytic function by inhibiting PtdSer exposure. This result was confirmed in HUVECs (Figure 18 B), which were stimulated in the presence or absence of DIDS or marimastat with ionomycin, PMA and the physiological ADAM stimuli thrombin and analysed for TNFR1 shedding. Again, pretreatment of the cells with marimastat or DIDS significantly reduced the stimulated shedding of TNFR1.

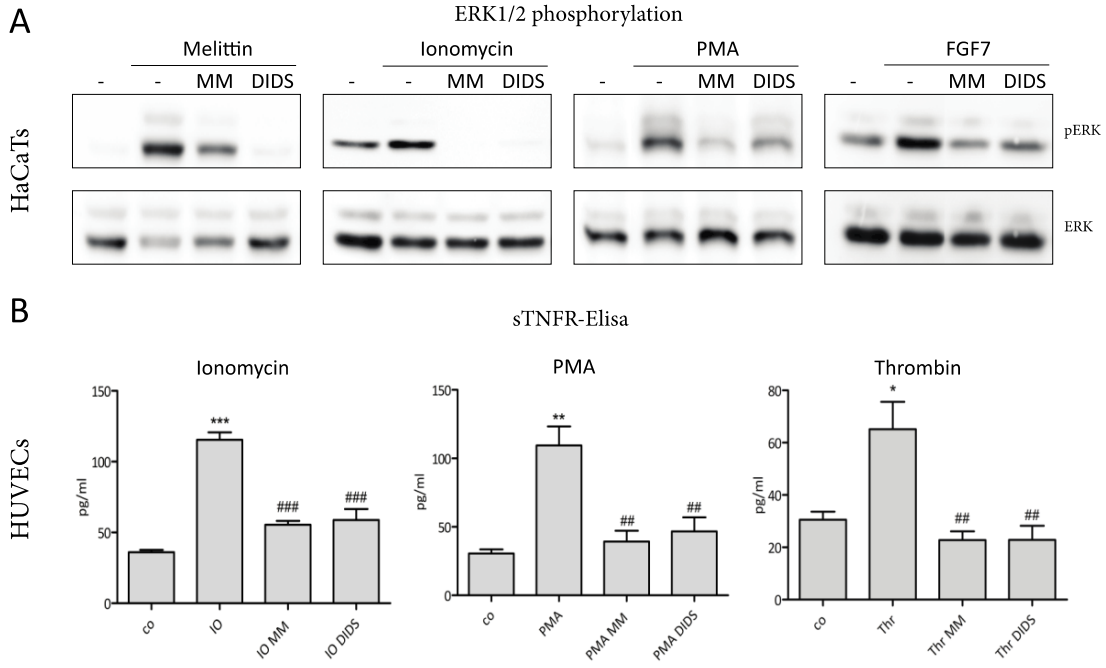

Figure 18: DIDS inhibits ADAM17-mediated ERK1/2 phosphorylation in HaCaT keratinocytes and TNFR1 shedding in HUVECs. A: HaCaTs were mock treated (-, co), pretreated with the indicated inhibitors marimastat (MM, 10 µM) or DIDS (100 µM) for 15 min before addition of the stimulants melittin (1 µM), ionomycin (1 µM), PMA (300 ng/ml) or FGF7 (100 ng/ml) respectively for 15 min. Subsequently cells were analysed for ERK1/2 phosphorylation by immunoblotting. **B:** HUVECs were mock treated (co), pretreated with marimastat (MM, 10 µM) or DIDS (100 µM) and stimulated with ionomycin (1 µM), PMA (100 ng/ml) or thrombin (Thr, 5 U) for 1 h. Conditioned supernatant was afterwards analysed for soluble TNFR1 by ELISA (n = 3, ANOVA, Boferroni multiple comparison post test: Asterisks indicate significance in stimulation, octothorps indicate significance in inhibition. */# $p<0.05$; **/## $p<0.01$; *** /###$p<0.001$.).

Due to the observed morphological changes induced by DIDS another inhibitor was used to verify the results obtained with DIDS. SITS (4-Acetamido-4′-isothiocyanato-2,2′-stilbenedisulfonic acid) is like DIDS a stilbene derivate that is used to inhibit PtdSer exposure

with comparable pharmacological properties as DIDS (Cytlak et al., 2013; Kucherenko et al., 2013). HaCaT keratinocytes exhibited less PtdSer exposure upon melittin stimulation when pretreated with SITS (Figure 19 A). To investigate if SITS also inhibits ADAM17-mediated shedding, HaCaT keratinocytes were treated with melittin (1 μM) or PMA (300 ng/ml) for 1h in the presence or absence of SITS or marimastat and analyzed for TNFR1 shedding. As expected, SITS strongly reduced TNFR1 shedding. Although the effect of DIDS and SITS on ADAM-mediated shedding and PtdSer exposure were not tested for all stimuli, cell types and read outs, the results obtained so far clearly indicate that both inhibitors can block PtdSer exposure and ADAM17-mediated shedding.

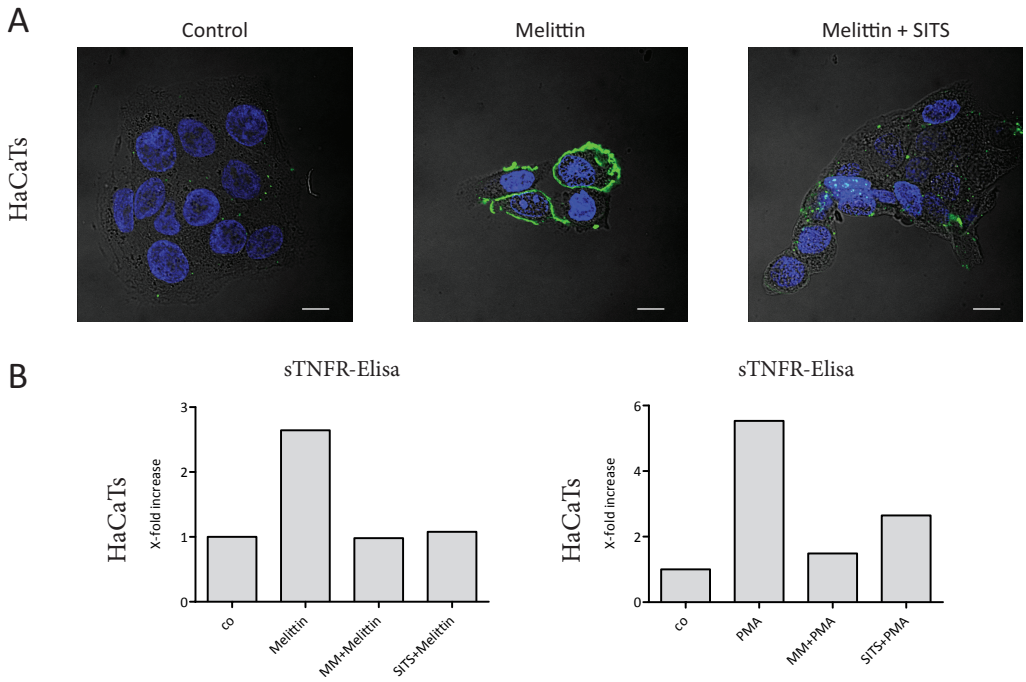

Figure 19: SITS inhibits PtdSer exposure and TNFR1 shedding in HaCaT keratinocytes. A: HaCaTs were grown on cover slips and mock treated (control), pretreated for 15 min with SITS (0.5 mM) before melittin (1 µM) was added. Cells were stimulated for 15 min and immediately stained with annexinV-FITC for PtdSer exposure. Representative images of one experiment are shown (bars represent 10 µm). **B:** HaCaT keratinocytes were mock treated (co), pretreated with marimastat (MM, 10 µM) or SITS (1 mM) and stimulated with melittin (1 µM), respectively PMA (300 ng/ml) for 1 h. Conditioned supernatant was analyzed for soluble TNFR1 by ELISA (n=1).

4.2.4. Cells defective in PtdSer synthesis exhibit reduced PtdSer externalisation and decreased ADAM17-mediated shedding of TGF-α

Mammalian cells contain two PtdSer synthases (PSS). PSS1 can synthesize PtdSer from PtdCho and PSS2 synthesizes Ptdser from PtdEtn (Figure 20). PSA3 is a mutant CHO-K1 cell line defective in PSS1 activity. When PSA3 cells are cultured in the absence of exogeneous PtdSer the cellular PtdSer level decreases (Kuge et al., 1986). This PtdSer reduction can be avoided by supplementing the cells with exogenous ethanolamine, which drives the PtdSer synthesis in an PSS2-dependent manner (Kuge and Nishijima, 1997; S. Lee et al., 2012).

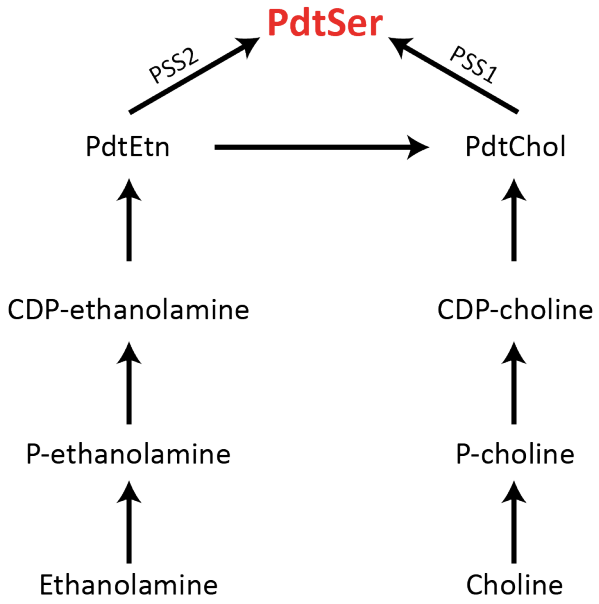

Figure 20: Biosynthetic pathway of PtdSer in mammals. Mammals contain two PtdSer synthases (PSS). PSS1 and -2 synthesize PtdSer by exchanging the headgroup of PtdCho or PtdEtn for serine. PtdEtn is generated by a multistep synthesis from ethanolamine and PtdCho from choline.

To analyze the PtdSer exposure the cells were either cultured in medium supplemented with dialyzed FCS and ethanolamine or for PtdSer reduction in medium supplemented only with dialyzed FCS. After 96 hours cells were stimulated with ionomycin or melittin and analyzed by PSIVA-IANBD live cell imaging for PtdSer exposure (supplementary movies). Representative images of starved (w/o Etn) or supplemented cells (+Etn) of ionomycin treated cells are depicted in Figure 21 A. Fluorescence area quantification of ionomycin or melittin treated cells is shown in Figure 21 B, respectively C (left side). In parallel, cells cultured identically were transfected after 72 h with TGF-α-AP and stimulated after 96 h with ionomycin or melittin. The ADAM17-mediated relative increase of stimulated TGF-α-AP shedding was determined as described. (Figure 21 B and C, right side). Starving of PSA3 cells resulted in less PtdSer exposure

and in significantly reduced TGF-α-AP processing compared to unstarved cells after stimulation with ionomycin or melittin (Figure 21).

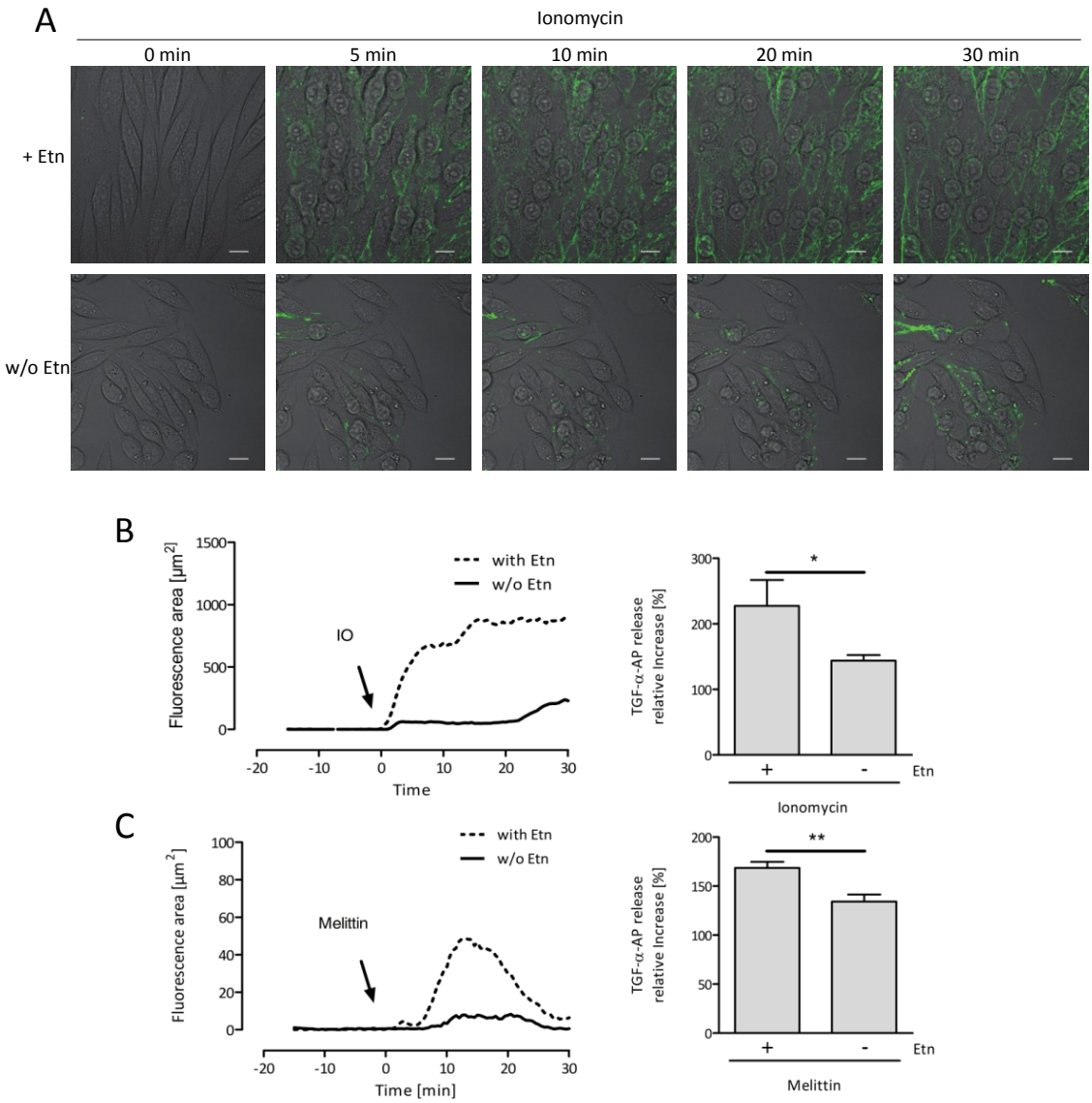

Figure 21: Starved PSA3 cells show decreased PtdSer exposure upon stimulation and decreased ADAM17 activity. PSA3 cells were PtdSer deprivated by starving in HamsF12 medium with 6% dialyzed FCS with or without ethanolamine for 96 h. **A:** Representative images of unstarved (+Etn) or starved (w/o Etn) PSA3 cells stimulated with ionomycin (1 µM) and analysed with pSIVA-IANBD confocal life cell imaging for PtdSer exposure (bars represent 10 µm). **B and C:** Fluorescence area quantification of starved and unstarved ionomycin (B) or melittin (C) treated PSA3 cells, stained with the PtdSer probe pSIVA-IANBD (left side). In parallel starved and unstarved TGF-α-AP transfected PSA3 cells were analyzed for ADAM17-dependent TGF-α-AP processing upon stimulation and compared to untreated controls (right side, unpaired t-test: *, $p< 0.05$; **, $p< 0.01$).

4.2.5. Structural basis for ADAM17-phosphatidylserine interaction

ADAM17 sheds its substrates directly above the cell surface. A hypothetic interaction of ADAM17 with PtdSer could pull down the metalloprotease domain ensuring the correct positioning of the protease to the substrate. Proteins that bind to acidic phospholipids often share some specific characteristics. This includes pattern of polybasic amino acids near to a membrane anchor. To validate if ADAM17 fulfills these criteria the sequences of acidic phospholipid binding proteins were compared with the sequence of ADAM17. As shown in Table 19 the membrane proximal domain of ADAM17 contains several basic amino acids. This pattern resembles the motifs of other acidic phospholipid binding proteins, for example Raf-1.

Table 19: Sequence comparison of ADAM17 and proteins binding to acididc phospholipids. The amino acid sequence of the membrane proximal domain of ADAM17 (MPD17) is compared to sequences of proteins that are able to bind to acidic phospholipids. Basic amino acids are marked in blue.

Protein	Polybasic sequences binding to acidic phospholipids
MPD17	^{581}FCKREQELESCACVDTDNSCKVCCRNLSGPCVPYVDAEQKNLFLRKGKPCTVGFCDMNGKCE^{642}
Raf-1	^{141}FARKTFLKLAFCDICQKFLLNGFRCQTCGY^{170}
Rac1	^{171}EAIRAVLCPPPVKKRKRKCL^{190}
Src	^{2}GSSKSKSKPKDPSQRRR^{16}
RALA	^{184}SKEKNGKKKRKSLAKRIRECCIL^{206}
EGFR	^{645}RRRHIVRKRTLRRLLQ^{660}
MARCKS	^{145}KKKKKRFSFKKS^{156}
K-Ras4B	^{174}GKKKKKKSKTSC^{185}
HIV-1 Gag	^{2}GARASVLSGGELDRWEKIRLRPGGKKKYKL^{31}

The membrane proximal domain of ADAM17 exists in two forms, the flexible/open and the inflexible/closed conformation. The three-dimensional structure of the closed MPD was solved by heteronuclear NMR spectroscopy by Düsterhöft et al. in 2013 (Figure 22 A, right side). Due to the flexibility of the open conformation in the lower PDI-sensitive part ($C_{600}XXC_{603}$) no NMR structure is solved. To get an idea about how the charges of the MPD could be distributed, the structures of the human and murine MPD were analyzed for electrostatic potentials. The structures were prepared with the PDB2PQR tool of the UCSF chimera software package using the CHARMM force field method and the electrostatic potential map was calculated with the Adaptive Poisson-Boltzmann Solver (APBS) (Baker et al., 2001; Dolinsky et al., 2007; 2004; MacKerell et al., 1998; Unni et al., 2011). Even though the calculations were performed with the closed conformation of the MPD, the electrostatic surface coloring indicates that the basic amino acids $R_{625}K_{626}XK_{628}$ in the flexible part may contribute to PtdSer binding through electrostatic interaction (Figure 22 B and C).

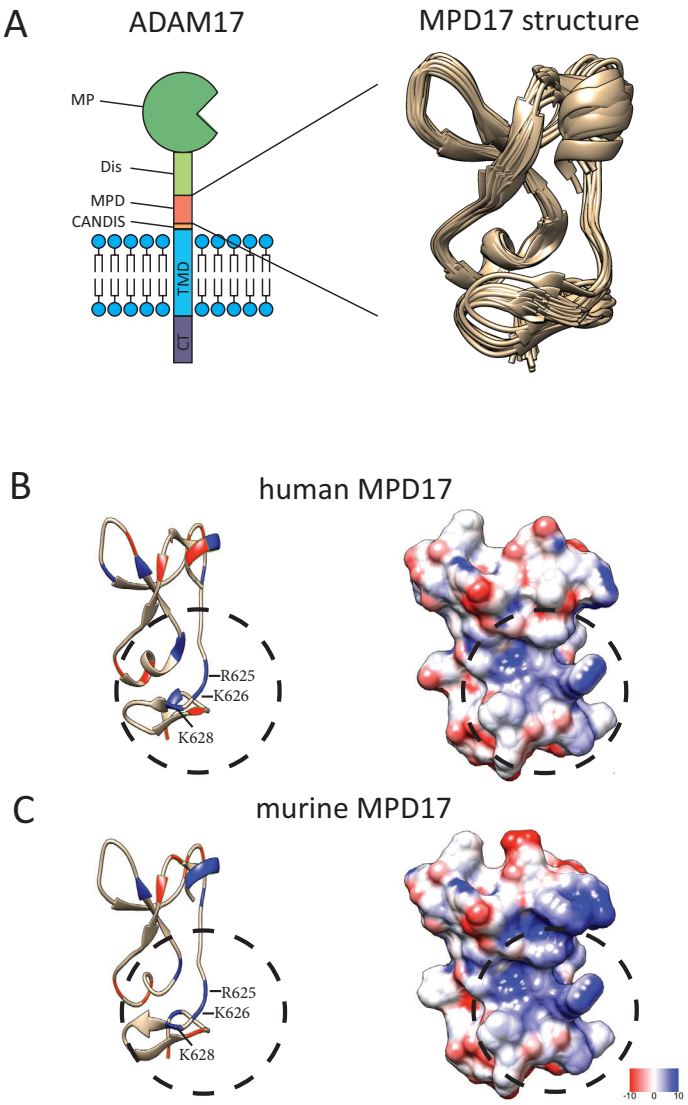

Figure 22: Structure and electrostatic potential of the closed membrane proximal domain of ADAM17. A: Schematic model of ADAM17 (MP: metalloprotease domain; Dis: disintegrin-like domain; MPD: membrane proximal domain; CANDIS: conserved ADAM17 dynamic interaction sequence; TMD: transmembrane domaine; CT: cytotail) and the three-dimensional structures of the closed conformation of the MPD resolved by Düsterhöft et al., 2013. **B and C**: Left side: structure of the human and murine MPD with positively charged amino acids in blue and negatively charged amino acids in red. Right side: electrostatic surface map of the human and murine MPD. The structures were prepared with the PDB2PQR tool of the UCSF chimera software package using the CHARMM force field method and the electrostatic potential map was calculated with the Adaptive Poisson-Boltzmann Solver (APBS). Electrostatic potential is shown as gradient from -10 (red) to +10 (blue). The polybasic motif ($R_{625}K_{626}XK_{628}$), which is located in the flexible part, is highlighted with dashed black circles.

4.2.6. The membrane proximal domain of ADAM17 binds to phosphatidylserine

Assuming that the PtdSer interactions take place in the membrane proximal domain of ADAM17 the interaction of recombinant MPD with PtdSer and PtdCho liposomes was analyzed. In cooperation with C. Nehls and T. Gutsmann (FZ Borstel, Department of Biophysics) isothermal titration calorimetry (ITC) and surface acoustic wave (SAW) measurements were performed. In the ITC experiments the MPD was titrated with PtdSer-liposomes or with PtdCho:PtdSer (9:1) liposomes. As shown in Figure 23 A, titration of the open MPD with PtdSer liposomes led to an exothermic reaction, as indicated by a downward signal at every titration step. This indicates a considerable reactivity of the MPD with PtdSer liposomes, whereas this reaction is significantly lower when titrating with PtdCho-liposomes. Interestingly, conversion of the open MPD to a closed confirmation by PDI treatment, almost completely abrogated PtdSer liposome interaction (Figure 23 B), indicating that the PtdSer binding motif is located in the N-terminal flexible part of the MPD.

The binding of the open MPD to PtdSer was confirmed by surface acoustic wave biosensor measurements (Figure 23 C). In short, SAW chips were coated with the indicated liposomes and buffer containing the MPD was applied. An increase in the amplitude signal indicates a higher mass loading of the chip, indicating a binding of the MPD to the liposomes. The amplitude and phase shift diagram shows that the MPD interacts with PtdSer liposomes but not with PtdCho liposomes. Unspecific protein binding to the chip surface was ruled out by using BSA as negative control.

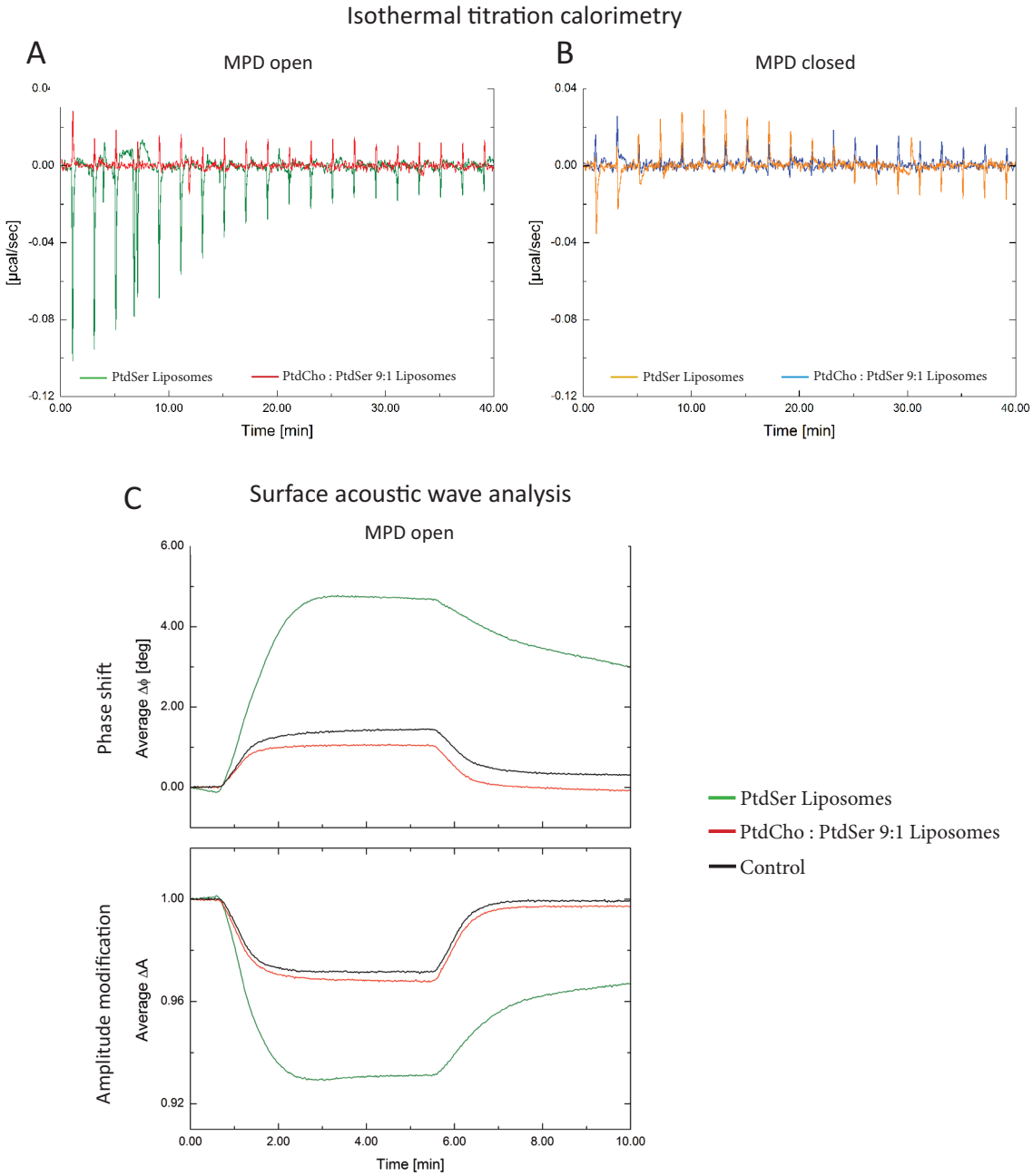

Figure 23: The membrane proximal domain of ADAM17 binds to Ptdser. A and B: Isothermal titration calorimetry measurements to study the interaction of the open (A) and closed (B) form of the MPD with either PtdSer (green) or PtdCho (red) liposomes. The MPD (0.5 mM dissolved in 5 mM HEPES, pH 7.4) was titrated 20 times in 1.5 µl injections into 250 µl of the respective lipid solution (0.1 mM dissolved in 5 mM HEPES, pH 7.4) at 22 °C and the heat of the interaction were recorded. The final lipid:protein ratio was 5:3 [M:M]. An upwards signal indicates a exothermic reaction of the open MPD with PtdSer liposomes. **C:** Binding of the open form of the ADAM17 MPD to the CM-dextran/PLL functionalization of sensor chip surfaces (black) and to additionally immobilized PtdSer membranes (green) or to PtdCho:PtdSer (9:1) membranes (red) in SAW biosensor experiments. Shown is the average phase shift ΔΦ (top) of five individual sensor channels indicating a mass loading on the surface and the average amplitude shift ΔA (bottom) indicating a decrease of viscosity. (Lena Heinbockel and Christian Nehls from FZ Borstel performed these experiments).

4.2.7. O-Phospho-L-serine inhibits ADAM17 activation

Phosphatidylserine consists of diacylglycerol, saturated or unsaturated fatty acids and the hydrophilic phosphoserine headgroup. When ADAM17 activation is due to direct interaction with PtdSer in the membrane, the exogenously applied soluble headgroup of PtdSer O-phospho-L-serine (OPLS) should inhibit ADAM17 activation competitively. To test this hypothesis, HaCaT keratinocytes were stimulated in the presence or absence of increasing amounts of OPLS, or the headgroup oft PtdCho phosphocholine (PC) and analyzed for ADAM17-dependent ERK1/2 phosphorylation (Figure 24 A). To verify that ERK1/2 phosphorylation was metalloprotease dependent, the general metalloprotease inhibitor marimastat (MM) was used as an additional control. As shown in Figure 24 A, PMA-induced ERK1/2 phosphorylation was dose-dependently inhibited with OPLS and a complete inhibition were observed with 10 mM. In contrast to OPLS, PC had no effect on PMA-induced ERK1/2 phosphorylation. To confirm this result, primary umbilical vein endothelial cells (HUVECs) were stimulated with PMA, ionomycin or melittin in the presence or absence of OPLS or PC and the supernatant was analyzed for soluble TNFR1 (Figure 24 B). The membrane receptor TNFR1 is a substrate for ADAM17 and is shed after ADAM17 activation (Reddy et al., 2000). Stimulation of the cells with the indicated stimuli led to a 4- to 8-fold increase of soluble TNFR1 in the supernatant. This increase was significantly inhibited in the presence of OPLS, but not with PC (Figure 24 B).

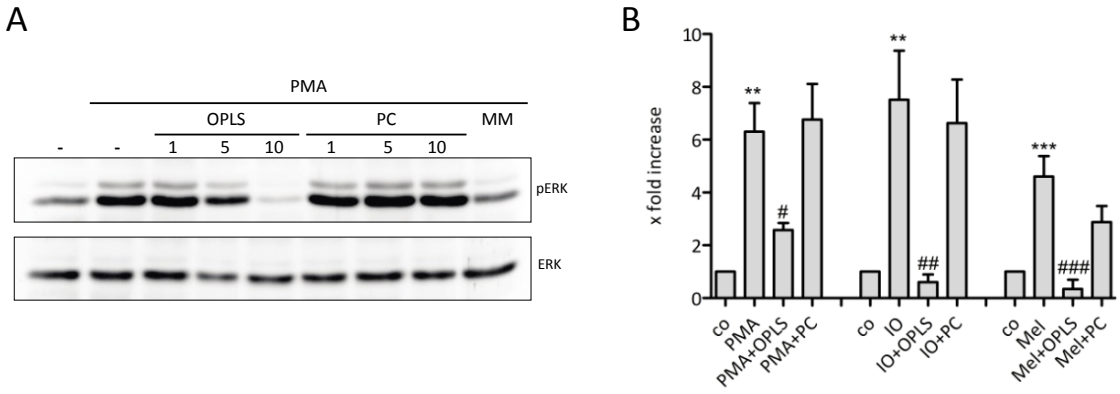

Figure 24: Competition of ADAM17-phosphatidylserine interaction abrogates ADAM17 activity. A: HaCaT keratinocytes were stimulated with PMA (300ng/ml) for 30 min and subsequently analyzed for ADAM-dependent ERK1/2 phosphorylation by immunoblot. PMA-induced ERK1/2 phosphorylation was dose-dependently reduced by addition of the PtdSer headgroup O-phospho-l-serine (OPLS). In contrast, phosphocholine (PC), the headgroup of PtdCho, did not reduce ERK1/2 phosphorylation. One representative immunoblot out of three is shown. **B:** Primary endothelial cells (human umbilical veine endothelial cells, HUVECs) were analyzed for ADAM17-dependent TNFR1 shedding by ELISA. PMA (200ng/ml), ionomycin (IO, 1 µM) and melittin (Mel, 1 µM) induced a strong increase in TNFR1 shedding measured after 1 h that was significantly inhibited with OPLS (10mM) but not with PC (10mM) (n = 5, ANOVA, Boferroni multiple comparison post test: Asterisks indicate significance in stimulation, octothorps indicate significance in inhibition. */# $p<0.05$; **/## $p< 0.01$; ***/### $p<0.001$).

4.2.8. The polybasic motif $R_{625}K_{626}XK_{628}$ of ADAM17 is necessary for stimulated and constitutive shedding of TGF-α

The electrostatic modeling and the finding that the open, but not the closed form of the MPD bind to PtdSer indicates that the polybasic motif $R_{625}K_{626}XK_{628}$ could be responsible for ADAM17 PtdSer interaction. This motif is located in the N-terminal flexible part of the MPD in close proximity to the CANDIS and the transmembrane domain. To verify if this motif is involved in modulating ADAM17 activity, the basic amino acids were substituted with glycine by site-directed mutagenesis in a murine ADAM17 plasmid. This mutant (A17 3x) was transfected in ADAM17 and ADAM10 double-deficient murine MEFs. These cells were analyzed for constitutive and stimulated shedding of TGF-α-AP (Figure 25 A-C). The mutagenesis and in parts the AP-assays were done by F. Kordowski (Institute of Dermatology and Allergology, UKSH Kiel; as part of his work as PhD student). The ADAM17 stimulant PMA induced a strong increase in TGF-α-AP release in wildtype ADAM17 transfected cells. The A17 3x mutant lost its ability to shed TGF-α-AP almost completely in a manner that was comparable to that of the inactive E/A ADAM17 variant (Figure 25 A). Additionally, melittin and ionomycin induced TGF-α-AP processing was significantly lower compared to wildtype ADAM17 (Figure 25 B). To answer the question if only the stimulated shedding is affected by the mutated polybasic motif, the constitutive TGF-α-AP processing was determined over 6 h. As shown in Figure 25 C the constitutive shedding of the 3x mutant is almost completely abolished to an extent comparable to the E/A mutant. In summary, despite a similar expression level (not shown), the 3x mutant loses the ability to shed TGF-α-AP. TGF-α-AP resembles the natural occurring ADAM17 substrate TGF-α, which is a transmembrane protein that is cleaved in close proximity to the membrane. To elucidate if the 3x mutant is still proteolytically active, experiments with a soluble metalloprotease substrate were performed. This peptide is based on the TNF-α sequence and carries a quenched fluorophore that can be detected after cleavage. ADAM17 wildtype, 3x and the E/A variant were overexpressed in highly transfectable Cos-7 cells and incubated for 6 h in the presence of the fluorogenic substrate. As shown in Figure 25 D, overexpression of the 3x mutant increased the substrate processing almost to the same level as wildtype ADAM17, indicated by an increase in fluorescence. Overexpression of the E/A variant did not increase substrate processing. The increase of fluorescence was metalloprotease-dependent as shown by the inhibition with marimastat.

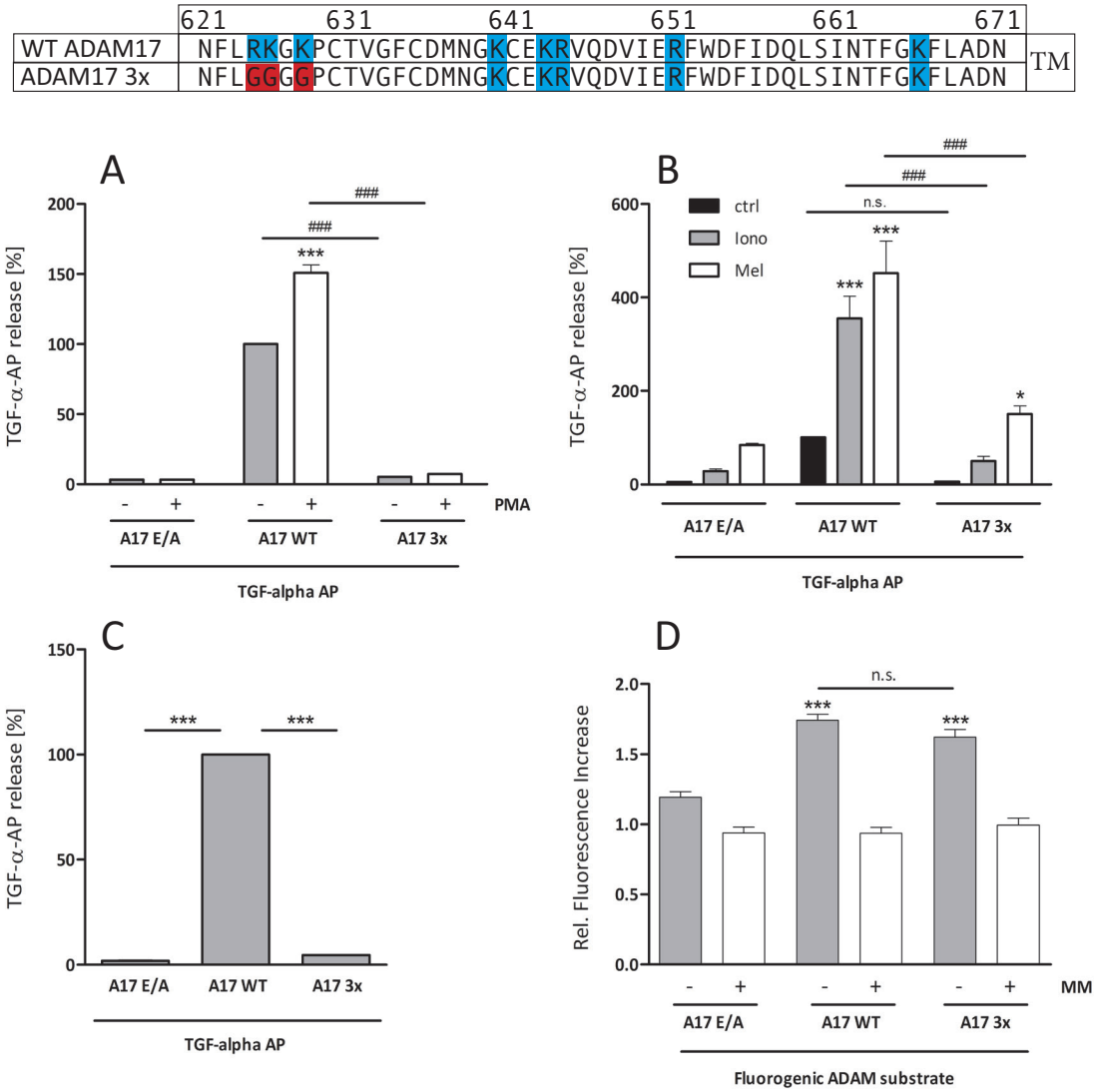

Figure 25: ADAM17 lacking the polybasic motif (R625, K626, K628) loses the ability to shed the transmembrane substrate TGF-α even though it is able to cleave soluble peptides. The inactive murine ADAM17 variant E/A, the wildtype murine ADAM17 or the mutated murine ADAM17 3x (R625, K626, K628, each substituted to G; upper scheme) were transfected together with TGF-α-AP to ADAM10 and -17-deficient murine embryonic fibroblasts (**A-C**, performed by F. Kordowski; Institute of Dermatology and Allergology, UKSH Kiel). The TGF-α-AP shedding rate was determined after 2 h of PMA stimulation (200 ng/ml; **A**), 1 h of melittin (1 µM) or ionomycin (1 µM; **B**) or after 6 h of untreated cells (**C**) and compared to their related controls (ADAM17 wt transfected, untreated cells). **D:** Cos7 cells were transfected with ADAM17 E/A, wt or 3x respectively and incubated with a soluble fluorogenic ADAM substrate with or without marimastat (MM, 10 µM). The fluorescence of the cleaved peptide in the supernatant was measured after 6 h of incubation and compared to untransfected cells. The data show the mean ± S.E. of 5 independent experiments and were testet for statistical significance with ANOVA Boferroni multiple comparison post test (Asterisks indicate significance in stimulation, octothorps indicate significance in inhibition. */# $p < 0.05$; **/## $p < 0.01$; ***/### $p < 0.001$).

5. Discussion

5.1. Melittin modulates keratinocyte function through P2-receptor-dependent ADAM activation

The bee venom component melittin has been discussed as promising supplement for anti-microbial, anti-inflammatory and anti-cancer therapy (Duclohier, 2010; Oršolić, 2012). It was shown that melittin selectively destroys cancer cells in vitro and it was tested in animal models for hepatocellular carcinoma, breast cancer and prostate cancer, with positive outcome (Liu et al., 2008; Son et al., 2007). Other investigations revealed that melittin enhances permeability in CaCo-2 epithelial cell monolayers and that melittin provokes proliferation of gastrointestinal cells (Maher et al., 2007; Maher and McClean, 2008). Both are physiological events that are often associated with ADAM-mediated shedding of cell adhesion molecule and release of EGFR-ligands. Therefore, the aim was to investigate the effects of melittin on ADAM-mediated substrate release and consecutively the functional consequences. It is demonstrated that subcytotoxic melittin concentrations evoked a rapid up-regulation of ADAM10 and -17 functions in different celltypes. This was mediated by ATP-release from the cells and subsequent P2-receptor activation. In HaCaT keratinocytes, this finally lead to the functional consequences of de-adhesion, migration and proliferation.

5.1.1. Melittin in sublethal concentration induces ATP-release from cells

Little is known about the molecular mechanisms of the melittin action. A cellular receptor is not known to exist, instead melittin binds via its cationic domain to the membrane and this is followed by membrane insertion of the hydrophobic part (Dawson et al., 1978). Additionally, melittin induces the release of marker molecules from liposomes (Sessa et al., 1969). In analogy with poreforming toxins, this could indicate that melittin oligomers may be able to form transmembrane pores. Consistent with this theory, it is shown in this thesis, that melittin, even in sublethal dosages, evoked ATP-release in a nanomolar concentration range. However, how ATP is released and how sufficient concentrations of ATP should accumulate to trigger P2-receptor response is not clear. Different mechanisms are known to trigger ATP-release from cells. To these belong stretch, osmolarity changes, oxidative stress and microbial products (Schwiebert and Zsembery, 2003). In conclusion, beside the possible pore-forming properties of melittin, ATP-release could also occur as a normal physiological stress response. Moreover, P2X7 activation leads to Pannexin-1 pore formation through which ATP release could occur, so that a self-amplifying activation loop may be created (Baroja-Mazo et al., 2013).

5.1.2. Melittin induces ADAM-dependent substrate cleavage

This investigation focuses on the two major members ADAM10 and -17 of the ADAM family. Subtoxic melittin treatment enhanced substrate processing of both proteases. In different cell types cadherins, a classical ADAM10 substrate family, were cleaved after melittin stimulation. To these belong N-cadherin in MEFs, VE-cadherin in endothelial cells and E-cadherin in HaCaT keratinocytes. Shedding of N-cadherin results in diminished adhesive behavior and redistribution of β-catenin in the cells (Reiss et al., 2005); cleavage of VE-cadherin increases vascular permeability and leukocyte transmigration (Schulz et al., 2008); shedding of E-cadherin provokes loss of epithelial cell-cell contacts and is associated with eczematous dermatitis (Maretzky et al., 2008; 2005). The result that ADAM10 is responsible for the melittin-induced N-cadherin cleavage was confirmed by the use of ADAM10-deficient MEFs, which showed no shedding of N-cadherin upon melittin stimulation. These findings that melittin induces ADAM10-mediated cadherin cleavage would provide retrospectively an explanation for the report that melittin enhances permeability of CaCo-2 epithelial cell monolayers (Maher et al., 2007). Besides ADAM10 activation, melittin stimulation also provoked processing of ADAM17 substrates. In HaCaT keratinocytes soluble TGF-α was ADAM17-dependent significantly increased after melittin stimulation. Additionally, also in leukocytes melittin stimulated shedding of the ADAM17 substrate L-selectin. These data together indicate that melittin truly can be seen as an ADAM10 and -17-activator, that works independent of the cell type and the kind of substrate. Further analysis is required to reveal if melittin is a broad-spectrum metalloprotease activator not only affecting ADAM10 and -17.

5.1.3. Melittin induces keratinocyte proliferation and migration

ADAM17 sheds a large subset of substrates. To these belong inter alia the EGFR ligands TGF-α, HB-EGF and amphiregulin (Sahin et al., 2004). Activation of the EGFR cascade causes cell proliferation and migration (Koivisto et al., 2006). Melittin induced shedding of TGF-α in HaCaT keratinocytes. This resulted in EGFR and subsequently ERK1/2 activation. Since all EGFR ligands are released through proteolysis, it is quite likely that also other ligands contribute to the observed EGFR activation. In any case functional consequences would follow. The functional consequences were confirmed by proliferation and migration analyses of melittin stimulated HaCaT keratinocytes. Both were significantly enhanced in a metalloprotease and EGFR-dependent manner. This is of particular interest because melittin is considered as a anti-tumor agent (Duclohier, 2010; Oršolić, 2012). Detailed analysis using specific inhibitors or siRNA would be required to determine the proportion of ADAM10 and -17 or even additional proteases to these processes. Nevertheless, melittin in subcytotoxic concentrations evoked proliferation

and migration in these cells. This finding is in line with the reported melittin-induced proliferation of gastrointestinal cells (Maher and McClean, 2008). With regard to the usefulness of melittin as anti-cancer agent, these results bring these approaches into question.

5.1.4. Melittin effects depend on ATP-release and P2-receptor activation

Different approaches were undertaken to elucidate the pathway leading to ADAM activation by melittin. Biophysical membrane properties may participate in controlling ADAM function by influencing the velocity of molecular movements in the lipid bilayer. Enhancement of membrane fluidity by free unsaturated fatty acids increases ADAM-mediated substrate processing (Reiss et al., 2011). Although melittin is known to disturb membranes, no changes in membrane fluidity were observed. A prime candidate for ADAM-activation is intracellular calcium elevation (Horiuchi et al., 2007b; Le Gall et al., 2010). It was already shown that melittin induces Ca^{2+}-influx and PLA_2-activation in ras-transformed cells (Sharma, 1993). In this thesis, melittin induced dose-dependently cytosolic Ca^{2+}-elevations by extracellular influx and by depletion of intracellular Ca^{2+}-stores. Interestingly, neither chelation of intracellular or extracellular Ca^{2+} was sufficient to prevent ADAM-mediated substrate processing. Although not shown, inhibition of PLA_2, PLC and PKC did not prevent ADAM-mediated substrate shedding. The fact that ATP is released after melittin treatment and that P2-receptors can contribute to ADAM function turned the focus to these receptors. It was shown that ADAM-dependent shedding of L-selectin and CD23 from human leukemic B-cells is inducible by extracellular ATP (Gu et al., 1998; Jamieson et al., 1996). Additionally, P2X7 is responsible for inducing cleavage of CD23 and CD27, two important mediators of the immune system (H. Moon et al., 2006; Sluyter et al., 2007). In those studies, supra-physiological ATP concentrations were used to stimulate ADAM-mediated functions. This point differs from the mechanism of melittin-induced ADAM-mediated shedding proposed here. Melittin in subtoxic concentrations induced ATP release at nanomolar concentrations. Concentrations, which would not be sufficient to induce ADAM-mediated shedding in experiments with extracellular applied ATP. However, since the cells themselves release ATP, it is probable that the local ATP concentration at the cell surface is much higher before it gets diluted in the supernatant. Three lines of evidence proved the involvement of ATP and P2-receptors in melittin-induced ADAM function. At first, PPADS, Evans blue and suramin, three commonly employed inhibitors of purinergic receptors suppressed melittin-mediated ADAM activation. Second, transfection of P2X7 in HEK293 increased melittin-induced ADAM function. Third, the melittin-induced ADAM-mediated shedding was reduced in the presence of ATPases.

Although not very specific, PPADS, Evans blue and suramin are commonly used to inhibit P2-receptors (Lambrecht, 2000; Ralevic and Burnstock, 1998). Whereas suramin and Evans blue block P2-receptor in general, PPADS exhibits more specifity towards P2X-receptors. To further validate the role P2-receptors in melittin-induced ADAM function P2X7 was transfected into HEK293 cells. Hek293 are widely used as model to investigate the role of P2-receptors, because they express only low amounts of P2Y receptors and do not express P2X receptors (Schachter et al., 1997). Overexpression of P2X7 in Hek293 remarkably increased the response to melittin stimulation. This indicates that at least P2X7 is important for the melittin-induced ADAM-activation. Due to the diversity and complexity of the purinergic receptor families, no further analyses were done to elucidate the contribution of individual receptors to the melittin-evoked effects. Most likely other P2 receptor contribute to the melittin response, eventually by modulating the signals leading to ADAM activation. One study highlights the role of P2Y2 in modulating intracellular Ca^{2+} responses to inflammatory stimuli. Rowlands et al. demonstrated that P2Y2 prolonged mitochondrial Ca^{2+} elevations in mouse lung micro vessels upon TNF-α stimulation and that this contributed to ROS generation and TNFR1 shedding (Rowlands et al., 2011). Additionally, the contribution of ROS to the melittin-induced ADAM activation cannot be excluded. Melittin can induce release of ROS and ROS can activate ADAM-mediated shedding (Myers et al., 2009; Stuhlmeier, 2007).

The role of ATP in the melittin-induced P2-receptor response was demonstrated by addition of ATPases to melittin treated cells. The different ATPases apyrase and hexokinase both reduced melittin-induced ERK1/2 phosphorylation. The ERK1/2 phosphorylation was not completely abrogated by ATPases, indicating that either the sufficiency was not enough or other additional mechanisms may play a role. One report suggests that melittin additionally interacts directly with transmembrane proteins (Keith et al., 2011). It might be speculated that direct binding of melittin to P2 receptors can occur to modulate their activation. A similar mechanism has been proposed for the antimicrobial peptide LL37 (Wewers and Sarkar, 2009). The studies on the role of this peptide in P2-receptor and EGFR activation showed striking similarities with the melittin-induced effects described here (Tokumaru et al., 2005; Tomasinsig et al., 2008). Both induce transient ATP release in the absence of overt cytotoxicity (Elssner et al., 2004). Both induce functions which are P2-receptor dependent and at least, both exhibit migration and proliferation promoting functions (Tokumaru et al., 2005; Tomasinsig et al., 2008).

5.1.5. Model of melittin evoked ADAM10 and -17-mediated substrate release

In conclusion, it was shown in this investigation that melittin in subcytotoxic concentrations is a general ADAM10 and -17-mediated shedding activator. This downstream event of melittin

leads to diverse functional consequences depending on the cell target. In HaCaT keratinocytes melittin induces de-adhesion, migration and proliferation, which puts the therapeutic potential of melittin as an anti-cancer agent into question. Since ADAM17 is the prime TNF-α processing enzyme, the anti-inflammatory potential of melittin should also be reconsidered. The proposed model of melittin-stimulated effects is depicted in Figure 26.

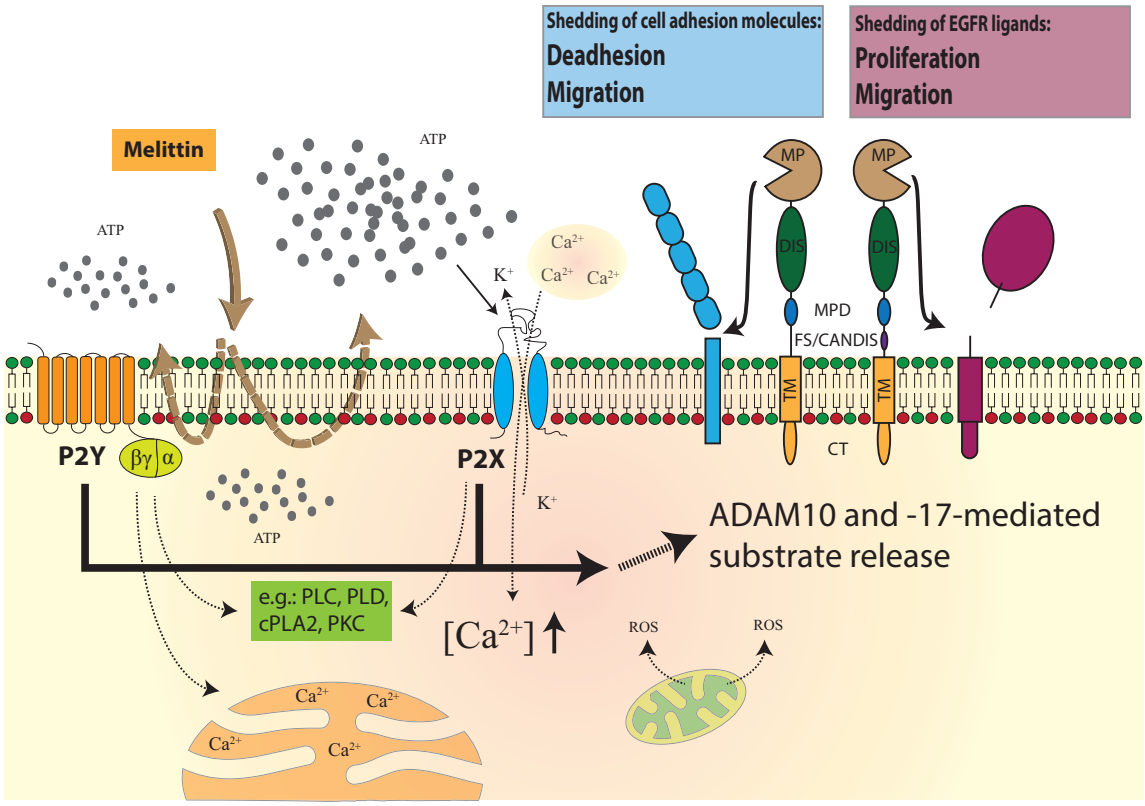

Figure 26: Melittin induces ADAM10- and -17-mediated substrate processing in an ATP and P2-receptor dependent manner. Melittin stimulation leads to ATP egress, which in turn activates P2X and P2Y receptors. Activation of these receptors induces multifaceted signaling cascades. To these belongs for example intracellular Ca^{2+}-elevation, Phospholipase activation (e.g. PLC, PLD, $cPLA_2$), protein kinase activation (e.g. PKC), K^+-efflux and mitochondrial ROS generation. Through not yet defined mechanisms ADAM10 and -17 are than activated and shed their substrates. These substrates can be cell-adhesion molecules and EGFR-ligands. Shedding of these substrates leads to the functional consequences of de-adhesion, proliferation and migration.

Melittin evokes its effect by releasing ATP from the cells by a mechanism that is not yet fully solved. One possibility is that melittin forms pores by which ATP egress. This ATP would activate purinergic receptors leading to diverse signaling events. These include cytosolic and mitochondrial Ca^{2+}-elevation, K^+-efflux, phospholipase activation, cAMP decrease and kinase activation. The mechanisms leading than to ADAM activation will be discussed in more detail in the second part of this chapter. Possible mechanisms could be spontaneous local Ca^{2+}-

concentration elevations, which are not chelated by EGTA or BAPTA-AM, mitochondrial ROS generation or potassium efflux.

However, melittin induces ADAM-mediated shedding in a P2-recpetor dependent manner. Which P2-receptors are involved may differ in different cell types due to the different expression pattern. The different receptors would lead to different signaling cascades, which might lead to ADAM-activation, which is different in time-course, strength and localization. Finally this would lead to substrate and tissue specific effects with yet unpredictable functional consequences. In HacAT keratinocytes these functional consequences of melittin stimulation were primarily mediated by shedding of cell adhesion molecules and EGFR-transactivation.

5.2. The role of phosphatidylserine exposure for ADAM17-mediated proteolysis

ADAM17-mediated shedding is upregulated by several physiological and unphysiological stimuli. The fast increase in substrate release is independent of the intracellular part of ADAM17 (Le Gall et al., 2010). Rather than intracellular ADAM17 modulations, the membrane seems to play an important role in determining ADAM17 activity. The impact of membrane modulations in determining ADAM17 activity was shown in the context of ADAM17 localization in the membrane, raft disruption and membrane fluidity. Despite these findings, the final trigger for ADAM17 activation was unknown. One possible mechanism for membrane-dependent inside-out signaling leading to ADAM17 activation is phosphatidylserine translocation from the inner leaflet to the outer leaflet of the membrane. Therefor the aim of this investigation was to examine the role of phosphatidylserine exposure on ADAM17 activation.

In this thesis it has been demonstrated that activators of ADAM17-mediated shedding lead to PtdSer exposure and that this correlates with the proteolytic activity of ADAM17. Inhibition of PtdSer externalization either by reducing the PtdSer contents of cells or by using inhibitors diminished ADAM17-mediated shedding. Assuming a direct interaction of PtdSer with ADAM17, the ability of the membrane proximal domain of ADAM17 to bind to PtdSer was proven by in vitro analyses. In functional shedding analyses, competition for PtdSer binding with the soluble head group of PtdSer decreased significantly ADAM17-mediated substrate release. Moreover, mutating the probable PtdSer-binding motif of ADAM17 completely abolished stimulated and constitutive shedding.

Taken together, these findings lead to the final model that PtdSer exposure serves as ultimate trigger for ADAM17-activation. ADAM17 binds via its polybasic motif to PtdSer ensuring the right positioning of ADAM17 to its substrate and this finally enables the shedding events. These results and conclusions will be discussed in more detail in this chapter.

5.2.1. Phosphatidylserine exposure correlates with ADAM17-mediated shedding

As shown by live cell imaging and annexinV staining, the ADAM17 stimuli melittin, ionomycin, PMA and FGF7 induced PtdSer exposure in cells. Except ionomycin, all stimuli lead to a transient externalization of PtdSer. This was characterized by a time-dependent increase followed by a decrease in fluorescence. This PtdSer translocation correlated with ADAM17-mediated ERK1/2 phosphorylation. Most important, specific signaling inhibitors inhibited PdtSer translocation as well as ERK1/2 phosphorylation. No direct link between PtdSer exposure and ADAM activation is reported. However, several stimuli, which are described to induce

ADAM-mediated shedding, are often also described to induce PtdSer exposure. In the literature, permanent PtdSer exposure is the classical hallmark of apoptosis (Martin et al., 1995). Apoptosis is a suicidal process that occurs during all stages of life (M. D. Jacobson et al., 1997; Raff et al., 1994). During apoptosis ADAM-mediated shedding of the membrane proteins IL6R, E-cadherin, L-selectin, TNFR1 and CD46 was observed (Chalaris et al., 2007; Hakulinen and Keski-Oja, 2006; Madge et al., 1999; Steinhusen et al., 2001; Walcheck et al., 2006). In this thesis ionomycin induced a fast and permanent PtdSer exposure accompanied by ADAM-mediated shedding. Ionomycin has been shown to induce apoptosis in different cell types and it is often used as potent ADAM10 and -17 activator (Garbers et al., 2011; Möller-Hackbarth et al., 2013; Stasik et al., 2007; Takei and Endo, 1994). In contrast to ionomycin, melittin induced PtdSer exposure was transient. As shown in the first part of this thesis melittin stimulated ATP- and P2-receptor-dependent ADAM10 and -17 substrates release. Both, ATP and P2 receptors, in particular P2X7, are reported to induce PtdSer exposure (Qu et al., 2009; Sluyter et al., 2007). Additionally, P2-receptor activation induces ADAM-mediated shedding of TNF-α, TNFR1 and L-selectin (Elliott et al., 2005; Le Gall et al., 2009; Rowlands et al., 2011). In contrast to ionomycin and melittin, the selective ADAM17 activators PMA and FGF7 induced punctuated PtdSer spots, which were located at the cell boarders. PMA is a PKC activator that is often used to induce fast ADAM17-mediated shedding (Le Gall et al., 2010). It also induces PKC-mediated Ca^{2+}-influx and PtdSer exposure in red blood cells (Andrews et al., 2002; Nguyen et al., 2011). The growth factor FGF7 has recently been described to induce ADAM17-mediated EGFR signaling (Maretzky et al., 2011a). Here, it is shown for the first time that PMA and FGF7 induce PtdSer exposure in nucleated cells. If this punctuated PtdSer exposure is exclusively typical for ADAM17 activation and if this pattern resembles membrane micro domains needs to be further validated, it is conceivable that staining of ADAM17 and/or its substrates would yield in a co-staining with PtdSer.

Interestingly, inhibition of the signaling cascades of the above-mentioned ADAM activators, decreased not only ADAM17-mediated ERK1/2 phosphorylation, it also inhibited PtdSer exposure. Also, other ADAM stimuli are reported to induce PtdSer exposure. These include fMLP, a chemotactic factor derived from bacteria, thrombin, a serine protease, or LL-37, an antimicrobial peptide. fMLP was shown to induce L-selectin shedding from neutrophils and also to induce PtdSer exposure at uropod rafts in neutrophils (Ball and King, 2011; Frasch et al., 2004). Thrombin causes PtdSer exposure in platelets in an TMEM16F-dependent mechanism (van Kruchten et al., 2013). Additionally, thrombin induces ADAM17-mediated shedding of GPIbα from platelets (Bergmeier et al., 2004). The antimicrobial peptide LL-37 induces caspase-independent PtdSer externalization and also ADAM-mediated transactivation of the EGFR (Ren et al., 2012; Tjabringa et al., 2003; Tokumaru et al., 2005; Tomasinsig et al., 2008).

The underlying general mechanisms of PdtSer exposure are complex and not well understood. Lipid scramblases are under suspicion to participate in the stimulus and apoptosis-induced PtdSer exposure. Lipid scramblases are often Ca^{2+}-activated lipid transporters, which randomize lipids between the leaflets and counteract ATP-dependent flippases upon activation (Pomorski and Menon, 2006). In red blood cells and platelets PLSCR1 is involved in PtdSer exposure, which activates blood clotting and phagocytosis (Bassé et al., 1996; Bevers et al., 1982; Comfurius et al., 1996; Zhou et al., 1997). However, mouse blood cells from PLSCR1-deficient mice were still able to scramble phospholipids. This indicates that PLSCR1 is not solely responsible for PtdSer exposure (Zhou et al., 2002). Until now five PLSCR (PLSCR1-5) have been identified (Wiedmer et al., 2000). In conjunction with other scramblases, for example TMEM16F and Xkr8, they may contribute to PtdSer exposure (Kmit et al., 2013; Suzuki et al., 2013a; 2014; 2010). TMEM16F, also known as anoctamin6, is a transmembrane Ca^{2+}-activated Cl^--channel (Kunzelmann et al., 2009). Beside this action, it was shown that TMEM16F is also an inward rectifying unselective ction channel and a PtdSer scramblase itself (Kunzelmann et al., 2009; 2014; Suzuki et al., 2010; van Kruchten et al., 2013). Patients of the rare Scott syndrome carry a loss-of-function mutation in the TMEM16F gene in platelets and other hematopoietic cells. These cells are unable to perform Ca^{2+} -dependent phosphatidylserine exposure and, hence, are impaired in supporting blood coagulation (Suzuki et al., 2010). If these cells are defective in ADAM-mediated substrate release is currently unknown. Xkr8 is a recently identified apoptosis-related scramblase that is activated by caspase-3 cleavage (Suzuki et al., 2013a). This scramblase contributes to the late PtdSer exposure in apoptosis and is at least not directly regulated by calcium.

Nevertheless, most of the known scramblases are thought to be Ca^{2+}-dependent (Bucki et al., 2001; Suzuki et al., 2013b). Beside Ca^{2+}-dependent scramblase activation, inhibition of flippases might also contribute to PtdSer exposure. ATP-dependent flippases, including family members of P-type-ATPases and ABC-transporters, are maintaining the lipid asymmetry between the membrane leaflets (Pomorski and Menon, 2006). Due to the complex network of phospholipid scrambling and flipping with its multifaceted possibilities of regulations, one could speculate that the ADAM stimulants might culminate in signaling events that drive PtdSer exposure most likely by activating scramblases and/or inhibiting flippases (Figure 27).

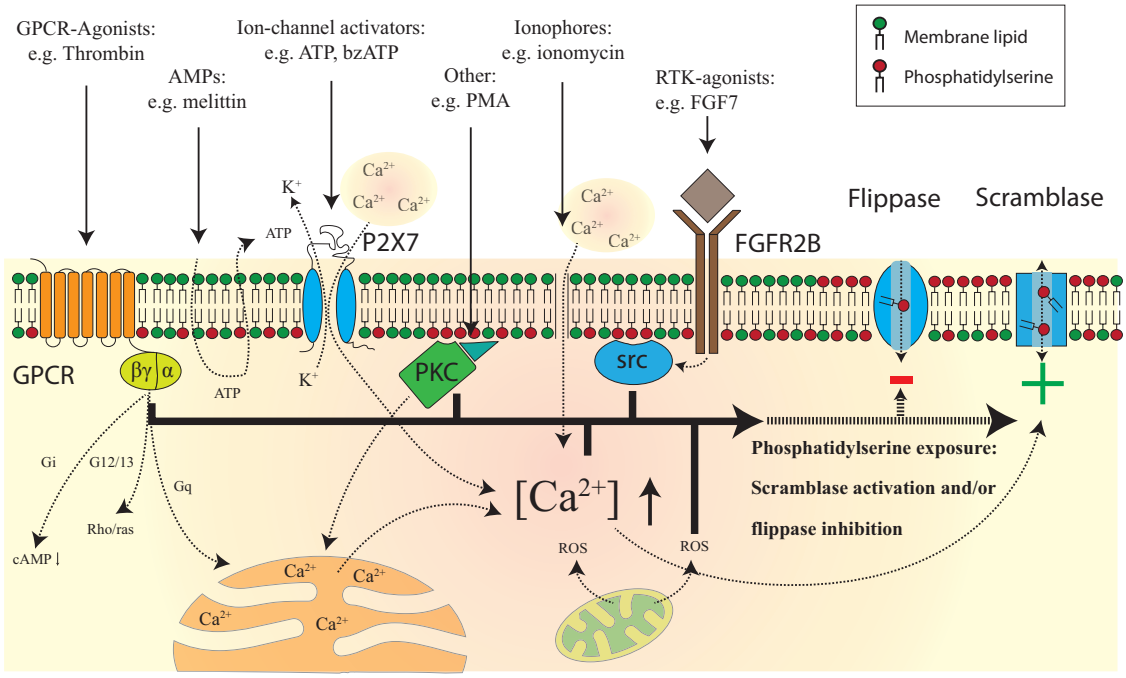

Figure 27: ADAM stimuli signaling lead to PtdSer scrambling. The multifaceted signaling cascades of ADAM activators culminate in the end in PtdSer exposure. The mechanisms involved are complex and not yet understood. Thrombin activates GPCRs of the protease activated receptor family. Depending on the G-proteins, are cAMP-levels downregulated, rho/ras activated or Ca^{2+}-released from the ER leading to complex downstream events. Melittin leads to ATP egress from the cells and this activates P2-receptors (**Figure 26**). In the case of P2X7 activation, this increases Ca^{2+}-influx and K^{+}-efflux. PMA mimicks diacylglycerol and activates PKCs, which in turn initiate diverse signaling cascades and Ca^{2+}-release. FGFR2b signaling leads to src kinase activation and activation of many downstream effector molecules. In these signaling cascades plays often Ca^{2+} a role, but also kinases and ROS may contribute to the observed PtdSer exposure. Although not known, the PdSer scrambling is most likely due to scramblase activation and flippases inhibition.

5.2.2. Inhibition of PtdSer translocation diminished ADAM17-mediated substrate release

The correlation of PtdSer exposure and ADAM17-mediated ERK1/2 phosphorylation indicates that PdtSer exposure might be a trigger for ADAM17 activation. This was evaluated by inhibiting PtdSer translocation with DIDS. DIDS is a unspecific Cl^{-}-channel and anion exchanger blocker, which is additionally often used to prevent PtdSer externalization (Elliott et al., 2005; Kucherenko et al., 2013). DIDS treatment of stimulated cells prevented PtdSer scrambling as well as ADAM17-mediated substrate release. The underlying mechanism of DIDS in preventing PtdSer exposure is not known. A recent study indicates that DIDS is not able to modulate Ca^{2+} homeostasis, at least in RBC stimulated with ionomycin (Kucherenko et al., 2013). This indicates that DIDS prevents PtdSer scrambling independent of intracellular Ca^{2+} elevations. DIDS

inhibits anion channels by covalently binding to specific amino acids in the channel pore through two isothiocyanate groups (Bridges et al., 1989; Laver and Bradley, 2006). These NH_2-specific crosslinking can probably also occur with other proteins, such as scramblases- hence inhibiting PtdSer exposure. Unfortunately, it cannot be ruled out that DIDS affect ADAM17 or its substrate directly by crosslinking them. Therefore the effect of DIDS on ADAM17-mediated shedding was confirmed with the DIDS derivate SITS. SITS has only one isothiocyanate group and no potential to crosslink primary amines, but exhibits comparable pharmacological properties as DIDS (Cytlak et al., 2013; Kucherenko et al., 2013). Indeed, SITS suppressed PtdSer exposure and ADAM17-mediated TNFR1 release in HaCaT keratinocytes. These findings supported the results obtained with DIDS, especially in the context that SITS is reported to inhibit PtdSer exposure (Cytlak et al., 2013). Due to the limitations of pharmacological approaches to inhibit PtdSer exposure these studies were not intensified. Instead, PSA3 cells were used to proof the concept that PtdSer scrambling directly induces ADAM17-mediated shedding. PSA3 cells, a CHO-K1 cell line defective in PSS1, showed reduced PtdSer exposure and TGF-α-AP shedding upon ionomycin and melittin treatment when starved without ethanolamine. This starving results in a decreased cellular level of PtdSer (Kuge et al., 1986). Beside its translocation from the inner to the outer leaflet of membranes, PtdSer has several intracellular functions. To these belong ionic interactions with proteins, for example with Rho, Rac and src. PtdSer binding of these proteins is important for their function (Finkielstein et al., 2006; Lemmon, 2008; Sigal et al., 1994). Additionally, PtdSer plays a role in targeting proteins to phagosomes (Yeung et al., 2009). Due to these roles of phosphatidylserine, intracellular side effects that might affect ADAM17 activation cannot be ruled out when the cellular PtdSer content decreases. However, in all experiments, PtdSer externalization correlated with ADAM17-mediated shedding.

5.2.3. The membrane proximal domain of ADAM17 binds to PtdSer

Proteins that bind to PtdSer typically contain polybasic amino acids at their binding site (Lemmon, 2008; L. Li et al., 2014). The membrane proximal domain of ADAM17 contains several basic amino acids, which might contribute to the assumed binding to PtdSer. The potential binding ability for PtdSer was identified by sequence comparison of proteins that bind to PtdSer with that of ADAM17 and by electrostatic surface calculations. Even though, sequence comparison and electrostatic calculations are just an approximation, it indicates that the polybasic motif $R_{625}K_{626}XK_{628}$ located in the flexible part of the MPD is the most probable interaction site for PtdSer binding. The MPD exists in a flexible/active form and can be inactivated by PDI-induced reshuffling of disulfide bridges (Düsterhöft et al., 2013). The electrostatic calculations were

performed on the only structure available, the inactive/closed MPD and can therefore not reflect the real situation. Nevertheless, the most promising region for interactions with PtdSer is in the part of the MPD that is in the open form highly flexible. This flexibility would facilitate interactions with PtdSer rather than hinder them.

The ability of the MPD to bind to PtdSer was confirmed by in vitro isothermal titration calorimetry (ITC) and surface acoustic wave (SAW) experiments. Titrating PtdSer containing liposomes with the open/flexible MPD resulted in a considerably exothermic reaction. The closed/inflexible MPD showed no binding reaction to these liposomes. This indicates that only the open MPD of ADAM17 is able to bind to PtdSer. In SAW experiments, the modulation of a surface-confined acoustic wave is utilized for the analysis of surface binding. Biomolecular interaction processes on the surface of the sensor chip can result in changes of phase and amplitude of the surface acoustic wave. Changes of these parameters correlate with mass loading and viscoelastic alterations (Andrä et al. 2008). In these experiments, the recombinant MPD in its flexible/open conformation bound at physiological conditions preferential to PtdSer containing liposomes, indicated by an increase in mass loading and a decrease in viscosity. Together this led to the hypothesis that ADAM17 binds to exposed PtdSer with its flexible MPD.

5.2.4. Competing for PtdSer binding decreases ADAM17-mediated shedding

The hypothesis that PtdSer exposure serves as trigger for ADAM17 activation by a direct interaction was further validated by using the soluble head group of PtdSer as competitor. OPLS is often used to inhibit the phagocytosis of PtdSer exposing cells (Ohnishi et al., 2010). In this case, OPLS competes with the binding sites for PtdSer on phagocyting cells, thus preventing phagocytosis (Stolzing and Grune, 2004). In the ADAM17 stimulation experiments, OPLS dose-dependently inhibited ADAM17-mediated shedding in HaCaT keratinocytes and HUVECs. In contrast, PC the head group of the uncharged PtdCho had no effect on ADAM17-mediated shedding. This indicates that there is a specific interaction between ADAM17 and the head group of PtdSer. In conclusion, OPLS competes with the binding site for PtdSer in ADAM17, abrogating the interaction of ADAM17 with exposed PtdSer in the membrane.

5.2.5. The polybasic motif of ADAM17 is necessary for shedding of transmembrane substrates

To further validate this hypothesis, the polybasic motif was mutated to uncharged glycines in ADAM17 expression plasmids. This mutated A17 3x was transfected into ADAM10/17 double deficient MEFs and shedding analyses were performed. Mutating basic amino acids to prevent possible ionic binding interactions is a common tool to study the specificity and functional con-

sequences of the binding. For example, it was used to identify the binding of src and the T-cell receptor cytoplasmic tail to acidic phospholipids (Sigal et al., 1994; C. Xu et al., 2008). Even the expression level was comparable to wildtype ADAM17, the 3x mutant almost completely lost the ability to shed TGF-α in AP-assays. In contrast, this mutant was still able to cleave soluble fluorogenic ADAM substrates. That indicates that the bona fide proteolytic potential of ADAM17 3x is not impaired. Interestingly, also the constitutive shedding of the 3x mutant was almost completely abolished. This could be due to the unresponsiveness to low amounts of spontaneous PtdSer exposure. It is worth speculating that nanoscale PtdSer exposure in the local environment of ADAM17 would be sufficient to induce shedding. This nanoscale PtdSer exposure cannot be detected with conventional confocal microscopy due to the diffraction limit. Those nanoscale lipid environments for membrane proteins were discovered for caveolin-1 and the T-cell receptor. Both are accompanied by acidic lipids in the inner leaflet, which is necessary for the proper function of these proteins (Ariotti et al., 2014; Molnár et al., 2012; Shi et al., 2013). Together, this leads to the conclusion that the ADAM17 proteolytic activity is triggered by binding of ADAM17 to exposed PtdSer.

5.2.6. Model of ADAM17 activation

Based on the findings of this thesis, a model for ADAM17 activation is proposed. ADAM17-mediated substrate cleavage is triggered by PtdSer translocation from the inner to the outer leaflet. Ionic interactions between the positively charged amino acid motif, located in the membrane proximal domain of ADAM17 and negatively charged PtdSer pulls the metalloprotease domain down. This enables the active site to reach the cleavage site of the substrate, which is for all substrates located in close proximity to the membrane. This model explains the ultimate activating step for ADAM17-mediated substrate release (Figure 28).

Proteins, which interact with negatively charged phospholipids, have generally three characteristics in common. They bind via fast ionic attraction, followed by a slow integration of hydrophobic amino acid side chains into the membrane. At least, this binding occurs for almost every protein in close proximity to a membrane anchor (Lemmon, 2008; McLaughlin and Murray, 2005). These membrane anchors can either be myristoyl anchors, GPI anchors or even a transmembrane domain. In a recently submitted report, Düsterhöft et al. could show that the CANDIS domain of ADAM17 is able to integrate into lipid membranes via insertion of hydrophobic amino acids. This would stabilize the active confirmation of ADAM17 proposed here, which resulted by ionic interactions with PtdSer. In conclusion, ADAM17 fulfills all three criteria of a peptide interacting with membrane lipids. It is anchored in the membrane, it interacts ironically with PtdSer and the CANDIS domain can most likely integrate into the membrane (Figure 28).

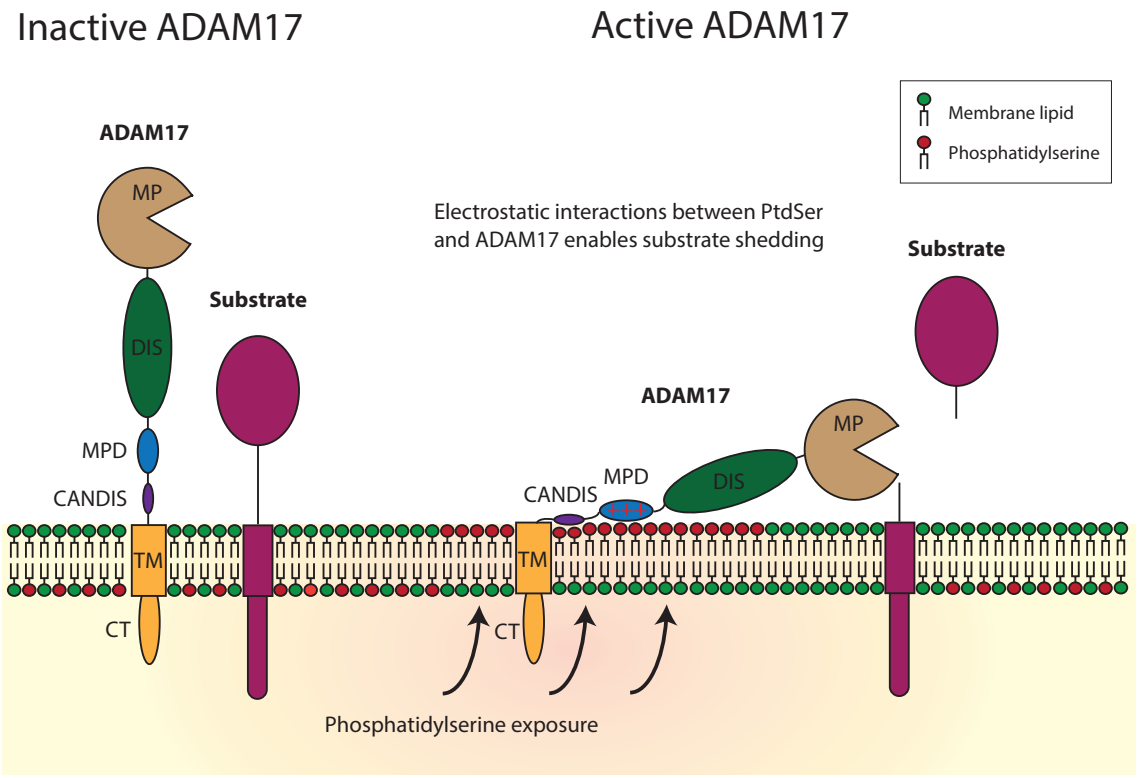

Figure 28: Schematic model of the final activation step of ADAM17-mediated substrate release. Phosphatidylserine translocation from the inner to the outer membrane leaflet enables ionic interactions with the polybasic motif of ADAM17. The membrane proximal domain of ADAM17 (MPD) adheres to the membrane and pulls the metalloprotease domain down to the cleavage site of the substrate. This conformation is stabilized by subsequent integration of the CANDIS domain into the membrane.

The conclusions of this thesis are based on *in vitro* and cell-based assay with different cell types. Most of the experiments were done in humane keratinocytes, primary endothelial cell, mouse embryonic fibroblasts and monkey fibroblast-like cell lines. These cells cover a broad range of cell types and reflect the diversity of tissue composition. This together with the inter species conserved MPD and CANDIS region in mammals, indicates that the proposed model of ADAM17 activation can probably be generalized. All stimuli led to PtdSer activation. This demonstrates that the final trigger for ADAM17-mediated proteolytic shedding is independent of the kind of stimuli. This raises the question how substrate selectivity, tissue specificity and varying functional consequences can be obtained when all stimuli culminate in PtdSer exposure. First, this model explains the final step leading to ADAM17-mediated substrate processing. Therefore the substrate should be already in close proximity to ADAM17, if not bound to the protease. This selection of the substrates may need specific signaling events as it was shown for TGF-α, HB-EGF, or AREG (Dang et al., 2013). Thus, ADAM17 shedding activators may act two-sided: On one hand by making the substrate available for shedding, and on the other hand by inducing PtdSer exposure to trigger the cleavage. Another report demonstrated that iRhoms

contribute to tissue specific substrate selectivity (Maretzky et al., 2013). In conclusion, substrate and tissue specificity of shedding events are obtained by the availability of the substrates, their localization and by signaling events that directs the substrates to the proteases. Additionally, the signaling that induces PtdSer exposure may vary in their characteristics and localization between different stimuli and/or tissues because of different expression of ion channels, different scramblases or flippases and of the ADAMs and substrates.

The proposed model describes for the first time the final triggering mechanism for ADAM17-mediated substrate release and underlines the importance of the membrane composition and dynamics in cell function. A better understanding of this membrane dynamics would allow to specifically influencing pathological situations with high ADAM17 proteolytic activity. Cancer cells and the supplying blood vessels are known to have high rates of exposed PtdSer. In the context of ADAM-mediated EGFR-signaling and enhanced proliferation and migration, this would provide one explanation of increased ADAM17 activity in cancer.

Finally, ADAM17 is the first transmembrane protein, which activity is extra-cellularly regulated by binding to acidic phospholipids. If also other transmembrane proteins, such as ADAM10, interact with exposed PtdSer needs to be evaluated. The unspecific ADAM stimuli ionomycin and melittin are known to induce ADAM10-mediated substrate release and as shown in this thesis also PtdSer exposure. Although ADAM10 is lacking a polybasic motif in its membrane proximal domain, it is possible that there might be another mode of interaction with PtdSer, e.g. like annexins via Ca^{2+} -bridges. In general, transient and locally restricted PtdSer exposure could be a signaling mechanism also for other transmembrane and membrane associated proteins. This would be a new mechanism of inside-out signaling of cells, which expands the knowledge of principle biological processes.

6. Outlook

In the first part of this thesis, it was demonstrated that the bee venom component melittin evokes ADAM10 and -17-mediated substrate processing, even in subcytotoxic concentrations. These shedding events were ATP- and P2-receptor dependent and led to the functional consequences of de-adhesion, proliferation and migration in HaCaT keratinocytes. How melittin induces ATP release is not clear and needs further investigations. Possible mechanisms are either the pore forming properties of melittin or the direct binding of melittin to proteins, such as P2-receptors. A direct activation of P2X7 would lead to pannexin pore formation and subsequent ATP release, which would facilitate the melittin-induced cell response.
Since some antimicrobial peptides are described to induce ADAM-mediated functional consequences, it would be of interest to investigate if this is a common feature of all AMPs and how this could work. Most of the AMPs are small cationic peptides. It is possible that they share a specific sequence or structure motif that is needed for the proper function and may contribute to ADAM activation. By using a synthesized peptide with antimicrobial and ADAM-activating properties, which was generated by Klaus Brandenburg (FZ Borstel), it would be possible to identify the sequence or structure responsible for its action. Therefore peptides with deleted or exchanged amino acids should be generated and tested for the ability to activate ADAM-mediated proteolysis.

In the second part of this thesis it was demonstrated that PtdSer exposure serves as final trigger for ADAM17-dependent substrate release. This is mediated by ionic interactions between negatively charged PtdSer and a polybasic motif of ADAM17. To further validate and extend our knowledge of this process additional approaches are considered as useful. Although the $R_{625}K_{626}XK_{628}$ motif is most likely the motif mediating the ionic binding, this should be verified. For example by mutating this motif in an MPD17-expression plasmid. This mutated MPD should be tested for the ability to bind to PtdSer by using the already established binding analyses described in chapter 4.2.6.
Moreover, the connection between ADAM-mediated shedding in apoptotic processes and PtdSer exposure should be analyzed in detail. It is imaginable that inhibiting PtdSer exposure in apoptosis without affecting apoptosis itself would prevent ADAM-mediated shedding. Joscha Büch studied this question in parallel for his MD thesis. The results obtained so far are totally in accordance with the results and hypothesis described in this thesis.
In this context a Ba/F3 cell line with a constitutively active scramblase TMEM16F should be analyzed for altered ADAM-mediated shedding as well as the physiological relevant B-cells from Scott patients, which do not expose PtdSer. Taken together, these experiments would pro-

vide additional support for the already obtained results and consolidate the role of PtdSer for ADAM-mediated substrate shedding.

Genetically modified mice, expressing ADAM17 without the polybasic motif, would be of particular interest to define the physiological role of the PtdSer-ADAM17 interaction. The questions to be solved are: is the interaction of ADAM17 and PtdSer absolutely required for normal development? Or, is the activity of ADAM17 just reduced, maybe comparable to ADAM17$^{ex/ex}$ mice (Chalaris et al., 2010). These mice are generated with the Crispr/Cas approach together with our cooperation partner R. Sedlacec (Prague). Depending on the phenotype of these mice, more analyses should be done to evaluate the physiological role of ADMA17-PtdSer interaction.

A quite challenging issue is how PtdSer is exposed and which are the underlying mechanisms. The complex network of signaling and the not well-understood contributions of the different, so far identified, scramblases and flippases to this process, make it conceivable that there is more than one final mechanism. Different ADAM stimuli may lead to different ways of PtdSer exposure that probably vary between cells and cell types. A good starting point would be to evaluate the contribution of a specific scramblase, such as TMEM16F to PtdSer exposure upon triggering the cells with different ADAM stimuli and analyse the shedding events. The already mentioned B-cells of Scott patients, pharmacolocical and siRNA approaches are here the methods of choice.

Another question, which remains to be solved, is the tissue-, substrate- and stimuli-specificity of ADAM-mediated functions. ADAMs exerts different functions in different tissues and in different stages of development. The mentioned different kind of PtdSer exposure mechanisms may also contribute to substrate selectivity. At least three kinds of substrate selection mechanisms are imaginable. The substrate itself should be made available for cleavage. This includes signaling that targets the substrate and protein-interaction partners, which directs the substrate to the destined location. For some substrate it has been reported that they directly interact with the ADAM-protease by binding. Protein-binding partners and/or lipid environments could additionally regulate this process. Once the substrate is available for the ADAM, the shedding is initiated by PtdSer scrambling, which in turn could also differ in localization and intensity. Taken together, due to this complex, diverse and multifaceted signaling that leads to regulated ADAM-mediated shedding, many questions remain unsolved and should be addressed in further investigations.

In a broader context, transient PtdSer exposure could be a general signaling mechanism that also affects other transmembrane or membrane-associated proteins. It would be of particular interest to look for those proteins with polybasic amino acid clusters in close proximity to the outer membrane leaflet and analyze their function in response to PtdSer exposure.

In summary, although the final triggering step for ADAM17-mediated shedding was figured out in this thesis, many open questions remain with regard to the mechanism of PtdSer exposure, the substrate selectivity and the generalization of PtdSer exposure as a new extracellular signaling mechanism for membrane-associated proteins.

7. Summary

The “a disintegrin and metalloproteases” (ADAM) -10 and -17 play pivotal roles in various physiological and pathophysiological situations. They are responsible for the proteolytic processing and release of many cell adhesion molecules, inflammatory cytokines, growth factors and receptors. To these substrates belong *inter alia* cadherins, selectins, TNF-α, EGFR-ligands as well as the receptors for VEGF and TNF-α. This wide variety of substrates requires that the activity of these proteases is tightly regulated. Indeed, the proteolytic activity of ADAM10 and ADAM17 can be rapidly upregulated by certain stimuli. Several studies indicate that different signaling processes are involved in this regulation, including kinase activation, elevation of intracellular Ca^{2+}-concentrations and interations with protein binding partners. Interestingly, the cytotail of ADAM17 as well as the cytotail of ADAM10 is dispensable for stimulated shedding. Therefore, other signaling mechanisms than modifications at the cytotail must be responsible for the rapid activation of ADAM10 and -17 proteolytic substrate processing. One candidate is the cell membrane itself. A recent study showed that the membrane fluidity affects the proteolytic release of ADAM substrates. The aim of this thesis was thus to investigate the influence of membrane modulations on ADAM-mediated shedding.

In the first instance, the impact of the membrane disturbing bee venom component melittin on ADAM10 and -17 mediated shedding was analyzed. Melittin is an antimicrobial peptide that is also being considered as an anti-inflammatory and anti-cancer agent. Shedding analyses revealed that melittin increases the release of ADAM10- and ADAM17-substrates. In HaCaT keratinocytes, the shedding of EGFR-ligands led to EGFR activation and consequently ERK1/2 phosphorylation. Together with E-cadherin shedding, this strikingly increased migration and proliferation of these cells. Melittin was shown to elicit these effects via ATP-release and subsequent P2-receptor activation. Degradation of extracellular ATP by ATPases, as well as inhibition of P2-receptors significantly decreased melittin evoked ADAM-mediated shedding. In Hek 293T cells, which lack the P2X7 receptor, retransfection of this receptor remarkably enhanced the responsiveness to melittin in terms of ADAM-dependent ERK1/2 phosphorylation. In conclusion, melittin modulates cellular functions through activation of ADAM-mediated shedding. Thus, the use of melittin as drug supplement may elicit unexpected and unwanted effects via ADAM activation.

In the second part of this thesis, the role of phosphatidylserine exposure on ADAM17-mediated shedding was analyzed. Phosphatidylserine is a negatively charged phospholipid, which is primarily localized at the cytoplasmic site of membrane bilayers. Upon activation of scramblases or inhibition of flippases, phosphatidylserine can rapidly be exposed, a process often, but not exclusively associated with apoptosis. It could be shown in this thesis, that all tested ADAM17-

stimuli induce phosphatidylserine scrambling in cells. This exposure was, except for ionomycin, temporary and transient. Moreover, phosphatidylserine exposure correlated with ADAM17-mediated ERK1/2 phosphorylation and could be inhibited by specific inhibitors, which inhibit the signaling cascades that lead to ADAM17 activation. The correlation of phosphatidylserine exposure and ADAM17-mediated shedding was additionally proven by either decreasing the cellular phosphatidylserine content in cells and by inhibiting the exposure with the stilbene derivates DIDS and SITS. Like other phosphatidylserine binding proteins, ADAM17 contains a polybasic amino acid cluster ($R_{625}K_{626}XK_{628}$), which is located in the extracellular membrane proximal domain. In *in vitro* binding assays it was shown that this domain binds to phosphatidylserine- but not to phosphatidylcholine-liposomes. Competition for the phosphatidylserine binding of ADAM17 with the soluble head group of phosphatidylserine OPLS, competitively inhibited ADAM17-mediated shedding. Exchanging the positively charged amino acids to uncharged amino acids by mutation completely abrogated the shedding of transmembrane substrates whereas the proteolytic potential to cleave a soluble substrate was unaffected. In conclusion, phosphatidylserine exposure serves as final trigger for ADAM17-mediated substrate processing. The binding of ADAM17 to phosphatidylserine probably orientates the metalloprotease domain to the cleavage site of the substrate and enables the shedding. This propagated model of ADAM17-phosphatidylserine interaction describes for the first time the final triggering step for ADAM17-mediated substrate processing. In this context, ADAM17 is the first transmembrane protein known, which activity is regulated by binding to acidic phospholipids at the extracellular site.

8. Zusammenfassung

Die “A Disintegrin and Metalloproteases” (ADAM) -10 und -17 spielen eine entscheidende Rolle in vielen physiologischen und pathophysiologischen Prozessen. Sie sind verantwortlich für die Freisetzung verschiedenster Transmembranproteine wie zum Beispiel Cadherine, Selektine, TNF-α, EGFR-Liganden und die Rezeptoren für VEGF und TNF-α. Aufgrund dieser Vielzahl an Substraten ist es notwendig, dass die proteolytische Aktivität von ADAM10 und -17 genau reguliert ist. Diverse physiologische Stimulanzien können diese proteolytische Aktivität sehr schnell erhöhen. Obwohl die Mechanismen, die der proteolytischen Aktivität von ADAM10 und -17 zu Grunde liegen, kaum verstanden sind, zeigen einige Studien, dass insbesondere eine Steigerung der intrazelluläre Ca^{2+}-Konzentration, Kinase-Aktivierungen und Interaktionen mit Protein-Bindungspartnern daran beteiligt sind. Interessanterweise sind die zytoplasmatischen Domänen von ADAM10 und auch ADAM17 für das stimulierte Shedding nicht notwendig. Deshalb können intrazelluläre Modifikationen von ADAM10 und -17 nicht die Ursache für die schnelle Aktivierung der Protease-Aktivität sein. Stattdessen könnte die Membran eine wichtige Rolle spielen, da unter anderem gezeigt wurde, dass die Membranfluidität die Sheddingrate beeinflusst. Ziel dieser Arbeit war es deshalb, den Einfluss von Membranveränderungen auf das von ADAM10 und -17 vermittelte Shedding näher zu untersuchen.

Im ersten Teil der Arbeit wurde der Einfluss von Melittin auf die von ADAM10 und -17 vermittelte Substrat-Freisetzung untersucht. Melittin ist ein Hauptbestandteil des Bienengiftes und beeinflusst die Membran-Integrität, da es sich in die Membranen einlagern kann. Gleichzeitig werden Melittin anti-inflammatorische und anti-kanzerogene Eigenschaften zugeschrieben.

Es wurde gezeigt, dass Melittin die Freisetzung sowohl von ADAM10-, als auch von ADAM17-Substraten erhöht. In HaCaT Keratinozyten führte das Shedding von EGFR-Liganden zu einer Aktivierung des EGFR und einer nachgelagerten Phosphorylierung von ERK1/2. Zusammen mit dem Shedding von E-Cadherin führte dies zu einer erhöhten Migration und Proliferation der Zellen. Das Melittin-induzierte Shedding von ADAM10- und -17-Substraten war dabei abhängig von ATP-Freisetzung und P2-Rezeptor Aktivierung. In Zellen, die keinen P2X7-Rezeptor exprimieren führte die Retransfektion dieses Rezeptors zu einer erhöhten Melittin-induzierten ADAM-abhängigen ERK1/2 Phosphorylierung. Zusammenfassend lässt sich sagen, dass Melittin das Shedding von ADAM-Substraten aktiviert und damit zelluläre Funktionen beeinflusst. Gerade im Hinblick auf den potentiellen therapeutischen Einsatz von Melittin könnte das zu unerwarteten und ungewollten Nebenwirkungen führen.

Im zweiten Teil dieser Arbeit wurde die Rolle von der Externalisierung von Phosphatidylserin auf das ADAM17-vermittelte Shedding untersucht. Phosphatidylserin ist ein negativ geladenes Phospholipid, dass überwiegend auf der zytoplasmatischen Seite von Zellmembranen lokalisiert

ist. Durch die Aktivierung von Scramblasen oder Inhibierung von Flippasen kann Phosphatidylserin sehr schnell externalisiert werden, ein Prozess der häufig, aber nicht ausschließlich mit Apoptose in Verbindung steht. Es konnte in dieser Arbeit gezeigt werden, dass alle untersuchten ADAM17-Stimulanzen auch eine Phosphatidylserin-Externalisierung auslösen. Diese war mit Ausnahme von Ionomycin transient und zeitlich begrenzt. Diese Phosphatidylserine-Translokation korrelierte mit ADAM17-abhängiger ERK1/2 Phosphorylierung und konnte mit spezifischen Inhibitoren für ADAM17-Aktivatoren verhindert werden. Diese Korrelation zwischen ADAM17-vermitteltem Shedding und Phosphatidylserin-Externalisierung konnte zusätzlich bestätigt werden, durch Verringerung der Phosphatidylserinmenge in Zellen und durch den Einsatz von Stilbene-Derivaten, die die Phosphatidylserine-Externalisierung inhibieren. ADAM17 enthält, wie andere Phospholipid bindende Proteine, eine polybasische Aminosäuregruppe ($R_{625}K_{626}XK_{628}$). Dieses Motiv liegt in der extrazellulären Membranproximalen Domäne. Mittels *in vitro* Untersuchungen konnte gezeigt werden, dass die Membranproximale Domäne von ADAM17 an Phosphatidylserin-Liposomen, nicht jedoch an Phosphatidylcholin-Liposomen bindet. ADAM17 vermitteltes Shedding konnte im Gegenzug durch die lösliche Kopfgruppe von Phosphatidylserine (OPLS) kompetitiv inhibiert werden. Ein Austausch der positiv geladenen Aminosäuren durch ungeladene Aminosäuren mittels Mutation verhinderte stimuliertes wie konstitutives Shedding von Transmembran-Substraten, ohne jedoch die Proteolyse eines löslichen ADAM Substrats zu beeinflussen. Aus diesen Ergebnissen lässt sich schließen, dass Phosphatidylserin Externalisierung der finale „Trigger“ für ADAM17-vermitteltes Substrat-Shedding ist. Die Bindung von ADAM17 an die Phosphatidylserin-präsentierende Membran bringt möglicherweise die Metalloprotease-Domäne in Position und ermöglicht so das Shedding von Transmembran Substraten. Das hier propagierte Modell einer Interaktion zwischen ADAM17 und Phosphatidylserin, beschreibt zum ersten mal den finalen Aktivierungsschritt für die ADAM17-vermittelte Proteolyse. In diesem Zusammenhang ist ADAM17 auch das erste bekannte Membranprotein, dessen Aktivität durch die Bindung an saure Phospholipide auf der extrazellulären Seite reguliert wird.

9. Abbrevations

% (v/v)	Percentage volume/volume
% (w/v)	Percentage weight/volume
% (w/w)	Percentage weight/weight
° C	Degree in Celsius
ABB	Annexin-binding buffer
ABC transporter	ATP-binding cassette transporters
ADAM	A disintegrin and metalloprotease
ADAMDEC-1	ADAM-like decysin 1
ADAMTS	A disintegrin and metalloprotease with thrombospondin motif
Amp	Ampicillin
AMP	Antimicrobial peptide
AMPA	α-Amino-3-hydroxy-5-methyl-4-isoxazolepropionic acid
ANOVA	Analysis of variance
AP	Alkaline phosphatase
APBS	Adaptive Poisson-Boltzmann Solver
APP	Amyloid precursor protein
AREG	Amphiregulin
ATP	Adenosine triphosphate
BSA	Bovine serum albumin
BTC	Betacellulin
bzATP	Benzoyl-adenosine triphosphate
CAM	Cell adhesion molecule
CANDIS	Conserved ADAM seventeen dynamic interaction sequence
CD (e.g. CD22)	Cluster of differentiation
Cetux	Cetuximab
co	control
CT	Cytoplasmic tail
CTF	C-terminal fragment
CX3CL1	Fractalkine
DAG	Diacylglycerol
DNA	Deoxyribonucleic acid
E-, N-, VE-cadherin	Epithelial-, neuronal-, vascular endothelial-cadherin
E. coli	*Escherichia coli*
ECM	Extracellular matrix
EGF	Epithelial growth factor
EGFR	Epithelial growth factor receptor
ELISA	Enzyme-linked immunosorbent assay
ER	Endoplasmic reticulum
ERK1/2	extracellular-signal-regulated kinases 1/2
Etn	Ethanolamine
FACS	Fluorescence-activated cell sorting
FCS	Fetal calf serum
FGF	Fibroblast growth factor
FGFR	Fibroblast growth factor receptor

Fig.	Figure
FITC	Fluorescein isothiocyanate
FS	Flexible stalk
GABA	Gamma aminobutyric acid
GPCR	G-protein coupled receptor
GPI	Glycosylphosphatidylinositol
Grb2	Growth factor receptor-bound protein 2
GSL	Glycosphingolipid
h	Hour
HB-EGF	Heparin binding EGF-like growth factor
HEK293T	Human embryonic kidney 293T cells
HIV-1	Human immunodeficiency virus type 1
HUVEC	Human umbilical vein endothelial cell
IL	Interleukin
ILR	Interleukin receptor
IO	Ionomycin
ITAM	Immunoreceptor tyrosine-based activation motif
ITC	Isothermal titration calorimetry
JAM-A	Junctional adhesion molecule A
l	Litre
L-selectin	Leukocyte selectin
LB medium	Lysogeny broth medium
LCI	Life cell imaging
LPA	Lysophosphatidic acid
LPS	Lipopolysaccharide
LSM	Lymphocyte separation medium
m	Meter
M	Molarity
MAPK	Mitogen activated protein kinase
MEF	Murine embryonic fibroblast
MEK	Mitogen-activated protein kinase kinase
Mel	Melittin
min	Minute
MM	Marimastat
MMP	Matrix metalloprotease
MPD	Membrane proximal domain
MPD17	Membrane proximal domain of ADAM17
Nef	Negative Regulatory Factor
NFκB	Nuclear factor kappa-light-chain-enhancer of activated B cells
NLR	Nod-like receptor
NMDA	N-Methyl-D-aspartic acid
NMR spectroscopy	Nuclear magnetic resonance spectroscopy
OD	Optical density
OPLS	O-phospho-L-serine
PA	Phosphatidic acid
PAR	Protease-activated receptor
PBMC	Peripheral blood mononuclear cells

PBS	Phosphate buffered saline
PC	Phosphatidylcholine
PCR	Polymerase chain reaction
PDGF	Platelet derived growth factor
PDGFR	Platelet derived growth factor receptor
PDI	Protein disulfide isomerase
PDK1	Phosphoinositide-dependent kinase 1
Pen/Strep	Penicillin/Streptomycin
PFT	Pore forming toxin
PH domain	Peckstring homology domain
PI	Propidium iodide
PKC	Protein kinase C
PKG	Protein kinase G
PLA	Phospholipase A
PLC	Phospholipase C
PMA	Phorbol-12-myristat-13-acetat
PSS	Phosphatidylserine synthase
PtdCho	Phosphatidylcholine
PtdEtn	Phosphatidylethanolamine
PtdIns	Phosphatidylinositol
PtdSer	Phosphatidylserine
PVDF	Polyvenylidene fluoride
rcf	Relative centrifugal force
RNA	Ribonucleic acid
rpm	Rounds per minute
RT	Room temperature
RT-PCR	Real-time polymerase chain reaction
s	Second
S.D.	Standard deviation
S.E.	Standard error
S.E.M.	Standard error of the mean
SAW	Surface acoustic wave
SH2/3 domain	Src homology 2/3 domain
siRNA	small interfering RNA
SLO	Streptolysin-O
SM	Sphingomyelin
SOB medium	Super optimal broth medium
SOC medium	SOB medium with glucose
Sos	Son of sevenless
SPINK9	Serine protease inhibitor kazal type 9
src	Proto-oncogene tyrosine-protein kinase
SVMP	Snake venom metalloprotease
TACE	TNF-α converting enzyme (ADAM17)
TGF-α	Transforming growth factor alpha
TIM-3	T cell immunoglobulin and mucin domain 3
TIMP	Tissue inhibitors of metalloproteinases
TLR	Toll-like receptor

TMD	Transmembrane domain
TNF-α	Tumor necrosis factor alpha
TNFR	Tumor necrosis factor alpha receptor
VEGF	Vascular endothelial growth factor
VEGFR	Vascular endothelial growth factor receptor
w/o	without
wt	wildtype

Amino acid abbrevations

Name	**3-letter**	**1-letter**
Alanine	Ala	A
Arginine	Arg	R
Asparagine	Asn	N
Aspartic acid	Asp	D
Cysteine	Cys	C
Glutamic acid	Glu	E
Glutamine	Gln	Q
Glycine	Gly	G
Histidine	His	H
Isoleucine	Ile	I
Leucine	Leu	L
Lysine	Lys	K
Methionine	Met	M
Phenylalanine	Phe	F
Proline	Pro	P
Serine	Ser	S
Threonine	Thr	T
Tyrosine	Tyr	Y
Tryptophan	Trp	W
Valine	Val	V

10. List of figures

11. References

Adrain, C., Zettl, M., Christova, Y., Taylor, N., Freeman, M., 2012. Tumor necrosis factor signaling requires iRhom2 to promote trafficking and activation of TACE. Science 335, 225–8. doi:10.1126/science.1214400

Akira, S., Takeda, K., 2004. Toll-like receptor signalling. Nature reviews. Immunology 4, 499–511. doi:10.1038/nri1391

Amour, A., Slocombe, P.M., Webster, A., Butler, M., Knight, C.G., Smith, B.J., Stephens, P.E., Shelley, C., Hutton, M., Knäuper, V., Docherty, A.J., Murphy, G., 1998. TNF-alpha converting enzyme (TACE) is inhibited by TIMP-3. FEBS Lett. 435, 39–44.

Anderson, R.G.W., Jacobson, K., 2002. A role for lipid shells in targeting proteins to caveolae, rafts, and other lipid domains. Science 296, 1821–5. doi:10.1126/science.1068886

Andrews, D.A., Yang, L., Low, P.S., 2002. Phorbol ester stimulates a protein kinase C-mediated agatoxin-TK-sensitive calcium permeability pathway in human red blood cells. Blood 100, 3392–3399. doi:10.1182/blood.V100.9.3392

Ariotti, N., Fernández-Rojo, M.A., Zhou, Y., Hill, M.M., Rodkey, T.L., Inder, K.L., Tanner, L.B., Wenk, M.R., Hancock, J.F., Parton, R.G., 2014. Caveolae regulate the nanoscale organization of the plasma membrane to remotely control Ras signaling. J. Cell Biol. 204, 777–92. doi:10.1083/jcb.201307055

Arribas, J., Bech-Serra, J.J., Santiago-Josefat, B., 2006. ADAMs, cell migration and cancer. Cancer metastasis reviews 25, 57–68. doi:10.1007/s10555-006-7889-6

Baker, N.A., Sept, D., Joseph, S., Holst, M.J., McCammon, J.A., 2001. Electrostatics of nanosystems: application to microtubules and the ribosome. Proc Natl Acad Sci U S A 98, 10037–10041. doi:10.1073/pnas.181342398

Ball, C.J., King, M.R., 2011. Role of c-Abl in L-selectin shedding from the neutrophil surface. Blood Cells Mol. Dis. 46, 246–251. doi:10.1016/j.bcmd.2010.12.010

Baroja-Mazo, A., Barberà-Cremades, M., Pelegrín, P., 2013. The participation of plasma membrane hemichannels to purinergic signaling. Biochimica et biophysica acta 1828, 79–93. doi:10.1016/j.bbamem.2012.01.002

Bartlett, R., Stokes, L., Sluyter, R., 2014. The P2X7 receptor channel: recent developments and the use of P2X7 antagonists in models of disease. Pharmacological reviews 66, 638–75. doi:10.1124/pr.113.008003

Bassé, F., Stout, J.G., Sims, P.J., Wiedmer, T., 1996. Isolation of an erythrocyte membrane protein that mediates Ca2+-dependent transbilayer movement of phospholipid. Journal of Biological Chemistry 271, 17205–17210.

Bennett, T.A., Edwards, B.S., Sklar, L.A., Rogelj, S., 2000. Sulfhydryl regulation of L-selectin shedding: phenylarsine oxide promotes activation-independent L-selectin shedding from leukocytes. J. Immunol. 164, 4120–9.

Bergmeier, W., Piffath, C.L., Cheng, G., Dole, V.S., Zhang, Y., Andrian, von, U.H., Wagner, D.D., 2004. Tumor necrosis factor-alpha-converting enzyme (ADAM17) mediates GPIbalpha shedding from platelets in vitro and in vivo. Circ. Res. 95, 677–683. doi:10.1161/01.RES.0000143899.73453.11

Bevers, E.M., Comfurius, P., van Rijn, J.L., Hemker, H.C., Zwaal, R.F., 1982. Generation of prothrombin-converting activity and the exposure of phosphatidylserine at the outer surface of platelets. Eur. J. Biochem. 122, 429–436.

Black, R.A., Rauch, C.T., Kozlosky, C.J., Peschon, J.J., Slack, J.L., Wolfson, M.F., Castner, B.J., Stocking, K.L., Reddy, P., Srinivasan, S., Nelson, N., Boiani, N., Schooley, K.A., Gerhart, M., Davis, R., Fitzner, J.N., Johnson, R.S., Paxton, R.J., March, C.J., Cerretti, D.P., 1997. A metalloproteinase disintegrin that releases tumour-necrosis factor-alpha from cells. Nature 385, 729–33. doi:10.1038/385729a0

Blobel, C.P., 1997. Metalloprotease-disintegrins: links to cell adhesion and cleavage of TNF alpha and Notch. Cell 90, 589–92.

Blobel, C.P., 2005. ADAMs: key components in EGFR signalling and development. Nature

reviews. Molecular cell biology 6, 32–43. doi:10.1038/nrm1548
Bode, W., Gomis-Rüth, F.X., Stöckler, W., 1993. Astacins, serralysins, snake venom and matrix metalloproteinases exhibit identical zinc-binding environments (HEXXHXXGXXH and Met-turn) and topologies and should be grouped into a common family, the 'metzincins'. FEBS Lett. 331, 134–40.
Borrell-Pagès, M., Rojo, F., Albanell, J., Baselga, J., Arribas, J., 2003. TACE is required for the activation of the EGFR by TGF-alpha in tumors. EMBO J. 22, 1114–24. doi:10.1093/emboj/cdg111
Bradford, M.M., 1976. A rapid and sensitive method for the quantitation of microgram quantities of protein utilizing the principle of protein-dye binding. Anal. Biochem. 72, 248–254.
Bridges, R.J., Worrell, R.T., Frizzell, R.A., Benos, D.J., 1989. Stilbene disulfonate blockade of colonic secretory Cl- channels in planar lipid bilayers. Am. J. Physiol. 256, C902–12.
Bucki, R., Janmey, P.A., Vegners, R., Giraud, F., Sulpice, J.C., 2001. Involvement of phosphatidylinositol 4,5-bisphosphate in phosphatidylserine exposure in platelets: use of a permeant phosphoinositide-binding peptide. Biochemistry 40, 15752–61.
Buser, C.A., Sigal, C.T., Resh, M.D., McLaughlin, S., 1994. Membrane binding of myristylated peptides corresponding to the NH2 terminus of Src. Biochemistry 33, 13093–101.
Buxbaum, J.D., Liu, K.N., Luo, Y., Slack, J.L., Stocking, K.L., Peschon, J.J., Johnson, R.S., Castner, B.J., Cerretti, D.P., Black, R.A., 1998. Evidence that tumor necrosis factor alpha converting enzyme is involved in regulated alpha-secretase cleavage of the Alzheimer amyloid protein precursor. Journal of Biological Chemistry 273, 27765–27767.
Bzowska, M., Jura, N., Lassak, A., Black, R.A., Bereta, J., 2004. Tumour necrosis factor-alpha stimulates expression of TNF-alpha converting enzyme in endothelial cells. European journal of biochemistry / FEBS 271, 2808–20. doi:10.1111/j.1432-1033.2004.04215.x
Capelluto, D.G.S., 2013. Lipid-mediated Protein Signaling. Springer Science & Business.
Chalaris, A., Adam, N., Sina, C., Rosenstiel, P., Lehmann-Koch, J., Schirmacher, P., Hartmann, D., Cichy, J., Gavrilova, O., Schreiber, S., Jostock, T., Matthews, V., Häsler, R., Becker, C., Neurath, M.F., Reiss, K., Saftig, P., Scheller, J., Rose-John, S., 2010. Critical role of the disintegrin metalloprotease ADAM17 for intestinal inflammation and regeneration in mice. J. Exp. Med. 207, 1617–24. doi:10.1084/jem.20092366
Chalaris, A., Rabe, B., Paliga, K., Lange, H., Laskay, T., Fielding, C.A., Jones, S.A., Rose-John, S., Scheller, J., 2007. Apoptosis is a natural stimulus of IL6R shedding and contributes to the proinflammatory trans-signaling function of neutrophils. Blood 110, 1748–55. doi:10.1182/blood-2007-01-067918
Chanthaphavong, R.S., Loughran, P.A., Lee, T.Y.S., Scott, M.J., Billiar, T.R., 2012. A role for cGMP in inducible nitric-oxide synthase (iNOS)-induced tumor necrosis factor (TNF) α-converting enzyme (TACE/ADAM17) activation, translocation, and TNF receptor 1 (TNFR1) shedding in hepatocytes. J. Biol. Chem. 287, 35887–98. doi:10.1074/jbc.M112.365171
Choi, O.H., Padgett, W.L., Daly, J.W., 1992. Effects of the amphiphilic peptides melittin and mastoparan on calcium influx, phosphoinositide breakdown and arachidonic acid release in rat pheochromocytoma PC12 cells. The Journal of pharmacology and experimental therapeutics 260, 369–375.
Christian, L.M., 2012. The ADAM family: Insights into Notch proteolysis. Fly 6, 30–4. doi:10.4161/fly.18823
Christova, Y., Adrain, C., Bambrough, P., Ibrahim, A., Freeman, M., 2013. Mammalian iRhoms have distinct physiological functions including an essential role in TACE regulation. EMBO reports 14, 884–90. doi:10.1038/embor.2013.128
Cohen, S., 1965. The stimulation of epidermal proliferation by a specific protein (EGF). Developmental biology 12, 394–407.
Comfurius, P., Williamson, P., Smeets, E.F., Schlegel, R.A., Bevers, E.M., Zwaal, R.F., 1996. Reconstitution of phospholipid scramblase activity from human blood platelets. Biochemistry 35, 7631–7634. doi:10.1021/bi9606859
Contreras, F.-X., Ernst, A.M., Wiel, F., Wieland, F., Brügger, B., 2011. Specificity of in-

tramembrane protein-lipid interactions. Cold Spring Harbor perspectives in biology 3, –. doi:10.1101/cshperspect.a004705

Cytlak, U.M., Hannemann, A., Rees, D.C., Gibson, J.S., 2013. Identification of the Ca^{2+} entry pathway involved in deoxygenation-induced phosphatidylserine exposure in red blood cells from patients with sickle cell disease. Pflugers Arch. 465, 1651–1660. doi:10.1007/s00424-013-1308-y

D Alessio, A., Esposito, B., Giampietri, C., Ziparo, E., Pober, J.S., Filippini, A., 2012. Plasma membrane microdomains regulate TACE-dependent TNFR1 shedding in human endothelial cells. Journal of Cellular and Molecular Medicine 16, 626–635. doi:10.1111/j.1582-4934.2011.01353.x

d'Anglemont de Tassigny, A., Berdeaux, A., Souktani, R., Henry, P., Ghaleb, B., 2008. The volume-sensitive chloride channel inhibitors prevent both contractile dysfunction and apoptosis induced by doxorubicin through PI3kinase, Akt and Erk 1/2. Eur. J. Heart Fail. 10, 39–46. doi:10.1016/j.ejheart.2007.11.002

Dang, M., Armbruster, N., Miller, M.A., Cermeno, E., Hartmann, M., Bell, G.W., Root, D.E., Lauffenburger, D.A., Lodish, H.F., Herrlich, A., 2013. Regulated ADAM17-dependent EGF family ligand release by substrate-selecting signaling pathways. Proc. Natl. Acad. Sci. U.S.A. 110, 1–12. doi:10.1073/pnas.1307478110

Dawson, C.R., Drake, A.F., Helliwell, J., Hider, R.C., 1978. The interaction of bee melittin with lipid bilayer membranes. Biochimica et biophysica acta 510, 75–86.

Derynck, R., Roberts, A.B., Winkler, M.E., Chen, E.Y., Goeddel, D.V., 1984. Human transforming growth factor-alpha: precursor structure and expression in E. coli. Cell 38, 287–97.

Devitt, A., Marshall, L.J., 2011. The innate immune system and the clearance of apoptotic cells. Journal of leukocyte biology 90, 447–57. doi:10.1189/jlb.0211095

Ding, X., Yang, L.-Y., Huang, G.-W., Wang, W., Lu, W.-Q., 2004. ADAM17 mRNA expression and pathological features of hepatocellular carcinoma. World journal of gastroenterology : WJG 10, 2735–9.

Dolinsky, T.J., Czodrowski, P., Li, H., Nielsen, J.E., Jensen, J.H., Klebe, G., Baker, N.A., 2007. PDB2PQR: expanding and upgrading automated preparation of biomolecular structures for molecular simulations. Nucleic Acids Res. 35, W522–5. doi:10.1093/nar/gkm276

Dolinsky, T.J., Nielsen, J.E., McCammon, J.A., Baker, N.A., 2004. PDB2PQR: an automated pipeline for the setup of Poisson-Boltzmann electrostatics calculations. Nucleic Acids Res. 32, W665–7. doi:10.1093/nar/gkh381

Drechsler, S., Andrä, J., 2011. Online monitoring of metabolism and morphology of peptide-treated neuroblastoma cancer cells and keratinocytes. Journal of bioenergetics and biomembranes 43, 275–85. doi:10.1007/s10863-011-9350-y

Duclohier, H., 2010. Antimicrobial peptides and peptaibols, substitutes for conventional antibiotics. Current pharmaceutical design 16, 3212–23.

Düsterhöft, S., Höbel, K., Oldefest, M., Lokau, J., Waetzig, G.H., Chalaris, A., Garbers, C., Scheller, J., Rose-John, S., Lorenzen, I., Grötzinger, J., 2014. A Disintegrin and Metalloprotease 17 Dynamic Interaction Sequence, the Sweet Tooth for the Human Interleukin 6 Receptor. J. Biol. Chem. 289, 16336–16348. doi:10.1074/jbc.M114.557322

Düsterhöft, S., Jung, S., Hung, C.-W., Tholey, A., Sönnichsen, F.D., Grötzinger, J., Lorenzen, I., 2013. Membrane-proximal domain of a disintegrin and metalloprotease-17 represents the putative molecular switch of its shedding activity operated by protein-disulfide isomerase. Journal of the American Chemical Society 135, 5776–81. doi:10.1021/ja400340u

Edwards, D.R., Handsley, M.M., Pennington, C.J., 2008. The ADAM metalloproteinases. Molecular aspects of medicine 29, 258–89. doi:10.1016/j.mam.2008.08.001

Elliott, J.I., Surprenant, A., Marelli-Berg, F.M., Cooper, J.C., Cassady-Cain, R.L., Wooding, C., Linton, K., Alexander, D.R., Higgins, C.F., 2005. Membrane phosphatidylserine distribution as a non-apoptotic signalling mechanism in lymphocytes. Nature cell biology 7, 808–16. doi:10.1038/ncb1279

Elssner, A., Duncan, M., Gavrilin, M., Wewers, M.D., 2004. A novel P2X7 receptor activator,

the human cathelicidin-derived peptide LL37, induces IL-1 beta processing and release. J Immunol 172, 4987–94.

Erb, L., Liao, Z., Seye, C.I., Weisman, G.A., 2006. P2 receptors: intracellular signaling. Pflügers Archiv : European journal of physiology 452, 552–62. doi:10.1007/s00424-006-0069-2

Ferguson, K.M., Berger, M.B., Mendrola, J.M., Cho, H.S., Leahy, D.J., Lemmon, M.A., 2003. EGF activates its receptor by removing interactions that autoinhibit ectodomain dimerization. Molecular Cell 11, 507–17.

Finkielstein, C.V., Overduin, M., Capelluto, D.G.S., 2006. Cell migration and signaling specificity is determined by the phosphatidylserine recognition motif of Rac1. Journal of Biological Chemistry 281, 27317–27326. doi:10.1074/jbc.M605560200

Firth, J.D., Putnins, E.E., 2004. Keratinocyte growth factor 1 inhibits wound edge epithelial cell apoptosis in vitro. J. Invest. Dermatol. 122, 222–231. doi:10.1046/j.0022-202X.2003.22124.x

Frasch, S.C., Henson, P.M., Nagaosa, K., Fessler, M.B., Borregaard, N., Bratton, D.L., 2004. Phospholipid flip-flop and phospholipid scramblase 1 (PLSCR1) co-localize to uropod rafts in formylated Met-Leu-Phe-stimulated neutrophils. Journal of Biological Chemistry 279, 17625–17633. doi:10.1074/jbc.M313414200

Gagnon, E., Schubert, D.A., Gordo, S., Chu, H.H., Wucherpfennig, K.W., 2012. Local changes in lipid environment of TCR microclusters regulate membrane binding by the CD3ε cytoplasmic domain. J. Exp. Med. 209, 2423–39. doi:10.1084/jem.20120790

Garbers, C., Jänner, N., Chalaris, A., Moss, M.L., Floss, D.M., Meyer, D., Koch-Nolte, F., Rose-John, S., Scheller, J., 2011. Species specificity of ADAM10 and ADAM17 proteins in interleukin-6 (IL-6) trans-signaling and novel role of ADAM10 in inducible IL-6 receptor shedding. J. Biol. Chem. 286, 14804–11. doi:10.1074/jbc.M111.229393

Gavert, N., Conacci-Sorrell, M., Gast, D., Schneider, A., Altevogt, P., Brabletz, T., Ben-Ze'ev, A., 2005. L1, a novel target of beta-catenin signaling, transforms cells and is expressed at the invasive front of colon cancers. J. Cell Biol. 168, 633–42. doi:10.1083/jcb.200408051

Gerlach, H., Laumann, V., Martens, S., Becker, C.F.W., Goody, R.S., Geyer, M., 2009. HIV-1 Nef membrane association depends on charge, curvature, composition and sequence. Nat Meth 6, 46–53. doi:10.1038/nchembio.268

Gilman, A.G., 1987. G proteins: transducers of receptor-generated signals. Annual review of biochemistry 56, 615–49. doi:10.1146/annurev.bi.56.070187.003151

Glomski, K., Monette, S., Manova, K., de Strooper, B., Saftig, P., Blobel, C.P., 2011. Deletion of Adam10 in endothelial cells leads to defects in organ-specific vascular structures. Blood 118, 1163–74. doi:10.1182/blood-2011-04-348557

Gu, B., Bendall, L.J., Wiley, J.S., 1998. Adenosine triphosphate-induced shedding of CD23 and L-selectin (CD62L) from lymphocytes is mediated by the same receptor but different metalloproteases. Blood 92, 946–51.

Hafezi-Moghadam, A., Thomas, K.L., Prorock, A.J., Huo, Y., Ley, K., 2001. L-selectin shedding regulates leukocyte recruitment. J. Exp. Med. 193, 863–72.

Hakulinen, J., Keski-Oja, J., 2006. ADAM10-mediated release of complement membrane cofactor protein during apoptosis of epithelial cells. Journal of Biological Chemistry 281, 21369–21376. doi:10.1074/jbc.M602053200

Hartmann, D., de Strooper, B., Serneels, L., Craessaerts, K., Herreman, A., Annaert, W., Umans, L., Lübke, T., Illert, A.L., Figura, von, K., Saftig, P., 2002. The disintegrin/metalloprotease ADAM 10 is essential for Notch signalling but not for alpha-secretase activity in fibroblasts. Human molecular genetics 11, 2615–24.

Heng, B.C., Aubel, D., Fussenegger, M., 2013. An overview of the diverse roles of G-protein coupled receptors (GPCRs) in the pathophysiology of various human diseases. Biotechnology advances 31, 1676–94. doi:10.1016/j.biotechadv.2013.08.017

Higashiyama, S., Abraham, J.A., Miller, J., Fiddes, J.C., Klagsbrun, M., 1991. A heparin-binding growth factor secreted by macrophage-like cells that is related to EGF. Science 251, 936–9.

Hirano, K., Kanaide, H., 2003. Role of protease-activated receptors in the vascular system. J. Atheroscler. Thromb. 10, 211–225.

Honigmann, A., van den Bogaart, G., Iraheta, E., Risselada, H.J., Milovanovic, D., Mueller, V., Müllar, S., Diederichsen, U., Fasshauer, D., Grubmüller, H., Hell, S.W., Eggeling, C., Kühnel, K., Jahn, R., 2013. Phosphatidylinositol 4,5-bisphosphate clusters act as molecular beacons for vesicle recruitment. Nature structural & molecular biology 20, 679–86. doi:10.1038/nsmb.2570

Horiuchi, K., Kimura, T., Miyamoto, T., Takaishi, H., Okada, Y., Toyama, Y., Blobel, C.P., 2007a. Cutting edge: TNF-alpha-converting enzyme (TACE/ADAM17) inactivation in mouse myeloid cells prevents lethality from endotoxin shock. J. Immunol. 179, 2686–9.

Horiuchi, K., Le Gall, S., Schulte, M., Yamaguchi, T., Reiss, K., Murphy, G., Toyama, Y., Hartmann, D., Saftig, P., Blobel, C.P., 2007b. Substrate selectivity of epidermal growth factor-receptor ligand sheddases and their regulation by phorbol esters and calcium influx. Mol. Biol. Cell 18, 176–88. doi:10.1091/mbc.E06-01-0014

Hundhausen, C., Misztela, D., Berkhout, T.A., Broadway, N., Saftig, P., Reiss, K., Hartmann, D., Fahrenholz, F., Postina, R., Matthews, V., Kallen, K.-J., Rose-John, S., Ludwig, A., 2003. The disintegrin-like metalloproteinase ADAM10 is involved in constitutive cleavage of CX3CL1 (fractalkine) and regulates CX3CL1-mediated cell-cell adhesion. Blood 102, 1186–95. doi:10.1182/blood-2002-12-3775

Issuree, P.D., Maretzky, T., McIlwain, D.R., Monette, S., Qing, X., Lang, P.A., Swendeman, S.L., Park-Min, K.-H., Binder, N., Kalliolias, G.D., Yarilina, A., Horiuchi, K., Ivashkiv, L.B., Mak, T.W., Salmon, J.E., Blobel, C.P., 2013. iRHOM2 is a critical pathogenic mediator of inflammatory arthritis. J. Clin. Invest. –. doi:10.1172/JCI66168

Iwashita, S., Kobayashi, M., 1992. Signal transduction system for growth factor receptors associated with tyrosine kinase activity: epidermal growth factor receptor signalling and its regulation. Cellular signalling 4, 123–132.

Jacobson, M.D., Weil, M., Raff, M.C., 1997. Programmed cell death in animal development. Cell 88, 347–354.

Jamieson, G.P., Snook, M.B., Thurlow, P.J., Wiley, J.S., 1996. Extracellular ATP causes of loss of L-selectin from human lymphocytes via occupancy of P2Z purinocepters. J. Cell. Physiol. 166, 637–642. doi:10.1002/(SICI)1097-4652(199603)166:3<637::AID-JCP19>3.0.CO;2-3

Jorissen, E., Prox, J., Bernreuther, C., Weber, S., Schwanbeck, R., Serneels, L., Snellinx, A., Craessaerts, K., Thathiah, A., Tesseur, I., Bartsch, U., Weskamp, G., Blobel, C.P., Glatzel, M., De Strooper, B., Saftig, P., 2010. The disintegrin/metalloproteinase ADAM10 is essential for the establishment of the brain cortex. J. Neurosci. 30, 4833–4844. doi:10.1523/JNEUROSCI.5221-09.2010

Keith, D.J., Eshleman, A.J., Janowsky, A., 2011. Melittin stimulates fatty acid release through non-phospholipase-mediated mechanisms and interacts with the dopamine transporter and other membrane-spanning proteins. Eur. J. Pharmacol. 650, 501–510. doi:10.1016/j.ejphar.2010.10.023

Killock, D.J., Ivetić, A., 2010. The cytoplasmic domains of TNFalpha-converting enzyme (TACE/ADAM17) and L-selectin are regulated differently by p38 MAPK and PKC to promote ectodomain shedding. The Biochemical journal 428, 293–304. doi:10.1042/BJ20091611

Kmit, A., van Kruchten, R., Ousingsawat, J., Mattheij, N.J.A., Senden-Gijsbers, B., Heemskerk, J.W.M., Schreiber, R., Bevers, E.M., Kunzelmann, K., 2013. Calcium-activated and apoptotic phospholipid scrambling induced by Ano6 can occur independently of Ano6 ion currents. Cell Death Dis 4, e611. doi:10.1038/cddis.2013.135

Koenen, R.R., Pruessmeyer, J., Soehnlein, O., Fraemohs, L., Zernecke, A., Schwarz, N., Reiss, K., Sarabi, A., Lindbom, L., Hackeng, T.M., Weber, C., Ludwig, A., 2009. Regulated release and functional modulation of junctional adhesion molecule A by disintegrin metalloproteinases. Blood 113, 4799–809. doi:10.1182/blood-2008-04-152330

Koivisto, L., Jiang, G., Häkkinen, L., Chan, B., Larjava, H., 2006. HaCaT keratinocyte migra-

tion is dependent on epidermal growth factor receptor signaling and glycogen synthase kinase-3alpha. Experimental cell research 312, 2791–2805. doi:10.1016/j.yexcr.2006.05.009

Kojro, E., Gimpl, G., Lammich, S., Marz, W., Fahrenholz, F., 2001. Low cholesterol stimulates the nonamyloidogenic pathway by its effect on the alpha -secretase ADAM 10. Proc. Natl. Acad. Sci. U.S.A. 98, 5815–20. doi:10.1073/pnas.081612998

Krebs, L.T., Xue, Y., Norton, C.R., Shutter, J.R., Maguire, M., Sundberg, J.P., Gallahan, D., Closson, V., Kitajewski, J., Callahan, R., Smith, G.H., Stark, K.L., Gridley, T., 2000. Notch signaling is essential for vascular morphogenesis in mice. Genes Dev. 14, 1343–1352.

Kucherenko, Y.V., Wagner-Britz, L., Bernhardt, I., Lang, F., 2013. Effect of chloride channel inhibitors on cytosolic Ca2+ levels and Ca2+-activated K+ (Gardos) channel activity in human red blood cells. J. Membr. Biol. 246, 315–326. doi:10.1007/s00232-013-9532-0

Kuge, O., Nishijima, M., 1997. Phosphatidylserine synthase I and II of mammalian cells. Biochimica et biophysica acta 1348, 151–156.

Kuge, O., Nishijima, M., Akamatsu, Y., 1986. Phosphatidylserine biosynthesis in cultured Chinese hamster ovary cells. III. Genetic evidence for utilization of phosphatidylcholine and phosphatidylethanolamine as precursors. Journal of Biological Chemistry 261, 5795–5798.

Kunzelmann, K., Kongsuphol, P., Aldehni, F., Tian, Y., Ousingsawat, J., Warth, R., Schreiber, R., 2009. Bestrophin and TMEM16-Ca(2+) activated Cl(-) channels with different functions. Cell Calcium 46, 233–241. doi:10.1016/j.ceca.2009.09.003

Kunzelmann, K., Nilius, B., Owsianik, G., Schreiber, R., Ousingsawat, J., Sirianant, L., Wanitchakool, P., Bevers, E.M., Heemskerk, J.W.M., 2014. Molecular functions of anoctamin 6 (TMEM16F): a chloride channel, cation channel, or phospholipid scramblase? Pflugers Arch. 466, 407–414. doi:10.1007/s00424-013-1305-1

Lambrecht, G., 2000. Agonists and antagonists acting at P2X receptors: selectivity profiles and functional implications. Naunyn Schmiedebergs Arch. Pharmacol. 362, 340–350.

Lammich, S., Kojro, E., Postina, R., Gilbert, S., Pfeiffer, R., Jasionowski, M., Haass, C., Fahrenholz, F., 1999. Constitutive and regulated alpha-secretase cleavage of Alzheimer's amyloid precursor protein by a disintegrin metalloprotease. Proc Natl Acad Sci U S A 96, 3922–3927.

Laver, D.R., Bradley, K.M., 2006. Disulfonic stilbene permeation and block of the anion channel from the sarcoplasmic reticulum of rabbit skeletal muscle. Am. J. Physiol., Cell Physiol. 290, C1666–77. doi:10.1152/ajpcell.00299.2005

Lavialle, F., Levin, I.W., Mollay, C., 1980. Interaction of melittin with dimyristoyl phosphatidylcholine liposomes: evidence for boundary lipid by Raman spectroscopy. Biochimica et biophysica acta 600, 62–71.

Le Gall, S.M., Bobé, P., Reiss, K., Horiuchi, K., Niu, X.-D., Lundell, D., Gibb, D.R., Conrad, D., Saftig, P., Blobel, C.P., 2009. ADAMs 10 and 17 represent differentially regulated components of a general shedding machinery for membrane proteins such as transforming growth factor alpha, L-selectin, and tumor necrosis factor alpha. Mol. Biol. Cell 20, 1785–94. doi:10.1091/mbc.E08-11-1135

Le Gall, S.M., Maretzky, T., Issuree, P.D., Niu, X.-D., Reiss, K., Saftig, P., Khokha, R., Lundell, D., Blobel, C.P., 2010. ADAM17 is regulated by a rapid and reversible mechanism that controls access to its catalytic site. J. Cell. Sci. 123, 3913–22. doi:10.1242/jcs.069997

Lee, A.G., 2003. Lipid-protein interactions in biological membranes: a structural perspective. Biochimica et biophysica acta 1612, 1–40.

Lee, C.-C., Sun, Y., Qian, S., Huang, H.W., 2011. Transmembrane pores formed by human antimicrobial peptide LL-37. Biophysical journal 100, 1688–96. doi:10.1016/j.bpj.2011.02.018

Lee, S., Uchida, Y., Emoto, K., Umeda, M., Kuge, O., Taguchi, T., Arai, H., 2012. Impaired retrograde membrane traffic through endosomes in a mutant CHO cell defective in phosphatidylserine synthesis. Genes to cells : devoted to molecular & cellular mechanisms 17, 728–36. doi:10.1111/j.1365-2443.2012.01622.x

Lemmon, M.A., 2008. Membrane recognition by phospholipid-binding domains. Nature reviews. Molecular cell biology 9, 99–111. doi:10.1038/nrm2328

Lentz, B.R., 2003. Exposure of platelet membrane phosphatidylserine regulates blood coagulation. Progress in lipid research 42, 423–38.

Li, L., Shi, X., Guo, X., Li, H., Xu, C., 2014. Ionic protein-lipid interaction at the plasma membrane: what can the charge do? Trends in biochemical sciences 39, 130–40. doi:10.1016/j.tibs.2014.01.002

Li, X., Pérez, L., Pan, Z., Fan, H., 2007. The transmembrane domain of TACE regulates protein ectodomain shedding. Cell research 17, 985–98. doi:10.1038/cr.2007.98

Liu, S., Yu, M., He, Y., Xiao, L., Wang, F., Song, C., Sun, S., Ling, C., Xu, Z., 2008. Melittin prevents liver cancer cell metastasis through inhibition of the Rac1-dependent pathway. Hepatology (Baltimore, Md.) 47, 1964–73. doi:10.1002/hep.22240

Lorenzen, I., Lokau, J., Düsterhöft, S., Trad, A., Garbers, C., Scheller, J., Rose-John, S., Grötzinger, J., 2012. The membrane-proximal domain of A Disintegrin and Metalloprotease 17 (ADAM17) is responsible for recognition of the interleukin-6 receptor and interleukin-1 receptor II. FEBS Lett. 586, 1093–100. doi:10.1016/j.febslet.2012.03.012

Lorenzen, I., Trad, A., Grötzinger, J., 2011. Multimerisation of A disintegrin and metalloprotease protein-17 (ADAM17) is mediated by its EGF-like domain. Biochem. Biophys. Res. Commun. 415, 330–6. doi:10.1016/j.bbrc.2011.10.056

Luetteke, N.C., Qiu, T.H., Peiffer, R.L., Oliver, P., Smithies, O., Lee, D.C., 1993. TGF alpha deficiency results in hair follicle and eye abnormalities in targeted and waved-1 mice. Cell 73, 263–78.

Lum, L., Reid, M.S., Blobel, C.P., 1998. Intracellular maturation of the mouse metalloprotease disintegrin MDC15. J. Biol. Chem. 273, 26236–47.

MacKerell, A.D., Bashford, D., Bellott, M., Dunbrack, R.L., Evanseck, J.D., Field, M.J., Fischer, S., Gao, J., Guo, H., Ha, S., Joseph-McCarthy, D., Kuchnir, L., Kuczera, K., Lau, F.T., Mattos, C., Michnick, S., Ngo, T., Nguyen, D.T., Prodhom, B., Reiher, W.E., Roux, B., Schlenkrich, M., Smith, J.C., Stote, R., Straub, J., Watanabe, M., Wiórkiewicz-Kuczera, J., Yin, D., Karplus, M., 1998. All-atom empirical potential for molecular modeling and dynamics studies of proteins. J Phys Chem B 102, 3586–3616. doi:10.1021/jp973084f

Madge, L.A., Sierra-Honigmann, M.R., Pober, J.S., 1999. Apoptosis-inducing agents cause rapid shedding of tumor necrosis factor receptor 1 (TNFR1). A nonpharmacological explanation for inhibition of TNF-mediated activation. Journal of Biological Chemistry 274, 13643–13649.

Maher, S., Feighery, L., Brayden, D.J., McClean, S., 2007. Melittin as an epithelial permeability enhancer I: investigation of its mechanism of action in Caco-2 monolayers. Pharm. Res. 24, 1336–1345. doi:10.1007/s11095-007-9288-2

Maher, S., McClean, S., 2008. Melittin exhibits necrotic cytotoxicity in gastrointestinal cells which is attenuated by cholesterol. Biochemical pharmacology 75, 1104–14. doi:10.1016/j.bcp.2007.10.029

Malekova, L., Tomaskova, J., Novakova, M., Stefanik, P., Kopacek, J., Lakatos, B., Pastorekova, S., Krizanova, O., Breier, A., Ondrias, K., 2007. Inhibitory effect of DIDS, NPPB, and phloretin on intracellular chloride channels. Pflugers Arch. 455, 349–357. doi:10.1007/s00424-007-0300-9

Mann, G.B., Fowler, K.J., Gabriel, A., Nice, E.C., Williams, R.L., Dunn, A.R., 1993. Mice with a null mutation of the TGF alpha gene have abnormal skin architecture, wavy hair, and curly whiskers and often develop corneal inflammation. Cell 73, 249–61.

Marcello, E., Saraceno, C., Musardo, S., Vara, H., La Fuente, de, A.G., Pelucchi, S., Di Marino, D., Borroni, B., Tramontano, A., Pérez-Otaño, I., Aless, Padovani, A., Padovani, R., Giustetto, M., Gardoni, F., Di Luca, M., 2013. Endocytosis of synaptic ADAM10 in neuronal plasticity and Alzheimer's disease. J. Clin. Invest. 123, 2523–38. doi:10.1172/JCI65401

Maretzky, T., Evers, A., Zhou, W., Swendeman, S.L., Wong, P.-M., Rafii, S., Reiss, K., Blobel, C.P., 2011a. Migration of growth factor-stimulated epithelial and endothelial cells depends on EGFR transactivation by ADAM17. Nat Commun 2, 229. doi:10.1038/ncomms1232

Maretzky, T., McIlwain, D.R., Issuree, P.D., Li, X., Malapeira, J., Amin, S., Lang, P.A., Mak,

T.W., Blobel, C.P., 2013. iRhom2 controls the substrate selectivity of stimulated ADAM17-dependent ectodomain shedding. Proc. Natl. Acad. Sci. U.S.A. 110, 11433–11438. doi:10.1073/pnas.1302553110

Maretzky, T., Reiss, K., Ludwig, A., Buchholz, J., Scholz, F., Proksch, E., de Strooper, B., Hartmann, D., Saftig, P., 2005. ADAM10 mediates E-cadherin shedding and regulates epithelial cell-cell adhesion, migration, and beta-catenin translocation. Proc. Natl. Acad. Sci. U.S.A. 102, 9182–7. doi:10.1073/pnas.0500918102

Maretzky, T., Scholz, F., Köten, B., Proksch, E., Saftig, P., Reiss, K., 2008. ADAM10-mediated E-cadherin release is regulated by proinflammatory cytokines and modulates keratinocyte cohesion in eczematous dermatitis. J. Invest. Dermatol. 128, 1737–46. doi:10.1038/sj.jid.5701242

Maretzky, T., Zhou, W., Huang, X.-Y., Blobel, C.P., 2011b. A transforming Src mutant increases the bioavailability of EGFR ligands via stimulation of the cell-surface metalloproteinase ADAM17. Oncogene 30, 611–8. doi:10.1038/onc.2010.443

Marinissen, M.J., Gutkind, J.S., 2001. G-protein-coupled receptors and signaling networks: emerging paradigms. Trends in pharmacological sciences 22, 368–76.

Martin, S.J., Reutelingsperger, C.P., McGahon, A.J., Rader, J.A., van Schie, R.C., LaFace, D.M., Green, D.R., 1995. Early redistribution of plasma membrane phosphatidylserine is a general feature of apoptosis regardless of the initiating stimulus: inhibition by overexpression of Bcl-2 and Abl. J. Exp. Med. 182, 1545–1556.

Matthews, V., Schuster, B., Schütze, S., Bussmeyer, I., Ludwig, A., Hundhausen, C., Sadowski, T., Saftig, P., Hartmann, D., Kallen, K.-J., Rose-John, S., 2003. Cellular cholesterol depletion triggers shedding of the human interleukin-6 receptor by ADAM10 and ADAM17 (TACE). J. Biol. Chem. 278, 38829–39. doi:10.1074/jbc.M210584200

McIlwain, D.R., Lang, P.A., Maretzky, T., Hamada, K., Ohishi, K., Maney, S.K., Berger, T., Murthy, A., Duncan, G., Xu, H.C., Lang, K.S., Häussinger, D., Wakeham, A., Itie-Youten, A., Khokha, R., Ohashi, P.S., Blobel, C.P., Mak, T.W., 2012. iRhom2 regulation of TACE controls TNF-mediated protection against Listeria and responses to LPS. Science 335, 229–32. doi:10.1126/science.1214448

McLaughlin, S., Murray, D., 2005. Plasma membrane phosphoinositide organization by protein electrostatics. Nature 438, 605–611. doi:10.1038/nature04398

Mechtersheimer, S., Gutwein, P., Agmon-Levin, N., Stoeck, A., Oleszewski, M., Riedle, S., Postina, R., Fahrenholz, F., Fogel, M., Lemmon, V., Altevogt, P., 2001. Ectodomain shedding of L1 adhesion molecule promotes cell migration by autocrine binding to integrins. J. Cell Biol. 155, 661–73. doi:10.1083/jcb.200101099

Meer, G., Voelker, D., Feigenson, G., 2008. Membrane lipids: where they are and how they behave. Nature reviews. Molecular cell biology 9, 112–24. doi:10.1038/nrm2330

Molnár, E., Swamy, M., Holzer, M., Beck-García, K., Worch, R., Thiele, C., Guigas, G., Boye, K., Luescher, I.F., Schwille, P., Schubert, R., Schamel, W.W.A., 2012. Cholesterol and sphingomyelin drive ligand-independent T-cell antigen receptor nanoclustering. J. Biol. Chem. 287, 42664–42674. doi:10.1074/jbc.M112.386045

Moon, D.-O., Park, S.-Y., Heo, M.-S., Kim, K.-C., Park, C., Ko, W.S., Choi, Y.H., Kim, G.-Y., 2006. Key regulators in bee venom-induced apoptosis are Bcl-2 and caspase-3 in human leukemic U937 cells through downregulation of ERK and Akt. International immunopharmacology 6, 1796–807. doi:10.1016/j.intimp.2006.07.027

Moon, H., Na, H.-Y., Chong, K.H., Kim, T.J., 2006. P2X7 receptor-dependent ATP-induced shedding of CD27 in mouse lymphocytes. Immunol. Lett. 102, 98–105. doi:10.1016/j.imlet.2005.08.004

Moreno-Càceres, J., Caja, L., Mainez, J., Mayoral, R., Martín-Sanz, P., Moreno-Vicente, R., Del Pozo, M.Á., Dooley, S., Egea, G., Fabregat, I., 2014. Caveolin-1 is required for TGF-β-induced transactivation of the EGF receptor pathway in hepatocytes through the activation of the metalloprotease TACE/ADAM17. Cell Death Dis 5, e1326. doi:10.1038/cddis.2014.294

Moss, M.L., Jin, S.L., Milla, M.E., Bickett, D.M., Burkhart, W., Carter, H.L., Chen, W.J., Clay,

W.C., Didsbury, J.R., Hassler, D., Hoffman, C.R., Kost, T.A., Lambert, M.H., Leesnitzer, M.A., McCauley, P., McGeehan, G., Mitchell, J., Moyer, M., Pahel, G., Rocque, W., Overton, L.K., Schoenen, F., Seaton, T., Su, J.L., Becherer, J.D., 1997. Cloning of a disintegrin metalloproteinase that processes precursor tumour-necrosis factor-alpha. Nature 385, 733–6. doi:10.1038/385733a0

Möller-Hackbarth, K., Dewitz, C., Schweigert, O., Trad, A., Garbers, C., Rose-John, S., Scheller, J., 2013. A disintegrin and metalloprotease (ADAM) 10 and ADAM17 are major sheddases of T cell immunoglobulin and mucin domain 3 (Tim-3). J. Biol. Chem. 288, 34529–44. doi:10.1074/jbc.M113.488478

Murai, T., Maruyama, Y., Mio, K., Nishiyama, H., Suga, M., Sato, C., 2011. Low cholesterol triggers membrane microdomain-dependent CD44 shedding and suppresses tumor cell migration. J. Biol. Chem. 286, 1999–2007. doi:10.1074/jbc.M110.184010

Murray, D., Ben-Tal, N., Honig, B., McLaughlin, S., 1997. Electrostatic interaction of myristoylated proteins with membranes: simple physics, complicated biology. Structure 1–5.

Myers, T.J., Brennaman, L.H., Stevenson, M., Higashiyama, S., Russell, W.E., Lee, D.C., Sunnarborg, S.W., 2009. Mitochondrial reactive oxygen species mediate GPCR-induced TACE/ADAM17-dependent transforming growth factor-alpha shedding. Mol. Biol. Cell 20, 5236–5249. doi:10.1091/mbc.E08-12-1256

Neves, S.R., Ram, P.T., Iyengar, R., 2002. G protein pathways. Science 296, 1636–9. doi:10.1126/science.1071550

Nguyen, D.B., Wagner-Britz, L., Maia, S., Steffen, P., Wagner, C., Kaestner, L., Bernhardt, I., 2011. Regulation of phosphatidylserine exposure in red blood cells. Cellular physiology and biochemistry : international journal of experimental cellular physiology, biochemistry, and pharmacology 28, 847–56. doi:10.1159/000335798

Ogiso, H., Ishitani, R., Nureki, O., Fukai, S., Yamanaka, M., Kim, J.-H., Saito, K., Sakamoto, A., Inoue, M., Shirouzu, M., Yokoyama, S., 2002. Crystal structure of the complex of human epidermal growth factor and receptor extracellular domains. Cell 110, 775–87.

Ohnishi, M., Katsuki, H., Izumi, Y., Kume, T., Takada-Takatori, Y., Akaike, A., 2010. Mitogen-activated protein kinases support survival of activated microglia that mediate thrombin-induced striatal injury in organotypic slice culture. J. Neurosci. Res. 88, 2155–2164. doi:10.1002/jnr.22375

Oršolić, N., 2012. Bee venom in cancer therapy. Cancer metastasis reviews 31, 173–94. doi:10.1007/s10555-011-9339-3

Pan, D., Rubin, G.M., 1997. Kuzbanian controls proteolytic processing of Notch and mediates lateral inhibition during Drosophila and vertebrate neurogenesis. Cell 90, 271–80.

Peiretti, F., Canault, M., Deprez-Beauclair, P., Berthet, V., Bonardo, B., Juhan-Vague, I., Nalbone, G., 2003. Intracellular maturation and transport of tumor necrosis factor alpha converting enzyme. Experimental cell research 285, 278–85.

Perez, D.M., Karnik, S.S., 2005. Multiple signaling states of G-protein-coupled receptors. Pharmacological reviews 57, 147–61. doi:10.1124/pr.57.2.2

Peschon, J.J., Slack, J.L., Reddy, P., Stocking, K.L., Sunnarborg, S.W., Lee, D.C., Russell, W.E., Castner, B.J., Johnson, R.S., Fitzner, J.N., Boyce, R.W., Nelson, N., Kozlosky, C.J., Wolfson, M.F., Rauch, C.T., Cerretti, D.P., Paxton, R.J., March, C.J., Black, R.A., 1998. An essential role for ectodomain shedding in mammalian development. Science 282, 1281–4.

Pomorski, T., Menon, A.K., 2006. Lipid flippases and their biological functions. Cell. Mol. Life Sci. 63, 2908–21. doi:10.1007/s00018-006-6167-7

Prenzel, N., Zwick, E., Daub, H., Leserer, M., Abraham, R., Wallasch, C., Ullrich, A., 1999. EGF receptor transactivation by G-protein-coupled receptors requires metalloproteinase cleavage of proHB-EGF. Nature 402, 884–8. doi:10.1038/47260

Prox, J., Willenbrock, M., Weber, S., Lehmann, T., Schmidt-Arras, D., Schwanbeck, R., Saftig, P., Schwake, M., 2012. Tetraspanin15 regulates cellular trafficking and activity of the ectodomain sheddase ADAM10. Cell. Mol. Life Sci. 69, 2919–32. doi:10.1007/s00018-012-0960-2

Pruessmeyer, J., Hess, F.M., Ahlert, H., Groth, E., Pasqualon, T., Schwarz, N., Nyamoya, S., Kollert, J., van der Vorst, E., Donners, M., Martin, C., Uhlig, S., Saftig, P., Dreymueller, D., Ludwig, A., 2014. Leukocytes require the metalloproteinase ADAM10 but not ADAM17 for cell migration and for inflammatory leukocyte recruitment into the alveolar space. Blood –. doi:10.1182/blood-2013-09-511543

Pupovac, A., Foster, C.M., Sluyter, R., 2013. Human P2X7 receptor activation induces the rapid shedding of CXCL16. Biochem. Biophys. Res. Commun. 432, 626–31. doi:10.1016/j.bbrc.2013.01.134

Qu, Y., Dubyak, G.R., 2009. P2X7 receptors regulate multiple types of membrane trafficking responses and non-classical secretion pathways. Purinergic Signal. 5, 163–173. doi:10.1007/s11302-009-9132-8

Qu, Y., Ramachandra, L., Mohr, S., Franchi, L., Harding, C.V., Nunez, G., Dubyak, G.R., 2009. P2X7 receptor-stimulated secretion of MHC class II-containing exosomes requires the ASC/NLRP3 inflammasome but is independent of caspase-1. J. Immunol. 182, 5052–5062. doi:10.4049/jimmunol.0802968

Raff, M.C., Barres, B.A., Burne, J.F., Coles, H.S., Ishizaki, Y., Jacobson, M.D., 1994. Programmed cell death and the control of cell survival. Philos. Trans. R. Soc. Lond., B, Biol. Sci. 345, 265–268. doi:10.1098/rstb.1994.0104

Raghuraman, H., Chattopadhyay, A., 2007. Melittin: a membrane-active peptide with diverse functions. Bioscience reports 27, 189–223. doi:10.1007/s10540-006-9030-z

Ralevic, V., Burnstock, G., 1998. Receptors for purines and pyrimidines. Pharmacol. Rev. 50, 413–492.

Rawlings, N.D., Morton, F.R., Kok, C.Y., Kong, J., Barrett, A.J., 2008. MEROPS: the peptidase database. Nucleic acids research 36, D320–5. doi:10.1093/nar/gkm954

Razzini, G., Brancaccio, A., Lemmon, M.A., Guarnieri, S., Falasca, M., 2000. The role of the pleckstrin homology domain in membrane targeting and activation of phospholipase Cbeta(1). J. Biol. Chem. 275, 14873–81.

Reddy, P., Slack, J.L., Davis, R., Cerretti, D.P., Kozlosky, C.J., Blanton, R.A., Shows, D., Peschon, J.J., Black, R.A., 2000. Functional analysis of the domain structure of tumor necrosis factor-alpha converting enzyme. J. Biol. Chem. 275, 14608–14.

Reiss, K., Cornelsen, I., Husmann, M., Gimpl, G., Bhakdi, S., 2011. Unsaturated fatty acids drive disintegrin and metalloproteinase (ADAM)-dependent cell adhesion, proliferation, and migration by modulating membrane fluidity. J. Biol. Chem. 286, 26931–42. doi:10.1074/jbc.M111.243485

Reiss, K., Maretzky, T., Ludwig, A., Tousseyn, T., de Strooper, B., Hartmann, D., Saftig, P., 2005. ADAM10 cleavage of N-cadherin and regulation of cell-cell adhesion and beta-catenin nuclear signalling. EMBO J. 24, 742–52. doi:10.1038/sj.emboj.7600548

Reiss, K., Saftig, P., 2009. The "a disintegrin and metalloprotease" (ADAM) family of sheddases: physiological and cellular functions. Semin. Cell Dev. Biol. 20, 126–37. doi:10.1016/j.semcdb.2008.11.002

Ren, S.X., Cheng, A.S.L., To, K.F., Tong, J.H.M., Li, M.S., Shen, J., Wong, C.C.M., Zhang, L., Chan, R.L.Y., Wang, X.J., Ng, S.S.M., Chiu, L.C.M., Marquez, V.E., Gallo, R.L., Chan, F.K.L., Yu, J., Sung, J.J.Y., Wu, W.K.K., Cho, C.H., 2012. Host immune defense peptide LL-37 activates caspase-independent apoptosis and suppresses colon cancer. Cancer Res. 72, 6512–6523. doi:10.1158/0008-5472.CAN-12-2359

Roghani, M., Becherer, J.D., Moss, M.L., Atherton, R.E., Erdjument-Bromage, H., Arribas, J., Blackburn, R.K., Weskamp, G., Tempst, P., Blobel, C.P., 1999. Metalloprotease-disintegrin MDC9: intracellular maturation and catalytic activity. J. Biol. Chem. 274, 3531–40.

Rousseau, S., Papoutsopoulou, M., Symons, A., Cook, D., Lucocq, J.M., Prescott, A.R., O'Garra, A., Ley, S.C., Cohen, P., 2008. TPL2-mediated activation of ERK1 and ERK2 regulates the processing of pre-TNF alpha in LPS-stimulated macrophages. J. Cell. Sci. 121, 149–54. doi:10.1242/jcs.018671

Rowlands, D., Islam, M., R, S., Huertas, A., Quadri, S., Horiuchi, K., Inamdar, N., Emin, M., Lindert, J., S, V., Bhattacharya, S., Bhattacharya, J., 2011. Activation of TNFR1 ectodo-

main shedding by mitochondrial Ca2+ determines the severity of inflammation in mouse lung microvessels. J. Clin. Invest. 121, 1986–99. doi:10.1172/JCI43839

Russell, P.J., Hewish, D., Carter, T., Sterling-Levis, K., Ow, K., Hattarki, M., Doughty, L., Guthrie, R., Shapira, D., Molloy, P.L., Werkmeister, J.A., Kortt, A.A., 2004. Cytotoxic properties of immunoconjugates containing melittin-like peptide 101 against prostate cancer: in vitro and in vivo studies. Cancer immunology, immunotherapy : CII 53, 411–21. doi:10.1007/s00262-003-0457-9

Sahin, U., Blobel, C.P., 2007. Ectodomain shedding of the EGF-receptor ligand epigen is mediated by ADAM17. FEBS Lett. 581, 41–4. doi:10.1016/j.febslet.2006.11.074

Sahin, U., Weskamp, G., Kelly, K., Zhou, H.-M., Higashiyama, S., Peschon, J., Hartmann, D., Saftig, P., Blobel, C.P., 2004. Distinct roles for ADAM10 and ADAM17 in ectodomain shedding of six EGFR ligands. J. Cell Biol. 164, 769–79. doi:10.1083/jcb.200307137

Schachter, J.B., Sromek, S.M., Nicholas, R.A., Harden, T.K., 1997. HEK293 human embryonic kidney cells endogenously express the P2Y1 and P2Y2 receptors. Neuropharmacology 36, 1181–1187.

Schäfer, B., Gschwind, A., Ullrich, A., 2004. Multiple G-protein-coupled receptor signals converge on the epidermal growth factor receptor to promote migration and invasion. Oncogene 23, 991–9. doi:10.1038/sj.onc.1207278

Scheller, J., Chalaris, A., Garbers, C., Rose-John, S., 2011. ADAM17: a molecular switch to control inflammation and tissue regeneration. Trends Immunol. 32, 380–387. doi:10.1016/j.it.2011.05.005

Schlöndorff, J., Becherer, J.D., Blobel, C.P., 2000. Intracellular maturation and localization of the tumour necrosis factor alpha convertase (TACE). The Biochemical journal 347 Pt 1, 131–8.

Schoch, P., Sargent, D.F., 1980. Quantitative analysis of the binding of melittin to planar lipid bilayers allowing for the discrete-charge effect. Biochimica et biophysica acta 602, 234–47.

Schulz, B., Pruessmeyer, J., Maretzky, T., Ludwig, A., Blobel, C.P., Saftig, P., Reiss, K., 2008. ADAM10 regulates endothelial permeability and T-Cell transmigration by proteolysis of vascular endothelial cadherin. Circ. Res. 102, 1192–201. doi:10.1161/CIRCRESAHA.107.169805

Schwarz, J., Broder, C., Helmstetter, A., Schmidt, S., Yan, I., Müller, M., Schmidt-Arras, D., Becker-Pauly, C., Koch-Nolte, F., Mittrücker, H.-W., Rabe, B., Rose-John, S., Chalaris, A., 2013a. Short-term TNFα shedding is independent of cytoplasmic phosphorylation or furin cleavage of ADAM17. Biochimica et biophysica acta 1833, 3355–67. doi:10.1016/j.bbamcr.2013.10.005

Schwarz, J., Schmidt, S., Will, O., Koudelka, T., Koehler, K., Boss, M., Rabe, B., Tholey, A., Scheller, J., Schmidt-Arras, D., Schwake, M., Rose-John, S., Chalaris, A., 2013b. Polo-Like Kinase 2, a Novel ADAM17 Signaling Component, Regulates TNFα Ectodomain Shedding. J. Biol. Chem. jbc.M113.536847. doi:10.1074/jbc.M113.536847

Schwiebert, E.M., Zsembery, A., 2003. Extracellular ATP as a signaling molecule for epithelial cells. Biochimica et biophysica acta 1615, 7–32.

Sessa, G., Freer, J.H., Colacicco, G., Weissmann, G., 1969. Interaction of alytic polypeptide, melittin, with lipid membrane systems. J. Biol. Chem. 244, 3575–82.

Sharma, S.V., 1993. Melittin-induced hyperactivation of phospholipase A2 activity and calcium influx in ras-transformed cells. Oncogene 8, 939–947.

Shi, X., Bi, Y., Yang, W., Guo, X., Jiang, Y., Wan, C., Li, L., Bai, Y., Guo, J., Wang, Y., Chen, X., Wu, B., Sun, H., Liu, W., Wang, J., Xu, C., 2013. Ca2+ regulates T-cell receptor activation by modulating the charge property of lipids. Nature 493, 111–5. doi:10.1038/nature11699

Shing, Y., Christofori, G., Hanahan, D., Ono, Y., Sasada, R., Igarashi, K., Folkman, J., 1993. Betacellulin: a mitogen from pancreatic beta cell tumors. Science 259, 1604–7.

Shoyab, M., Plowman, G.D., McDonald, V.L., Bradley, J.G., Todaro, G.J., 1989. Structure and function of human amphiregulin: a member of the epidermal growth factor family. Science 243, 1074–6.

Sigal, C.T., Zhou, W., Buser, C.A., McLaughlin, S., Resh, M.D., 1994. Amino-terminal basic residues of Src mediate membrane binding through electrostatic interaction with acidic phospholipids. Proc. Natl. Acad. Sci. U.S.A. 91, 12253–7.

Simons, K., Ikonen, E., 1997. Functional rafts in cell membranes. Nature 387, 569–72. doi:10.1038/42408

Simons, K., Sampaio, J.L., 2011. Membrane organization and lipid rafts. Cold Spring Harbor perspectives in biology 3, a004697. doi:10.1101/cshperspect.a004697

Skals, M., Jorgensen, N.R., Leipziger, J., Praetorius, H.A., 2009. Alpha-hemolysin from Escherichia coli uses endogenous amplification through P2X receptor activation to induce hemolysis. Proc. Natl. Acad. Sci. U.S.A. 106, 4030–5. doi:10.1073/pnas.0807044106

Sluyter, R., Shemon, A.N., Wiley, J.S., 2007. P2X(7) receptor activation causes phosphatidylserine exposure in human erythrocytes. Biochem. Biophys. Res. Commun. 355, 169–173. doi:10.1016/j.bbrc.2007.01.124

Soman, N.R., Baldwin, S.L., Hu, G., Marsh, J.N., Lanza, G.M., Heuser, J.E., Arbeit, J.M., Wickline, S.A., Schlesinger, P.H., 2009. Molecularly targeted nanocarriers deliver the cytolytic peptide melittin specifically to tumor cells in mice, reducing tumor growth. J. Clin. Invest. 119, 2830–42. doi:10.1172/JCI38842

Sommer, A., Fries, A., Cornelsen, I., Speck, N., Koch-Nolte, F., Gimpl, G., Andrä, J., Bhakdi, S., Reiss, K., 2012. Melittin modulates keratinocyte function through P2 receptor-dependent ADAM activation. J. Biol. Chem. 287, 23678–89. doi:10.1074/jbc.M112.362756

Son, D., Lee, J., Lee, Y., Song, H., Lee, C., Hong, J., 2007. Therapeutic application of anti-arthritis, pain-releasing, and anti-cancer effects of bee venom and its constituent compounds. Pharmacology & therapeutics 115, 246–70. doi:10.1016/j.pharmthera.2007.04.004

Soond, S.M., Everson, B., Riches, D.W.H., Murphy, G., 2005. ERK-mediated phosphorylation of Thr735 in TNFalpha-converting enzyme and its potential role in TACE protein trafficking. J. Cell. Sci. 118, 2371–80. doi:10.1242/jcs.02357

Sperrhacke, M., Fischer, J., Wu, Z., Klünder, S., Sedlacek, R., Schroeder, J.-M., Meyer-Hoffert, U., Reiss, K., 2014. SPINK9 stimulates metalloprotease/EGFR-dependent keratinocyte migration via purinergic receptor activation. J. Invest. Dermatol. 134, 1645–54. doi:10.1038/jid.2014.23

Stasik, I., Rapak, A., Kalas, W., Ziolo, E., Strzadala, L., 2007. Ionomycin-induced apoptosis of thymocytes is independent of Nur77 NBRE or NurRE binding, but is accompanied by Nur77 mitochondrial targeting. Biochimica et biophysica acta 1773, 1483–1490. doi:10.1016/j.bbamcr.2007.05.011

Steinhusen, U., Weiske, J., Badock, V., Tauber, R., Bommert, K., Huber, O., 2001. Cleavage and shedding of E-cadherin after induction of apoptosis. Journal of Biological Chemistry 276, 4972–4980. doi:10.1074/jbc.M006102200

Stolzing, A., Grune, T., 2004. Neuronal apoptotic bodies: phagocytosis and degradation by primary microglial cells. FASEB J. 18, 743–745. doi:10.1096/fj.03-0374fje

Stone, A.L., Kroeger, M., Sang, Q.X., 1999. Structure-function analysis of the ADAM family of disintegrin-like and metalloproteinase-containing proteins (review). Journal of protein chemistry 18, 447–65.

Strachan, L., Murison, J.G., Prestidge, R.L., Sleeman, M.A., Watson, J.D., Kumble, K.D., 2001. Cloning and biological activity of epigen, a novel member of the epidermal growth factor superfamily. J. Biol. Chem. 276, 18265–71. doi:10.1074/jbc.M006935200

Stuhlmeier, K.M., 2007. Apis mellifera venom and melittin block neither NF-kappa B-p50-DNA interactions nor the activation of NF-kappa B, instead they activate the transcription of proinflammatory genes and the release of reactive oxygen intermediates. J. Immunol. 179, 655–64.

Sud, M., Fahy, E., Cotter, D., Brown, A., Dennis, E.A., Glass, C.K., Merrill, A.H., Jr, Murphy, R.C., Raetz, C.R.H., Russell, D.W., Subramaniam, S., 2007. LMSD: LIPID MAPS structure database. Nucleic acids research 35, D527–32. doi:10.1093/nar/gkl838

Suzuki, J., Denning, D.P., Imanishi, E., Horvitz, H.R., Nagata, S., 2013a. Xk-related protein 8 and CED-8 promote phosphatidylserine exposure in apoptotic cells. Science 341, 403–406.

doi:10.1126/science.1236758
Suzuki, J., Fujii, T., Imao, T., Ishihara, K., Kuba, H., Nagata, S., 2013b. Calcium-dependent phospholipid scramblase activity of TMEM16 protein family members. J. Biol. Chem. 288, 13305–13316. doi:10.1074/jbc.M113.457937
Suzuki, J., Imanishi, E., Nagata, S., 2014. Exposure of Phosphatidylserine by Xk-related Protein Family Members during Apoptosis. J. Biol. Chem. 289, 30257–30267. doi:10.1074/jbc.M114.583419
Suzuki, J., Umeda, M., Sims, P.J., Nagata, S., 2010. Calcium-dependent phospholipid scrambling by TMEM16F. Nature 468, 834–838. doi:10.1038/nature09583
Swendeman, S., Mendelson, K., Weskamp, G., Horiuchi, K., Deutsch, U., Scherle, P., Hooper, A., Rafii, S., Blobel, C.P., 2008. VEGF-A stimulates ADAM17-dependent shedding of VEGFR2 and crosstalk between VEGFR2 and ERK signaling. Circ. Res. 103, 916–918. doi:10.1161/CIRCRESAHA.108.184416
Takeda, S., 2009. Three-dimensional domain architecture of the ADAM family proteinases. Semin. Cell Dev. Biol. 20, 146–52. doi:10.1016/j.semcdb.2008.07.009
Takei, N., Endo, Y., 1994. Ca2+ ionophore-induced apoptosis on cultured embryonic rat cortical neurons. Brain Res. 652, 65–70.
Tang, J., Zarbock, A., Gomez, I., Wilson, C.L., Lefort, C.T., Stadtmann, A., Bell, B., Huang, L.-C., Ley, K., Raines, E.W., 2011. Adam17-dependent shedding limits early neutrophil influx but does not alter early monocyte recruitment to inflammatory sites. Blood 118, 786–794. doi:10.1182/blood-2010-11-321406
Tellier, E., Canault, M., Rebsomen, L., Bonardo, B., Juhan-Vague, I., Nalbone, G., Peiretti, F., 2006. The shedding activity of ADAM17 is sequestered in lipid rafts. Experimental cell research 312, 3969–80. doi:10.1016/j.yexcr.2006.08.027
Tjabringa, G.S., Aarbiou, J., Ninaber, D.K., Drijfhout, J.W., Sørensen, O.E., Borregaard, N., Rabe, K.F., Hiemstra, P.S., 2003. The antimicrobial peptide LL-37 activates innate immunity at the airway epithelial surface by transactivation of the epidermal growth factor receptor. J. Immunol. 171, 6690–6.
Tokumaru, S., Sayama, K., Shirakata, Y., Komatsuzawa, H., Ouhara, K., Hanakawa, Y., Yahata, Y., Dai, X., Tohyama, M., Nagai, H., Yang, L., Higashiyama, S., Yoshimura, A., Sugai, M., Hashimoto, K., 2005. Induction of keratinocyte migration via transactivation of the epidermal growth factor receptor by the antimicrobial peptide LL-37. J. Immunol. 175, 4662–8.
Tomasinsig, L., Pizzirani, C., Skerlavaj, B., Pellegatti, P., Gulinelli, S., Aless, Tossi, A., Tossi, R., Di Virgilio, F., Zanetti, M., 2008. The human cathelicidin LL-37 modulates the activities of the P2X7 receptor in a structure-dependent manner. J. Biol. Chem. 283, 30471–81. doi:10.1074/jbc.M802185200
Toyoda, H., Komurasaki, T., Uchida, D., Takayama, Y., Isobe, T., Okuyama, T., Hanada, K., 1995. Epiregulin. A novel epidermal growth factor with mitogenic activity for rat primary hepatocytes. J. Biol. Chem. 270, 7495–500.
Trad, A., Riese, M., Shomali, M., Hedeman, N., Effenberger, T., Grötzinger, J., Lorenzen, I., 2013. The disintegrin domain of ADAM17 antagonises fibroblast-carcinoma cell interactions. International journal of oncology 42, 1793–800. doi:10.3892/ijo.2013.1864
Traynelis, S.F., Wollmuth, L.P., McBain, C.J., Menniti, F.S., Vance, K.M., Ogden, K.K., Hansen, K.B., Yuan, H., Myers, S.J., Dingledine, R., 2010. Glutamate receptor ion channels: structure, regulation, and function. Pharmacological reviews 62, 405–96. doi:10.1124/pr.109.002451
Tresckow, von, B., Kallen, K.-J., Str, von, E.P., Strandmann, von, E.P., mann, Borchmann, P., Lange, H., Engert, A., Hansen, H.P., 2004. Depletion of cellular cholesterol and lipid rafts increases shedding of CD30. J. Immunol. 172, 4324–31.
Tucher, J., Linke, D., Koudelka, T., Cassidy, L., Tredup, C., Wichert, R., Pietrzik, C., Becker-Pauly, C., Tholey, A., 2014. LC-MS based cleavage site profiling of the proteases ADAM10 and ADAM17 using proteome-derived peptide libraries. Journal of proteome research 13, 2205–14. doi:10.1021/pr401135u

Uemura, K., Kihara, T., Kuzuya, A., Okawa, K., Nishimoto, T., Ninomiya, H., Sugimoto, H., Kinoshita, A., Shimohama, S., 2006. Characterization of sequential N-cadherin cleavage by ADAM10 and PS1. Neuroscience letters 402, 278–83. doi:10.1016/j.neulet.2006.04.018

Unni, S., Huang, Y., Hanson, R.M., Tobias, M., Krishnan, S., Li, W.W., Nielsen, J.E., Baker, N.A., 2011. Web servers and services for electrostatics calculations with APBS and PDB2PQR. J Comput Chem 32, 1488–1491. doi:10.1002/jcc.21720

van den Eijnde, S.M., van den Hoff, M.J., Reutelingsperger, C.P., van Heerde, W.L., Henfling, M.E., Vermeij-Keers, C., Schutte, B., Borgers, M., Ramaekers, F.C., 2001. Transient expression of phosphatidylserine at cell-cell contact areas is required for myotube formation. J. Cell. Sci. 114, 3631–3642.

van Kruchten, R., Mattheij, N.J.A., Saunders, C., Feijge, M.A.H., Swieringa, F., Wolfs, J.L.N., Collins, P.W., Heemskerk, J.W.M., Bevers, E.M., 2013. Both TMEM16F-dependent and TMEM16F-independent pathways contribute to phosphatidylserine exposure in platelet apoptosis and platelet activation. Blood 121, 1850–1857. doi:10.1182/blood-2012-09-454314

Vance, J.E., Vance, D.E., 2008. Biochemistry of Lipids, Lipoproteins and Membranes. Elsevier.

Vernon, L.P., Bell, J.D., 1992. Membrane structure, toxins and phospholipase A2 activity. Pharmacology & therapeutics 54, 269–95.

Walcheck, B., Herrera, A.H., St Hill, C., Mattila, P.E., Whitney, A.R., Deleo, F.R., 2006. ADAM17 activity during human neutrophil activation and apoptosis. European journal of immunology 36, 968–976. doi:10.1002/eji.200535257

Walev, I., Vollmer, P., Palmer, M., Bhakdi, S., Rose-John, S., 1996. Pore-forming toxins trigger shedding of receptors for interleukin 6 and lipopolysaccharide. Proc. Natl. Acad. Sci. U.S.A. 93, 7882–7.

Wei, L., Xiao, A.Y., Jin, C., Yang, A., Lu, Z.Y., Yu, S.P., 2004. Effects of chloride and potassium channel blockers on apoptotic cell shrinkage and apoptosis in cortical neurons. Pflugers Arch. 448, 325–334. doi:10.1007/s00424-004-1277-2

Wewers, M.D., Sarkar, A., 2009. P2X(7) receptor and macrophage function. Purinergic Signal. 5, 189–195. doi:10.1007/s11302-009-9131-9

White, J.M., 2003. ADAMs: modulators of cell-cell and cell-matrix interactions. Current opinion in cell biology 15, 598–606.

Wiedmer, T., Zhou, Q., Kwoh, D.Y., Sims, P.J., 2000. Identification of three new members of the phospholipid scramblase gene family. Biochimica et biophysica acta 1467, 244–253.

Wild-Bode, C., Fellerer, K., Kugler, J., Haass, C., Capell, A., 2006. A basolateral sorting signal directs ADAM10 to adherens junctions and is required for its function in cell migration. J. Biol. Chem. 281, 23824–9. doi:10.1074/jbc.M601542200

Willems, S.H., Tape, C.J., Stanley, P.L., Taylor, N.A., Mills, I.G., Neal, D.E., McCafferty, J., Murphy, G., 2010. Thiol isomerases negatively regulate the cellular shedding activity of ADAM17. The Biochemical journal 428, 439–50. doi:10.1042/BJ20100179

Wolfsberg, T.G., Straight, P.D., Gerena, R.L., Huovila, A.P., Primakoff, P., Myles, D.G., White, J.M., 1995. ADAM, a widely distributed and developmentally regulated gene family encoding membrane proteins with a disintegrin and metalloprotease domain. Developmental biology 169, 378–83. doi:10.1006/dbio.1995.1152

Wolfsberg, T.G., White, J.M., 1996. ADAMs in fertilization and development. Developmental biology 180, 389–401. doi:10.1006/dbio.1996.0313

Xu, C., Gagnon, E., Call, M.E., Schnell, J.R., Schwieters, C.D., Carman, C.V., Chou, J.J., Wucherpfennig, K.W., 2008. Regulation of T cell receptor activation by dynamic membrane binding of the CD3epsilon cytoplasmic tyrosine-based motif. Cell 135, 702–713. doi:10.1016/j.cell.2008.09.044

Xu, D., Ch, Sharma, C., Sharma, A., Hemler, M.E., 2009. Tetraspanin12 regulates ADAM10-dependent cleavage of amyloid precursor protein. FASEB J. 23, 3674–81. doi:10.1096/fj.09-133462

Xu, P., Derynck, R., 2010. Direct activation of TACE-mediated ectodomain shedding by p38 MAP kinase regulates EGF receptor-dependent cell proliferation. Molecular Cell 37, 551–

66. doi:10.1016/j.molcel.2010.01.034
Xu, P., Liu, J., Sakaki-Yumoto, M., Derynck, R., 2012. TACE activation by MAPK-mediated regulation of cell surface dimerization and TIMP3 association. Science signaling 5, ra34. doi:10.1126/scisignal.2002689
Xue, L., Lucocq, J., 1998. ERK2 signalling from internalised epidermal growth factor receptor in broken A431 cells. Cellular signalling 10, 339–48.
Yarden, Y., Sliwkowski, M.X., 2001. Untangling the ErbB signalling network. Nature reviews. Molecular cell biology 2, 127–37. doi:10.1038/35052073
Yeung, T., Heit, B., Dubuisson, J.-F., Fairn, G.D., Chiu, B., Inman, R., Kapus, A., Swanson, M., Grinstein, S., 2009. Contribution of phosphatidylserine to membrane surface charge and protein targeting during phagosome maturation. J. Cell Biol. 185, 917–928. doi:10.1083/jcb.200903020
Yoshimura, T., Tomita, T., Dixon, M.F., Axon, A.T.R., Robinson, P.A., Crabtree, J.E., 2002. ADAMs (a disintegrin and metalloproteinase) messenger RNA expression in Helicobacter pylori-infected, normal, and neoplastic gastric mucosa. The Journal of infectious diseases 185, 332–40. doi:10.1086/338191
Zelová, H., Hošek, J., 2013. TNF-α signalling and inflammation: interactions between old acquaintances. Inflamm. Res. 62, 641–651. doi:10.1007/s00011-013-0633-0
Zhang, Q., Thomas, S.M., Lui, V.W.Y., Xi, S., Siegfried, J.M., Fan, H., Smithgall, T.E., Mills, G.B., Gr, J.R., Grandis, J.R., is, 2006. Phosphorylation of TNF-alpha converting enzyme by gastrin-releasing peptide induces amphiregulin release and EGF receptor activation. Proc. Natl. Acad. Sci. U.S.A. 103, 6901–6. doi:10.1073/pnas.0509719103
Zhou, Q., Zhao, J., Stout, J.G., Luhm, R.A., Wiedmer, T., Sims, P.J., 1997. Molecular cloning of human plasma membrane phospholipid scramblase. A protein mediating transbilayer movement of plasma membrane phospholipids. Journal of Biological Chemistry 272, 18240–18244.
Zhou, Q., Zhao, J., Wiedmer, T., Sims, P.J., 2002. Normal hemostasis but defective hematopoietic response to growth factors in mice deficient in phospholipid scramblase 1. Blood 99, 4030–4038. doi:10.1182/blood-2001-12-0271

12. Acknowledgement

In the first instance, I want to thank my supervisor Karina Reiss for the opportunity to work in her group, for the great support and for the freedom to develop own ideas.
At least as important as Karina was Björn Ahrens for this thesis. Without his excellent technical support, the generation of the data in this form would have not been possible. Thank you Björn!
Furthermore, I want to thank Felix Kordowski for doing the mutagenesis and AP-Assays with this mutant. I am also grateful for the proof-reading of my manuscript in its entirety or in parts by Karina Reiss, Ulrich Ehmke, Maria Sperrhacke, Astrid Evers, Nancy Speck and Britta Hansmann.

Of cause I want to thank all actual and former members of the AG Reiss. It was a pleasure for me to work with you: Maria Sperrhacke, Nancy Speck, Björn Ahrens, Felix Kordowski, Astrid Evers, Sarah Klünder, Marie Düppe, Joscha Büch, Martin Munz.

Additionally, I want to acknowledge all of our cooperation partners, which are involved in these projects: Anja Fries, Isabell Cornelsen, Fritz Koch-Nolte, Gerald Gimpl, Jörg Andrä, Sucharit Bhakdi, Astrid Evers, Torsten Maretzky, Matthias Michalek, Carl Blobel, Sascha Jung, Tanja Schirmeister, Karl Kunzelmann, S. Nagata, Stefan Düsterhöft, Christian Nehls, Lena Heinböckel, Thomas Gutsmann, Achim Grötzinger

I am very grateful to Thomas Roeder for agreeing to be the official first supervisor for my thesis

I am also thankful for the financial and scientific support by the SFB877 and its IRTG.

Finally I want to thank my parents Wolfgang und Gabriele Sommer for their patience and support over all the years. I am very happy to have you by my side.

13. Supplements

THE JOURNAL OF BIOLOGICAL CHEMISTRY VOL. 287, NO. 28, pp. 23678–23689, July 6, 2012

Melittin Modulates Keratinocyte Function through P2 Receptor-dependent ADAM Activation*[S]

Received for publication, March 15, 2012, and in revised form, May 9, 2012 Published, JBC Papers in Press, May 21, 2012, DOI 10.1074/jbc.M112.362756

Anselm Sommer[‡1], **Anja Fries**[§1], **Isabell Cornelsen**[§], **Nancy Speck**[‡], **Friedrich Koch-Nolte**[¶], **Gerald Gimpl**[‖], **Jörg Andrä**[**2], **Sucharit Bhakdi**[§3], **and Karina Reiss**[‡4]

From the [‡]*Department of Dermatology, Christian-Albrecht University Kiel, 24098 Kiel, the* [§]*Institute of Medical Microbiology and Hygiene, Gutenberg-University Mainz, Hochhaus am Augustusplatz, 55131 Mainz, Germany, the* [¶]*Institute of Immunology, University Medical Center Hamburg-Eppendorf, Martinistr. 52, 20246 Hamburg, Germany, the* [‖]*Department of Biochemistry, Gutenberg-University Mainz, J.J. Becherweg 30, 55128 Mainz, Germany, and the* [**]*Division of Biophysics, Research Center Borstel, Leibniz-Center for Medicine and Biosciences, Parkallee 10. 23845 Borstel, Germany*

Background: Melittin is an antimicrobial peptide that is also being considered as anti-inflammatory and anti-cancer agent.
Results: Melittin provokes P2 receptor activation, which leads to ADAM-dependent transactivation of the EGFR and augments keratinocyte proliferation and migration.
Conclusion: Melittin modulates cellular functions through activation of ADAM-mediated shedding.
Significance: The use of melittin may elicit unexpected and unwanted effects via ADAM activation.

Melittin, the major component of the bee venom, is an amphipathic, cationic peptide with a wide spectrum of biological properties that is being considered as an anti-inflammatory and anti-cancer agent. It modulates multiple cellular functions but the underlying mechanisms are not clearly understood. Here, we report that melittin activates disintegrin-like metalloproteases (ADAMs) and that downstream events likely contribute to the biological effects evoked by the peptide. Melittin stimulated the proteolysis of ADAM10 and ADAM17 substrates in human neutrophil granulocytes, endothelial cells and murine fibroblasts. In human HaCaT keratinocytes, melittin induced shedding of the adhesion molecule E-cadherin and release of TGF-α, which was accompanied by transactivation of the EGF receptor and ERK1/2 phosphorylation. This was followed by functional consequences such as increased keratinocyte proliferation and enhanced cell migration. Evidence is provided that ATP release and activation of purinergic P2 receptors are involved in melittin-induced ADAM activation. E-cadherin shedding and EGFR phosphorylation were dose-dependently reduced in the presence of ATPases or P2 receptor antagonists. The involvement of P2 receptors was underscored in experiments with HEK cells, which lack the P2X7 receptor and showed strikingly increased response to melittin stimulation after transfection with this receptor. Our study provides new insight into the mechanism of melittin function which should be of interest particularly in the context of its potential use as an anti-inflammatory or anti-cancer agent.

Bee venom produced by the honey bee (*Apis mellifera*) contains a large number of bioactive peptides including melittin, apamin, adolapin, and mast cell-degranulating peptide. Melittin is the most abundant component, constituting 50% of whole bee venom (1). This amphipathic peptide of 26 residues contains a hydrophobic stretch of 19 amino acids followed by a cluster of 4 positively charged residues at the C terminus. Melittin is able to intercalate into cell membranes, causing changes in biophysical membrane properties (2–5). It belongs to the family of antimicrobial peptides (AMPs)[5] that have become the subject of increasing discussion as promising anti-cancer drugs and substitutes for conventional antibiotics (6, 7). Several cancer cells including renal, lung, breast, and bladder cells can be selectively destroyed by melittin *in vitro* (8). Its potential use as an agent to treat hepatocellular carcinoma, breast cancer, and prostate cancer has been tested in animal models, with positive outcome (9–11).

Moreover, melittin has been described to exert anti-inflammatory, anti-rheumatoid, anti-arthritic, and pain-relieving effects (8), but the mode of action is still largely unknown (12). Besides biophysical membrane interaction, melittin might directly influence cellular function by activating downstream signaling. It is discussed as a potent activator of phospholipase A_2 (PLA_2) thereby also promoting arachidonic acid synthesis (13). PLA_2-dependent cytotoxic effects and activation of caspase-3 are reported to contribute to anti-cancer cytotoxicity (14). Melittin has also been suggested to reduce inflammatory

* This work was supported by the Deutsche Forschungsgemeinschaft, CRC 490 (to S. B.), DFG AN301/5-1 (to J. A.), CRC 877 (to K. R.), and the Cluster of Excellence "Inflammation at Interfaces" (to K. R.).
[S] This article contains supplemental Figs. S1 and S2.
[1] Both authors contributed equally to this work.
[2] Present address: Department of Biotechnology, Hamburg University of Applied Sciences, Lohbrügger Kirchstr. 65, 21033 Hamburg, Germany.
[3] To whom correspondence may be addressed: Institute of Medical Microbiology and Hygiene, Gutenberg-University Mainz. Tel.: 49-6131-179362; Fax: 49-6131-179037; E-mail: sbhakdi@uni-mainz.de.
[4] To whom correspondence may be addressed: Dept. of Dermatology, Christian-Albrecht University Kiel. Tel.: 49-431-5974786; Fax: 49-431-2972624; E-mail: kreiss@dermatology.uni-kiel.de.

[5] The abbreviations used are: AMP, antimicrobial peptides; PPADS, pyridoxalphosphate-6-azophenyl-2′,4′,-disulfonic acid; PLA, phospholipase A; MMP, matrix metalloprotease; ADAM, a disintegrin like metalloprotease; VE, vascular-endothelial; MTT, 3-(4,5-dimethylthiazol-2-yl)-2,5 diphenyltetrazolium-bromide; CTF, C-terminal fragment; MEF, murine embryonic fibroblast.

responses by inhibiting the DNA binding activity of NF-κB (15), but this concept remains controversial (12).

Metalloproteases play important roles in inflammatory diseases and cancer progression. It has been proposed that melittin could contribute to anti-rheumatoid effects by inhibiting matrix metalloprotease (MMP)-3 production (16). In another study, MMP-9 expression in MCF-7 cells was abolished by melittin treatment (17). Besides MMPs, disintegrin like metalloproteases (ADAMs) play important roles in health and disease (18). They control diverse cellular functions through the release of transmembrane molecules from the cell surface (19). ADAM10 and ADAM17 are the best characterized members of this family. ADAM10 is critically involved in Notch receptor signaling and ADAM17 activity is essential for epidermal growth factor receptor (EGFR) activation. Deletion of both genes leads to embryonic death in knock-out mouse models (20, 21). Several substrates have been identified for both proteases. ADAM10 is the major protease involved in the cleavage of cell adhesion molecules such as neuronal (N)-cadherin (22), epithelial (E)-cadherin (23), or vascular-endothelial (VE)-cadherin (24), but also releases the EGFR ligands betacellulin and EGF (25). ADAM17, also known as TACE (TNF-α converting enzyme), was identified as the enzyme releasing soluble TNF-α from its transmembrane precursor form. Because of the release of this pro-inflammatory cytokine and other cell surface molecules that modulate inflammation, ADAM17 is being discussed as a potential drug target for several inflammatory pathologies.

Up to now a large number of ADAM17 substrates have been identified. *Inter alia*, the protease controls the function of cell adhesion molecules such as L-selectin on neutrophil granulocytes (21) and the release of the EGFR ligands amphiregulin, epiregulin, TGF-α, or heparin-binding EGF (HB-EGF) (26). ADAM10 as well as ADAM17 appear to promote cancer progression by EGFR activation and release of cell adhesion molecules (18).

Recently, we demonstrated that biophysical alterations of cell membrane properties modulate ADAM10 and ADAM17-mediated substrate cleavage (27). Application of free unsaturated fatty acids induced ADAM-mediated shedding by increasing cell membrane fluidity and augmenting the mobility of enzyme and substrate in the membrane. From these findings, the suspicion arose that other membrane active agents such as melittin might also augment the function of ADAMs.

In this communication, we report that melittin indeed provokes rapid substrate cleavage by ADAMs in diverse cell types. We found, however, that the increase in ADAM-mediated shedding was not due to changes in membrane fluidity. Instead, evidence is presented that exposure of cells to sublethal concentrations of melittin results in P2 receptor activation. This in turn is responsible for augmentation of ADAM activity and downstream EGFR transactivation in HaCaT keratinocytes.

EXPERIMENTAL PROCEDURES

Reagents and Antibodies—Melittin was synthesized with an amidated C terminus by the Fmoc solid-phase peptide synthesis technique on an automatic peptide synthesizer (model 433 A; Applied Biosystems) as described (28). Monoclonal antibodies against the cytoplasmic domain of E-cadherin (C36) and N-cadherin were purchased from BD Bioscience. ADAM10 was detected using a polyclonal antiserum described previously (20). Rabbit polyclonal anti-ADAM17 cytotail antibody was kindly provided by Carl Blobel (NY) (29). Monoclonal antibody against VE-cadherin and peroxidase-conjugated immunoglobulins to mouse or rabbit IgG were obtained from Santa Cruz Biotechnology, Inc. The EGFR-function blocking antibody Cetuximab (C225) was from Merck. CD62L antibodies were from eBioscience. Pyridoxalphosphate-6-azophenyl-2′,4′,-disulfonic acid (PPADS), suramin, hexokinase, apyrase, BAPTA-AM (1,2- bis(o-aminophenoxy)ethane-*N*,*N*,*N*′,*N*′-tetraacetic acid, sodium), EGTA, TAPI-0, and MTT (3-(4,5-dimethylthiazol-2-yl)-2,5 diphenyltetrazolium-bromide) were obtained from Sigma. Evans Blue and marimastat were purchased from Tocris. Hydroxamate-based inhibitors GW280264 ((2*R*,3*S*)-3-(formyl-hydroxyamino)-2-(2-methyl-1-propyl) hexanoic acid [(1*S*)-5-benzyloxycarbamoylamino-1-(1,3-thiazol-2-ylcarbamoyl)-1-pentyl] amide) and GI254023 ((2*R*,3*S*)-3-(formyl-hydroxyamino)-2-(3-phenyl-1-propyl) butanoic acid [(1*S*)-2,2-dimethyl-1-methylcarbamoyl-1-propyl] amide) were synthesized as described in US patents US 6 172 064, US 6 191 150, and US 6 329 400. They were kindly provided by Dr. A. Ludwig (UK Aachen, Germany) and are described in detail elsewhere (30). The human P2X7R cDNA was kindly provided by Carl Blobel (31).

Cell Culture—HUVECs were obtained from Provitro and cultured in Endothelial Cell Growth Medium (PromoCell). All experiments were performed with HUVECs from passages 3–7. HaCaT keratinocytes were provided by Dr. N. E. Fusenig (DKFZ, Heidelberg, Germany) (32). Mouse embryonic fibroblast (MEF) cell lines from ADAM10$^{-/-}$ mice and respective wild-type animals were generated and characterized as described elsewhere (20, 33). MEFs, HaCaT keratinocytes and HEK-293T cells (ATCC) were grown in high glucose DMEM (PAA, Linz, Austria) supplemented with 10% FCS and 1% penicillin/streptomycin.

Transfection—HEK cells were seeded in six-well plates and transfected on the next day with 1 μg/well plasmid DNA encoding for P2X7. Transfection was performed using TurboFect™ *in vitro* Transfection Reagent (Fermentas, St. Leon-Rot, Germany) according to the manufacturer's instructions. Cells were grown for 48 h prior to stimulation and protein extraction for Western blot analysis.

MTT Assay—Metabolic activity was determined in 96-well plates in triplicates by quantifying the reduction of MTT to formazan. Briefly, cells were incubated with the indicated amounts of melittin in 100 μl serum-free medium for 30 min. Untreated and 2.5% Triton-X treated cells served as controls. Afterward medium was replaced by 100 μl of 0.5 mg/ml MTT in 10% standard cell culture medium and 90% PBS and incubated for 2 h at 37 °C. Formed formazan crystals were dissolved by adding 100 μl of 10% Triton-X in isopropanol. Extinction was measured at 590 nm and absorbance values were normalized to untreated and Triton-X treated controls.

Bioluminescence Assay for Determination of Cellular ATP—CellTiter-Glo Luminescent Cell Viability Assay (Promega) was used to determine the release of soluble ATP. The assay was performed according to manufacturer's instructions.

Membrane Fluidity—HaCaT keratinocytes (1 ml, 5×10^8 cells) were incubated for 30 min at 32 °C with diphenyl hexatriene (DPH, 4 μM). To remove unbound DPH, the cells were centrifuged for 5 min at 3000 × *g*, were washed twice with PBS and were resuspended in 10 ml PBS. The cells were then transferred to a thermostated cuvette under continuous stirring. Anisotropy was measured in a Quantamaster (PTI, Canada) fluorimeter using Glan-Thompson polarizers at excitation and emission wavelengths of 360 ± 4 nm and 430 ± 4 nm, respectively, including a GG390 cut-off filter at the emission site. Steady-state fluorescence anisotropy (r) was determined according to $r = (I_{VV}\text{-}I_{VH}G)/(I_{VV}+2\,I_{VH}G)$, where I_{VV} and I_{VH} are the fluorescence intensities observed with the excitation polarizer in the vertical position, and the analyzing emission polarizer in both the vertical (I_{VV}) and horizontal (I_{VH}) configuration. Factor G corrects for the unequal transmission of differently polarized light.

Calcium Influx—Peptide-mediated calcium influx in HaCaT keratinocytes was monitored over time by fluorescence spectroscopy using the Ca^{2+}-sensitive dye Indo-1. The assay and all washing steps were performed either in PBS, pH 7.4 containing 1% FCS (buffer A) or in the same buffer supplemented with 1 mM $CaCl_2$ and 1 mM $MgCl_2$ (buffer B). Cells were washed in buffer A or B and adjusted to 10^6 cells/ml, preloaded with 1 μM Indo-1-AM (Invitrogen, Molecular Probes) for 45 min at 37 °C, washed again, and adjusted to 10^5 cells/ml in the respective buffer. The assay was performed at room temperature in 2 ml glass cuvettes using a spectrofluorometer (Fluorolog-3, Horiba) with an excitation wavelength of 355 nm as well as emission wavelengths of 405 and 485 nm to detect the Ca^{2+}-bound and the Ca^{2+}-free form of the dye. Fluorescence of the cell suspension was monitored for 1 min before the addition of peptide without any measurable change in fluorescence. Then, melittin was added in indicated concentrations and the fluorescence was monitored for additional 4 min. Data are represented as the quotient (F_{405}/F_{485}) of the normalized emission intensities (F_t/F_0) of the two wavelengths, *i.e.* the fluorescence intensity at a certain time point (F_t) divided by the mean fluorescence intensity before addition of peptide (F_0). At least two independent experiments were performed and one representative experiment is shown.

L-selectin FACS Analysis—PMN were isolated from heparinized peripheral blood of healthy donors using Biocoll Separating Solution (Biochrom AG) according to the manufacturer's recommendations. Residual erythrocytes were removed using lysis buffer containing NH_4Cl. PMN purity was >90% as determined by flow cytometric analysis and by counting in a hemocytometer. Stock suspensions of the cells ($20–30 \times 10^6$ per ml) were kept in PBS on ice and used within 2 h. Experiments were conducted in HBSS using 3×10^6 cells/ml.

Immunoblotting—Immunoblots for the analysis of VE-cadherin, N-cadherin, and E-cadherin were performed as described elsewhere (22–24). Signals were recorded by a luminescent image analyzer (Fuji image reader LAS1000) and analyzed with image analyzer software (GEL-PROANALYSER, Media Cybernetics, Silver Spring, MD). To generate the control blots for expression of ERK1/2 and EGFR, Western blots were incubated in stripping reagent (100 mM 2-mercaptoethanol, 2% (w/v) SDS, 62.5 mM Tris-HCl pH 6.7) at 55 °C for 30 min and then re-probed with anti ERK1/2 or EGFR antibody, respectively.

In Vitro Wound Healing—HaCaT keratinocytes were seeded in 12-well plates (Sarstedt) and grown until they reached confluence (48 h). A cell-free area was introduced by scraping the monolayer with a pipette tip (10 μl, Sarstedt). To avoid a proliferative effect, cells were treated with 2 mM hydroxyurea (Sigma-Aldrich) for 24 h. For stimulation experiments, FCS-free medium containing metalloprotease inhibitors or DMSO was added. After 15 min pre-incubation, the cells were treated with melittin (0.5 μM). Cells were photographed before stimulation and 24 h after stimulation by using an inverted phase-contrast microscope (Zeiss). The cell free area was quantified using AxioVision (Zeiss) before and after stimulation, respectively.

Cell Proliferation Assays—HaCaT keratinocytes were cultured overnight in medium containing FCS before starvation for 48 h. Subsequently, medium containing various agents was added, and cells were incubated for 24 h. PI cell cycle analysis was performed as previously described (34).

Quantitative Real-time-PCR—mRNA was isolated with peqGOLDTriFast (Peqlab) and reverse transcribed by Maxima Reverse Transcriptase (Thermofisher Scientific) as described by the manufacturer's protocol. The quantitative real-time-PCR was performed in a Lightcycler II (Roche). The reaction mixture consisted of 10 ng cDNA, 0.5 μM of each primer (hb2M, forward: ATGAGTATGCCTGCCGTGTGA, reverse: GGCATCTTCAAACCTCCATG; hADAM10, forward: AGTGGACCCATCAACTTGTG, reverse: CCAGCCATTAGCATGATCAG; hADAM17, forward: AGACAGAGAACCACCTGAAG reverse: CCCATGAAGTGTTCCGATAG), and 2 μl of My budget 5× EvaGreen QPCR Mix Capillary (BioBudget) per 10 μl mixture. Water was used as a control. Each mRNA expression was normalized against beta-2 microglobulin mRNA (ΔΔCT-method) and all data are presented as fold change against the unstimulated control. Each experiment was performed in duplicate and the S.E. has been calculated on the basis of the two experiments.

Statistical Analysis of CTF Generation—All values are expressed as means ± S.E. or as otherwise indicated. Variance analysis was performed with one-way ANOVA (SigmaStat 3.1 software; Erkrath, SYSSTAT, Germany). Pair wise and multiple comparison procedures were performed with Bonferroni test or Dunnett's test. p values < 0.05 were classified as statistically significant.

RESULTS

Melittin Effects on Cellular Viability Are Cell Type Dependent—High concentrations of melittin are known to induce necrosis and apoptosis, while low concentrations have been shown to enhance cell proliferation (35). To exclude that potential cytotoxic effects would affect substrate processing and to define sublethal concentrations of melittin in our experiments, MTT reduction was measured and taken as a parameter of cell viability. The yellow tetrazolium MTT is reduced by metabolically active cells leading to generation of intracellular purple formazan which can be quantified. As

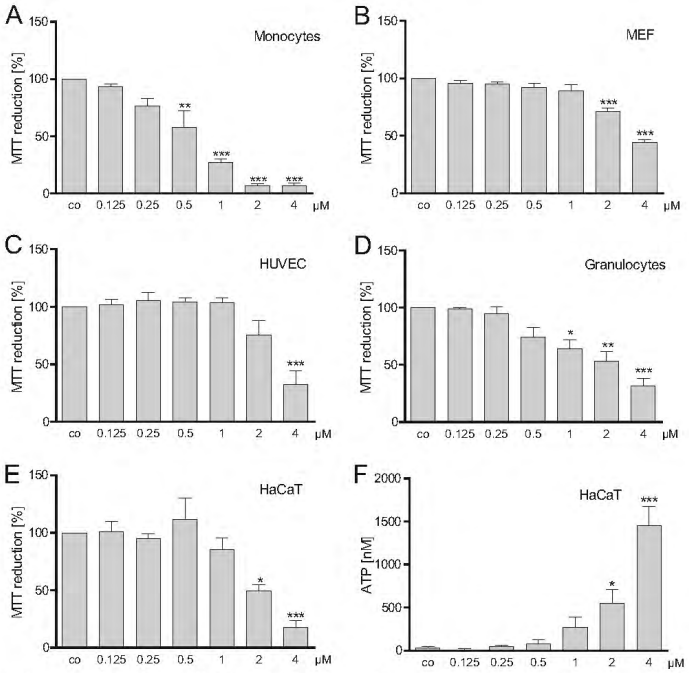

FIGURE 1. **Low concentrations of melittin do not affect cell viability.** Primary human monocytes (*A*), murine embryonic fibroblasts (MEFs) (*B*), human umbilical vein endothelial cells (HUVECs) (*C*), human neutrophil granulocytes (*D*), and HaCaT keratinocytes (*E*, *F*) were incubated with different dosages of melittin for 30 min. Reduction of MTT was measured as readout for cell viability (*A–E*) and ATP release (*F*) was determined using a luminescent ATP-based assay. Data represent mean values ± S.E. of three independent experiments all measured in triplicates. * indicates significant difference compared with control (*, $p < 0.05$; **, $p < 0.01$; ***, $p < 0.001$).

shown in Fig. 1, all cells tested responded to melittin treatment with a decrease in MTT reduction. Human monocytes were most sensitive and were not used in the following experiments (Fig. 1*A*). Murine embryonic fibroblasts (MEFs) and human umbilical vein endothelial cells (HUVECs) were least sensitive and significant reduction in cellular viability occurred at 2 and 4 μM melittin, respectively (Fig. 1, *B* and *C*). Melittin concentrations $\geq$ 0.5 μM led to a significant decrease of MTT reduction in human neutrophil granulocytes (Fig. 1*D*). HaCaT keratinocytes tolerated melittin effects up to a threshold concentration of 1 μM (Fig. 1*E*).

The same results for melittin-induced cytotoxicity in HaCaT keratinocytes have been previously reported (36). We concluded that concentrations between 0.5 μM and 1 μM melittin were tolerable and they were usually employed, except in experiments with MEFs where higher doses were required to induce a significant increase in shedding events.

To discern whether melittin treatment would also lead to ATP release, we additionally measured ATP in the supernatant of melittin-treated HaCaT keratinocytes. As shown in Fig. 1*F*, melittin evoked ATP release dose-dependently. Nanomolar concentrations became detectable in the supernatants also when non-toxic melittin concentrations were applied.

Melittin Induces ADAM-dependent Substrate Cleavage—Shedding of certain substrates is preferentially elicited by specific members of the ADAM family. ADAM10 is critically involved in the release of the adhesion molecule N-cadherin in fibroblasts and neuronal cells (22, 37, 38). To discern whether melittin would stimulate ADAM10-dependent shedding, we analyzed N-cadherin processing in MEFs using monoclonal antibodies against the C terminus of the adhesion molecule. The generation of the N-cadherin C-terminal fragment (CTF) in wild-type cells was compared with ADAM10-deficient fibroblasts. As shown in Fig. 2*A*, melittin dose-dependently induced N-cadherin shedding in wild-type cells while the CTF was not generated in ADAM10-deficient cells.

Analogously, shedding of VE-cadherin was found to occur in response to 0.5–1 μM melittin. Shedding was inhibited by the broadspectrum metalloprotease inhibitor marimastat (Fig. 2*B*), and also by GI254023X, a preferential inhibitor of ADAM10 (data not shown).

To analyze the stimulated cleavage of a preferential ADAM17 substrate, the release of soluble L-selectin (CD62L) was determined in neutrophil granulocytes using FACS analysis (21, 31, 39). L-selectin was rapidly shed from cells following treatment with 0.5 μM melittin. This effect was abrogated in the

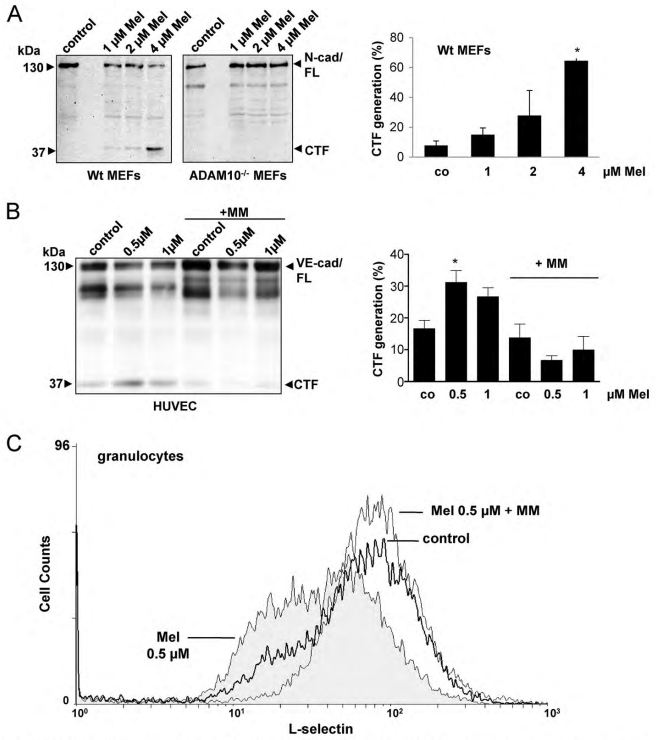

FIGURE 2. **Melittin increases ADAM-mediated proteolysis in different cell types.** *A*, MEFs were mock treated (control) or stimulated with increasing amounts of melittin for 30 min. Total cell extracts from wild type-MEFs (*Wt*) and ADAM10$^{-/-}$ fibroblasts were subjected to immunoblot analysis and stained with a C-terminal anti-N-cadherin antibody. N-cadherin CTF generation in Wt-MEFs was calculated by densitometric analysis of three independent experiments (*right panel*). Results are expressed as mean ± S.E. ($n = 3$). CTF formation was significantly increased after melittin treatment (*, $p < 0.05$). *B*, HUVECs were stimulated with melittin in the presence or absence of broadspectrum metalloprotease inhibitor marimastat (MM, 10 μM). VE-cadherin cleavage was analyzed with a C-terminal VE-cadherin antibody by immunoblot. *D*, densitometric analysis of three independent experiments is shown in the *right panel* (*, $p < 0.05$). *C*, human neutrophil granulocytes were stimulated with 0.5 μM melittin for 15 min in the presence or absence of marimastat (MM, 10 μM). Cell surface expression of CD62L was determined by FACS analysis.

presence of the broad-spectrum metalloprotease inhibitor marimastat (Fig. 2*C*).

Melittin Induces ADAM-dependent E-cadherin Shedding and Transactivation of the EGFR in HaCaT Keratinocytes—The effects of melittin on HaCaT keratinocytes were then investigated. In these cells, E-cadherin is preferentially cleaved by ADAM10 (23), while shedding of TGF-alpha is dependent mainly on ADAM17 (21). Melittin dose-dependently augmented proteolysis of E-cadherin (Fig. 3*A*), and this effect could be significantly reduced by the use of broadsprectrum-metalloprotease inhibitor marimastat but also by the preferential ADAM10 inhibitor GI254023X and GW280264, an inhibitor of ADAM10 and ADAM17 (Fig. 3*B*). Melittin simultaneously provoked release of TGF-α into the supernatant. As to be expected, this event was strongly reduced by the mixed ADAM10/ADAM17 inhibitor GW280264 and marimastat, but only slightly affected by the preferential ADAM10 inhibitor GI254023X (Fig. 3*C*).

TGF-α is a potent ligand of the EGFR which critically participates in the control of cell differentiation, proliferation and cell survival. In addition to TGF-α, six other ligands are known to activate the EGFR via EGF-like motifs, and all are shed by ADAM10 and/or ADAM17 (25, 40). It followed that treatment of cells with melittin might lead to EGFR activation. Indeed, exposure of HaCaT keratinocytes to melittin-induced EGFR phosphorylation with downstream activation of ERK1/2, which were prone to inhibition by marimastat (Fig. 3*D*).

Melittin Induces Metalloprotease-dependent HaCaT Keratinocyte Cell Proliferation and Migration—The results suggested that functional consequences might follow the shedding processes (23, 24, 41).

Incubation of HaCaT keratinocytes with melittin indeed resulted in increased cell proliferation, as determined by propidium iodide (PI) cell cycle analysis (Fig. 4*A*). This effect was essentially abrogated in the presence of the broad-spectrum metalloprotease inhibitor TAPI-0. To address the role of melit-

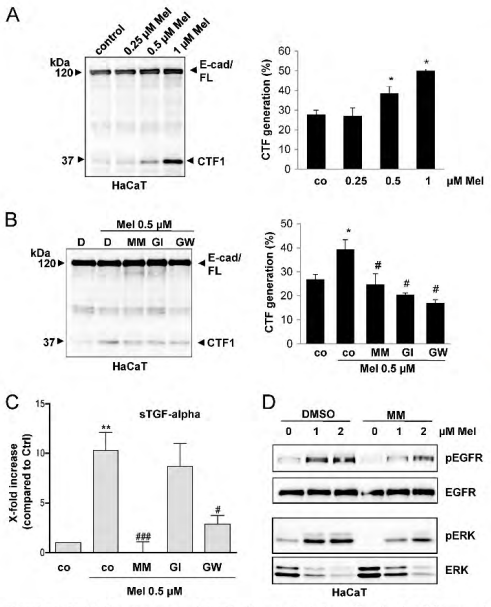

FIGURE 3. **Melittin augments ADAM-dependent E-cadherin shedding and EGFR activation in HaCaT keratinocytes.** *A*, after incubation with different amounts of melittin, HaCaT keratinocyte pellets were subjected to immunoblot analyses using a C-terminal E-cadherin antibody. E-cadherin CTF generation was calculated by densitometric analysis of three independent experiments (*right panel*). Results are expressed as mean ± S.E. ($n = 3$). *B*, cells were treated with the ADAM10 inhibitor GI254023X (GI, 3 μM), the ADAM17/ADAM10 inhibitor GW280264X (GW, 3 μM), the broad-spectrum metalloprotease inhibitor marimastat (MM, 10 μM), or DMSO (*D*) as a control for 10 min before stimulation. E-cadherin CTF generation was calculated by densitometric analysis of three independent experiments (*right panel*). Melittin significantly increased E-cadherin proteolysis (*, $p < 0.05$, $n = 3$). Marimastat, GI and GW significantly decreased this melittin effect (#, $p < 0.05$, $n = 3$). *C*, release of soluble TGF-α (sTGF-α) from HaCaT keratinocytes was analyzed by ELISA and compared with mock-treated cells. Cells were stimulated with 0.5 μM melittin for 30 min in the presence or absence of the ADAM10 inhibitor GI254023X (*GI*) or the ADAM17/ADAM10 inhibitor GW280264X (*GW*). Data represent mean values of five independent experiments with S.E. Melittin significantly induced sTGF-α release (**, $p < 0.01$, $n = 5$). Marimastat and GW significantly decreased melittin-induced TGF-α shedding (#, $p < 0.05$, ###, $p < 0.001$, $n = 5$). *D*, HaCaT keratinocytes were treated with melittin for 30 min in the presence or absence of marimastat (MM, 10 μM). Representative Western blot analyses of EGFR phosphorylation and ERK1/2 phosphorylation are shown with an immunoblot of total EGFR and total ERK1/2 included as loading control.

tin for HaCaT keratinocyte migration, we used an *in vitro* model for wound healing. In this assay, scrape wounds were generated in confluent HaCaT keratinocyte cultures, and cells were allowed to migrate for 24 h. The scratch assays were performed in the presence of 2 mM hydroxyurea to prevent HaCaT keratinocyte proliferation (42). While mock-treated cells just started to cover the denuded area, melittin stimulation led to nearly complete wound closure. This effect was abolished in the presence of the broad-spectrum metalloprotease inhibitor marimastat (Fig. 4*B*). Application of the monoclonal antibody Cetuximab, which blocks access of ligands to the EGF receptor, significantly reduced HaCaT keratinocyte migration (Fig. 4*C*), indicating that EGFR activation indeed plays a key role in the observed cellular reaction.

Cell Membrane Fluidity and ADAM10/ADAM17 Expression Are Not Changed by Melittin—We have presented evidence that alterations in membrane fluidity have a direct impact on ADAM function, and found that application of unsaturated fatty acids to cells augmented cleavage of ADAM substrates in a manner that now seemed to be mimicked by melittin (27). Because the peptide modulates the biophysical properties of membranes (43), the diffusion of fatty acyl chains in HaCaT keratinocyte membranes was determined using steady-state fluorescence anisotropy with diphenyl hexatriene (DPH) as a probe. Melittin at concentrations that induced ADAM substrate processing exerted no effects on membrane fluidity. Even much higher concentrations remained without effect (supplemental Fig. S1). In contrast, rapid decrease in anisotropy was observed in response to oleic acid, which was used as positive control.

The possibility was considered that melittin might activate signaling pathways leading to modulation of ADAM expression, stability, or maturation. Removal of the prodomain by furin-type proprotein convertases is necessary to convert the inactive pro-form to the mature active enzyme. However, even prolonged treatment of cells with melittin led to no changes in expression of ADAM10 or ADAM17, or to increased maturation of the enzymes (supplemental Fig. S1).

Increase in Cytosolic Calcium Is Not Involved in ADAM Activation—Melittin stimulation has been shown to induce calcium influx in different cell types. To determine whether extracellular calcium influx would contribute to ADAM activation, HaCaT keratinocytes were stimulated with increasing concentrations of this compound in calcium-containing and in calcium-free medium. A rapid dose-dependent increase in free intracellular Ca^{2+} was observed immediately after addition of melittin to HaCaT keratinocytes (supplemental Fig. S2, *left panel*). A pronounced effect was visible down to 0.2–0.4 μM melittin. The melittin-induced increase of intracellular Ca^{2+} in buffer lacking Ca^{2+} and Mg^{2+} (*right panel*) was reduced by 20 and 15% for 1 and 0.4 μM melittin compared with the Ca^{2+} increase in buffer containing Ca^{2+} and Mg^{2+}. This indicated that melittin induced the influx of extracellular Ca^{2+} as well as the release of Ca^{2+} from intracellular stores.

Calcium can act in signal transduction and calcium ionophores are widely used to induce the shedding of several ADAM10 substrates such as N-cadherin, E-cadherin, CD44, or betacellulin (23, 31, 38, 44). However, the melittin-induced E-cadherin shedding did not rely on the increase of free calcium because neither chelation of extracellular calcium by 5 mM EGTA nor the use of the membrane-permeable calcium chelator BAPTA-AM affected the cellular response (supplemental Fig. S2). The same applied to the activation of EGFR signaling (supplemental Fig. S2).

Melittin Effects Depend on ATP Release and P2 Receptor Activation—Purinergic P2 receptors participate in the regulation of several physiological processes. They are divided into two major families, the P2X receptors, which are ATP-gated ion channels, and the P2Y receptors, which are G-protein-coupled receptors (45). HaCaT keratinocytes express both P2X and

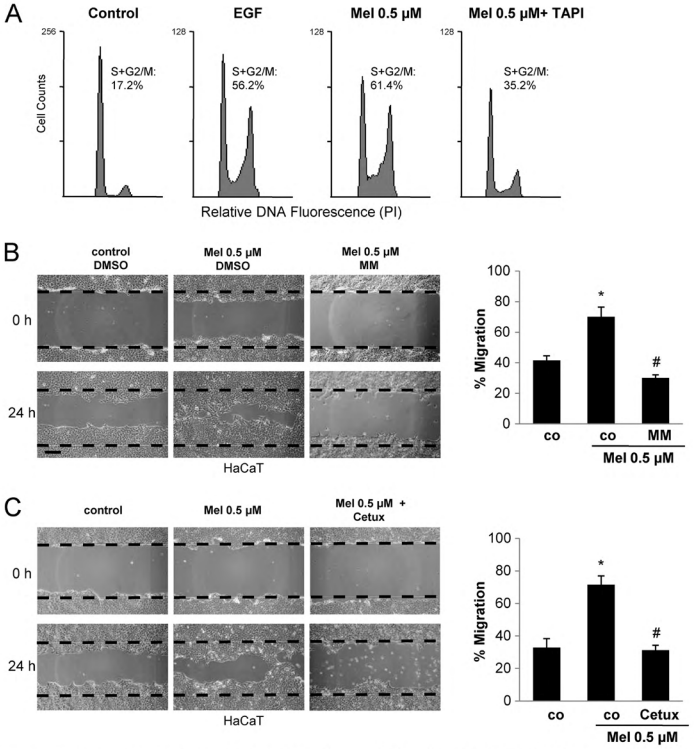

FIGURE 4. **Melittin augments metalloprotease-dependent proliferation and migration of epithelial cells.** *A*, cell cycle analysis was determined by propidium iodide (*PI*) staining and flow cytometry. HaCaT keratinocytes were seeded at 20,000 cells/well in microtiter plates and stimulated with EGF (4 nM) as positive control and with melittin (0.5 μM). After 24 h, increased percentages of EGF and melittin-treated cells are in S+G2/M phase. TAPI (10 μM) abrogated the melittin-induced effect. Analyses are representative of two independent experiments. *B* and *C*, melittin stimulates epithelial cell migration. HaCaT keratinocytes were grown to confluence and a cell-free area was introduced by scratching with a pipette tip. After washing, cells were mock treated or incubated with the indicated amounts of melittin (*B*) in the presence of the broad-spectrum metalloprotease inhibitor marimastat (MM, 10 μM) or (*C*) with the EGFR blocking antibody Cetuximab (Cetux, 10 μg/ml). Migration was evaluated after 24 h. Micrographs of one representative of three independent experiments are shown, respectively. Bar: 100 μm. Migration of three independent assays was quantified in the *right panel*. *Asterisk* (*) indicates a significant increase compared with mock-treated samples (*, $p < 0.05$, $n = 3$). MM and Cetux significantly inhibited melittin-induced migration (#, $p < 0.05$, $n = 3$).

P2Y receptors (46) and can thus be activated by ATP. Since melittin stimulation led to ATP release and P2 receptors have been discussed in the context of ADAM activation (31, 47–54), we performed experiments using the broad-spectrum P2R inhibitor, pyridoxalphosphate-6-azophenyl-2′,4′,-disulfonic acid (PPADS) (55, 56). As shown in Fig. 5*A*, PPADS abolished ERK1/2 activation dose-dependently (*upper panel*). Melittin-induced E-cadherin shedding was strongly reduced by PPADS to an extent comparable with marimastat effects (*lower panel*). To confirm these results, we additionally used the broad-spectrum P2 inhibitor suramin (Fig. 5*B*) and Evans Blue (Fig. 5*C*), a more selective P2X receptor antagonist. Both compounds reduced melittin-stimulated E-cadherin shedding and ERK1/2 activation in HaCaT keratinocytes.

To further validate a role of ATP in melittin-activation, cells were stimulated in the presence of the ATPase hexokinase. Addition of hexokinase reduced E-cadherin shedding and ERK1/2 activation dose-dependently (Fig. 5*D*), although the effects were not completely abrogated. Endogenously released ATP therefore appears to represent one, but possibly not the sole trigger of P2 receptor-mediated ADAM activation.

HEK cells are widely used as models to study the role of purinergic receptors because they only express low amounts of certain P2Y receptors (57) and do not express P2X receptors. We compared the melittin response in HEK cells with HEK cells transiently transfected with the P2X7 receptor. As shown in Fig. 5*E*, P2X7 transfection strikingly increased the response to melittin stimulation. The stimulation was abrogated by pretreatment with metalloprotease inhibitor marimastat and by treatment with the ATPase apyrase. Stimulation with the P2X7 agonist benzoyl-ATP (bzATP), which was used as positive control, elicited comparable effects.

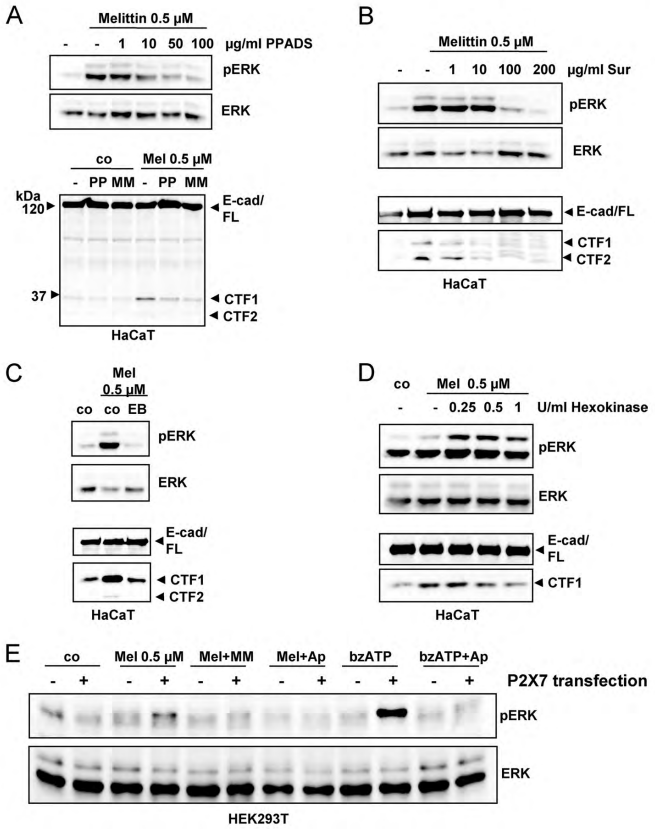

FIGURE 5. **P2 receptor signaling is involved in activation of melittin effects in HaCaT keratinocytes.** *A*, HaCaT keratinocytes were stimulated with melittin (0.5 μM) for 30 min in the presence of increasing amounts of PPADS. Representative Western blot analyses of ERK1/2 phosphorylation with an immunoblot of total ERK1/2 included as loading control is shown in the *upper panel*. PPADS (PP, 100 μM) inhibition of melittin-induced E-cadherin proteolysis was nearly as effective as marimastat (MM, 10 μM), *lower panel*. *B*, P2 receptor antagonist suramin (*Sur*) led to decrease of ERK1/2 phosphorylation and E-cadherin CTF generation at concentrations of 100 and 200 μM. *C*, P2 receptor antagonist Evans blue (*EB*) was found to inhibit melittin effects effectively at a concentration of 1 μM. *D*, ATPase hexokinase dose-dependently decreased ERK1/2 phosphorylation and E-cadherin shedding. *E*, HEK293T cells were mock-transfected or transfected with P2X7. 48 h afterward, cells were stimulated with melittin (0.5 μM) in the presence of marimastat (MM, 10 μM) or ATPase apyrase (Ap, 2 units/ml). Stimulation with bzATP (300 μM) was used as positive control. One representative immunoblot of three independent experiments is shown for all analyses.

DISCUSSION

The effects of melittin on cells are remarkably diverse and the functional outcomes essentially unpredictable (12, 58, 59). Reports on its anti-inflammatory and growth-suppressing action stand alongside with observations to the contrary. How the amphipathic peptide elicits these myriad reactions remains quite enigmatic. A cellular receptor is not known to exist. The cationic domain mediates binding, which is followed by membrane insertion of the hydrophobic sequence whose length suffices to span only half of the lipid bilayer. In analogy with pore-forming toxins, one possibility is that transmembrane pores are formed by melittin oligomers. While increases in membrane permeability for ions have been demonstrated and cell lysis occurs when critical concentrations are reached, data on the composition and structure of the putative pore are not available. Equally nebulous are the events that underlie triggering of the signaling pathways and the mediators that are involved in eliciting the sublethal effects of melittin.

This study adds another facet to the complex theme. We report that subcytotoxic concentrations of melittin cause rapid up-regulation in function of ADAMs, the central shedding proteinases of nucleated cells. The roles fulfilled by the individual ADAMs are varied, their pattern of tissue expression diverse, and the signaling pathways leading to their activation heterogeneous (31).

We elected to focus our investigation on the effects of melittin on ADAM10 and ADAM17, two major members of the

ADAM proteinase family. Our results indicate that melittin treatment leads to activation of both proteases. Further analyses will reveal whether the agent does indeed represent a broad-spectrum ADAM activator as may be anticipated at this stage, and which would accord very satisfactorily with its propensity to evoke such a wide range of biological effects.

ADAM10 is the major sheddase of classical cadherins. We investigated the shedding of N-cadherin in murine fibroblasts, VE-cadherin in human endothelial cells, and E-cadherin in human HaCaT keratinocytes. Melittin rapidly stimulated cleavage of each substrate. Cleavage of VE-cadherin increases endothelial permeability. Cleavage of E-cadherin likely provokes loss of epithelial cell-cell contacts and may contribute to the genesis of eczematous dermatitis (41). Thus, an explanation retrospectively emerges for the recent finding that melittin enhances permeability of CaCo-2 epithelial cell monolayers (60). ADAM17 cleaves a large number of substrates including cytokines (*e.g.* TNF-α) and their receptors (*e.g.* IL6R), TGF-α, and other EGFR ligands, and L-selectin. We investigated whether melittin would induce shedding of L-selectin in neutrophil granulocytes and TGF-α in HaCaT keratinocytes. The affirmative results obtained in both cases corroborate the contention that melittin truly can be viewed as an ADAM activator.

TGF-α can activate the EGFR signaling pathway to induce cell proliferation and migration (61). Since all EGFR ligands are released through proteolysis, it is quite likely that the shedding of additional ligands contributes to EGFR activation. In any case functional consequences would have to follow. The question whether cell growth would be promoted in our experiments was of particular interest since melittin is being considered as an anti-tumor agent. Subtoxic concentrations were indeed found to induce ERK1/2-phosphorylation. This process was metalloprotease and EGFR-dependent and vigorously stimulated proliferation and migration of human HaCaT keratinocytes. Detailed analyses using specific inhibitors or siRNA experiments will be required to differentiate the contribution of ADAM10, ADAM17, or even additional metalloproteases to these processes.

However, these proliferation promoting features are in line with and provide an explanation for the melittin-induced proliferation of gastrointestinal cells (35). With regard to the usefulness of melittin as anti-cancer agent (9), our results bring these approaches into question.

The pathway leading to ADAM activation by melittin is under investigation and has led to a number of findings that are of interest. The physical properties of membranes may participate in controlling ADAM function by influencing the velocity of molecular movement in the lipid bilayer. Enhancement of fluidity by unsaturated free fatty acids accelerates cleavage of membrane anchored substrates. The rapid kinetics of substrate cleavage provoked by melittin were reminiscent of those previously observed to be invoked by free fatty acids. We therefore examined the effect of melittin on membrane fluidity, but could observe no effects in the HaCaT keratinocytes.

Melittin is known to provoke Ca^{2+}-influx, which in turn would be a prime candidate for triggering ADAM activity. Dose-dependent increases of cytosolic Ca^{2+} concentrations were indeed detected upon exposure to melittin. Surprisingly, however, ADAM up-regulation by melittin displayed no requirement for Ca^{2+} and was observed in the presence of EGTA and in cells loaded with the intracellular calcium chelator BAPTA-AM. In the course of these investigations, we also employed conventional inhibitors of intra-cellular signaling pathways but could not identify any substance that effectively inhibited melittin-mediated ADAM activation (data not shown).

The link between melittin and ADAMs emerged as attention then turned to a possible involvement of purinergic receptors. A few studies have demonstrated that, among their many functions, these receptors also play a role in regulating ADAM activity. ADAM-dependent cleavage of L-selectin from human leukemic B-cells is inducible by extracellular ATP (49, 52), and in mice, shedding of this adhesion molecule is dependent on P2X7R (62). The same receptor controls shedding of CD23 and CD27, two important mediators of the immune system (53, 54). In those studies, ADAM activation was provoked by application of ATP at supraphysiological concentrations. Here, we propose that purinergic receptor activation via membrane attack by an extrinsic agent can lead to up-regulation of ADAM function in the responding cell. The conclusion is derived from two lines of evidence. First, melittin-mediated ADAM activation was suppressed by PPADS, Evans Blue, and suramin, three commonly employed inhibitors of purinergic receptors. Second, transfection of P2X7 in HEK293 cells increased the ERK-activating capacity of melittin, which was again abrogated in the presence of apyrase, clearly indicating that ATP release represents a critical step for downstream transduction mechanisms. Given the complexity and redundancy of the large receptor family, no attempts were here undertaken to identify other members that might be involved in ADAM activation. As in previous studies (31), our report is limited to the description of the phenomenon. Elucidation of the molecular links between purinergic receptors and ADAMs remains a challenge for the future.

According to our data, melittin induced P2 receptor activation appears to involve ATP. However, how ATP is released and how sufficient concentrations of ATP should accumulate to trigger the receptors is not clear. Multiple mechanisms mediate the release of intracellular ATP in response to diverse stimuli, including mechanical stimulation, stretch, osmolarity change, oxidative stress, and microbial products (63). The MTT assays indicate that egress of ATP from cells occurs already at non-toxic melittin concentrations. Thus, we assume that this process represents a physiological cellular response. The human cathelicidin-derived antimicrobial peptide LL-37 has similarly been reported to induce transient release of ATP in the absence of overt cell cytotoxicity (64).

Even though melittin membrane interaction is quite likely to directly induce ATP release, additional mechanisms might be involved such as the generation of reactive oxygen species (ROS) (12). P2X7 receptor activation leads to Pannexin-1 pore formation through which ATP release could occur, so that a self-amplifying activation loop may furthermore be created.

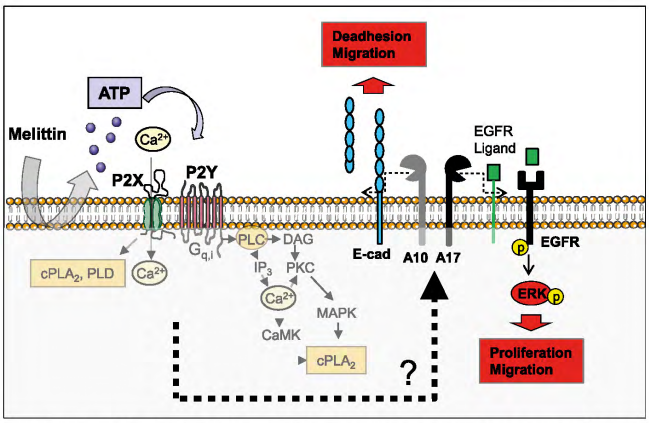

FIGURE 6. **Schematic representation of melittin-stimulated effects.** Melittin-induced ATP release leads to activation of P2X and P2Y receptors, which trigger several signaling pathways. Whether and how these signaling cascades activate ADAM10 and ADAM17 remains nebulous. ADAM10 and ADAM17 activation results in shedding of E-cadherin (E-cad) and in the release of EGFR ligands. E-cadherin shedding decreases cell-cell adhesion and induces cell migration. EGFR phosphorylation triggers downstream signaling cascades leading to increased HaCaT keratinocyte migration and proliferation.

However, the melittin concentrations employed incurred little depletion of cellular ATP, and only nanomolar concentrations were measureable in the supernatants. Although local ATP concentrations at the cell surface may be considerably higher, P2 receptor and ADAM activation might also be effected through more complex events. This would be in accord with the finding that the ATPase hexokinase reduced but did not completely abrogate the melittin effects. Melittin has been suggested to interact with membrane proteins at the cell surface (65), and it might also be speculated that direct binding of melittin to P2 receptors can occur to effect their triggering.

Such a direct interaction with P2 receptors has recently been proposed for the antimicrobial peptide LL-37 (66), and reports on the P2R and EGFR-activation properties of this peptide are of particular interest here (67, 68). There is evidence that the peptide induces IL-1β release in lipopolysaccaride-primed monocytes through activation of P2X7 (64). Furthermore, the same receptor appears to mediate the mitogenic effect of the peptide on epithelial cells. The latter finding accorded with earlier studies in which ATP had been shown to stimulate cell proliferation (69, 70), most likely due to ADAM activation.

To sum, this study has revealed that ADAM activation is a major downstream event occurring in the wake of membrane attack by melittin (Fig. 6). Depending on the cell target, very diverse functional consequences are likely to follow that can hardly be predicted or controlled. This should be of interest particularly to investigators who are engaged in the development of melittin as a therapeutic agent.

Acknowledgments—We thank Björn Ahrens, Fatima Boukhallouk, Silvia Weis, and Sabrina Groth for their excellent technical assistance. Some data of this publication are part of the PhD thesis of Isabell Cornelsen and Anja Fries. We are grateful to the Blood Transfusion Center of the University of Mainz for providing blood samples from healthy donors.

REFERENCES

1. Raghuraman, H., and Chattopadhyay, A. (2007) Melittin: a membrane-active peptide with diverse functions. *Biosci. Rep.* **27,** 189–223
2. Sessa, G., Freer, J. H., Colacicco, G., and Weissmann, G. (1969) Interaction of alytic polypeptide, melittin, with lipid membrane systems. *J. Biol. Chem.* **244,** 3575–3582
3. Dawson, C. R., Drake, A. F., Helliwell, J., and Hider, R. C. (1978) The interaction of bee melittin with lipid bilayer membranes. *Biochim. Biophys. Acta* **510,** 75–86
4. Schoch, P., and Sargent, D. F. (1980) Quantitative analysis of the binding of melittin to planar lipid bilayers allowing for the discrete-charge effect. *Biochim. Biophys. Acta* **602,** 234–247
5. Lavialle, F., Levin, I. W., and Mollay, C. (1980) Interaction of melittin with dimyristoyl phosphatidylcholine liposomes: evidence for boundary lipid by Raman spectroscopy. *Biochim. Biophys. Acta* **600,** 62–71
6. Orsolic, N. (2012) Bee venom in cancer therapy. *Cancer Metastasis Rev.* **31,** 173–194
7. Duclohier, H. (2010) Antimicrobial peptides and peptaibols, substitutes for conventional antibiotics. *Curr. Pharm. Des.* **16,** 3212–3223
8. Son, D. J., Lee, J. W., Lee, Y. H., Song, H. S., Lee, C. K., and Hong, J. T. (2007) Therapeutic application of anti-arthritis, pain-releasing, and anti-cancer effects of bee venom and its constituent compounds. *Pharmacol. Ther.* **115,** 246–270
9. Liu, S., Yu, M., He, Y., Xiao, L., Wang, F., Song, C., Sun, S., Ling, C., and Xu, Z. (2008) Melittin prevents liver cancer cell metastasis through inhibition of the Rac1-dependent pathway. *Hepatology* **47,** 1964–1973
10. Russell, P. J., Hewish, D., Carter, T., Sterling-Levis, K., Ow, K., Hattarki, M., Doughty, L., Guthrie, R., Shapira, D., Molloy, P. L., Werkmeister, J. A., and Kortt, A. A. (2004) Cytotoxic properties of immunoconjugates containing melittin-like peptide 101 against prostate cancer: *in vitro* and *in vivo* studies. *Cancer Immunol. Immunother.* **53,** 411–421
11. Soman, N. R., Baldwin, S. L., Hu, G., Marsh, J. N., Lanza, G. M., Heuser, J. E., Arbeit, J. M., Wickline, S. A., and Schlesinger, P. H. (2009) Molecularly targeted nanocarriers deliver the cytolytic peptide melittin specifically to tumor cells in mice, reducing tumor growth. *J. Clin. Invest.* **119,** 2830–2842
12. Stuhlmeier, K. M. (2007) Apis mellifera venom and melittin block neither NF-κB-p50-DNA interactions nor the activation of NF-κB, instead they activate the transcription of proinflammatory genes and the release of reactive oxygen intermediates. *J. Immunol.* **179,** 655–664
13. Vernon, L. P., and Bell, J. D. (1992) Membrane structure, toxins and phos-

pholipase A2 activity. *Pharmacol. Ther.* **54,** 269–295
14. Moon, D. O., Park, S. Y., Heo, M. S., Kim, K. C., Park, C., Ko, W. S., Choi, Y. H., and Kim, G. Y. (2006) Key regulators in bee venom-induced apoptosis are Bcl-2 and caspase-3 in human leukemic U937 cells through downregulation of ERK and Akt. *Int. Immunopharmacol.* **6,** 1796–1807
15. Park, H. J., Son, D. J., Lee, C. W., Choi, M. S., Lee, U. S., Song, H. S., Lee, J. M., and Hong, J. T. (2007) Melittin inhibits inflammatory target gene expression and mediator generation via interaction with IκB kinase. *Biochem. Pharmacol.* **73,** 237–247
16. Nah, S. S., Ha, E., Mun, S. H., Won, H. J., and Chung, J. H. (2008) Effects of melittin on the production of matrix metalloproteinase-1 and -3 in rheumatoid arthritic fibroblast-like synoviocytes. *J. Pharmacol. Sci.* **106,** 162–166
17. Cho, H. J., Jeong, Y. J., Park, K. K., Park, Y. Y., Chung, I. K., Lee, K. G., Yeo, J. H., Han, S. M., Bae, Y. S., and Chang, Y. C. (2010) Bee venom suppresses PMA-mediated MMP-9 gene activation via JNK/p38 and NF-κB-dependent mechanisms. *J. Ethnopharmacol.* **127,** 662–668
18. Saftig, P., and Reiss, K. (2011) The "A Disintegrin And Metalloproteases" ADAM10 and ADAM17: novel drug targets with therapeutic potential? *Eur. J. Cell Biol.* **90,** 527–535
19. Reiss, K., and Saftig, P. (2009) The "a disintegrin and metalloprotease" (ADAM) family of sheddases: physiological and cellular functions. *Semin. Cell Dev. Biol.* **20,** 126–137
20. Hartmann, D., de Strooper, B., Serneels, L., Craessaerts, K., Herreman, A., Annaert, W., Umans, L., Lübke, T., Lena, Illert, A., von Figura, K., and Saftig, P. (2002) The disintegrin/metalloprotease ADAM 10 is essential for Notch signaling but not for α-secretase activity in fibroblasts. *Hum. Mol. Genet.* **11,** 2615–2624
21. Peschon, J. J., Slack, J. L., Reddy, P., Stocking, K. L., Sunnarborg, S. W., Lee, D. C., Russell, W. E., Castner, B. J., Johnson, R. S., Fitzner, J. N., Boyce, R. W., Nelson, N., Kozlosky, C. J., Wolfson, M. F., Rauch, C. T., Cerretti, D. P., Paxton, R. J., March, C. J., and Black, R. A. (1998) An essential role for ectodomain shedding in mammalian development. *Science* **282,** 1281–1284
22. Reiss, K., Maretzky, T., Ludwig, A., Tousseyn, T., de Strooper, B., Hartmann, D., and Saftig, P. (2005) ADAM10 cleavage of N-cadherin and regulation of cell-cell adhesion and β-catenin nuclear signaling. *EMBO J.* **24,** 742–752
23. Maretzky, T., Reiss, K., Ludwig, A., Buchholz, J., Scholz, F., Proksch, E., de Strooper, B., Hartmann, D., and Saftig, P. (2005) ADAM10 mediates E-cadherin shedding and regulates epithelial cell-cell adhesion, migration, and β-catenin translocation. *Proc. Natl. Acad. Sci. U.S.A.* **102,** 9182–9187
24. Schulz, B., Pruessmeyer, J., Maretzky, T., Ludwig, A., Blobel, C. P., Saftig, P., and Reiss, K. (2008) ADAM10 regulates endothelial permeability and T-cell transmigration by proteolysis of vascular endothelial cadherin. *Circ. Res.* **102,** 1192–1201
25. Sahin, U., Weskamp, G., Kelly, K., Zhou, H. M., Higashiyama, S., Peschon, J., Hartmann, D., Saftig, P., and Blobel, C. P. (2004) Distinct roles for ADAM10 and ADAM17 in ectodomain shedding of six EGFR ligands. *J. Cell Biol.* **164,** 769–779
26. Sahin, U., and Blobel, C. P. (2007) Ectodomain shedding of the EGF-receptor ligand epigen is mediated by ADAM17. *FEBS Lett.* **581,** 41–44
27. Reiss, K., Cornelsen, I., Husmann, M., Gimpl, G., and Bhakdi, S. (2011) Unsaturated fatty acids drive disintegrin and metalloproteinase (ADAM)-dependent cell adhesion, proliferation, and migration by modulating membrane fluidity. *J. Biol. Chem.* **286,** 26931–26942
28. Andrä, J., Koch, M. H., Bartels, R., and Brandenburg, K. (2004) Biophysical characterization of endotoxin inactivation by NK-2, an antimicrobial peptide derived from mammalian NK-lysin. *Antimicrob. Agents Chemother.* **48,** 1593–1599
29. Schlondorff, J., Becherer, J. D., and Blobel, C. P. (2000) Intracellular maturation and localization of the tumour necrosis factor α convertase (TACE). *Biochem. J.* **347,** 131–138
30. Ludwig, A., Hundhausen, C., Lambert, M. H., Broadway, N., Andrews, R. C., Bickett, D. M., Leesnitzer, M. A., and Becherer, J. D. (2005) Metalloproteinase inhibitors for the disintegrin-like metalloproteinases ADAM10 and ADAM17 that differentially block constitutive and phorbol ester-inducible shedding of cell surface molecules. *Comb. Chem. High Throughput. Screen.* **8,** 161–171
31. Le Gall, S. M., Bobé, P., Reiss, K., Horiuchi, K., Niu, X. D., Lundell, D., Gibb, D. R., Conrad, D., Saftig, P., and Blobel, C. P. (2009) ADAMs 10 and 17 represent differentially regulated components of a general shedding machinery for membrane proteins such as transforming growth factor α, L-selectin, and tumor necrosis factor α. *Mol. Biol. Cell* **20,** 1785–1794
32. Boukamp, P., Petrussevska, R. T., Breitkreutz, D., Hornung, J., Markham, A., and Fusenig, N. E. (1988) Normal keratinization in a spontaneously immortalized aneuploid human keratinocyte cell line. *J. Cell Biol.* **106,** 761–771
33. Black, R. A., Rauch, C. T., Kozlosky, C. J., Peschon, J. J., Slack, J. L., Wolfson, M. F., Castner, B. J., Stocking, K. L., Reddy, P., Srinivasan, S., Nelson, N., Boiani, N., Schooley, K. A., Gerhart, M., Davis, R., Fitzner, J. N., Johnson, R. S., Paxton, R. J., March, C. J., and Cerretti, D. P. (1997) A metalloproteinase disintegrin that releases tumour-necrosis factor-α from cells. *Nature* **385,** 729–733
34. Haugwitz, U., Bobkiewicz, W., Han, S. R., Beckmann, E., Veerachato, G., Shaid, S., Biehl, S., Dersch, K., Bhakdi, S., and Husmann, M. (2006) Pore-forming *Staphylococcus aureus* α-toxin triggers epidermal growth factor receptor-dependent proliferation. *Cell Microbiol.* **8,** 1591–1600
35. Maher, S., and McClean, S. (2008) Melittin exhibits necrotic cytotoxicity in gastrointestinal cells which is attenuated by cholesterol. *Biochem. Pharmacol.* **75,** 1104–1114
36. Drechsler, S., and Andra, J. (2011) Online monitoring of metabolism and morphology of peptide-treated neuroblastoma cancer cells and keratinocytes. *J. Bioenerg. Biomembr.*
37. Jorissen, E., Prox, J., Bernreuther, C., Weber, S., Schwanbeck, R., Serneels, L., Snellinx, A., Craessaerts, K., Thathiah, A., Tesseur, I., Bartsch, U., Weskamp, G., Blobel, C. P., Glatzel, M., De Strooper, B., and Saftig, P. (2010) The disintegrin/metalloproteinase ADAM10 is essential for the establishment of the brain cortex. *J. Neurosci.* **30,** 4833–4844
38. Uemura, K., Kihara, T., Kuzuya, A., Okawa, K., Nishimoto, T., Ninomiya, H., Sugimoto, H., Kinoshita, A., and Shimohama, S. (2006) Characterization of sequential N-cadherin cleavage by ADAM10 and PS1. *Neurosci. Lett.* **402,** 278–283
39. Li, Y., Brazzell, J., Herrera, A., and Walcheck, B. (2006) ADAM17 deficiency by mature neutrophils has differential effects on L-selectin shedding. *Blood* **108,** 2275–2279
40. Blobel, C. P. (2005) ADAMs: key components in EGFR signaling and development. *Nat. Rev. Mol. Cell Biol.* **6,** 32–43
41. Maretzky, T., Scholz, F., Köten, B., Proksch, E., Saftig, P., and Reiss, K. (2008) ADAM10-mediated E-cadherin release is regulated by proinflammatory cytokines and modulates keratinocyte cohesion in eczematous dermatitis. *J. Invest Dermatol.* **128,** 1737–1746
42. Firth, J. D., and Putnins, E. E. (2004) Keratinocyte growth factor 1 inhibits wound edge epithelial cell apoptosis *in vitro*. *J. Invest Dermatol.* **122,** 222–231
43. Needham, L., Dodd, N. J., and Houslay, M. D. (1987) Quinidine and melittin both decrease the fluidity of liver plasma membranes and both inhibit hormone-stimulated adenylate cyclase activity. *Biochim. Biophys. Acta* **899,** 44–50
44. Nagano, O., Murakami, D., Hartmann, D., De Strooper, B., Saftig, P., Iwatsubo, T., Nakajima, M., Shinohara, M., and Saya, H. (2004) Cell-matrix interaction via CD44 is independently regulated by different metalloproteinases activated in response to extracellular Ca(2+) influx and PKC activation. *J. Cell Biol.* **165,** 893–902
45. Fredholm, B. B., Abbracchio, M. P., Burnstock, G., Daly, J. W., Harden, T. K., Jacobson, K. A., Leff, P., and Williams, M. (1994) Nomenclature and classification of purinoceptors. *Pharmacol. Rev.* **46,** 143–156
46. Yoshida, H., Kobayashi, D., Ohkubo, S., and Nakahata, N. (2006) ATP stimulates interleukin-6 production via P2Y receptors in human HaCaT keratinocytes. *Eur. J. Pharmacol.* **540,** 1–9
47. Camden, J. M., Schrader, A. M., Camden, R. E., González, F. A., Erb, L., Seye, C. I., and Weisman, G. A. (2005) P2Y2 nucleotide receptors enhance α-secretase-dependent amyloid precursor protein processing. *J. Biol. Chem.* **280,** 18696–18702
48. Ratchford, A. M., Baker, O. J., Camden, J. M., Rikka, S., Petris, M. J., Seye, C. I., Erb, L., and Weisman, G. A. (2010) P2Y2 nucleotide receptors me-

diate metalloprotease-dependent phosphorylation of epidermal growth factor receptor and ErbB3 in human salivary gland cells. *J. Biol. Chem.* **285,** 7545–7555
49. Gu, B., Bendall, L. J., and Wiley, J. S. (1998) Adenosine triphosphate-induced shedding of CD23 and L-selectin (CD62L) from lymphocytes is mediated by the same receptor but different metalloproteases. *Blood* **92,** 946–951
50. Le Gall, S. M., Maretzky, T., Issuree, P. D., Niu, X. D., Reiss, K., Saftig, P., Khokha, R., Lundell, D., and Blobel, C. P. (2010) ADAM17 is regulated by a rapid and reversible mechanism that controls access to its catalytic site. *J. Cell Sci.* **123,** 3913–3922
51. Sengstake, S., Boneberg, E. M., and Illges, H. (2006) CD21 and CD62L shedding are both inducible via P2X7Rs. *Int. Immunol.* **18,** 1171–1178
52. Jamieson, G. P., Snook, M. B., Thurlow, P. J., and Wiley, J. S. (1996) Extracellular ATP causes of loss of L-selectin from human lymphocytes via occupancy of P2Z purinocepters. *J. Cell Physiol.* **166,** 637–642
53. Sluyter, R., and Wiley, J. S. (2002) Extracellular adenosine 5′-triphosphate induces a loss of CD23 from human dendritic cells via activation of P2X7 receptors. *Int. Immunol.* **14,** 1415–1421
54. Moon, H., Na, H. Y., Chong, K. H., and Kim, T. J. (2006) P2X7 receptor-dependent ATP-induced shedding of CD27 in mouse lymphocytes. *Immunol. Lett.* **102,** 98–105
55. Ralevic, V., and Burnstock, G. (1998) Receptors for purines and pyrimidines. *Pharmacol. Rev.* **50,** 413–492
56. Lambrecht, G. (2000) Agonists and antagonists acting at P2X receptors: selectivity profiles and functional implications. *Naunyn Schmiedebergs Arch. Pharmacol.* **362,** 340–350
57. Schachter, J. B., Sromek, S. M., Nicholas, R. A., and Harden, T. K. (1997) HEK293 human embryonic kidney cells endogenously express the P2Y1 and P2Y2 receptors. *Neuropharmacology* **36,** 1181–1187
58. Park, H. J., Lee, S. H., Son, D. J., Oh, K. W., Kim, K. H., Song, H. S., Kim, G. J., Oh, G. T., Yoon, D. Y., and Hong, J. T. (2004) Antiarthritic effect of bee venom: inhibition of inflammation mediator generation by suppression of NF-κB through interaction with the p50 subunit. *Arthritis Rheum.* **50,** 3504–3515
59. Lee, S. Y., Park, H. S., Lee, S. J., and Choi, M. U. (2001) Melittin exerts multiple effects on the release of free fatty acids from L1210 cells: lack of selective activation of phospholipase A2 by melittin. *Arch. Biochem. Biophys.* **389,** 57–67
60. Maher, S., Feighery, L., Brayden, D. J., and McClean, S. (2007) Melittin as an epithelial permeability enhancer I: investigation of its mechanism of action in Caco-2 monolayers. *Pharm. Res.* **24,** 1336–1345
61. Koivisto, L., Jiang, G., Häkkinen, L., Chan, B., and Larjava, H. (2006) HaCaT keratinocyte migration is dependent on epidermal growth factor receptor signaling and glycogen synthase kinase-3α. *Exp. Cell Res.* **312,** 2791–2805
62. Elliott, J. I., Surprenant, A., Marelli-Berg, F. M., Cooper, J. C., Cassady-Cain, R. L., Wooding, C., Linton, K., Alexander, D. R., and Higgins, C. F. (2005) Membrane phosphatidylserine distribution as a non-apoptotic signaling mechanism in lymphocytes. *Nat. Cell Biol.* **7,** 808–816
63. Schwiebert, E. M., and Zsembery, A. (2003) Extracellular ATP as a signaling molecule for epithelial cells. *Biochim. Biophys. Acta* **1615,** 7–32
64. Elssner, A., Duncan, M., Gavrilin, M., and Wewers, M. D. (2004) A novel P2X7 receptor activator, the human cathelicidin-derived peptide LL37, induces IL-1β processing and release. *J. Immunol.* **172,** 4987–4994
65. Keith, D. J., Eshleman, A. J., and Janowsky, A. (2011) Melittin stimulates fatty acid release through non-phospholipase-mediated mechanisms and interacts with the dopamine transporter and other membrane-spanning proteins. *Eur. J. Pharmacol.* **650,** 501–510
66. Wewers, M. D., and Sarkar, A. (2009) P2X(7) receptor and macrophage function. *Purinergic. Signal.* **5,** 189–195
67. Tomasinsig, L., Pizzirani, C., Skerlavaj, B., Pellegatti, P., Gulinelli, S., Tossi, A., Di Virgilio, F., and Zanetti, M. (2008) The human cathelicidin LL-37 modulates the activities of the P2X7 receptor in a structure-dependent manner. *J. Biol. Chem.* **283,** 30471–30481
68. Tokumaru, S., Sayama, K., Shirakata, Y., Komatsuzawa, H., Ouhara, K., Hanakawa, Y., Yahata, Y., Dai, X., Tohyama, M., Nagai, H., Yang, L., Higashiyama, S., Yoshimura, A., Sugai, M., and Hashimoto, K. (2005) Induction of keratinocyte migration via transactivation of the epidermal growth factor receptor by the antimicrobial peptide LL-37. *J. Immunol.* **175,** 4662–4668
69. Dixon, C. J., Bowler, W. B., Littlewood-Evans, A., Dillon, J. P., Bilbe, G., Sharpe, G. R., and Gallagher, J. A. (1999) Regulation of epidermal homeostasis through P2Y2 receptors. *Br. J. Pharmacol.* **127,** 1680–1686
70. Greig, A. V., Linge, C., Terenghi, G., McGrouther, D. A., and Burnstock, G. (2003) Purinergic receptors are part of a functional signaling system for proliferation and differentiation of human epidermal keratinocytes. *J. Invest Dermatol.* **120,** 1007–1015

Supplementary Figure S1

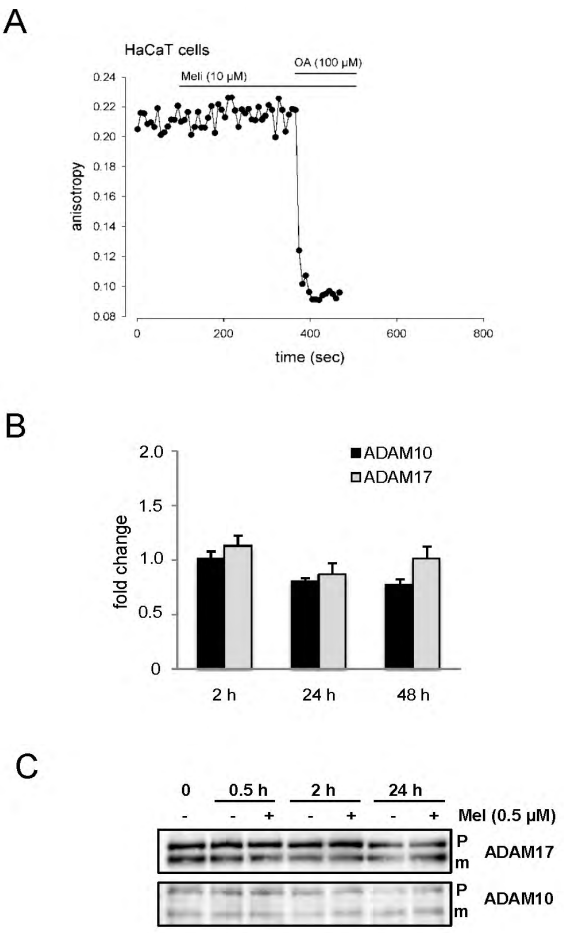

Supplementary Figure S1. Melittin effects are independent of changes in membrane fluidity and ADAM expression. (A) Anisotropy measurements were performed with HaCaT cells loaded with 4 µM diphenyl hexatriene (DPH). The anisotropy values were monitored as a function of the time. Melittin (Meli) was added at the indicated time. Oleic acid (OA) was used as positive control. (B) Real-time RT–PCR analysis and (C) ADAM10/ADAM17 immunoblot analysis. HaCaTs were left untreated or stimulated with 0.5 µM melittin for the indicated time. Melittin treatment did not significantly increase RNA expression or protein level of ADAM10 and ADAM17. p: proform; m: mature form.

Supplementary Figure S2

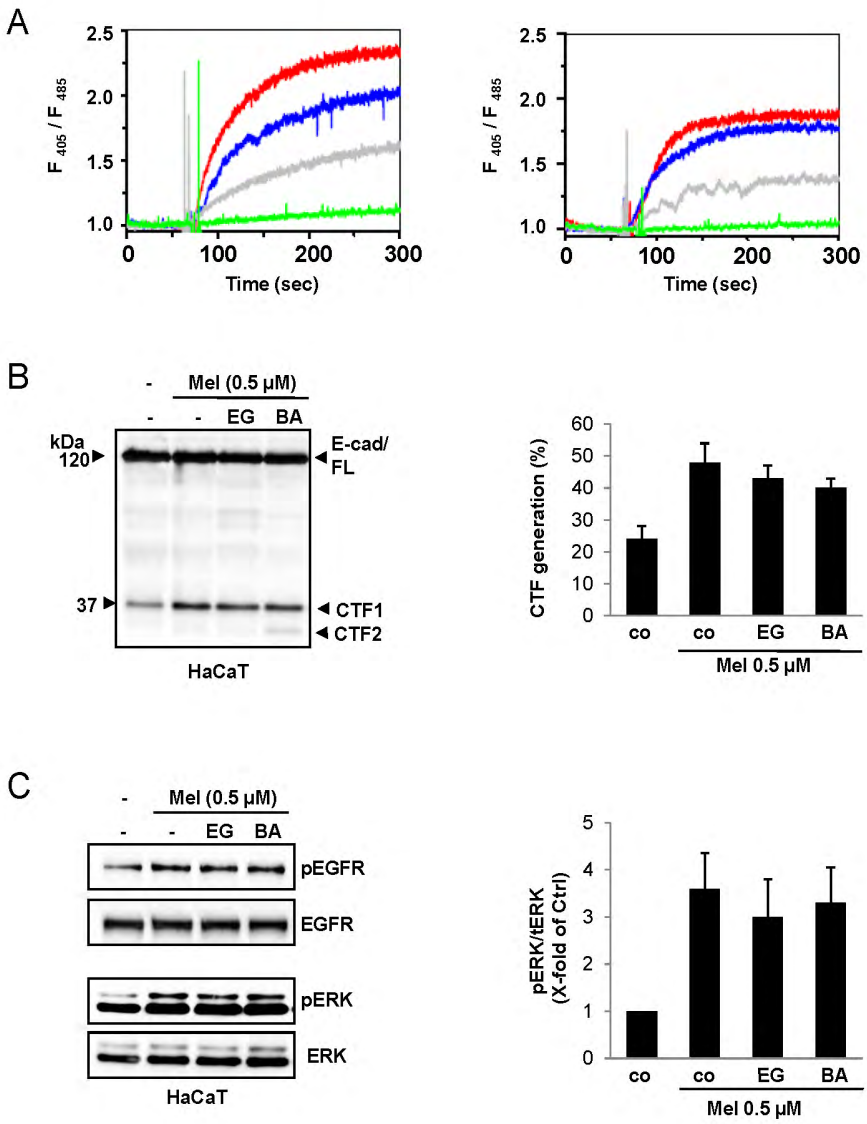

Supplementary Figure S2. Melittin-induced calcium influx is not essential for ADAM activation. (A) HaCaT cells were stimulated with increasing concentrations of melittin (green line: 0.2 µM, grey line: 0.4 µM, blue line 0.8 µM, red line: 1µM) in calcium-containing buffer (left panel) and in buffer lacking Ca^{2+} and Mg^{2+} (right panel). Calcium influx was determined by fluorescence spectroscopy. (B) HaCaT cells were stimulated with melittin (0.5 µM) for 30 min in the presence of extracellular calcium chelator EGTA (EG, 5 mM), intracellular calcium chelator BAPTA-AM (BA, 50 µM) and analyzed for E-cadherin shedding. Quantification of three independent experiments is shown in the right panel. (C) Representative western blot analyses of EGFR activation and ERK1/2 phosphorylation with an immunoblot of total EGFR and total ERK1/2 included as loading control. The results of a densitometric quantification of ERK1/2 phosphorylation (pERK) relative to total ERK (tERK) (n=3) are shown in the right panel.

14. Erklärung

Hiermit erkläre ich, Anselm Sommer, dass ich die vorliegende Arbeit - abgesehen von der wissenschaftlichen Beratung durch meinen akademischen Betreuer- selbstständig und nur mit den von mir angegebenen Quellen und Hilfsmitteln verfasst habe. Die vorliegende Arbeit entstand unter Einhaltung der Regeln guter wissenschaftlicher Praxis der Deutschen Forschungsgemeinschaft. Die Arbeit wurde bisher an keiner anderen Universität zur Begutachtung im Rahmen eines Prüfungsverfahren vorgelegt.

Teile dieser Arbeit wurden in dem folgenden Artikel veröffentlicht:

Sommer, A.*, Fries, A.*, Cornelsen, I., Speck, N., Koch-Nolte, F., Gimpl, G., Andrä, J., Bhakdi, S., Reiss, K., 2012. **Melittin modulates keratinocyte function through P2 receptor-dependent ADAM activation**. J. Biol. Chem. 287, 23678-89. doi:10.1074/jbc.M112.362756
*equal contribution

Darüber hinaus wurde ein weiteres Manuskript, das Daten aus dieser Arbeit enthält zur Publikation vorbereitet:

Sommer, A., Kordowski, F., Büch, J., Evers, A., Maretzky, T., Michalek, M., Andrä, J., Blobel, C.P., Jung, S., Schirmeister, T., Kunzelmann, K., Nagata, S., Düsterhöft, S., Nehls, C., Heinbockel, L., Gutsmann, T., Grötzinger, J., Bhakdi, S., Reiss, K. **Phosphatidylserine exposure represents the decisive step of ADAM17-mediated proteolysis.**

Kiel, Dezember 2014

Anselm Sommer

15. Curriculum vitae

Name	Anselm David Sommer
born on	27.02.1982
in	Herdecke
Citizenship	german

Tertiary education

08/2010 - 12/2014	**Dissertation** at the Department of Dermatology and Allergology, UKSH Kiel, in the group of Prof. Dr. Karina Reiss as part of the SFB 877 ”Proteolysis as a Regulatory Event in Pathophysiology” project A4 . **Titel:** “Analyses of melittin-induced ADAM10 and -17-activation and of phosphatidylserine exposure for ADAM17-mediated substrate processing”
07/2009-07/2010	**Diploma thesis** at the Institute for Pharmacology and Toxicology, Medical Faculty Aachen in the group of Prof. Dr. Stefan Uhlig. **Titel:** “Transzytose und parazelluläre Permeabilität von pulmonalen Endothelzellen”.
10/2002-07/2009	**Study of biology** at the Rheinisch-Westfälische Technische Hochschule (RWTH) Aachen. Focal subjects: Neurobiology, Molecular biology, Developmental biology and Pharmacology.

School education

2002	Abitur degree at the Freie Waldorfschule Kiel
1992-2002	Freie Waldorfschule Kiel
1989-1993	Freie Waldorfschule Kaltenkirchen